BULGARIAN ACADEMY of SCIENCES
1869

PhD thesis

STUDY OF THE LIGAND-DEPENDENT DYSREGULATION OF PPARγ: ADVERSE OUTCOME PATHWAYS DEVELOPMENT AND MOLECULAR MODELLING

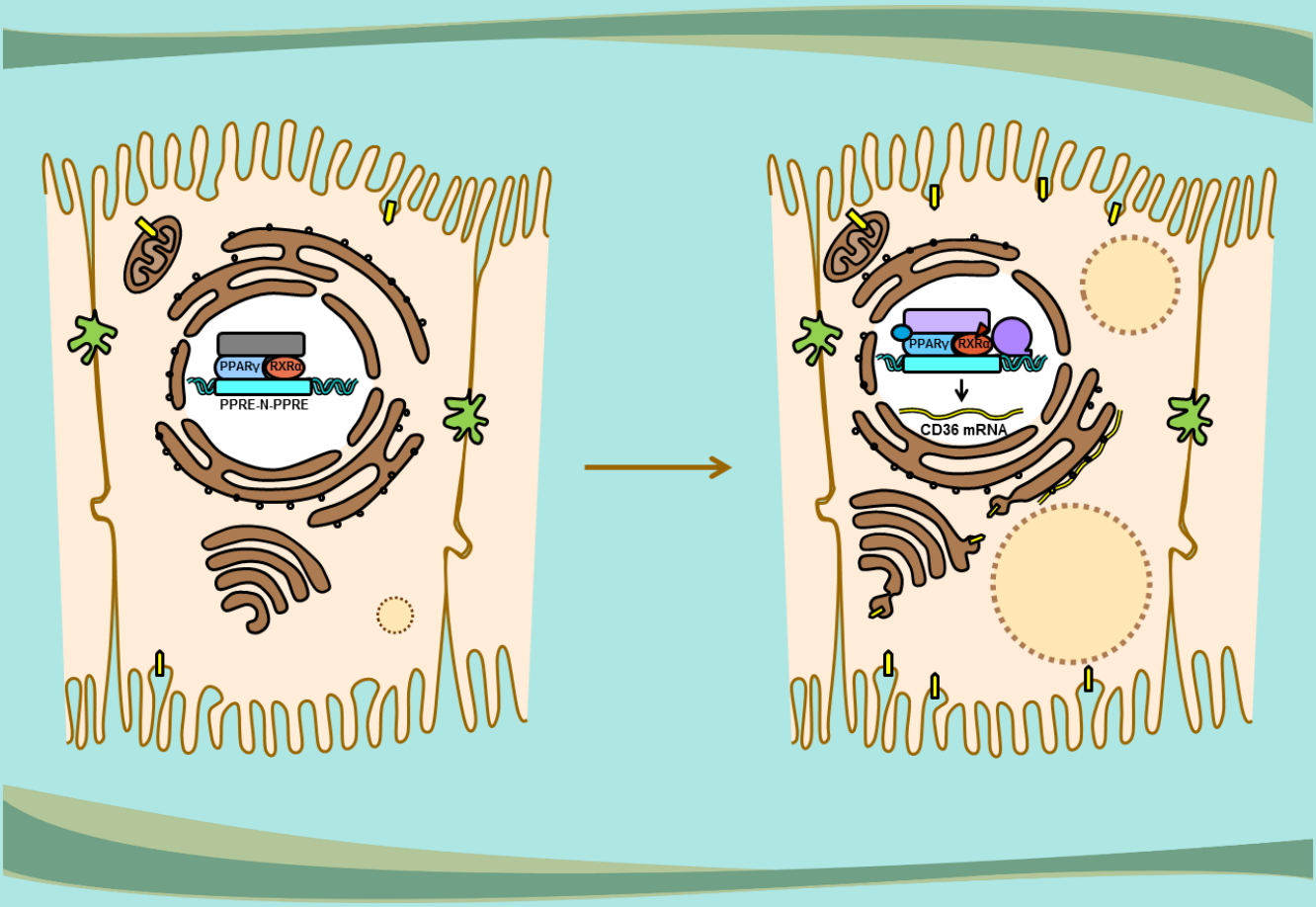

MERILIN AL SHARIF

2016

Bulgarian Academy of Sciences

Institute of Biophysics and Biomedical Engineering

Department of QSAR and Molecular Modelling

STUDY OF THE LIGAND-DEPENDENT DYSREGULATION OF PPARγ: ADVERSE OUTCOME PATHWAYS DEVELOPMENT AND MOLECULAR MODELLING

A DISSERTATION SUBMITTED FOR THE DEGREE OF

DOCTOR OF PHILOSOPHY

MERILIN MAZEN AL SHARIF

SUPERVISORS:

ASSOC. PROF. IVANKA TSAKOVSKA, PhD

AND

CORR. MEMBER OF BAS, PROF. ILZA PAJEVA, DSc

Sofia

2016

ACKNOWLEDGEMENTS

I would like to express my heartfelt gratitude to my parents, who supported me, and incented me to strive towards my goal, for their understanding and encouragement in every possible way.

I deeply appreciate and acknowledge my erudite professors from the Faculty of Biology, Sofia University "St. Kliment Ohridski", who laid the foundations for my career development.

I am sincerely thankful to my supervisors Assoc. Prof. Ivanka Tsakovska, PhD, and Corr. Member of BAS, Prof. Ilza Pajeva, DSc, for their excellent guidance, for the immense knowledge they gave me and for allowing me to grow as a research scientist. I would especially like to thank specialist Petko Alov for his expert contribution, influence and care during the entire course of my PhD.

I would also like to thank the rest of my thesis committee: Prof. Stefka Taneva, DSc; Prof. Irini Doytchinova, DSc; Prof. Mariela Odjakova, PhD, and Assoc. Prof. Vessela Vitcheva, PhD, for their insightful comments and suggestions as well as for the encouragement.

My special thanks are extended to the Institute of Biophysics and Biomedical Engineering – BAS and the Department of QSAR and Molecular Modelling as well as to our foreign partners within the SEURAT-1 cluster for the fruitful and enriching collaboration.

Last but not least, the funding from the European Community's 7th Framework Program COSMOS Project (grant n°266835) and from the Ministry of Education, Youth and Science, Bulgaria (grant n°D01-169/14.07.2014) is gratefully acknowledged.

Thank you for making me more than I am.

Merilin Al Sharif

2016

TABLE OF CONTENTS

ABBREVIATIONS

%max, percent efficacy in relation to the maximum efficacy of a reference compound

(Q)SAR, (quantitative) structure-activity relationship

ΔG or ΔE, change in the free energy formation of the ligand-receptor complex

ΔH, enthalpy

ΔS, entropy

3Rs, replacement, reduction and refinement of animal testing

Acc, acceptor

ACC, acetyl-CoA carboxylase

Acc2, projected acceptor

ADIPOQ, adiponectin

Ad-PPARγ, adenovirus-mediated transfection of PPARγ

AF1, activation function domain 1

AF2, activation function domain 2

AhR, aryl hydrocarbon receptor

AMPK, 5'-adenosine monophosphate-activated protein kinase

Ani, anion

AO, adverse outcome effect

AOP, adverse outcome pathway

AOP-KB, AOP Wiki Knowledge Base

aP2, adipose fatty acid binding protein

ApoCIV, apolipoprotein C IV

Aro, aromatic

BHK21 ATCC CCL10, baby hamster kidney cell line from the American Type Culture Collection

C, cellular level

CAR, constitutive androstane receptor

CAS, chemical abstracts service

Cat, cation

CD, normal chow diet

CM, community level

CoMFA, Comparative Molecular Field Analysis

CoMSIA, Comparative Molecular Similarity Indices Analysis

COS-1 and COS-7, CV-1 in origin, with SV40 genetic material

COSMOS, Integrated *In Silico* Models for the Prediction of Human Repeated Dose Toxicity of COSMetics to Optimise Safety

cSDEP, the estimated cross-validated standard error at the specified critical point

CSRML, Chemical Subgraphs and Reactions Markup Language

CV-1, simian - *Cercopithecus aethiops* or normal African green monkey kidney Fibroblast Cells

DBD, DNA-binding domain

DGAT1, diglyceride acyltransferase 1

DGAT2, diglyceride acyltransferase 2

Don, donor

Don2, projected donor

dq/dr, the slope of q_{cv}^2 at the specified critical point with respect to the correlation of the original dependent variables versus the perturbed dependent variables

DUD-E database, a database of useful decoys: enhanced

e, efficacy

EC, environmental contamination

EC_{50}, effective concentration (the concentration of a drug that gives half-maximal response)

E_{max}, maximal efficacy

ER, estrogen receptor

EX, exposure

FA, fatty acids

FABP4, fatty acid binding protein 4 (synonym of aP2)

FABPpm, plasma membrane fatty acid binding protein

FAS, fatty acid synthase

FASEs. fatty acid synthesising enzymes

FAT/CD36, fatty acid translocase/cluster determinant 36

FAT/UPs, fatty acid transport/uptake related proteins

FDA CFSAN's CERES, Chemical Evaluation and Risk Estimation System at the U.S. Food and Drug Administration, Center for Food Safety and Applied Nutrition

FN, false negative

FP, false positive

FSP27/CIDE-C, fat-specific protein 27/cell death-inducing DFF45-like effector

FXR, farnesoid X receptor

GR, glucocorticoid receptor

H, helix

HB, hydrogen bond

HCC, hepatocellular carcinoma

HEK293, human embryonic kidney 293 cell line

HepG2, human liver hepatocellular carcinoma cell line

HFD, high-fat diet

HSCs, hepatic stellate cells

Huh-7, human liver hepatocellular carcinoma cell line

Hyd, hydrophobic

HydA, hydrophobic atom

I, individual level

IC_{50}, half maximal inhibitory concentration

K_d, dissociation constant

KEs, key events

K_i, inhibitory constant

L, ligand

LBD, ligand-binding domain

LD, lipid droplet

LDAPs, lipid droplet associated proteins

LOO, leave-one-out cross-validation

LPL, lipoprotein lipase

LXR, liver X receptor

M, molecular level

MGAT1, monoacylglycerol O-acyltransferase 1

MIE, molecular initiating event

ML, metal ligator

ML2, projected metal ligator

MM, molecular modelling

MoA, mode of action

NAFL, non-alcoholic fatty liver

NAFLD, non-alcoholic fatty liver disease

NASH, non-alcoholic steatohepatitis

NFkB, nuclear factor – kappaB

N_{opt}, optimal number of PLS components

NR1C3, nuclear receptor subfamily 1, group C, member 3 (synonym of PPARγ)

O, organelle level

OECD, Organisation for Economic Co-operation and Development

oRepeatTox DB, oral repeated dose toxicity database

P, population level

PDB, Protein Data Bank

PiN, ring projection

PiR, pi-ring

Plin 1, 2 and 4, Perilipins 1, 2, and 4

PLS, partial least squares analysis

PPARα, peroxisome proliferator-activated receptor α

PPARγ, peroxisome proliferator-activated receptor γ

PXR, pregnane X receptor

Q^2, the expected value of q^2 at the specified critical point for $r^2_{yy'}$ (the correlation of the scrambled responses with the unperturbed data)

qAOP, quantitative AOP

q_{cv}^2, cross-validated coefficient

R, gas constant

R, receptor

R', the response of a tissue to some stimulus

RAR, retinoic acid receptor

RDT, repeated dose toxicity

RL, receptor-ligand complex

RMSD, root-mean-square deviation

r_{pred}^2, predictive correlation coefficient

RT-PCR, real time polymerase chain reaction

RXRα, retinoid X receptor alpha

S, stimulus

SCD1, stearoyl-CoA desaturase1

SEE, standard error of estimate

SEPcv, cross-validated standard error of prediction

SEURAT-1, Safety Evaluation Ultimately Replacing Animal Testing

SLC 27A2, solute carrier family 27 fatty acid transporter member 2

SLC 27A5, solute carrier family 27 fatty acid transporter member 5

SOP, source to outcome pathway

SREBP-1, sterol regulatory element-binding protein-1

StDev*Coeff, the standard deviation of the 3D field at each grid point multiplied by the 3D QSAR coefficient

T, tissue level

TG, triglycerides

TGSEs, triglyceride synthesising enzymes

TN, true negative

ToP, toxicity pathway

TP, true positive

TZDs, thiazolidinediones

VLDL, very low-density lipoprotein

VS, virtual screening

WoE, weight-of-evidence

WT, wild type

y, fractional receptor occupancy

α, intrinsic activity

The current PhD thesis contains 48 figures, 20 tables and 306 references.

INTRODUCTION

Since ancient times till nowadays, people's quests for self-awareness, natural lifestyle and combat with the oncoming diseases and epidemics have given impetus to the development of many scientific fields related to human health. One of them is biomedical engineering – an interdisciplinary field combining medicine, toxicology, pharmacology, biochemistry, molecular biology, physics, chemistry, methods of structure analysis, mathematical and engineering methods.

Even Hippocrates used to claim that the human organism is related to the environment, which influences its natural life functions. Unfortunately, mankind's desire for more material wealth, comfort and luxury in everyday life has brought about today's over-industrialized world, generating a number of adverse effects and influences on living systems. For the last century, tons of xenobiotics have flooded the Earth and its biosphere in the form of chemical weapons, industrial pollutants, pharmaceuticals and cosmetics, thus posing a serious risk to the stability and functioning of biosystems and to human health in particular. Therefore, qualitative and quantitative characterizations of potential toxins are crucial moments in health risk analysis and assessment.

The founder of toxicology, Paracelsus, defines very clearly the quantity aspects of the adverse effects, postulating that "the dose makes the poison." Establishing quantitative structure-activity relationships, molecular modelling, and elucidating the specific mode of action of potential toxins are among the modern approaches of computational (predictive) toxicology.

In line with the 3Rs principles of replacement, reduction and refinement of animal toxicity testing, the current PhD thesis is focused on the development of alternative *in silico* approaches supporting hazard identification and characterisation related to repeated dose hepatotoxicity. The toxicity-induced liver injury, in particular the non-alcoholic fatty liver disease (NAFLD), represents a special interest. NAFLD involves a spectrum of liver pathologies (steatosis/steatohepatitis/fibrosis) increasing the incidence of liver cirrhosis and hepatocellular carcinoma. Nuclear-receptor disruption has been considered one of the potential mechanisms involved in the development of NAFLD. Among the receptors reported to be potentially involved in disease development and progression is the peroxisome proliferator-activated receptor gamma (PPARγ). PPARγ is a transcriptional regulator from the nuclear receptor superfamily which:

- is expressed in multiple tissues: mainly in white and brown adipose tissue but also in intestines, liver, kidneys, retina, immunologic system (bone marrow, lymphocytes, monocytes and macrophages) and muscles (to a lesser extent);

- regulates crucial cellular pathways, related to: adipogenesis (adipocyte proliferation and differentiation), lipid and glucose homeostasis, inflammatory responses, vascular biology and placental development;

- is an attractive therapeutic target for the treatment of a wide spectrum of diseases: metabolic diseases, especially hyperglycemia; cardiovascular disorders; inflammatory and auto-immune diseases: multiple sclerosis, inflammatory bowel diseases, rheumatoid arthritis; cancer; Alzheimer's disease; age-related macular degeneration; skin-related disorders; addiction control – in terms of substances (alcohol, nicotine, opioids or cocaine) or addictive behavior (kleptomania and others).

The potential for an adverse prosteatotic effect of PPARγ full agonists has been explored through the Mode of Action/Adverse Outcome Pathway (MoA/AOP) methodology by systematisation and analysis of the available scientific knowledge. The study involves the development of two AOPs with different molecular initiating events (MIEs): PPARγ inhibition in adipocytes and PPARγ full activation in hepatocytes as well as a weight-of-evidence (WoE) evaluation of key events with an emphasis on the array of assays supporting the outlined biochemical and histological disease markers. The complex nature of the inter-tissue cross-talks and their description within the AOP framework is discussed in the light of the link adipose tissue-related disorders – NAFLD.

For the MIE in hepatocytes (PPARγ full activation), a dataset with structural and biological (binding affinity, potency, and relative efficacy) data for more than 400 full and partial agonists was generated from PDB (http://www.rcsb.org/) and literature sources. It is publicly available (http://biomed.bas.bg/qsarmm/) and serves as a source of data for *in silico* modelling.

Further, an analysis of the PPARγ-full agonist complexes available in PDB was performed to derive a pharmacophore model of PPARγ full agonists. The model was incorporated in a virtual screening (VS) procedure to predict PPARγ full agonism of compounds.

A successful integration of the VS procedure in two battery approaches is discussed as an example for the supportive role of the *in silico* predictive models complementing each other in the process of hazard identification.

A 3D QSAR model to predict the PPARγ full agonists' potency (transactivation activity EC_{50}) was developed as an improvement over previously reported ones, based on the largest and structurally diverse training set used so far. Emphasis is given on the mechanistically justified selection of the dependent variable.

The developed AOPs and predictive models provide a mechanistically justified rationale for the screening of potential prosteatotic chemicals and their prioritisation for further testing.

This work is a part of an *in silico* strategy for predicting potential hepatotoxicity of cosmetic ingredients (COSMOS project, http://www.cosmostox.eu).

CHAPTER 1. LITERATURE REVIEW

1.1. Replacement, Reduction and Refinement (3Rs) of animal testing: MoA/AOP framework and *in silico* approaches

1.1.1. The advent of predictive toxicology

Modern toxicology is based on the concept of the 3Rs, defined as Replacement, Reduction and Refinement of animal testing. Since first proposed by Russel and Burch in 1959 (Russell and Burch, 1959), these principles have gained wide acceptance, being embedded in national and international legislation regulating the use of animals in scientific procedures and driving the establishment of national 3R centres (NC3Rs; Törnqvist et al., 2014) (**Figure 1**).

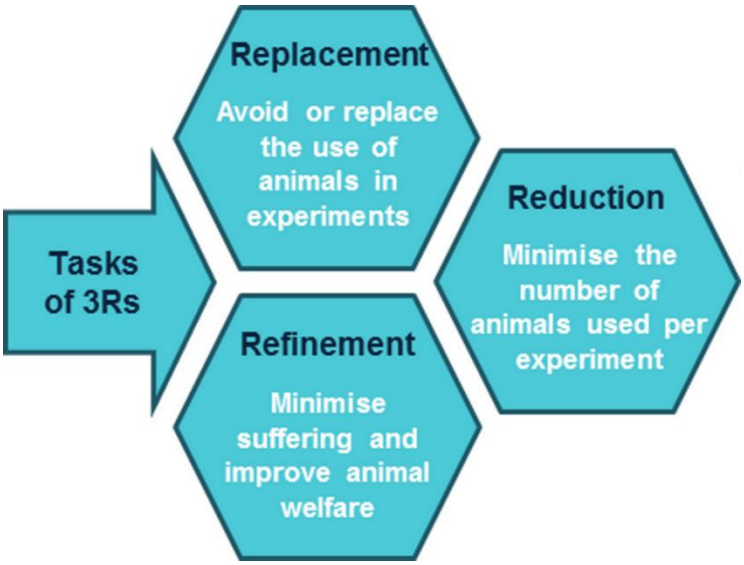

Figure 1. Main tasks related to the three Rs principles

This historical paradigm shift stems from safety, ethical and economic issues and it is expected to ensure the robustness and reproducibility of the experiments, increasing the human relevance of the model systems in a more humane, time- and cost-saving manner. It is driven by the advent of science and technology, and is strongly dependent on data sharing and knowledge exchange, which in the ideal scenario delivers high quality experimental data, acquired and reported according to unified and commonly accepted protocols and formats (NC3Rs; Burden et al, 2014; ENV/JM/MONO(2013)6; Gocht et al., 2015).

The establishment of alternatives to animal testing involves: pathways approaches in toxicology; systems biology; computational chemistry; bioinformatics and mathematical modelling. All of them power the development of and/or benefit from a variety of new technologies that could be classified in a different manner. Depending on the considered level of biological organisation, there are three main groups of technologies: (i) molecular level ("omics"-based technologies generating genomic (genotyping, gene expression, and epigenomic), proteomic, and metabolomic/metabonomic biomarkers), (ii) tissue/organ levels (3D cell cultures, bioreactors, artificial organs), (iii) organism/multisystem levels (micro-flow chips: tissue-on-a-chip / human-on-a-chip) (Burden et al, 2014; Fowler, 2012; Rabinowitz et al., 2008; Huh et al., 2011; Altex Proceedings, 2014). Individually or in a combination, they are known to support main aspects of risk assessment (**Figure 2**) such as: 1) hazard identification, 2) hazard characterisation, 3) exposure assessment and 4) risk characterisation in the light of various toxicological endpoints (topical toxicity, repeated dose toxicity, skin sensitisation, endocrine disruption, reproductive and developmental toxicology, genotoxicity / carcinogenicity, inhalation toxicology) and levels of exposure (bioavailability, bioaccumulation, ecotoxicology) (FAO/WHO, 2008; WHO, 2009a).

The generation of a wide spectrum of new methods and the growing number of toxicity-related databases is a prerequisite for the development of superior approaches based on alternative models (*in vitro* and *in silico*) that being involved in the so-called intelligent (integrated) testing strategies or also expert systems will be able to predict the adverse effects of chemicals, thus replacing *in vivo* toxicity testing (Adler et al., 2011). Such measures are believed to bring benefits for human safety assessments like: (i) reduced uncertainty and increased relevance, (ii) robustness, (iii) reduced cost and time, (iv) higher humanity, (v) adequacy to the legislative requirements within regulations (Burden et al, 2014). Achieving these goals is a continuous and dynamic process that is running at the interface of scientific advancement and legislative requirements, with all positives and negatives of the collective effort it depends on.

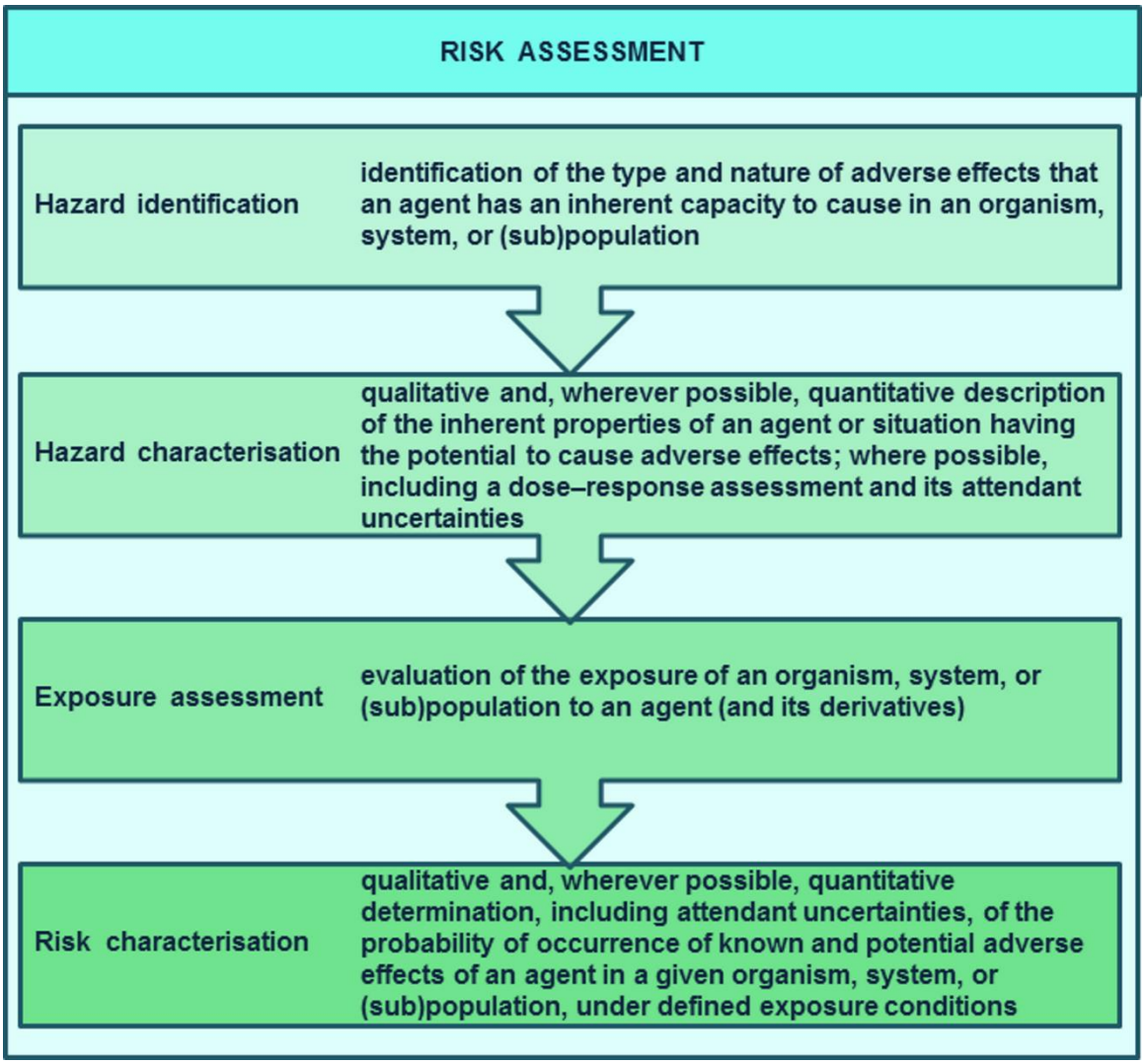

Figure 2. The main steps in risk assessment and their definitions by the Food and Agriculture Organisation/World Health Organisation (FAO/WHO, 2008).

Therefore, the role of the large-scale collaborative initiatives in tuning the scientific approach according to the regulatory demands has become central. An example of such an initiative is SEURAT-1 (Safety Evaluation Ultimately Replacing Animal Testing, http://www.seurat-1.eu/). Working towards animal free chronic toxicity testing, the European FP7 Research Initiative SEURAT-1 adopted a framework focused on better understanding of human adverse health effects related to the repeated exposure to chemicals, exploring the precise MoA/AOP of the toxicants. SEURAT-1 was launched on 1 January 2011 as a cluster, composed of seven projects (http://www.seurat-1.eu/). One of them is the COSMOS Project, focused on the development of mechanism-based *in silico* tools to predict the risk of chronic toxicity induced

by cosmetic ingredients, in accordance with the full EU marketing ban of cosmetics tested on animals since 2013 (Regulation 1223/2009/EC OJ L 342, 22.12.2009, p. 59; COM(2013) 135 final) and other legislation such as the EU REACH and Biocides Regulations and the general 3Rs Principles (Richarz et al., 2014). The current PhD thesis includes a case study performed within the COSMOS Project.

1.1.2. MoA/AOP approach

Historically, among the earliest published scientific papers dealing with MoA of a given compound is "On Digitalis: Its Mode of Action and its Use" by Fothergill JM in 1871 (Fothergill, 1871). This work includes suggestions for possible initiating mechanisms and extensively describes the observed adverse effects related to digitalis administration. This exemplifies the general principle *"Primum non nocere"* (*First, do no harm*) outlined within the Hippocratic Oath, which is implemented in the current drug development strategies. However, consumers' safety issues have gone far beyond the domain of pharmaceuticals, considering the continuously increasing spectrum of xenobiotics they are exposed to. This has strengthened the role of the mechanism-based understanding of the undesired health effects, making it one of the pillars of modern predictive toxicology.

The work on the MoA in animals of the U.S. Environmental Protection Agency (U.S. EPA, 1999) and the WHO's International Programme on Chemical Safety (IPCS) (Sonich-Mullen et al., 2001), followed by further initiatives of the International Life Sciences Institute Risk Sciences Institute (ILSI RSI) (Meek et al., 2003; Seed et al., 2005) and IPCS (Boobis et al., 2006; Boobis et al., 2008), grew into a mode of action/human relevance analysis framework, whose principles, in combination with multiple existing assays and the systems biology approach, became the heart of the AOP concept (ENV/JM/MONO(2013)6). Further, the Organisation for Economic Co-operation and Development initiated an AOP development programme (OECD, www.oecd.org/chemicalsafety/testing/adverse-outcome-pathways-molecular-screening-and-toxicogenomics.htm) to support the OECD Test Guidelines programme, QSAR (quantitative structure-activity relationship) project and Hazard Assessment activities. According to the OECD's definition, the AOP methodology is "an approach which provides a framework to collect, organise and evaluate relevant information on chemical, biological and toxicological effect of chemicals". It integrates a variety of *in chemico*, *in vitro* and *in silico* approaches to potentiate the systematisation, analysis and exchange of knowledge as well as the establishment of reliable expert systems to support decision making (**Figure 3**).

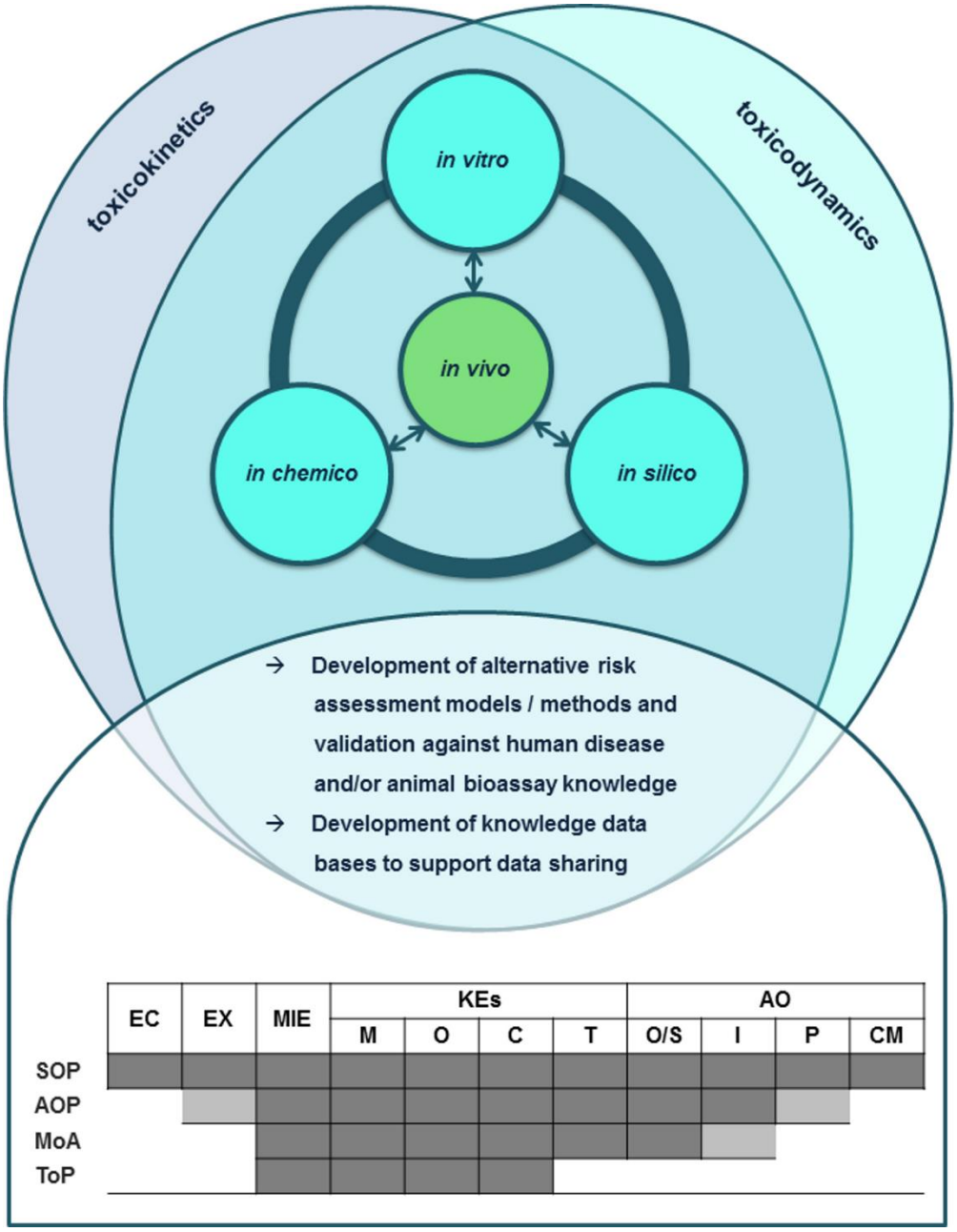

Figure 3. Integration of the alternative models/methods development within the MoA/AOP framework to support decision making in risk assessment: SOP – source to outcome pathway, AOP – adverse outcome pathway, MoA – mode of action, ToP – toxicity pathway, EC – environmental contamination, EX – exposure, MIE – molecular initiating event, KEs – key events at M – molecular level, O – organelle level, C – cellular level, T – tissue level, AO – adverse outcome effect at O/S – organ/system level, I – individual level, P – population level, CM – community level. Dark grey boxes mean that the corresponding level is by definition included in the unit, light boxes are the theoretical extension(s) of the given unit, and white boxes mean that the level is not covered by the unit (adapted from ENV/JM/MONO(2013)6).

Within this concept, the so-called source to outcome pathway covers all steps from environmental contamination to adverse effects at the community level (U.S. EPA, 2005) and incorporates three main units: AOP, MoA and toxicity pathway. However, the heart of the AOP approach is the comprehensive understanding of the MoA of particular chemical initiator(s) triggering a cascade of sequential events: MIE and multiple downstream key events (KEs) related to biologically significant perturbations at all levels of organisation and finally ending with particular adverse outcome (AO) effect, where compensatory mechanisms and feedback loops are overcome.

In particular, the MIE involves a direct interaction of a chemical with a specific target biomolecule (e.g. DNA-binding, protein oxidation, or receptor/ligand interaction) initiating the toxicity pathway (Villeneuve and Garcia-Reyero, 2011; Schultz, p. c.; ENV/JM/MONO(2011)8). The last is enclosed within the MoA but lacks a direct link to an apical effect as it covers the key events to the cellular level (Krewski et al., 2010; Watanabe et al., 2011). In fact, the key events, being biological markers by their nature, represent the main intermediate elements of the AOP as they are: (i) toxicologically relevant to the AO; (ii) experimentally observable and quantifiable; (iii) evolving between the MIE and the AO (ENV/JM/MONO(2011)8; U.S. EPA, 2005; Boobis et al., 2008; ENV/JM/MONO(2008)35.). Although MoA goes further to the organ response, its cornerstone remains the presence of robust experimental observations and mechanistic data supporting the key events (World Health Organisation, 2009b). The site of action also represents a key anchor in the MoA/AOP development and could be interpreted in view of the different levels of biological organisation from the target biological molecule or a more specific site on it (e.g. the ligand binding domain of a receptor) to a particular cell or tissue type in which the molecular initiating event takes place (Schultz, p. c.). Therefore, an AOP may go beyond the confines of a single organ or a system as it represents “a sequence of events from the exposure of an individual or population to a chemical substance through a final adverse (toxic) effect at the individual level (for human health) or population level (for ecotoxicological endpoints).” (ENV/JM/MONO(2013)6). The adverse effect itself represents an impairment of functional/compensatory capacity or an increase in susceptibility to other influences. This effect is caused by a change in the morphology, physiology, growth, development, reproduction, or lifespan of an organism, system, or (sub)population (IPCS, 2004; Keller et al., 2012 ; ENV/JM/MONO(2013)6). Often, the terms endpoint and adverse effect are used interchangeably. This stems from some common

elements in their definitions. However, the term endpoint includes various *in chemico*, *in vitro* or *in vivo* observed chemical or biological properties (hydrophobicity, electrophilicity, lethality, carcinogenicity, immunological responses, organ effects, developmental and reproductive effects, etc.) used in regulatory assessments of chemicals. A more precise definition within the MoA/AOP concept involves two types of endpoints: (i) apical (final) endpoint – directly measured whole-organism outcomes (gross changes) of exposure in *in vivo* tests, generally death, reproductive failure, or developmental dysfunction (ENV/JM/MONO(2011)8; Villeneuve and Garcia-Reyero, 2011; North American Free Trade Agreement NAFTA, 2011), which is closer to if not the same as adverse effect/adverse outcome and (ii) non-apical endpoint – occurring at suborganism-level, i.e. at a level of biological organisation below that of the apical endpoint related to *in vitro* responses, biomarkers, genomics (Villeneuve and Garcia-Reyero, 2011; Schultz, p. c.), which is more likely an intermediate event.

Currently, within the OECD's initiative for chemical safety, the ongoing development of AOPs is organised in 37 main projects (http://www.oecd.org/chemicalsafety/testing/projects-adverse-outcome-pathways.htm, last access: 19 August 2015). The statistics clearly demonstrate the recent advent of the field, which is obviously progressing at a good pace (**Figure 4a, 4b**). Twenty out of 37 projects have already been included in the Adverse Outcome Pathways Knowledge Base (AOP-KB, last access: 19 August 2015) presenting 91 different AOPs, which are classified as: (i) AOPs ready for commenting and currently under OECD Extended Advisory Group on Molecular Screening and Toxicogenomics review (14); (ii) AOPs ready for commenting and open for general comments (3); (iii) AOPs under development (74). The majority of them are still under development (**Figure 5**). The MIEs are related to a variety of target biomolecules – proteins (receptors, transporters, enzymes) and DNA, involving a non-covalent disruption (activation, inhibition) of their function or covalent modifications triggering mutagenesis or oxidative stress. The wide range of final endpoints covers organ- and system-specific adverse effects. **Figure 6** summarises the distribution of AOs with respect to the affected organs/systems. When the effects are too complex/fuzzy to be related to a particular target organ/system or when they are involved in mutagenesis, embryotoxicity or disruption in the normal metabolism/energy balance, they are classified as indefinable.

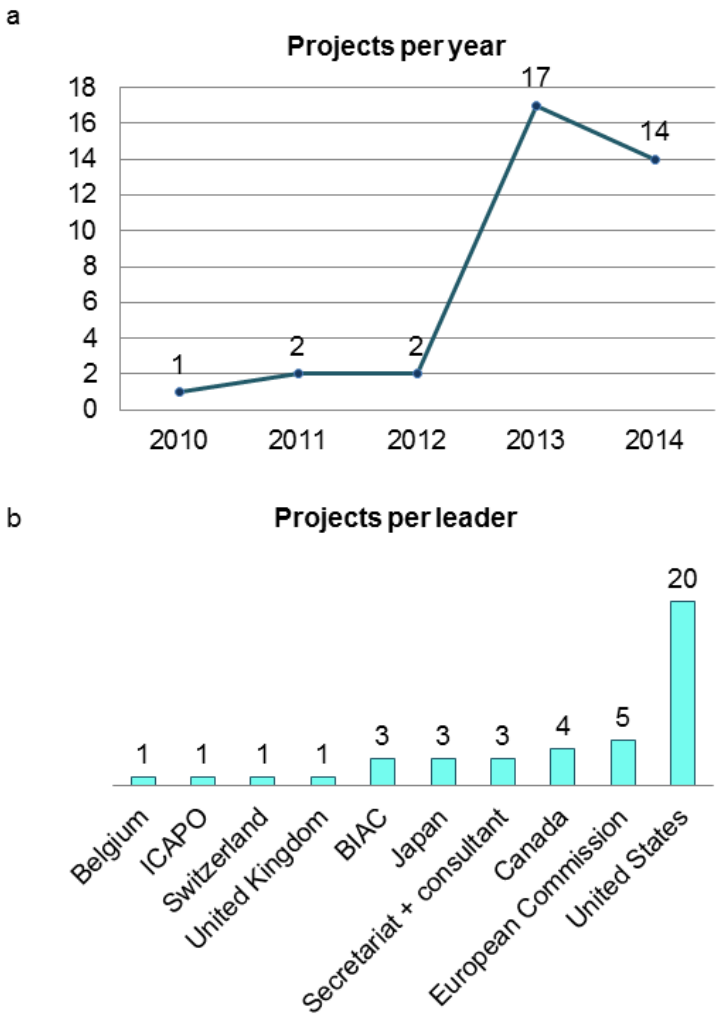

Figure 4. Distribution of the AOP-related projects within the OECD initiative (AOP-KB, AOP Wiki Knowledge Base) by (a) years and (b) country leaders.

Obviously, hepatotoxicity is among the most frequent adverse effects within the reported AOPs. Recently, the dysregulations of several nuclear receptors, including: LXR, PXR, AhR, PPARs (subtypes α and γ), ER, FXR, CAR, GR and RAR, have been proposed as possible MIEs leading to liver steatosis, which not only underlines the role of this class of transcriptional regulators but also raises the question with the AOPs' networking (Landesmann et al., 2012; Mellor et al., 2015). The general understanding is that a single AOP may link only one particular MIE with a single adverse effect.

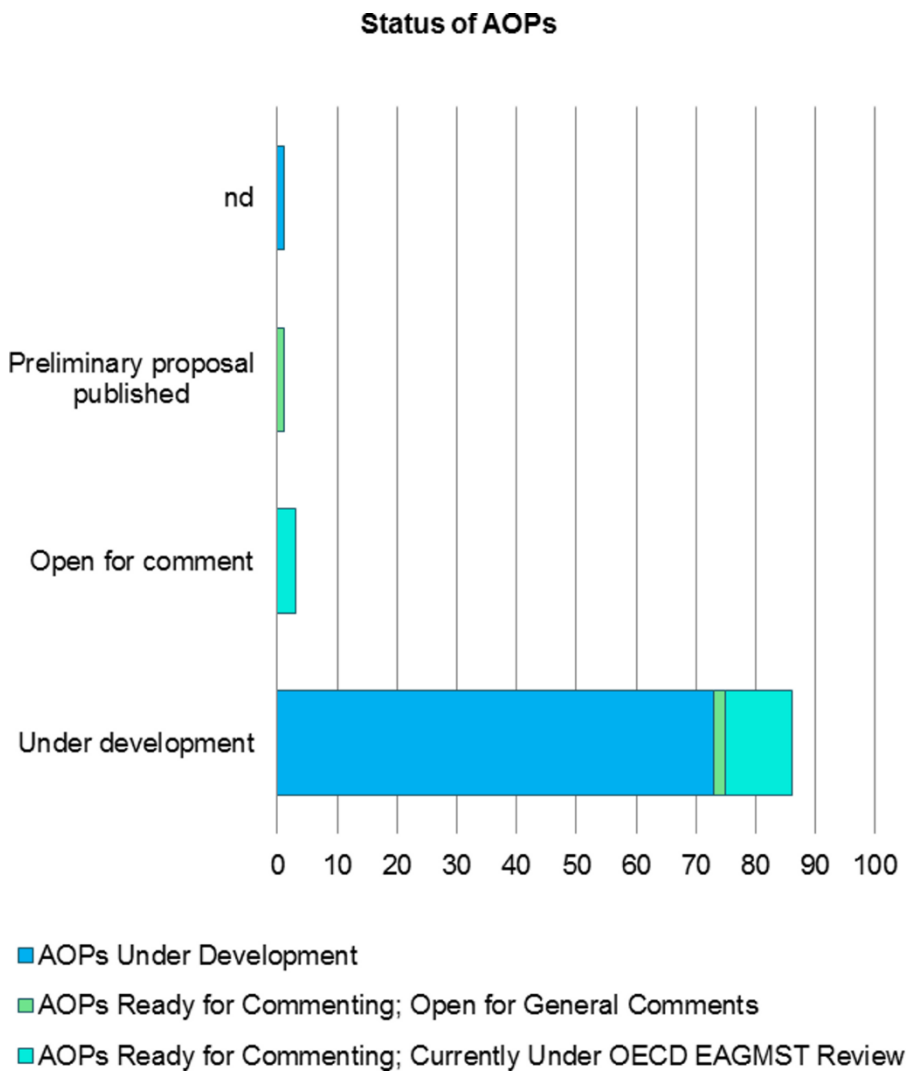

Figure 5. Distribution of the AOPs in the AOP-KB according to their status (nd – no data)

The evolution of the linear AOPs toward networks of many cross-related pathways is rooted in the fact that a particular MIE may lead to several intermediate events and/or final outcomes and, conversely, several MIEs may share common downstream events. The networking of the AOPs depends on the degree of organisation of the collected knowledge, while their quantification – on the extent of evaluation of the quantitative relationships between all events. Once a qualitative AOP is established, it may be further evaluated quantitatively.

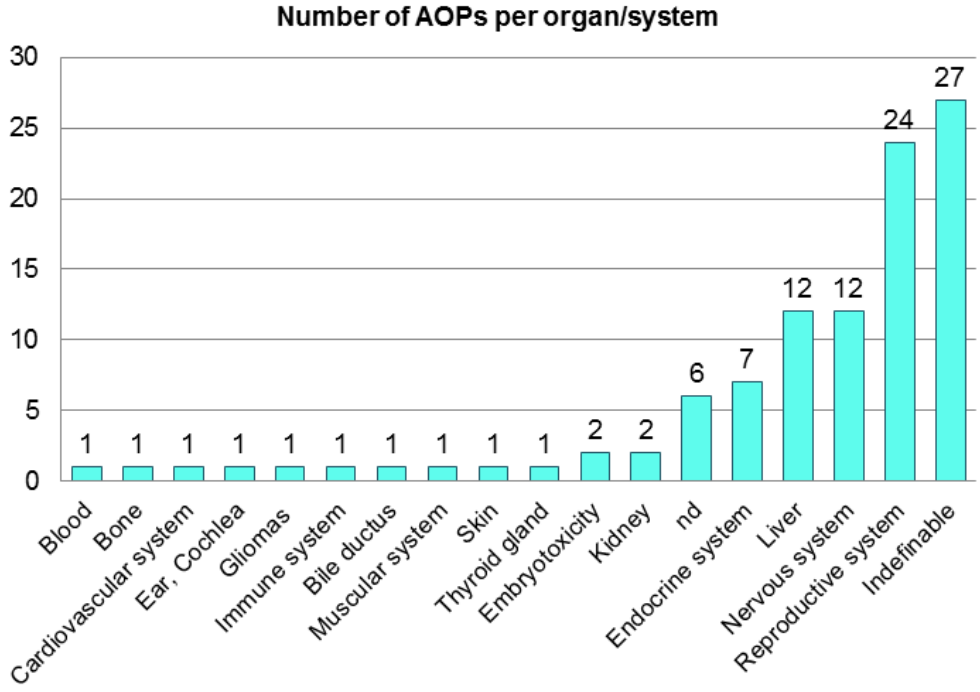

Figure 6. Distribution of the AOPs in the AOP-KB by target organ (nd – no data)

According to the OECD's Guidance document on developing and assessing adverse outcome pathways (or simply OECD's guideline), the quantitative AOP (qAOP) is one where the methods for assessing the key events have been identified and sufficient data generated to identify the applicability domain, threshold values and/or the response relationships with other key events.

Thus the more explored, the more complex and quantifiable become the networks established to meet the challenges of risk assessment, in particular: (1) priority setting for further testing, (2) hazard identification, and (3) classification and labelling. The potential of AOPs to become a basis for the development of an integrated approach to testing and assessment or an integrated testing strategy for toxicity endpoints is enclosed in their central role in channelling the development and/or refinement of chemical categories, *in vitro* and *ex vivo* assays for direct detection of chemical effects or responses at the cellular or higher levels of biological organisation as well as screening assays for targets related to the molecular initiating events identified (ENV/JM/MONO(2011)8).

1.1.3. *In silico* approaches in predictive toxicology

Computational modelling is emerging as an indispensable bridging element in the modern science, which links theory and experiment by simulating and predicting the behaviour of real-world systems, processes and phenomena. It is suggested that methodological advancements (i.e. the progress in computer technologies, computational chemistry, cheminformatics, statistical and machine-learning approaches) are the main drivers of the rise and development of predictive toxicology, which emphasises the strong interdisciplinarity of this modern scientific field (**Figure 7**) (Cronin and Livingstone, 2004; Cherkasov et al., 2014). In view of the demands of risk assessment and regarding the complexity of biological systems, exploration of the mechanisms of toxicity is a challenging task. Therefore, computational toxicology is foreseen as a perspective alternative of the traditional toxicity testing, offering a wide spectrum of *in silico* approaches addressing toxicokinetics or toxicodynamics by various (Q)SARs (SAR heuristic, chemotypes alerts, 2D QSAR) and molecular modelling (MM) methods (pharmacophore modelling, docking, 3D QSAR) (**Figure 8**) (Cronin, 2010; Combes, 2012; Hartung and Hoffmann, 2009; Patlewicz et al., 2013; Cherkasov et al., 2014; Geenen et al., 2009; EFSA, 2014; Rabinowitz et al., 2008). Moreover, the *in silico* tools have been underlined as a potential important element of the integrated testing strategies defined by Blaauboer et al. as "any approach to the evaluation of the toxicity, which serves to reduce, refine or replace an existing animal procedure, and which is based on the use of two or more of the following: physicochemical, *in vitro*, human (e.g. epidemiological, clinical case reports), and animal data (where unavoidable), and computational methods, such as (quantitative) structure-activity relationships ([Q]SAR) and biokinetic models" (Blaauboer et al., 1999). The role of QSAR in safety assessment of food, cosmetics, and industrial chemicals has been established for decades, being integrated in multiple areas of environmental research and regulation. There is an increasing tendency for application of QSAR methods in screening, testing prioritisation, pollution prevention initiatives, green chemistry, hazard identification, and risk assessment. (Cronin and Livingstone, 2004; Patlewicz et al., 2013; Cherkasov et al., 2014).

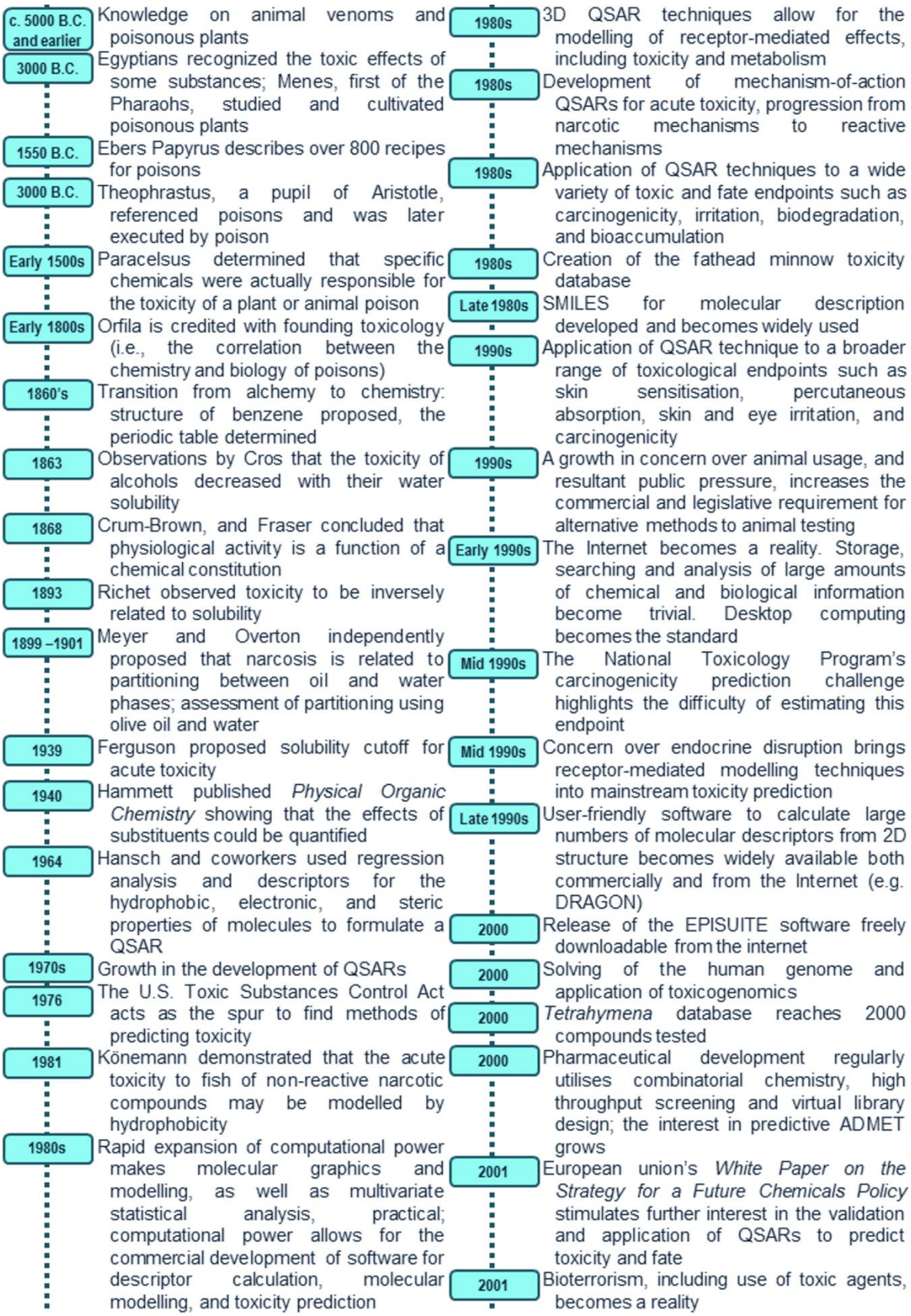

Figure 7. Timeline of key events driving the rise of predictive toxicology (adapted from Cronin and Livingstone, Predicting chemical toxicity and fate, 2004)

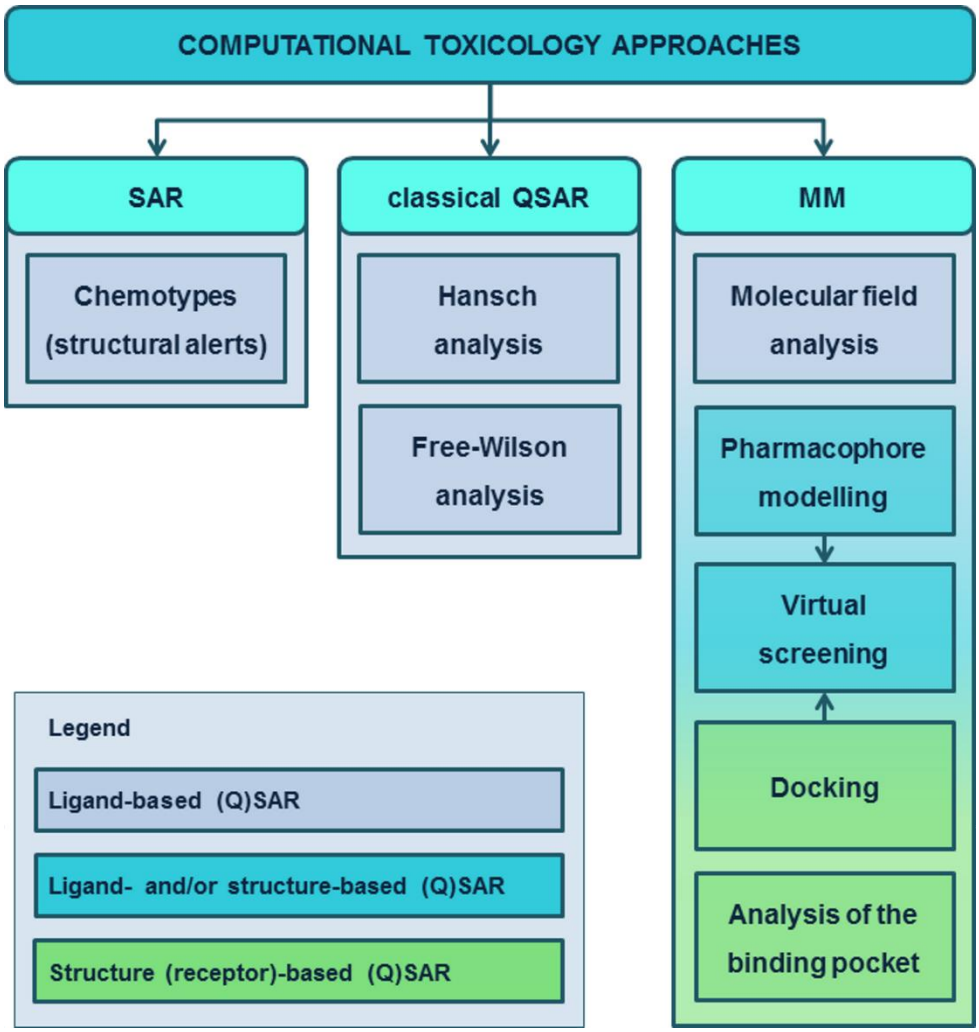

Figure 8. Classification of main computational toxicology methods.

Among the number of endpoints with regulatory importance, modelling repeated–dose toxicity (RDT) is a daunting task dealing with the delayed effects of multiple or repeated administration of chemicals, their accumulation in tissues or other mechanisms of homeostasis perturbation (Krewski et al., 2010). By definition, RDT comprises adverse general toxicological effects which occur as a result of repeated daily dosing with or exposure to a substance for a specified period up to the expected lifespan of the test species (ECHA, 2013). Although challenged by the multi MoA nature of this endpoint and thus represented by limited and mostly local (Q)SARs (Patlewicz et al, 2013), the pathway-based alternative approaches are able to overcome the limitations of the traditional *in vivo* repeated dose toxicity tests (Prieto, et al., 2011; Cronin et al., 2012). Examples of *in silico* models for RDT were summarised by Adler et al., 2011 (**Table 1**).

Table 1. Summary of repeated dose toxicity related *in silico* methods (adapted from Adler et al., 2012); * R&D, optimisation, prevalidation, validation, regulatory acceptance; ** Maximum recommended therapeutic dose

Alternative tests available	Part of mechanism covered	Area(s) of application	Status *	Comments	Estimated time until entry into pre-validation
TOPKAT	Predicts LOAEL for chronic toxicity	Prioritisation/ screening	Optimised		No formal validation necessary, methods have to follow the OECD principles for the validation of QSARs for regulatory purposes
DEREK	Hepatotoxicity	Hazard identification	Optimised	Not quantitative – predicts potential hepatotoxicity (yes/no answer)	Formal validation not necessary
DEREK	DEREK hERG channel inhibition – cardiotoxicity	Hazard identification	Optimised	Not quantitative – predicts potential hERG inhibition (yes/no answer)	Formal validation not necessary
LAZAR (Maunz and Helma 2008)	Predicts MRTD for chronic toxicity **	Prioritisation/ screening	Optimised	Developed using data on pharmaceuticals from clinical trials	Formal validation not necessary
Garcia-Domenech et al. (2006)	Predicts LOAEL for chronic toxicity	Prioritisation/ screening	Optimised	Major work needed to develop software for wider use	Formal validation not necessary
Mazzatorta et al. (2008)	Predicts LOAEL for chronic toxicity	Prioritisation/ screening	Optimised	Major work needed to develop software for wider use	Formal validation not necessary
Matthews et al. (2004a, b)	Predicts MRTD for chronic toxicity **	Prioritisation/ screening	Optimised	Major work needed to develop software for wider use	Formal validation not necessary

Cherkasov et al. have summarised the general conditions one or more of which are necessary for successful application of QSAR in modelling toxicity: "(i) compounds within the training set are structurally similar (i.e. congeneric), implying that a single target-mediated mechanism, even if unknown, is more likely; (ii) the toxicity endpoint being modelled is either non-target specific (e.g. narcosis in aquatic toxicity due to membrane concentration effects), or a subject to relatively well-understood chemical reactivity principles (e.g. electrophilic theory of carcinogenicity); (iii) the toxicity endpoint is linked to a well-defined molecular target (e.g. estrogen receptor) or phenotype (e.g. cleft palate malformation, or liver tumours in rats); or (iv) toxicity data are available for a sufficiently large number of diverse chemicals to capture all or most of the possible structure-activity associations, representing multiple possible adverse outcome pathways within the same dataset (e.g. genotoxicity)" (Cherkasov et al., 2014). In November 2004, the 37th OECD's Joint Meeting of the Chemicals Committee and the Working Party on Chemicals, Pesticides and Biotechnology (http://www.oecd.org/env/ehs/organisationoftheenvironmenthealthandsafetyprogramme.htm) agreed on the OECD Principles for the Validation, for Regulatory Purposes, of (Q)SAR Models. These principles are as follows:

"To facilitate the consideration of a (Q)SAR model for regulatory purposes, it should be associated with the following information:

1. a defined endpoint;

2. an unambiguous algorithm;

3. a defined domain of applicability;

4. appropriate measures of goodness-of-fit, robustness and predictivity;

5. a mechanistic interpretation, if possible."

There are numerous advantages of *in silico* methods compared with *in vitro* and especially *in vivo* approaches (Valerio, 2009; Combes, 2012):

- higher throughput
- less expensive
- less time consuming
- constant optimisation possible
- higher reproducibility if the same model is used

- low compound synthesis, laboratory equipment and facilities requirements
- potential to reduce the use of animals
- very useful for compound prioritisation
- appropriate for being incorporated into decision-trees and expert systems with the capability of predicting a wide range of endpoints and properties, including bioavailability, biodegradation and toxicity
- usually based on a mechanism of action related to toxicity endpoint
- readily amenable to being incorporated into test batteries comprising models with complementary and overlapping applicability domains

However, a range of disadvantages should be also considered toward their full acceptance by end-users (toxicologists, regulators, industry): (Weaver and Gleeson, 2008; Valerio, 2009; Combes, 2012):

- quality and transparency of training set experimental data
- transparency of the program (what is being modelled)
- descriptors sometimes confusing
- applicability domain sometimes limited or not clear
- complex terminology and poorly understood procedures sometimes used
- ADME features, especially metabolism, not taken into account
- carcinogenicity prediction does not work on non-genotoxic compounds

Within the AOP continuum, the level of application of the predictive models is a function of: (i) their inherent uncertainties rooted in the quality of the experimental data and the limitations of the particular *in silico* approaches and (ii) the level of the confidence in the AOP – e.g. the presence and the relevance of scientific evidence supporting each event (**Figure 9**)

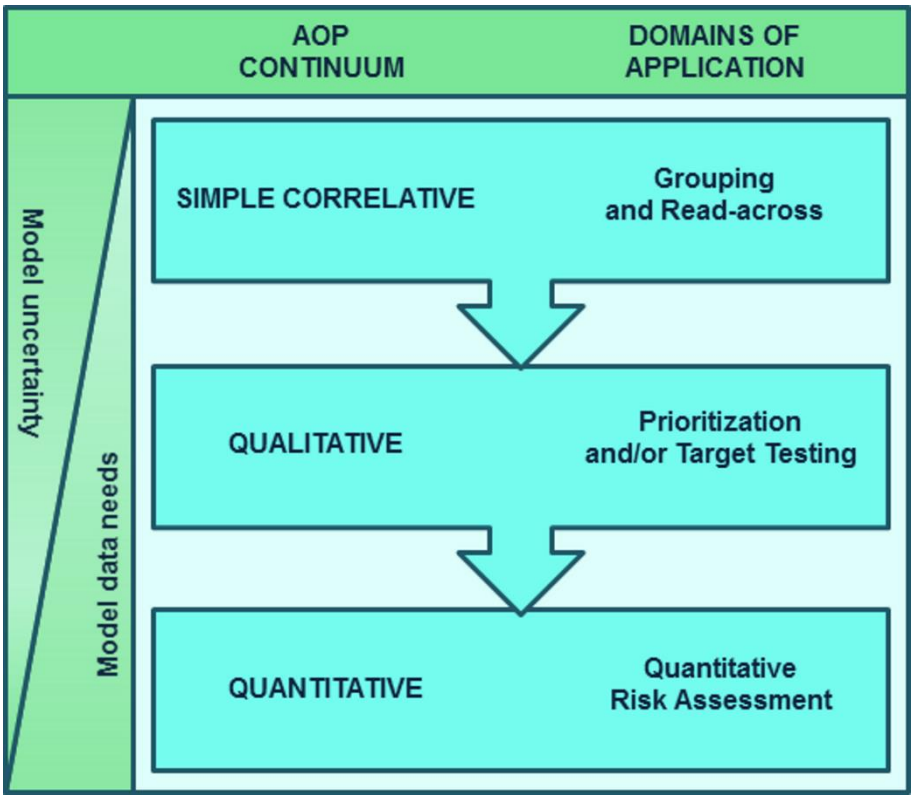

Figure 9. Domains of application of the predictive models according to the matrix uncertainty/data requirements in relation to the AOP continuum (adapted from Bal-Price, et al., 2015).

While the (Q)SAR modelling approaches (**Figure 8**) are widely used in the field of predictive toxicology (ENV/JM/MONO(2007)2; ECHA, 2008), the application of MM techniques for such needs is still in its infancy, albeit its well established role in drug design. Computer aided drug design has extensively exploited MM for more than three decades, saving resources and time by directing the synthesis of highly selective, specific and potent ligands of particular therapeutic targets. Such strategy generally involves exploration of key intermolecular interactions which are central for both therapeutic and toxic effects. That explains why MM approaches have also proved helpful in estimating potential toxicity related to ligand-dependent dysregulation of key biomolecules (nucleic acids or proteins) crucial for downstream metabolic/signalling pathways. Therefore, at the interface of drug discovery and risk assessment, we may find common molecular mechanisms and apply unified *in silico* techniques. However, a number of differences in goals, chemical spaces and tasks have to be overcome for the successful transfer of MM approaches toward solving safety issues.

While the aim of drug discovery is to screen for a molecule with well characterised target, mode of action and desired activity, risk assessment is expected to evaluate more complex, sometimes mixed and less well understood toxic outcomes, considering both exposure and various interaction mechanisms in the context of possible chemical initiators. Moreover, the span of the chemical-activity domain is a function of the mode of action (therapeutic or adverse) to be modelled, which means that the complex and often cross-related adverse effects suggest a larger spectrum of structures, range of activities and may depend on strong or weak interactions with targets in both a specific and a nonspecific manner. The focus of such expertise shifts from reducing the number of molecules incorrectly predicted as potential drug candidates (false positives) toward narrowing the pool of harmful chemicals that are underestimated (false negatives). Yet, the main difference is the ultimate purpose of the screening approaches, e.g. lead generation and optimisation in the rational drug design versus mechanism elucidation, prioritisation, and safety assessment in the predictive toxicology (Cherkasov et al., 2014; Rabinowitz et al., 2008).

1.2. Peroxisome proliferator-activated receptor γ (PPARγ) and non-alcoholic fatty liver disease (NAFLD)

1.2.1. Hepatotoxicity and NAFLD

The better assessment of repeated dose toxicity in hepatic, cardiac, renal, neuronal, muscle and skin tissues implies great research efforts (Landesmann et al., 2012; Adler et al., 2010). Among them hepatotoxicity is an endpoint that has recently drawn significant interest (Hengstler et al., 2012; Vinken et al., 2012).

Liver is a frequent target for toxicity as it is central in the metabolism of the xenobiotics and thus is highly exposed to many potentially toxic substances. It is also responsible for the maintenance of the whole body lipid homeostasis, meeting the energy demands of the extra-hepatic tissues. Therefore, it is important to note that its primary function is fat redistribution in contrast to the adipose tissue (another key organ related to lipid exchange), which is mainly involved in the storage of fatty acids (**Figure 10**).

Direct hepatocyte damage, hepatic tumour, and/or accumulation of lipids or phospholipids (fatty liver disorder) are common reasons for liver injury and thus important hepatotoxic endpoints. The NAFLD is a medical condition which includes non-alcoholic fatty liver (NAFL or liver steatosis) and non-alcoholic steatohepatitis (NASH) and may progress to fibrosis, cirrhosis and hepatocellular carcinoma (HCC) (**Figure 11**) (Sass et al., 2005**;** Bedogni et al., 2010). As this pathology is a common cause of chronic liver injury, its pathogenesis is of particular interest in view of the application of MoA/AOP framework to repeated-dose hepatotoxicity endpoints. NAFLD is the most common cause of liver disease worldwide, with a prevalence of 20%-40% in Western populations (Bedogni et al., 2004; Rusu et al, 2015) and between 20-30% in Europe (World Gastroenterology Organisation Global Guidelines, 2012). The prevalence increases to 58% in overweight individuals and can be as high as 98% in non-diabetic obese individuals (Machado et al., 2006). Generally, some 12-40% of the patients diagnosed with NAFL develop NASH and nearly 15% of these demonstrate progression to cirrhosis (Bhatia et al., 2012).

Disruption of the normal functionality of PPARγ by chemical initiators has been recently proposed as one of the possible MIEs related to the early manifestation of NAFLD (liver steatosis), characterised by excessive hepatic lipid accumulation (Sass et al., 2005; Landesmann et al., 2012).

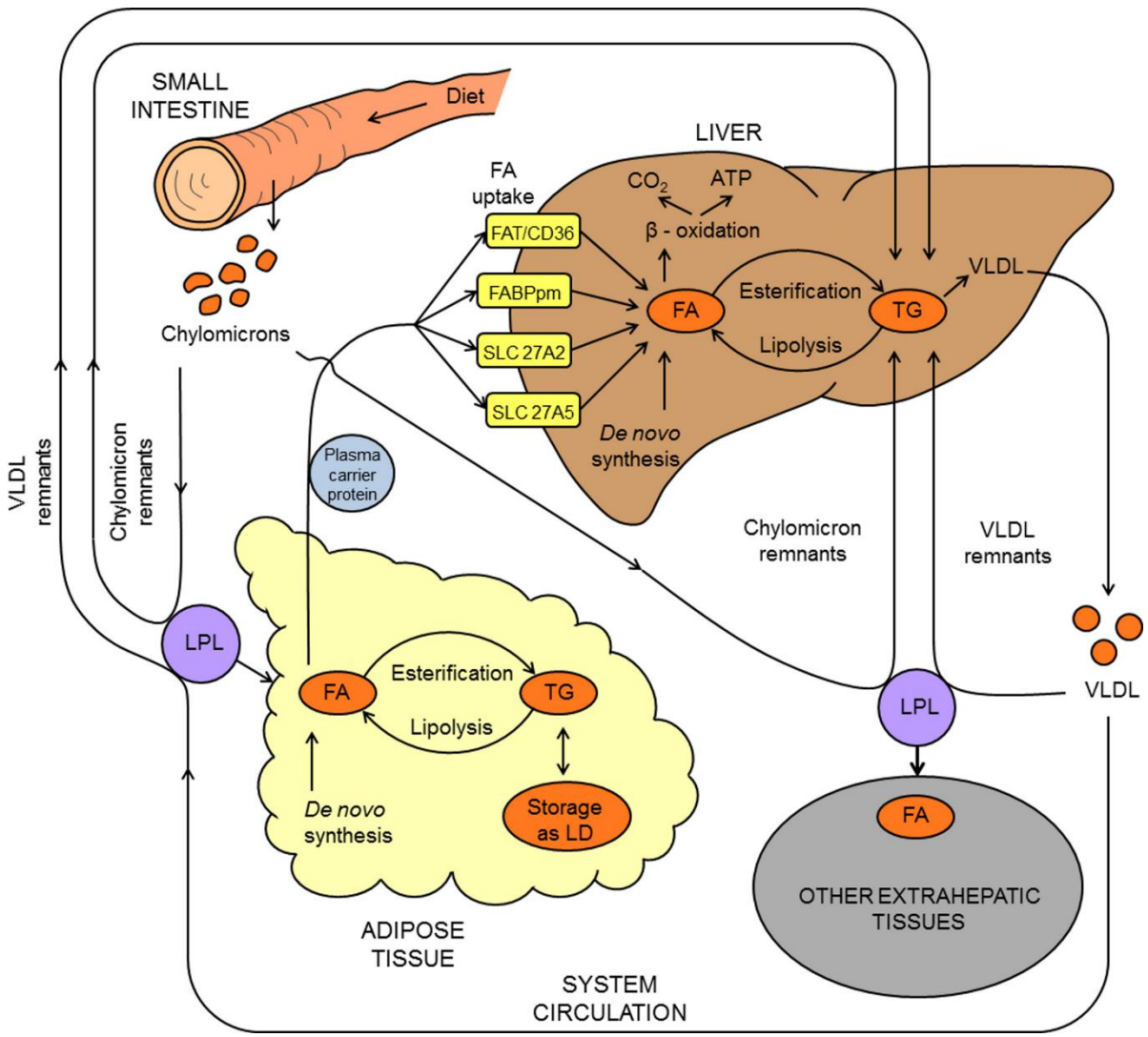

Figure 10. Overview on the complementary roles of hepatic and adipose tissues in the context of lipid homeostasis: FAT/CD36 – fatty acid translocase/cluster determinant 36; FABPpm – plasma membrane fatty acid binding protein; SLC 27A2 and SLC 27A5 – solute carrier family 27 fatty acid transporters (member 2 and member 5); FA – fatty acids; TG – triglycerides; VLDL – very low-density lipoprotein; LPL – lipoprotein lipase; LD – lipid droplet.

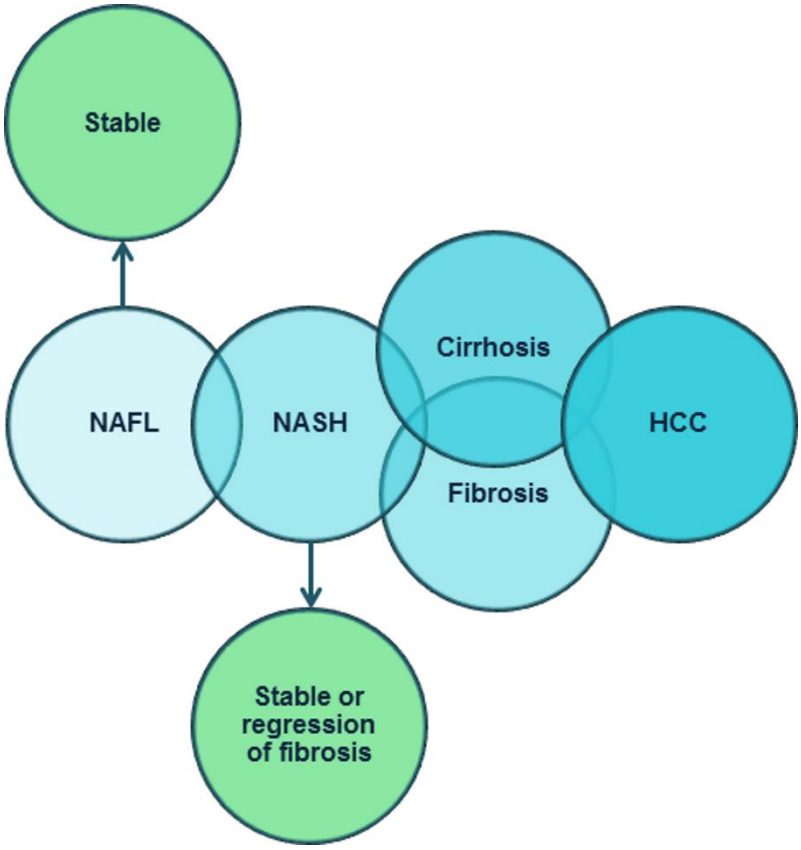

Figure 11. Progression of NAFLD (NAFL and NASH) to fibrosis, cirrhosis and hepatocellular carcinoma (HCC)

1.2.2. PPARγ

1.2.2.1.Biology of PPARγ

The PPARγ also known as NR1C3 (nuclear receptor subfamily 1, group C, member 3) is a ligand-activated transcription factor from the steroid-thyroid hormone superfamily (Nuclear Receptors Nomenclature Committee, 1999). It is a part of the PPAR family (including also the PPARα and PPARβ/δ isotypes) and is expressed mainly in white and brown adipose tissue but also in intestines, liver, kidneys, retina, immunologic system (bone marrow, lymphocytes, monocytes and macrophages) and muscles (to a lesser extent). PPARγ is central in the regulation of crucial cellular pathways related to adipogenesis (adipocyte proliferation and differentiation), lipid and glucose homeostasis, inflammatory responses, vascular biology and placental development (Virtue and Vidal-Puig, 2010; Azhar, 2010; Fournier et al., 2007.; Grygiel-Górniak, 2014; Brown and Plutzky, 2007; Ahmadian et al., 2013). While several transrepression strategies have been reported for the genomic control of the adaptive inflammatory responses (Luconi et al., 2010), the PPARγ-mediated transactivation of genes associated with lipid transport, metabolism, storage, and adipogenesis is governed by a well-defined single mechanism (Costa et al., 2010; Luconi et al., 2010). The latter involves heterodimerisation with another nuclear receptor, the retinoid X receptor alpha (RXRα), DNA binding at the promoter regions of target genes and stabilisation of the active PPARγ conformation by diverse endogenic lipid metabolites, including eicosanoids and fatty acids or synthetic agonists like rosiglitazone (**Figure 12**) (Gampe et al., 2000; Chandra et al., 2008; Costa et al., 2010;;). Thus agonist-induced corepressor dissociation, accompanied by the permanent exposure of the coactivator binding surface, permits coactivator recruitment necessary for transcription initiation (Nolte et al., 1998; Brown and Plutzky, 2007; Batista et al., 2015).

The PPARγ 2 isoform, predominantly expressed in adipocytes, has thirty amino acids more at the N-terminus than PPARγ 1, and it is available in multiple tissues, including liver (Ahmadian et al., 2013; Chandra et al., 2008). However, the two isoforms bear the common domain structure of the nuclear hormone receptors with an N-terminal AF-1 (activation function 1) domain, involved in the interaction with cofactors and the ligand-independent transactivation; a DBD (DNA binding domain), which is highly conserved among nuclear receptors; a hinge region with high flexibility, which guarantees nuclear localisation and cofactor docking; and a

C-terminal LBD/AF-2 (ligand binding domain/activation function 2), which participates in the ligand-binding, ligand-dependent transactivation, coactivator recruitment and corepressor release (**Figure 13**) (Azhar, 2010; Ahmadian et al., 2013).

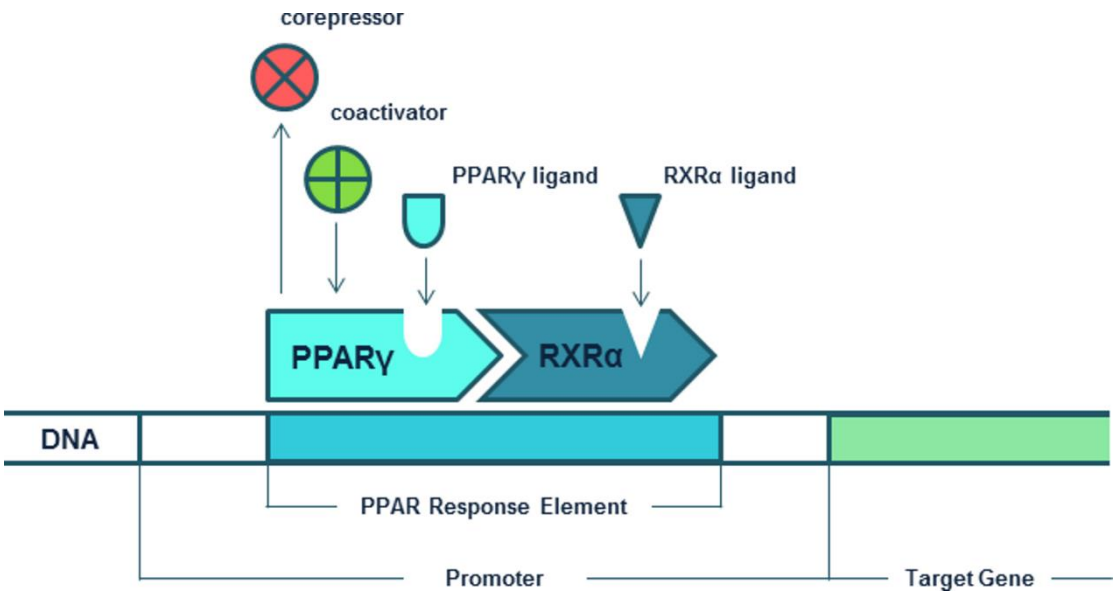

Figure 12. The mechanism of PPARγ-mediated transactivation.

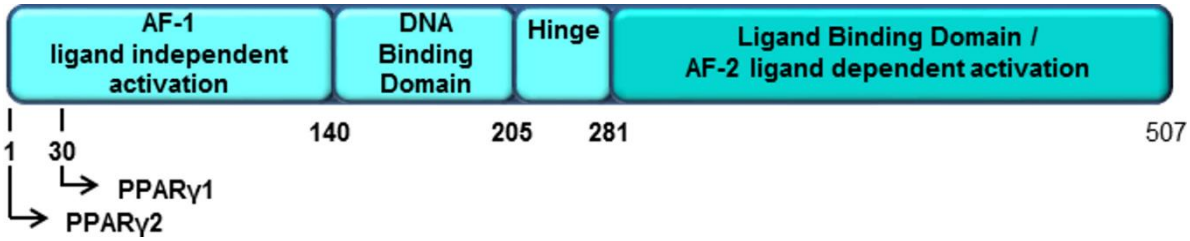

Figure 13. PPARγ functional domain organisation: AF1 – activation function domain 1, DBD – DNA-binding domain, hinge, LBD – ligand-binding domain, AF2 – activation function domain 2.

1.2.2.2.PPARγ ligands and NAFLD

The most notable natural PPARγ ligands are eicosanoids and related compounds, including lipoxygenase (LOX) products – hydroxyoctadecadienoic acids (9- and 13-HODE) and 15-hydroxyeicosatetraenoic acid (15-HETE), and cyclooxygenase (COX) products – prostaglandins (PG), e.g. PGJ2 and its derivative 15-deoxy-Δ^{12-14}-PGJ2 (15d-PGJ2), which is involved in adipogenesis, anti-tumororogenesis and modulation of inflammation (Bishop-Bailey and Wray, 2003; Nosjean and Boutin, 2002). Anti-cancer effects are reported also for PUFAs like mainly docosahexaenoic acid and eicosapentaenoic acid) (Trombetta et al., 2007; Edwards et al., 2004; Sun et al., 2005; Sun et al., 2008) while other natural PPARγ ligands are claimed to ameliorate obesity-related metabolic dysfunction (long-chain monounsaturated fatty acids (LC-MUFAs) like C20:1 and C22:1 isomers) (Yang et al., 2013) and to increase glucose uptake and insulin sensitivity (phytanic acid) (Heim et al., 2002). Triterpenoids are also among the natural PPARγ ligands. (Weng et al., 2013; Jingbo et al., 2015).

Because of its wide tissue distribution and important regulatory role, PPARγ is also an attractive therapeutic target for multiple synthetic ligands. In a systematic review on patents (2008-2012) for therapeutic modulators of PPARs, Lamers et al. proposed an overview over possible future indications of PPARγ ligands: metabolic diseases; especially hyperglycemia; cardiovascular disorders; inflammatory and auto-immune diseases: multiple sclerosis, inflammatory bowel diseases, rheumatoid arthritis; cancer; Alzheimer's disease; age-related macular degeneration; skin related disorders; addiction control (in terms of substances (alcohol, nicotine, opioids or cocaine) or addictive behaviour (kleptomania and others)) (Lamers et al., 2012). Altogether, these emphasise the increasing actuality of PPARγ ligands' safety evaluation.

Troglitazone, rosiglitazone and pioglitazone are among the most studied anti-diabetic PPARγ ligands from the thiazolidinediones (TZDs) class and their mechanism of therapeutic action is well known (Day, 1997; Grossman and Lessem, 1997). These ligands sharing a common scaffold (**Figure 14**) are known to induce conformational changes involved in the receptor activation (Berger et al., 1996). Interestingly, apart from activating PPARγ, troglitazone has been shown to induce its expression and nuclear translocation in MCF-7 cells examined by confocal microscopy (Weng et al., 2013).

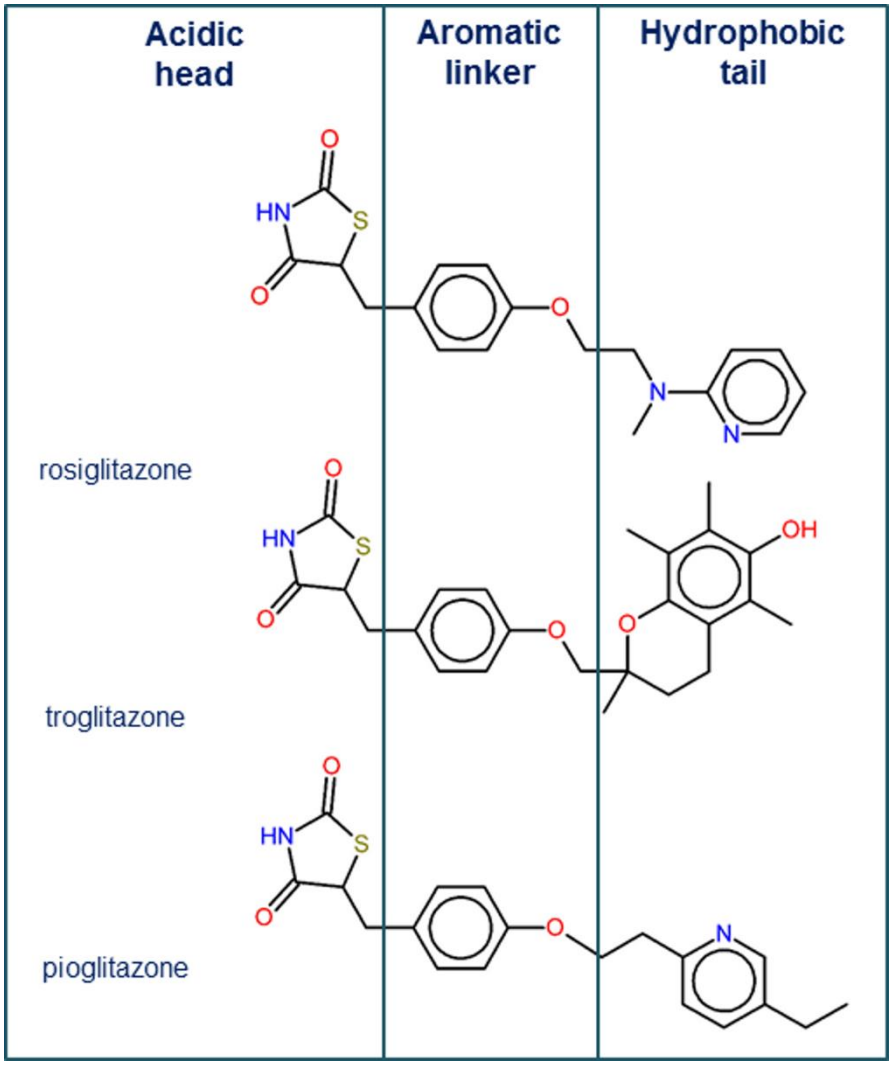

Figure 14. Main substructures within the common TZDs' scaffold (adapted from Guasch et al., 2012; Lamers et al., 2012; Scheen, 2001)

Studies show that binding to the helix12 (H12) of the receptor involves formation of key hydrogen bonds (HBs) with particular residues (Ser289, His323, His449 and Tyr473), thus driving the conformational change of H12 required for full agonist activity (Bruning et al., 2007). This molecular event lies in the PPARγ-mediated: (i) adipocyte differentiation from fibroblasts, associated with increased uptake, storage and potentially catabolism of circulating lipids and carbohydrates; (ii) production of adipose-derived factors with potential insulin-sensitising activity; (iii) increased glucose uptake and decreased gluconeogenesis in liver; (iv) increase in skeletal muscles' glucose uptake, oxidation and glycogenesis; and (v) reduction

of the circulating levels and/or actions of insulin resistance-causing adipose-derived factors (e.g. TNFα); all of which synergistically restore the glycemic balance (Berger and Moller, 2002; Grossman and Lessem, 1997; Semple et al., 2006; Chawla et al., 1994; Garg, 2004; Gee et al., 2014).

Apart from the therapeutic potential of TZDs, several adverse effects were reported, which led to the withdrawal of rosiglitazone (fluid retention/oedema, weight gain, bone loss, adverse hepatic effects and increased incidence of cardiovascular events) and troglitazone (hepatoxicity due to significant ROS-mediated damage of mitochondrial DNA) from the market (Pan et al., 2006; Moya et al., 2010; Chigurupati et al., 2015; Viccica et al., 2010; Graham et al., 2010; Nissen et al., 2010; Shen et al., 2012; Rachek et al., 2009). Pharmacological treatment of NAFLD is still evolving with vitamin E and pioglitazone being the only approved drugs as of now (Agrawal and Duseja, 2014). Therefore, the concerns for adversity underlined the necessity of additional studies treating the role of PPARγ activation in other tissues, especially in terms of the possible risk for their ligand-induced adipogenic transformation and its secondary effects at a system level (Teboul et al., 1995). Some authors report a correlation between this MIE and the development of NAFLD (Rull et al., 2014; Kus et al., 2011; Hemmeryckx et al., 2013) while others underline the therapeutic potential of receptors' modulation in reversing the progression of this disease (Le and Loomba, 2012; Rogue et al., 2014). Thus, a debate on the impact of PPARγ activation on NAFLD still exists and its double-edged role has been extensively reviewed (Tailleux et al., 2012; Ables, 2012). However, as synthetic PPARγ ligands are primarily categorised based on their transactivation activity into full and partial agonists (Kouskoumvekaki et al., 2013), the understanding that PPARγ full agonists hold more negatives than positives is out of debate (Merk and Schubert-Zsilavecz, 2012), and there is a firm tendency toward development of novel ligands: partial agonists (Chigurupati et al., 2015), multitargeted cooperative agonists (dual- and pan-PPAR) (Wang et al., 2014; Fiévet et al., 2006; Gonzalez et al., 2007), non-agonists (Choi et al., 2014; Kamenecka et al., 2011) and even antagonists of the receptor (Marciano et al., 2015). Moreover, partial PPARγ activation, as well as dual or pan-PPAR activation, has been shown to be beneficial for liver structure and functioning (Souza-Mello, 2015).

Apart from pharmaceuticals, hormone nuclear receptors are claimed as primary targets of various non-drug endocrine disrupting chemicals since their natural ligands are small, lipoidal

molecules (i.e. steroid hormones, fatty acids and their derivatives) which can be mimicked by many environmental chemicals. Among PPAR activators are xenobiotics such as: industrial and consumer chemicals, pesticides, and environmental contaminants (Rogue et al., 2010; ENV/JM/MONO(2012)23; Landesmann et al., 2012). Furthermore, PPARs signaling pathways have been considered as a separate axis in the context of endocrine disruption by exogenous chemicals, and there have been reviewed general aspects of the assessment of such dysregulation, including: PPAR transactivation reporter assays, microarray analyses of livers of exposed animals, cell-based assays (adipocyte differentiation) and apical endpoints (lipid accumulation, weight gain in chronically exposed animals) (ENV/JM/MONO(2012)23). In view of the multiple roles of PPARγ in maintaining energy and metabolism homeostasis and regarding the potency-related variations in the physiological effects of its activators, *in silico* analysis of the PPARγ full agonistic effect is of specific interest in the field of toxicology. That explains the significant efforts which have been made for understanding and predicting the binding to and activation of PPARγ.

1.2.2.3.Molecular modelling of PPARγ

In view of the increased therapeutic interest on modulation of PPARγ activity, the prevalence of the drug design related studies (Al-Najjar et al., 2011; Carrieri et al., 2013; Dixit et al., 2008; Guasch et al., 2012a; Liao et al., 2004; Lu et al., 2006; Rücker et al., 2006; Shah et al., 2008; Guasch et al., 2011; Vedani et al., 2007) over those treating predictive toxicology issues (Vedani et al., 2007) can be expected. The *in silico* studies on PPARγ are focused on 2D (Al-Najjar et al., 2011; Carrieri et al., 2013; Dixit et al., 2008), 3D (Carrieri et al., 2013; Guasch et al., 2011; Guasch et al., 2012a; Liao et al., 2004; Lu et al., 2006; Shah et al., 2008; Sundriyal et al., 2009) or 6D QSAR (Vedani et al., 2007) analysis and pharmacophore modelling (Al-Najjar et al., 2011; Carrieri et al., 2013; Lu et al., 2006; Guasch et al., 2011; Sohn et al., 2013, Sharma et al., 2014). The latter has outlined mainly hydrophobic and some hydrogen-bond donor/acceptor features, varying in the total number of pharmacophoric points (between 3 and 7), by means of ligand- and/or structure-based modelling (Markt et al., 2007; Carrieri et al., 2013; Goebel et al., 2010; Sohn et al.; 2011, Guasch et al., 2012b; Sohn et al., 2013). The pharmacophore models have been applied for SAR analysis (Pingali et al., 2008; Goebel et al., 2010; Xiao et al., 2014) or combined with a separate step of molecular docking within a virtual screening (VS) procedure (Guasch et al., 2011; Sohn et al.; 2011, Sohn et al., 2013; Fakhrudin et al., 2012). However, most of the PPARγ-related pharmacophore-based studies have been particularly applied for design of dual PPARα/γ agonists (Pingali et al., 2008) or identification/analysis of partial PPARγ agonists (Goebel et al., 2010; Guasch et al., 2011; Fakhrudin et al., 2012). This illustrates the prevailing tendency toward the discovery of novel drug-like PPARγ agonists to serve as lead molecules (Markt et al., 2008; Sohn et al. 2011, Sohn et al.; 2013, Fakhrudinet al., 2012; Guasch et al., 2012b; Guasch et al., 2013; Lewis et al., 2015). The studies targeted toward distinguishing between full and partial agonists are few. Among them are the reports of Vidović et al., who identified a partial agonist-like ligand cluster within a binding mode similarity dendrogram based on an analysis of co-crystallised PPARγ modulators (Vidović et al., 2011), Guash et al., who developed separate pharmacophore models for full and partial agonists of PPARγ, applied them for a virtual screening of natural ligands with partial agonism (Guasch et al., 2012a) and performed 3D QSAR modelling, particularly of PPARγ full agonists (Guasch et al., 2012b), and Lewis et al., who selected criteria for filtering the full agonism activity type (Lewis et al., 2015).

Therapeutic application has also been the driving stimulus for 3D QSAR modelling studies. The developed models have been based on dependent variables such as: potency (transactivation activity) – pEC_{50} (Carrieri et al., 2013; Guasch et al., 2012a; Rücker et al., 2006; Shah et al., 2008; Sundriyal et al., 2009) or binding affinity – pIC_{50} (Al-Najjar et al., 2011; Guasch et al., 2012a; Rücker et al., 2006) or pK_i (Liao et al., 2004; Rücker et al., 2006; Vedani et al., 2007) values of PPARγ agonists. It should be noted that most of the 3D QSAR models are based on pEC_{50} values. Although considered more interesting from a pharmacological point of view, potency data is hard to be modelled due to its complex nature. Transactivation activity involves not only receptor binding but also its activation and a sequence of downstream molecular events culminating with expression of a target reporter protein (Rücker et al., 2006). The last is the quantifiable event within the corresponding assay (usually Luciferase transcriptional reporter gene assay) which reflects the variations in the levels of protein expression as a function of the structural diversity of the chemical initiators. Interestingly, some authors use an additive dependent variable called "sum of biological activities" (pEC_{50}) to build 3D QSAR models for dual (γ/δ or α/δ) and pan (α/γ/δ) PPAR agonists (Shah et al., 2008; Sundriyal et al., 2009). The number of compounds within the training sets varies between 22 and 77 with training to test set (tr/ts) ratio in the range from 5:1 to 1:1. Briefly, the generalised diapasons of some reported statistical parameters are as follows: $N_{opt} = 2 – 10$, $q^2 = 0.549 – 0.744$, $r^2_{pred} = 0.150 – 0.336$. The fields most frequently involved in the developed 3D QSAR models are steric and electrostatic. In particular, there is a prevalence in the number of the pEC_{50} based models with 22 to 95 compounds (total set) and 19-28 (training sets), a tr/ts ratio from 1:1 to 3:1, q^2 between 0.549 and 0.744 and steric and electrostatic fields involved–. However, no r^2_{pred} values are reported. Among the pEC_{50} based 3D QSAR models possessing the fullest array of statistical parameters the highest q^2_{cv} is 0.633 ($SEP_{cv} = 0.017$, $N_{opt} = 5$, tr/ts = 19/4, steric and electrostatic fields) (Shah et al., 2008). Although the current pEC_{50} based models are statistically poorer compared with those involving pIC_{50} or pK_i values, predicting potency is mechanistically justified because the input data is observed in the biologically relevant *in vitro* model system of the MIE (PPARγ activation) and is directly related to the earliest downstream key events – increased levels of an array of target proteins, outlined in the developed liver AOP and discussed later.

Based on the literature review presented above, the following conclusions can be made:

1. Predictive toxicology is a new promising field that has many advantages.
2. MoA/AOP framework is a powerful approach that organises the existing knowledge and underlines both data gaps to be explored and key events to be comprehensively analysed.
3. NAFLD is a complex pathological condition that is crucial for the chronic liver injury, and thus predicting potential prosteatotic activity of chemicals is a key element in the strategy for minimising the risk for such adverse effect.
4. Full PPARγ agonists can be associated with various adverse effects, including liver toxicity.
5. *In silico* tools for modelling MIEs are pivotal for optimising safety assessment but they strongly depend on the available experimental data.
6. Currently, there is no report on PPARγ-related toxicophore (pharmacophore) model for the purposes of predictive toxicology since the focus of the pharmacophore-based approaches is the discovery of partial PPARγ or dual PPARα/γ agonists for therapeutic applications.
7. Many of the PPARγ-related 3D QSAR models published in the scientific literature address the transactivation activity as a dependent variable, albeit its complexity, and thus suffer from poorer statistical performance as compared to the binding affinity-based models. Among them only one is particularly focused on full agonists.

AIM AND TASKS OF THE PhD THESIS

Based on the conclusions above, the following aim and tasks were outlined.

AIM

The aim of this PhD thesis is the application of MoA/AOP concepts and computational toxicology methods to understand and predict the role of PPARγ ligand-dependent dysregulation in the development of NAFLD.

TASKS

1. **Development of AOP to connect in a logical sequence of events PPARγ ligand-dependent dysregulation (MIE) and NAFLD (adverse effect)**

   1.1. Collection of the existing knowledge and description of the AOP

   1.2. Evaluation of key events

2. ***In silico* study of the MIE**

   2.1. Data collection, curation and organisation of representative sets of biologically active compounds and ligand-receptor complexes for evaluation of toxicity pathways and for *in silico* prediction of biological effects

   2.2. Molecular modelling analysis of the interactions in crystallographic structures of protein-ligand complexes

   2.3. Development of an integrated *in silico* approach for chemical hazard identification and prioritisation, combining pharmacophore and 3D QSAR models to screen for potentially prosteatotic PPARγ full agonists and to predict their transactivation activity

CHAPTER 2. DATA AND METHODS

2.1. OECD principles for AOP development and evaluation

AOP development and evaluation is a continuous process which involves not only collection and analysis of scientific evidence but also AOP networking and quantification. Regarding the starting point for AOP development, two different approaches are available:

(i) a 'bottom-up approach' which uses chemistry and mechanistic information for hazard identification;

(ii) a 'top-down approach' which starts with the knowledge about the final adverse outcomes produced by well studied substances to develop chemical categories with a particular mode-of-action (Sonich-Mullin et al., 2001).

However, the OECD principles for establishing and assessing such logical sequence of events, are common for both approaches and are shown within the general workflow in **Figure 15.**

There are 5 categories for the evaluation of the weight-of-evidence (WoE) that OECD proposes when assessing the scientific value of the described key events (**Table 2**). They consider estimation of both the extent of development of the assay applied for experimental observation of the key event under evaluation and the mechanistical justification for the established causal relationship between the event and the adverse effect (ENV/JM/MONO(2013)6).

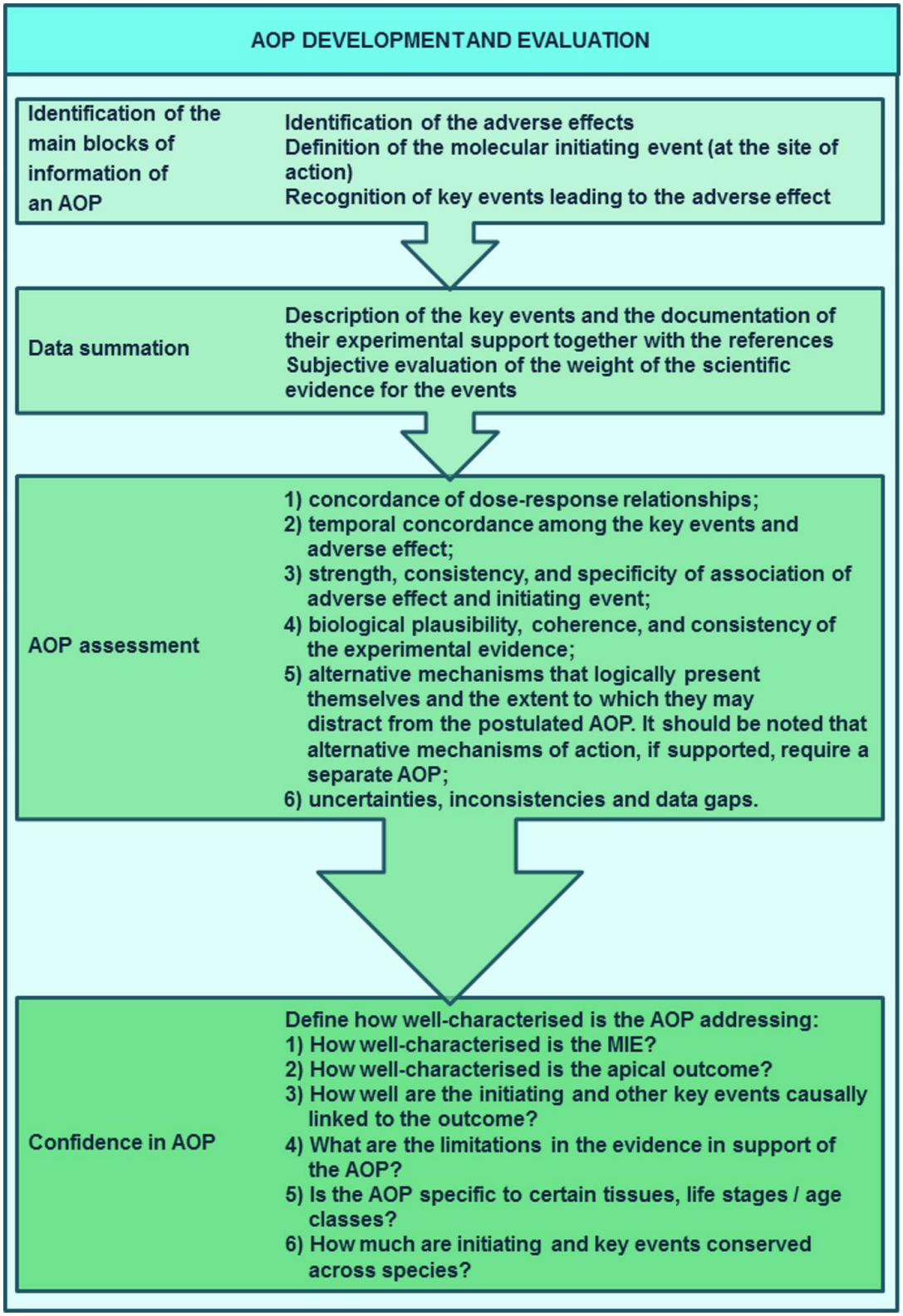

Figure 15. Main stages in developing and assessing AOPs (ENV/JM/MONO(2013)6).

Table 2. OECD classification of weight-of-evidence (ENV/JM/MONO(2013)6).

Weight-of-Evidence	Extent of Development of Assay for the Key Event / Intermediate Effect	Relationship Between Key Event and Apical Endpoint
Very Strong	OECD Guideline test or an assay that has progressed through a minimum of prevalidation. A large database of results for relevant chemicals supportive of the relationship between the key event and the apical endpoint.	Clear and unequivocal relationship and mechanistic basis for it.
Strong	A well developed assay, available in a form that could allow it to be submitted for prevalidation. A database of results for relevant chemicals supportive of the relationship between the key event and the apical endpoint.	General agreement that there is a strong relationship and a mechanistic basis for it.
Moderate	A robust and reliable method published in the peer-reviewed literature. A database of results for relevant chemicals supportive of the relationship between the key event and the apical endpoint.	An understanding that there is a relationship and a probable mechanistic basis for it.
Weak	An assay is available but is in the process of development. A small number of chemicals supportive of the relationship between the key event and the apical endpoint.	An understanding that there is some evidence of a relationship and a plausible mechanistic basis for it.
Very Weak	The key event is identified but no assay is available.	Hypothetical or literature based.

2.2. Molecular modelling approaches and QSAR

2.2.1. Collection and processing of the structural and biological data

To collect the necessary data for PPARγ ligands, the following sources were used: PDB (www.rcsb.org, Berman et al., 2000) and ChEMBL (https://www.ebi.ac.uk/chembl/; Bento et al., 2014) databases as well as the NIH PubMed system (http://www.ncbi.nlm.nih.gov/pubmed).

2.2.1.1. Biological data used

Generally, there are several main criteria in selecting the biological data regarding its quality and consistency as well as the performance of the experiment (Höltje at al., 2004):

(i) preferably identical experimental conditions
(ii) common mechanism/binding mode of the tested compounds
(iii) experimentally confirmed lack of activity where suggested
(iv) *in vitro* experimental setting only[1]
(v) at least 3 orders of magnitude span in the biological activities
(vi) exact 3D structural data
(vii) exclusion of stereochemically undefined mixtures (mixtures of enantiomers or diastereomers)

Applying all these rules is quite challenging in predictive toxicology. Often, experimental data suffers from intra- and inter-laboratory variations even when a standard protocol has been followed. Sometimes, the 3D structure of the ligands is not crystallised although there is at least one member of a reported chemical series that is deposited in the Protein Data Bank (PDB) and may serve as a template. The stereochemistry issue is also disputable as there are studies that involve corrective coefficients or rely on some mechanism-justified criteria for selecting a particular isomer instead of excluding data for racemic mixtures.

---

[1] *Achieving real equilibrium is suggested only for in vitro experiments since all other test systems undergo time-dependent changes, being cross-related with other biochemical processes (e.g. membrane permeation) and affected by transport phenomena and diffusion gradients.*

In addition, OECD outlined some key principles for endpoint selection in its Guidance document on the validation of QSAR models, as follows (ENV/JM/MONO(2007)2):

1. The endpoint should be defined by providing detailed information on the test protocols which were used to generate the training set data, especially with respect to factors which impact variability, knowledge of uncertainties, and possible deviations from standardised test guidelines.
2. Differences in the protocols that experimentally measure the described endpoint should not lead to markedly different values of the endpoint.
3. Differences within a protocol (e.g. media, reagents) should not lead to differences that cannot be rationalised (e.g. impact of hardness within a fish LC50 study).
4. The chemical domain of the (Q)SAR should be contained within the chemical domain of the test protocol.
5. The endpoint being predicted by a (Q)SAR should be the same as the endpoint measured by a defined test protocol that is relevant for the purposes of the chemical assessment.
6. A well-defined endpoint should reflect differences between chemical structures.

The collected biological data used in the modelling studies (transactivation activity, EC_{50}) was additionally processed in two steps for the CoMSIA modelling:

(i) transformation to pEC_{50} values;

(ii) pEC_{50} values' selection by favouring human over animal data and calculation of the mean pEC_{50} were necessary for each of the reference compounds (farglitazar, rosiglitazone and pioglitazone) that have been tested on human and animal cell lines by different research groups.

2.2.1.2.Structure preparation

Depending on the input data, three main procedures were applied in the structures' generation:

(i) For ligands with correct IUPAC names available in the literature source, SMILES were generated through NCI/CADD SIR (http://cactus.nci.nih.gov) or University of Cambridge OPSIN (http://opsin.ch.cam.ac.uk) services.

(ii) For ligands without IUPAC names available in the source or with incorrect/unresolvable IUPAC names, SMILES codes were generated from similar structures that were modified accordingly; IUPAC names were obtained through ChemAxon's chemicalize.org service (http://www.chemicalize.org).

(iii) For ligands with the PPARγ complexes deposited in PDB, ligand structures were extracted from the complexes, they were neutralised through the Wash procedure in MOE platform v. 2014.0901, (CCG Inc., http://www.chemcomp.com), and their stereochemistry was fixed where necessary.

The data processing step involved convertion of all SMILES codes to "inchified" SMILES by Openbabel 2.3.2 (http://openbabel.org, CLI parameters: -ismi -osmi -xI), generation of InChi keys to be used as connection table names and conversion of the binding affinity and transactivation activity data to micromolar concentrations.

As explained in greater detail in **Section 3.3.2.**, a subset of 170 PPARγ full agonists fitting the requirements for modelling purposes was selected from the initial dataset. This structurally diverse subset included ligands with relative efficacy ≥ 70% and/or PDB ligands with substructures matching the features of the developed PPARγ full agonists' pharmacophore (Tsakovska et al., 2014). Detailed information regarding the ligands retrieved from PDB and used for modelling is provided in **Table S.1., Appendix A. Supplementary Material**.

The selected modelling subset of 170 ligands encompasses data reported in PDB and in the literature. Among the 15 different homologous series collected (**Table 3**):

(i) eight contain a PPARγ ligand with a crystal structure deposited in the PDB that was used as a template in structure generation;

(ii) one contains a PPARα ligand used as a template;

(iii) six do not contain resolved PDB ligands and the corresponding structures were built either directly or from structurally similar PDB ligands.

The ligands' stereochemistry was adjusted as reported in the literature sources. Racemic mixtures were not excluded from the modelling set, but S stereoisomers were used instead, since this is the commonly accepted active form (Rücker et al., 2006; Shah et al., 2008). The protonation state of the ligands, if not reported in the PDB complexes, was assigned according to the predominant forms of the structures at pH = 7.4, as explored in ACD/Labs Percepta suite 2015 (ACD Inc.). When for a given compound the calculated proportions of the protonation states equaled, the corresponding forms were suggested to coexist and thus considered as different ligands. Structure minimisation was further performed with the MMFF94s force field, including electrostatics using the MM platform MOE (MOE, v. 2014.0901).

Table 3. PPARγ ligands selected for modelling: research group, molecular scaffold, numbers and PDB identifiers. * 1[a] – Bènardeau et al., 2009; 1[b] – Grether et al., 2009; 1[c] – Kuhn et al., 2006; 2[a] – Casimiro-Garcia et al., 2008; 2[b] – Casimiro-Garcia et al., 2009; 3 – Ohashi et al., 2013; 4[a] – Otake et al., 2011a; 4[b] – Otake et al., 2011b; 4[c] – Otake et al., 2012; 5[a] – Sauerberg et al., 2002; 5[b] – Sauerberg et al., 2003; 5[c] – Sauerberg et al., 2005; 6[a] – Devasthale et al., 2007, 6[b] – Zhang et al., 2009 and 6[c] – Ye et al., 2010., 7 – Cronet et al., 2001; 8 – Gampe et al., 2000; 9 – Xu et al., 2001; 10[a] – Mahindroo et al., 2005; 10[b] – Mahindroo et al., 2006a; 10[c] – Mahindroo et al., 2006b; 10[d] –Lin et al., 2009; 11 – DOI**:** 10.2210/pdb2xkw/pdb; 12 – Ohashi et al., 2011; 13 – Kuwabara et al., 2012. Indices a, b, and c correspond to different papers of one and the same research group designated by a number.

DATA SOURCE			TEMPLATES FOR STRUCTURE GENERATION		
Research group *	**Scaffold used in the source paper**	**Ligands (number)**	**PDB complex code**	**PDB ligand code**	**Comment**
1[a]	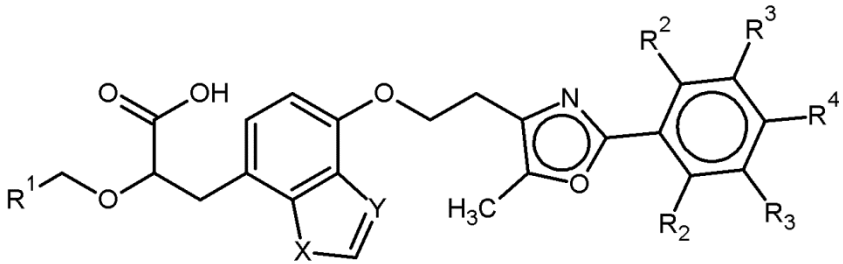	10	3G9E	RO7	

	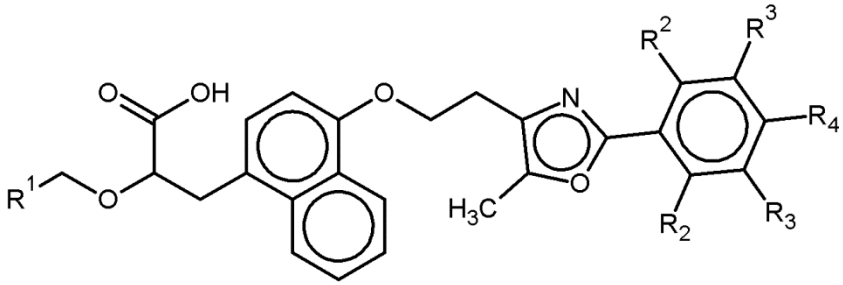			
1[b]	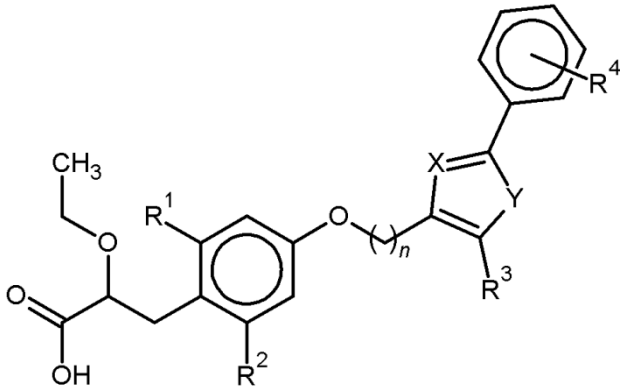	12	3FEJ	CTM

1[c]	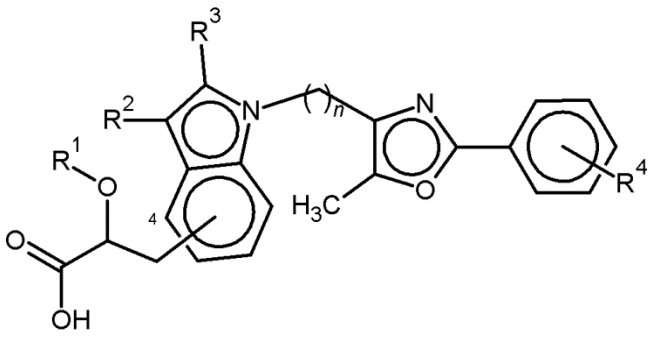	17	2GTK	208
2[a]	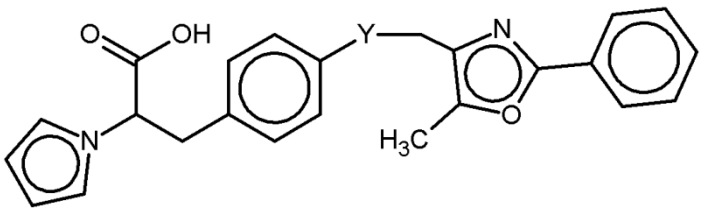	12	2Q8S	L92
	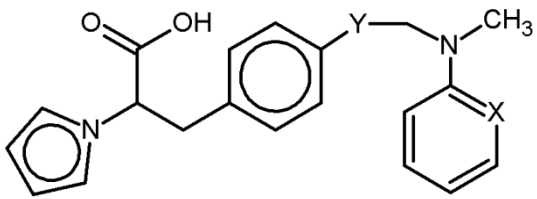			

2[b]	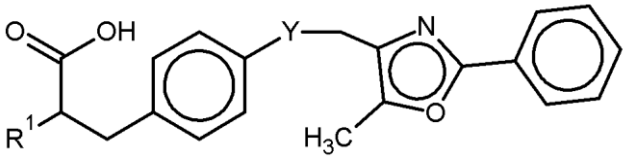	3	3IA6	UNT
3	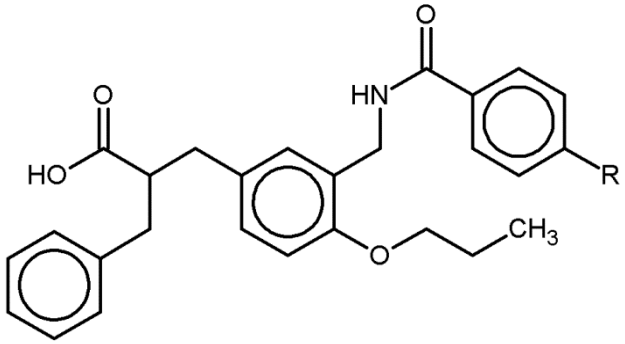	10	3VSO	EK1
4[a]	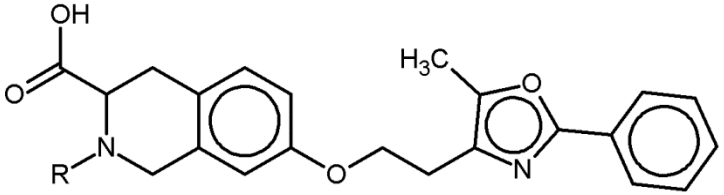	10	no	no

4[b]	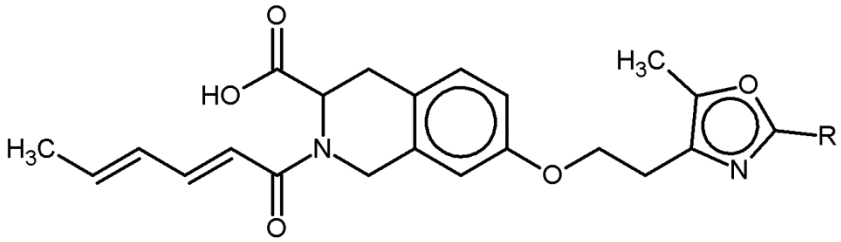	9	no	no	
4[c]	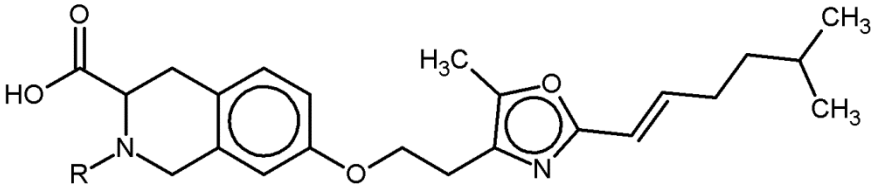	25	no	no	
5[a]	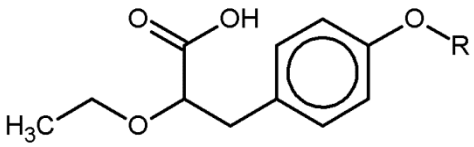	13	1KNU	YPA	
5[b]		2	no	no	1KNU/ YPA used as a template
5[c]		3	no	no	1KNU/ YPA used as a template

6[a]	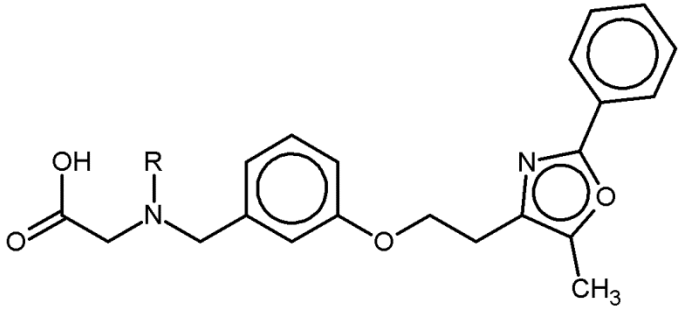	12	no	no	1FM9/570 used as a template
6[b]	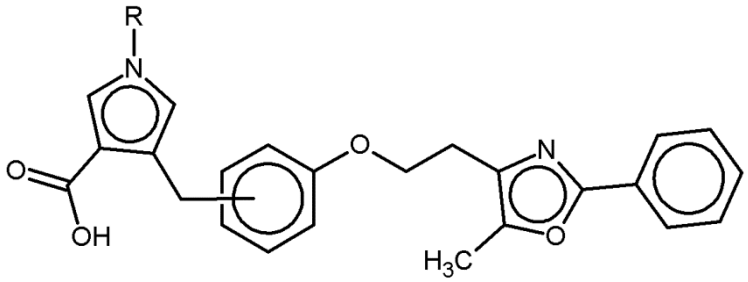	11	3BC5	ZAA	
	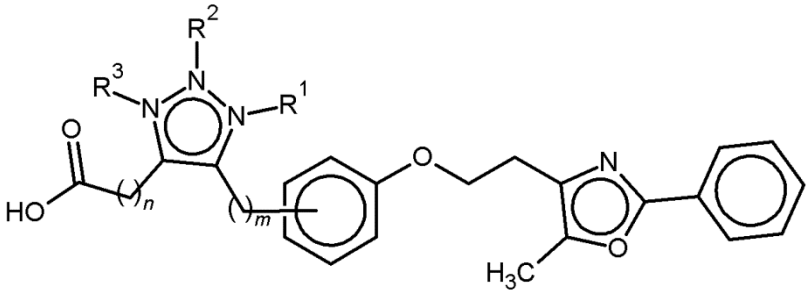				

6[c]	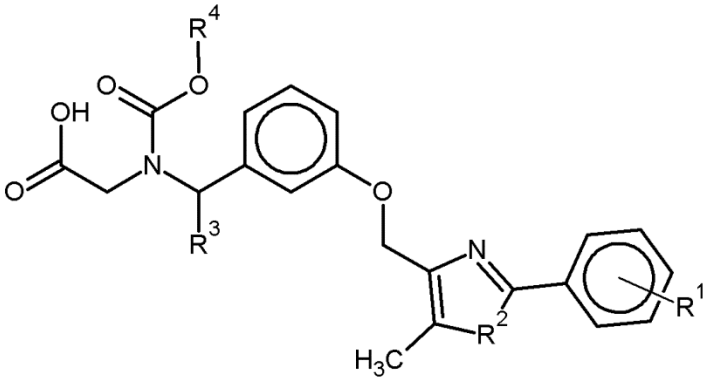	9	3KDU	NKS	NKS used only as a template, however, not included in the modelling dataset since 3KDU is a complex of PPARα
7	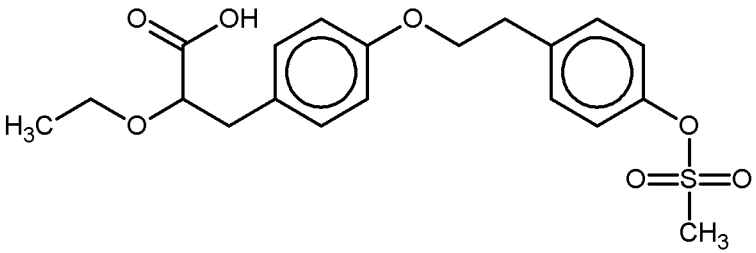	1	1I7I	AZ2	

	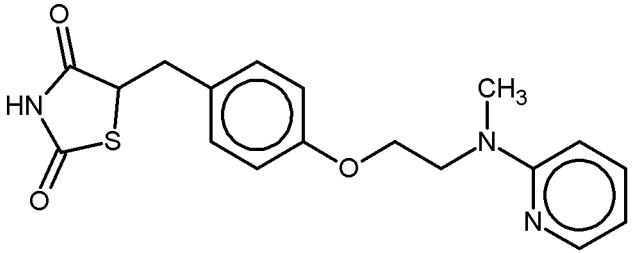	1	1FM6	BRL
8	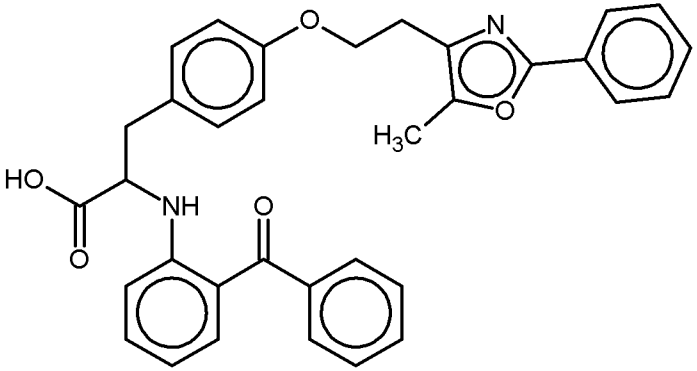	1	1FM9	570

9	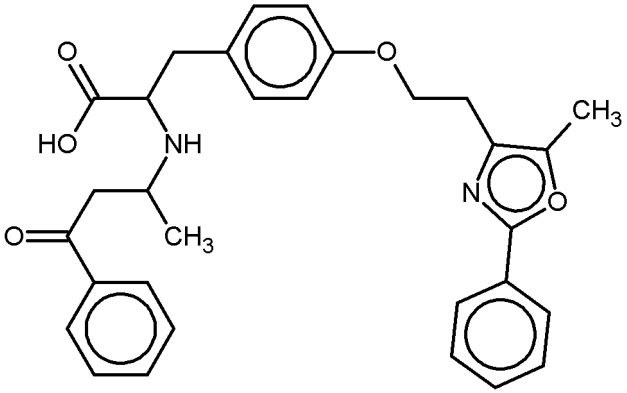	1	1K74	544
10[a]	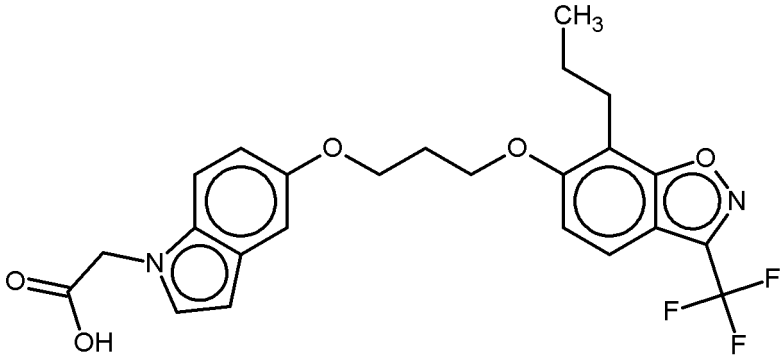	1	2ATH	3EA

10[b]	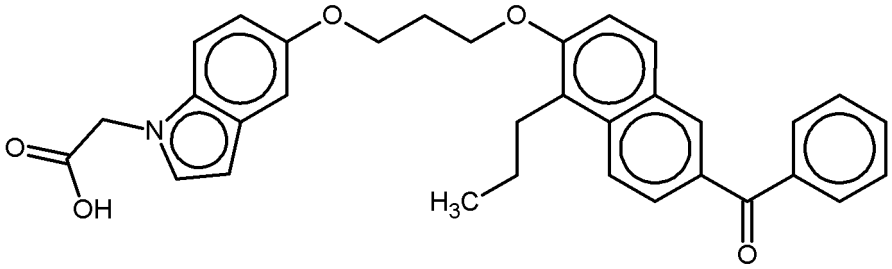	1	2F4B	EHA
10[c]	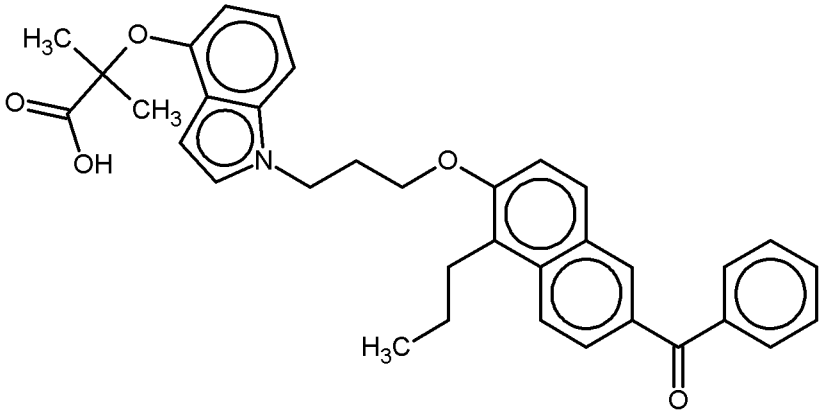	1	2HWR	DRD

10[d]	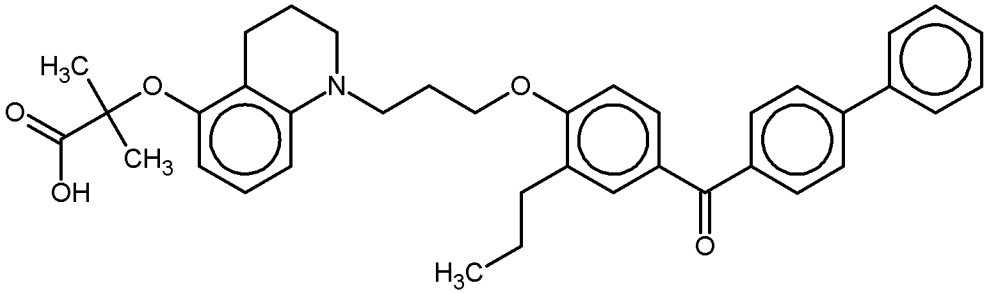	1	3GBK	2PQ
11	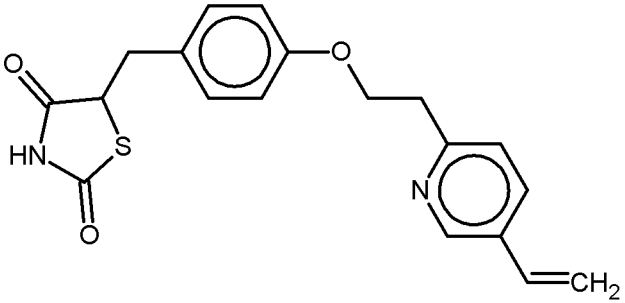	1	2XKW	PIB

12	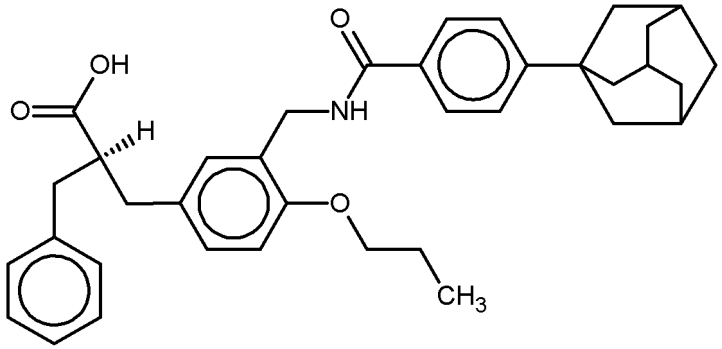	1	3AN3	M7S
	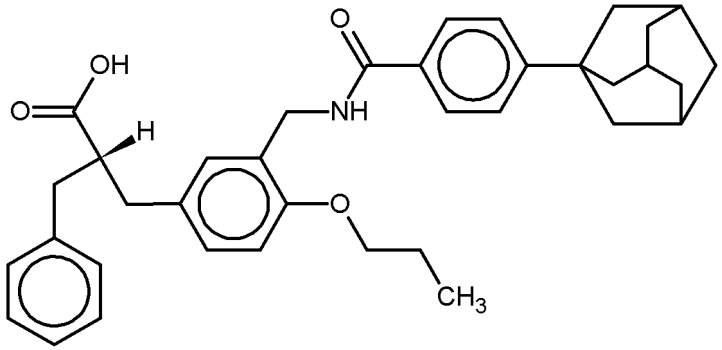	1	3AN4	M7R

13	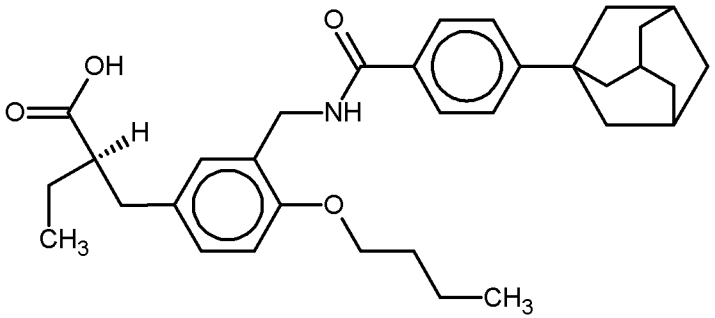	1	3VJI	J53

2.2.1.3.Protein preparation

The “Protonate 3D” tool within the MM platform of MOE v. 2014.0901 (CCG Inc.) was used to prepare the initial structures of PPARγ. That involved assignment of the correct ionisation states and addition of the hydrogen atoms in the X-ray protein structures by determining:

(i) the rotamers of –SH, –OH, –CH3 and –NH3 groups in Cys, Ser, Tyr, Thr, Met, Lys;

(ii) the ionisation states of acids and bases in Arg, Asp, Glu, Lys, His;

(iii) the tautomers of imidazoles (His) and carboxylic acids (Asp, Glu);

(iv) the protonation state of metal ligand atoms in Cys, His, Asp, Glu, *etc*.;

(v) the ionisation state of metals;

(vi) the element identities in His and the terminal amides (Asn, Gln).

Based on the generalized Born/volume integral electrostatics model within this application, an optimisation of the titration free energies of all titratable groups was performed at physiologically relevant conditions (temperature: 310 K; pH = 7.4; ion concentration: 0.152 mol/L).

2.2.2. Protein-ligand interactions

2.2.2.1. General principles

Molecular interaction and recognition are the primary events governing each biochemical process within a cell or an organism. In particular, complex formation between small molecules and their macromolecular targets is a frequent initiating event related to chemical-induced organ toxicity. The reversibility of receptor-ligand (*RL*) complex formation is rooted in the non-covalent nature of the driving interactions and is characterised by the rate constant of the forward reaction $k_{forward}$ and the rate constant of the backward reaction $k_{backward}$:

$$R + L \underset{k_{backward}}{\overset{k_{forward}}{\Leftrightarrow}} RL \qquad \text{Eq. 1}$$

A simplified illustration of such a relationship, disregarding migration of a ligand to the active site, activation of second-messenger transduction processes or interaction with the solvent and additional molecules, is presented in **Figure 16**.

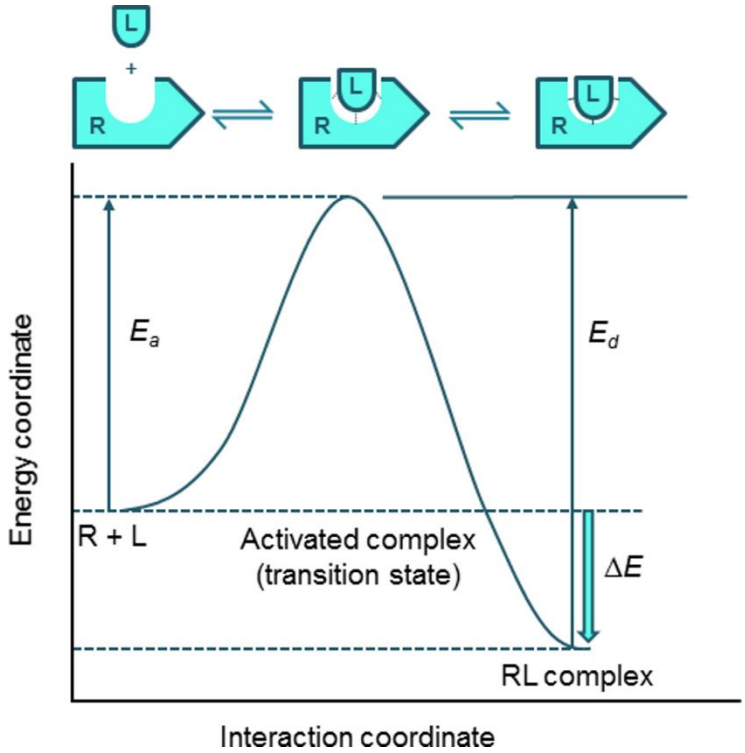

Figure 16. Interaction-energy diagram for the reversible receptor-ligand complex formation: ΔE – overall change in energy for the interaction; ΔE_a and ΔE_d – activation energies for the association and dissociation processes, respectively; *R* – receptor; *L* – ligand; *RL* – receptor-ligand complex. Adapted from Raffa et al., 2003 and Schneider et al., 2008.

The thermodynamical aspect of the receptor-ligand interactions is centred on the change in the free energy formation of the ligand-receptor complex ΔG as defined by Gibbs in 1873 and the general principle that a spontaneous occurrence of a receptor-ligand complex is possible if its overall energy level is lower than that of the free molecules. The "Gibbs energy" summarises the free energy changes associated with the electrostatic, non-polar and hydrophobic interactions which occur between the two molecules, and entropy costs associated with the interaction and is given by the Gibbs-Helmholtz equation:

$$\Delta G = \Delta H - T\Delta S \qquad \text{Eq. 2}$$

with ΔG giving the change in the free energy of binding, T – the temperature in Kelvin and the enthalpic and entropic contributions to ΔG designated by ΔH and ΔS, respectively. The change in enthalpy (ΔH) indicates the molecular forces involved in the receptor-ligand interaction characterised by formation and disruption of: hydrogen-bonds; electrostatic (e.g. ionic, polar); arene-arene (both electrostatic and hydrophobic) and dispersive (vdW) interactions (**Table 4**) (Schneider et al., 2008; Andrews, 1993).

Table 4. Non-covalent intra- and intermolecular interactions; r – distance separating the interacting particles

Type of the interaction / effect	Strength	Strength proportional to
ion – ion	Very strong	r^{-1}
ion – dipole	Strong	r^{-2}
vdW dipole – dipole	Moderately strong	r^{-3}
vdW ion – induced dipole	Weak	r^{-4}
vdW dipole – induced dipole	Very weak	r^{-6}
vdW London dispersion forces (induced dipole – induced dipole)	Very weak	r^{-6}
hydrogen bond	Moderately strong	the electronegativity of the H-donor and the H-acceptor
hydrophobic	Moderately strong	the size of the lipophilic surface area shed by the ligand in the complex

- The electrostatic interactions include ion-ion, ion-dipole and dipole-dipole interactions. Although the ion-ion interactions seem to be the most important for the ligands in view of the predominantly anionic (carboxylate, phosphate) or cationic (e.g. aliphatic amino) forms of their functional groups at physiological pH, the weaker ion-dipole and dipole-dipole interactions are more prevalent. This is due to the wider occurrence of bond, group or molecule dipole moments resulting from electronegativity differences. The inductive interactions (ion-induced dipole and dipole-induced dipole) are commonly characterised by intra- or intermolecular charge redistribution. While the first can be related either to the ligand or the receptor molecule (polarisation), the second reflects the charge transfer between the ligand and the receptor. Special cases of electrostatic interactions are the cation – π, and π – π (arene – arene) interactions.

- The dispersive interactions (London forces) occur between non-polar molecules, particularly at short intramolecular distances, and are rooted in the dipole moments generated from the movement of electrons around the nuclei. The total contribution of these interactions can be very significant, albeit their individual weakness, and is generally governed by attractive dispersion and short-range repulsive forces.

- The HB donor/acceptor interactions in most cases are best described as electrostatic ones. The most significant biologically relevant hydrogen-bond interactions involve the oxygen and nitrogen atoms of the carboxyl, hydroxyl, carbonyl, amino, imino and amido groups participating in the establishment of the tertiary structure of proteins and nucleic acids as well as in the complex formation with their corresponding ligands. Carboxylates are better HB acceptors than amides, ketones or ionised carboxyls, while substituted ammonium ions are better HB donors than unsubstituted ammonium ions or trigonal donors. This is explained by the fact that the greater is the electrostatic character of the groups sharing the hydrogen atom, the stronger is the HB formed (Andrews, 1993).

- The hydrophobic effect is a major driving force of receptor-ligand associations. The change in entropy (ΔS), which reflects the change in the degrees of freedom ("uncertainty") of the molecular system, is governed by this effect. Generally, the loss of degrees of freedom of the receptor and the ligand during complex formation is

countered by an increase in entropy, resulting from the release of receptor- and ligand-bound water molecules into the bulk solvent. Since the water molecules cannot form polar contacts with the hydrophobic protein surfaces, they are forced to adopt an entropically unfavourable ordered structure. The release from these strained structures significantly increases their degrees of freedom (ΔS, entropic contribution) and hydrogen bonding with bulk water molecules (ΔH, enthalpic contribution), which additionally contributes to an overall negative change in free energy. The contribution of the hydrophobic effect in many cases is approximately proportional to the size of the lipophilic surface area shed by the ligand in the complex (Schneider et al., 2008).

ΔG is related to the binding constant K_i by the equation:

$$\Delta G = -RT \ln K_i \qquad \text{Eq. 3}$$

with R being the gas constant. This relation links the free energy change to the aforementioned rate constants ($k_{forward}$ and $k_{backward}$) since K_i is a synonym of the dissociation constant K_d and is inversely related to the equilibrium constant K_{eq}:

$$K_{eq} = \frac{k_{forward}}{k_{backward}} = \frac{[RL]}{[R]*[L]} \qquad \text{Eq. 4}$$

$$K_i = K_d = \frac{[R]*[L]}{[RL]} \qquad \text{Eq. 5}$$

The biochemical competition assays are among the most frequent experimental approaches for estimation of the dissociation constant K_d of a ligand. Generally, this involves measuring the displacement of a known reference ligand from the receptor where the stronger displacement is related to higher binding affinity of the tested compound (hence the term “inhibition constant”, K_i). Typically, radioactive reference ligands are used (e.g. in a scintillation proximity assay), or the displacement is coupled to a detectable fluorescence signal (e.g. in a fluorescence polarisation binding assay). Several concentrations of the test compound are used to determine the one at which the competing ligand displaces 50% of the specific binding of the reference ligand (e.g. the IC_{50} value) (**Figure 17**).

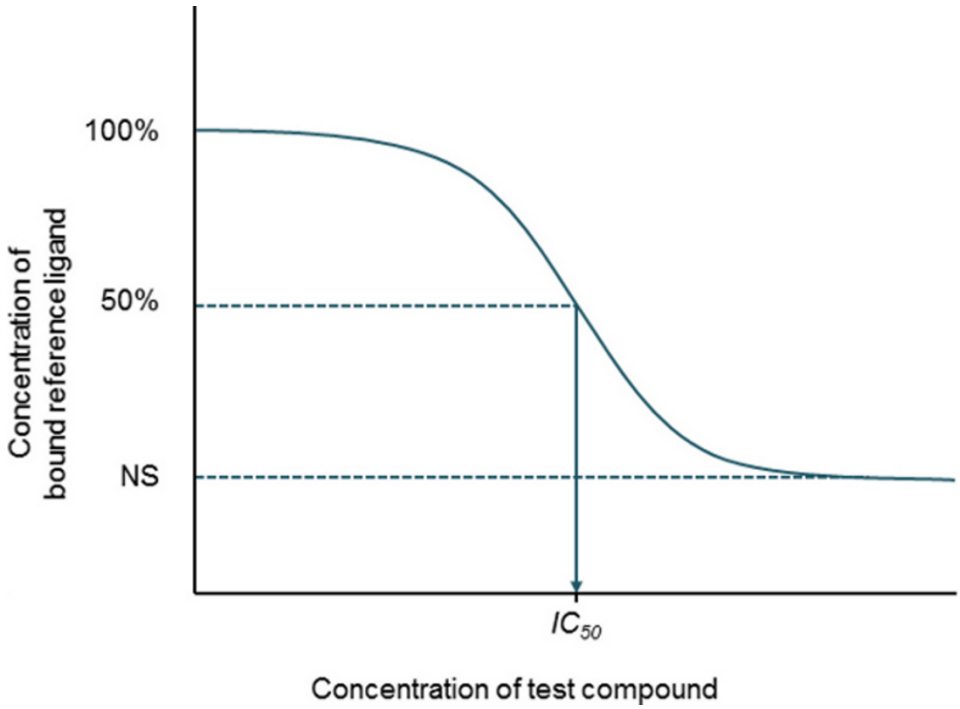

Figure 17. Competition curve for a test ligand in a receptor binding assay. The IC_{50} value is obtained from the turning point of the curve. The fraction of the reference ligand that is not displaced by the test ligand is designated as non-specific binding (NS). Adapted from Schneider et al., 2008.

The Cheng-Prussoff equation is used in the estimation of the K_i of the test compound based on the $K_d^{reference}$ value for binding of the reference ligand and the IC_{50} determined in the binding assay:

$$K_i = \frac{IC_{50}}{1 + \frac{[L]}{K_d^{reference}}} \qquad \text{Eq. 6}$$

where $[L]$ is the concentration of the reference ligand used in the assay. However, these apparent K_i values may not reflect the "true" K_i values of the tested compounds (Schneider et al., 2008).

According to the classical receptor theory developed by Clark (1933), it was assumed that the effect of a drug was proportional to the fraction of receptors it occupied in such a manner that occupation of all receptors was necessary for achieving the maximal effect.

$$R + L \underset{k_{backward}}{\overset{k_{forward}}{\Leftrightarrow}} RL \rightarrow effect \qquad \text{Eq. 7}$$

Adopting such understanding for the receptor-ligand interactions would produce the following equation:

$$E = \frac{E_{\max} * [L]}{K_d + [L]} \qquad \text{Eq. 8}$$

where E is the effect, E_{max} is the maximal effect, $[L]$ is the concentration of the free ligand and $[L]/(K_d + [L])$ is the fraction of the receptors that is occupied by ligand.

Based on the linear relationship between occupancy and response, three main cases can be considered:

(i) $[L] << K_d \rightarrow E = E_{max} * [L] / K_d$ Eq. 8.1

(effect depends on [L] linearly)

(ii) $[L] >> K_d \rightarrow E = E_{max}$ Eq. 8.2

(effect does not depend on [L])

(iii) $[L] = K_d \rightarrow E = E_{max} / 2$ Eq. 8.3

According to case (iii), the concentration at which the ligand is half-maximally effective (pEC_{50}) is equal to its pK_d (**Figure 18**).

For the nuclear receptors that are transcriptional regulators of target genes, the estimation of EC_{50} is often performed by transactivation reporter gene assays (for example, Luciferase assay), measuring the transactivation activity of the ligand. The resulting sigmoidal log dose-effect curve is the most helpful graphical representation for comparing the relative potencies and efficacies of agonists (**Figure 19a**).

In reality, however, the relationship occupancy-response is non-linear since signal amplification is triggered in-between as a cascade of intermediate molecular events. As a result, the observed EC_{50} for response is significantly shifted to the left of the K_d for receptor occupancy (**Figure 19b**).

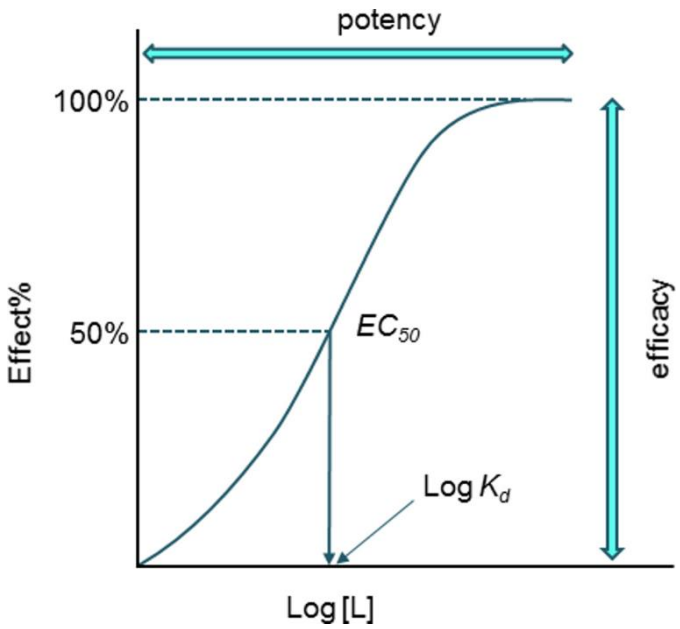

Figure 18. A log[*L*]-response curve reveals a sigmoidal relationship between occupancy and response, such that, in the absence of negative or positive cooperativity, 10% to 90% response occurs over approximately a 100-fold range of agonist concentration, "centred" about the EC_{50} for the agonist (Ross, 1996).

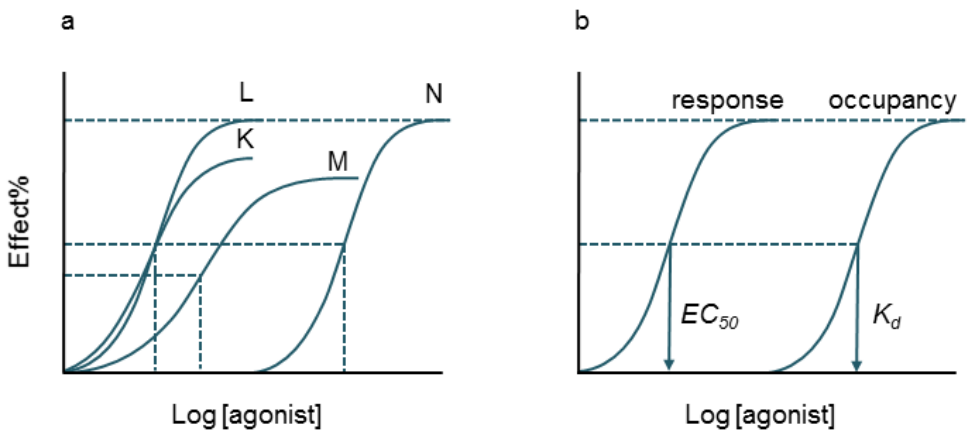

Figure 19. Agonists vary in terms of potency and efficacy. (a) Ligands *K* and *L* are equal in their potency, which is superior to that of ligands *M* and *N*. At the same time, ligands *L* and *N* are more efficacious than *K* and *M*, which are partial agonists. (b) Because occupancy is often not directly related to response and signal transduction cascades between receptor binding, effector activation, and the observed response amplifies the initial stimulus, dose-response curves often fall to the left of the receptor-occupancy profiles. Adapted from Ross (1996).

The nonlinear relationships were addressed first by Ariens (1954), who introduced the term "intrinsic activity" to describe the observation that some drugs did not elicit a maximal response, albeit the apparently maximal receptor occupancy:

$$E = \alpha[DR] \qquad \text{Eq. 9}$$

where *E* is the effect, *α* – the intrinsic activity and *DR* – the concentration of the drug-receptor complexes.

In order to reflect the property of an agonist, Stephenson (1956) introduced the term efficacy and further advanced the concept to the following relationship:

$$R' = f(S) \qquad \text{Eq. 10}$$

$$S = ey \qquad \text{Eq. 11}$$

where R' is the response of a tissue to some stimulus (S) which depends on the efficacy (e) and the fractional receptor occupancy (y).

It is postulated that the agonist's potency is determined by its efficacy, together with the affinity for its receptors. Moreover, the drug's characteristics, the properties of its receptor and of the target tissue (e.g. drug's distribution and metabolism, tissue-specific levels of the receptor, coupling the receptor occupancy to the final response) have their contributions to the variations in the ligands' effects in different tissues. The current form of the equation is:

$$E = f(S) = f\left(\frac{\alpha * [L]}{K_d + [L]}\right), \qquad \alpha = \frac{E\max_{agonist}}{E\max_{strongest\_agonist}} \qquad \text{Eq.12}$$

where intrinsic activity (α) is equal to the relative efficacy of the ligand compared to the reference compound, thus being a convenient criterion for classification of full agonists, partial agonists and antagonists (**Figure 20**).

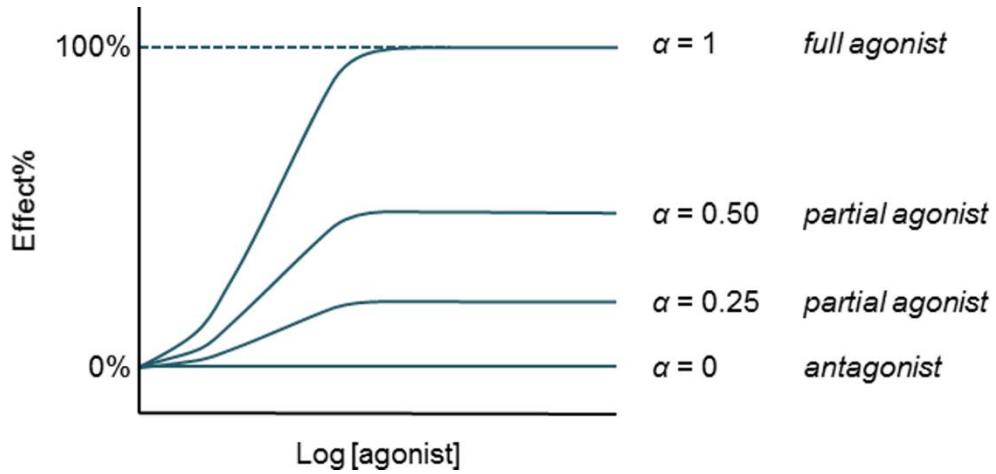

Figure 20. Application of intrinsic activity for discriminating between ligands with different types of action.

However, the relative efficacy calculated in percents (%max) is the most often reported value for a series of tested ligands. Since IC_{50}, EC_{50} and %max values are relatively easy to obtain, these are determined in first-pass screening campaigns and K_i values are determined during later stages.

2.2.2.2.Analysis of the receptor-ligand interactions

The PPARγ-ligand complexes were analysed using the MOE tool "Ligand Interactions" (MOE, v. 2014.0901). This application allows for identification of a number of interactions (hydrogen bonds, salt bridges, hydrophobic interactions, cation-π, sulphur-lone pair, halogen bonds and solvent exposure) between the ligand and the receptor-interacting entities as HB residues, close, but non-bonded residues (approaching the ligand but not having any strong interactions, i.e. HBs), solvent molecules and ions. The probability criteria considered in the identification of the HB donor-acceptor interactions were based on a large training set. The default HB scores (in percentages) and HB directionality were applied.

2.2.3. Pharmacophore modelling

2.2.3.1.Pharmacophore concept – general view

In 1909 Paul Ehrlich used the term *pharmacophore* in the sense of "a molecular framework that carries (*phoros*) the essential features responsible for a drug's (*pharmacon*) biological activity" (Ehrlich, 1909). Therefore, the pharmacophore could be considered as a 3D model describing the type and location of the binding interactions between a ligand and its target receptor. According to the IUPAC definition: "A pharmacophore is an ensemble of steric and electronic features that is necessary to ensure the optimal supramolecular interactions with a specific biological target and to trigger (or block) its biological response.", where the term *supramolecular* stands for non-covalent (Wermuth et al., 1998). The pharmacophoric features characterise the nature of a particular property rather than be associated with a specific chemical structure, thus one feature may integrate different chemical groups sharing the same property, for example: hydrogen bond donor, hydrogen bond acceptor, hydrophobic, and positively and negatively ionised areas.

Pharmacophore modelling involves generation of a pharmacophore hypothesis for the binding interactions in a particular active site and could be ligand-, target- or complex-based, depending on the type of the available data (**Figure 21**). The computerised representation of a hypothesised pharmacophore (pharmacophore query) could be used to screen virtual compound libraries for novel ligands, to filter conformer databases, e.g. output from molecular docking runs, for biologically active conformations (MOE, v. 2014.0901).

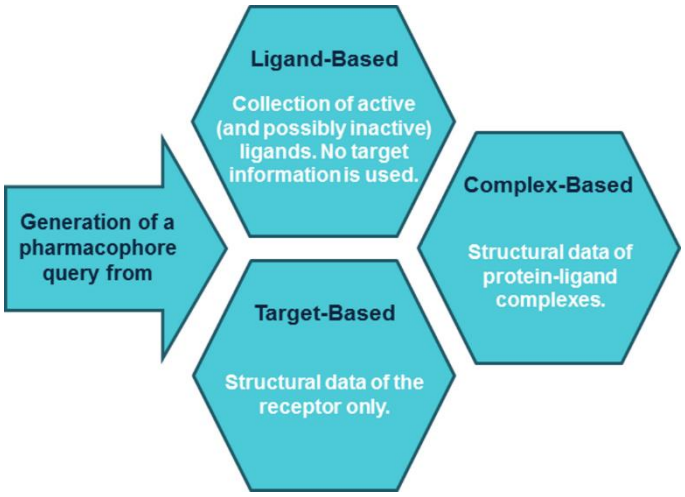

Figure 21. Main approaches for generating pharmacophore queries depending on the input data.

A toxicophore concept overlaps with the understanding for pharmacophore and is defined as the ensemble of steric and electronic features that is necessary to ensure the optimal intermolecular interaction with a specific biological target molecule, which results in the manifestation of a specific toxic effect (ENV/JM/MONO(2007)2). What is specific here is that the substructural features (toxicophores) are particularly associated with toxicity by a specific interaction and disruption of one or more subcellular components: (i) receptors; (ii) enzymes; or (iii) macromolecules such as proteins and DNA. Moreover, it is accepted that a chemical with a toxicophore could possess other toxicophores for the same or different toxicities, and it might also contain a region involved in prevention of its toxicity (biophobe) (Combes, 2012).

2.2.3.2.Pharmacophore model development and validation

The pharmacophore was developed using the "Pharmacophore Query Editor" tool in MOE. The set of query features was created from three main categories ligand annotation points that are automatically detected in MOE (MOE, v. 2014.0901):

(i) atom annotations, located directly on an atom of a molecule and typically indicating a function related to protein-ligand binding: the H-bond donor (Don), the H-bond acceptor (Acc), cation (Cat), anion (Ani), metal ligator (ML) and hydrophobic atom (HydA);

(ii) projected annotations, located along an implicit lone pair or implicit hydrogen directions and used to annotate the location of possible partners for a hydrogen bond or a metal ligation, or a possible R-group atom locations: projected donor (Don2), projected acceptor (Acc2), projected metal ligator (ML2) and ring projection (PiN);

(iii) centroid annotations (including bioisosteres), located at the geometric centre of a subset of the atoms of a molecule: aromatic (Aro), pi-ring (PiR) and hydrophobic (Hyd).

After selection of the annotation points that were relevant to the pharmacophore, they were given a non-zero radius that encoded the permissible variation in the pharmacophore query's geometry. This extra parameter converted these points into query features.

The predictive power of the developed model was evaluated on the basis of four classes of compounds (**Table 5**) and following the Cooper's statistics (**Table 6**) (Gleeson et al., 2012; ENV/JM/MONO(2007)2**)**:

Table 5. Contingency table: TP – true positive, FN – false negative, FP – false positive, TN – true negative. Adapted from Gleeson et al., 2012 and ENV/JM/MONO(2007)2.

		Assigned class		
		Toxic	**Non-toxic**	**Marginal totals**
Observed (*in vivo*) class	**Active**	TP	FN	TP + FN
	Non-active	FP	TN	FP + TN
	Marginal totals	TP + FP	FN + TN	TP + FP + FN + TN

Table 6. Definitions of the Cooper statistics. Adapted from Gleeson et al., 2012 and ENV/JM/MONO(2007)2.

Statistic	Formula	Definition
Sensitivity (True Positive rate)	TP/(TP+FN)	fraction of active chemicals correctly assigned
Specificity (True Negative rate)	TN/(TN+FP)	fraction of non-active chemicals correctly assigned
Concordance or Accuracy	(TP+TN)/(TP+FP+TN+FN)	fraction of chemicals correctly assigned
Positive Predictivity	TP/(TP+FP)	fraction of chemicals correctly assigned as active out of the active assigned chemicals
Negative Predictivty	TN/(TN+FN)	fraction of chemicals correctly assigned as non-active out of the non-active assigned chemicals
False Positive (over-classification) rate	FP/FP + TN 1-specificity	fraction of non-active chemicals that are falsely assigned to be active
False Negative (under-classification) rate	FN/TP + FN 1-sensitivity	fraction of active chemicals that are falsely assigned to be non-active

2.2.4. 3D QSAR (CoMSIA) modelling

2.2.4.1.CoMFA and CoMSIA approaches

The three-dimetional quantitative structure-activity relationship approach (3D QSAR) aims at establishing a correlation between the variations in the biological activity and the 3D properties of a series of structurally and biologically characterised molecules (**Figure 22**).

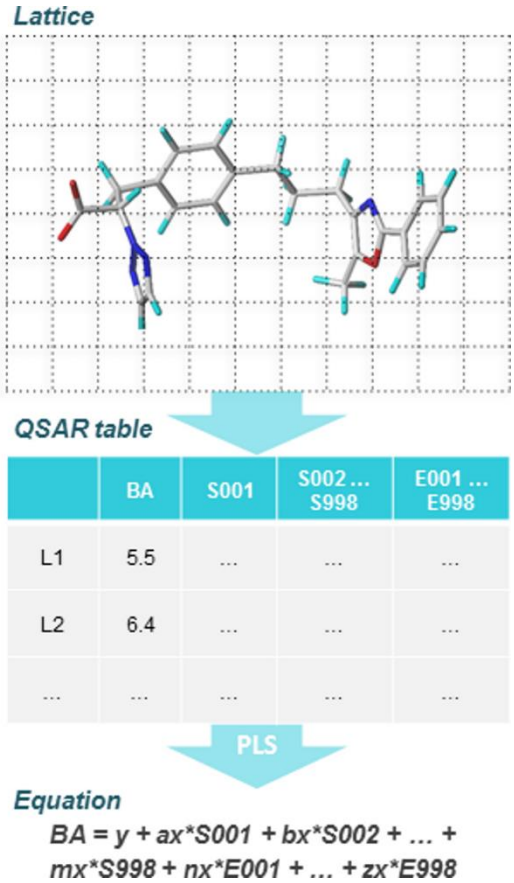

Figure 22. The spatial fingerprints of numerous field properties can be calculated at a lattice as in the approaches related to CoMFA which use the changes in the shapes and strengths of the non-covalent interaction fields (steric – S, electrostatic – E, etc.) surrounding the ligands (L1, L2, etc.) to explain the differences in their biological activity (BA).

Preliminary pharmacophore modelling is a reasonable first step in such a study since generation and alignment of bioactive molecular conformations is a prerequisite for robust and reliable analysis. The aligned molecules are located in a cubic grid simulating the active site. There, the gradual changes of the ligands' interaction properties are mapped by evaluating the potential energy at regularly spaced grid points surrounding the structures.

In the standard application of CoMFA, two potentials, namely, the steric potential as a Lennard-Jones function and the electrostatic potential as a simple Coulomb function are used, providing only the enthalpic contributions of the free energy (Höltje at al., 2004). Therefore, the CoMFA approach bears several limitations:

(i) Entropic influences seem to be neglected or insufficiently covered as their contributions to the binding affinity are more difficult to describe.

(ii) The steepness of Lennard-Jones potential close to the van der Waals surface results in a dramatic change of the potential energy at the vicinal grid points.

(iii) The singularities at the atomic positions that the Lennard-Jones and Coulomb potentials produce unacceptably large values. To overcome this problem, the potential evaluations are performed within regions that are outside the molecules and are restricted by arbitrarily fixed cutoff values. Since the two potentials (e.g. Lennard-Jones and Coulomb) differ in their slopes, these cutoff values are exceeded for the different terms at different distances from the molecules. Thus the loss of information for one of the fields is inevitable during their additional arbitrary adjustment for simultaneous evaluation (**Figure 23**).

(iv) The graphical representation is difficult to interpret since the resulting contour maps are discontinuous due to the cutoff settings and the steepness of the potentials close to the molecular surfaces.

A CoMSIA approach has been proposed to overcome these problems by:

(i) including entropic influences through a field, considering the differences in hydrophobic surface contributions;

(ii) replacement of the Lennard-Jones and Coulomb potentials by a Gaussian-type function (no singularities) so that no arbitrary definition of cutoff limits is required and the indices can be calculated at all grid points (**Figure 23**).

In CoMSIA analysis, the comparison between all mutual pairs of molecules is indirectly evaluated via the similarity of each molecule *j* of the data set with a common probe atom which is systematically placed at the intersections (grid point *q*) of a regularly spaced surrounding lattice (usually a grid spacing of 1 Å):

$$A_{F,k}^{q}(j) = \sum_{j} w_{probe,k} w_{i,k} e^{-\alpha r_{iq}^{2}} \qquad \text{Eq. 13}$$

where the similarity indices $A_{F,k}$ between the compounds of interest and the probe atom are calculated on the basis of the summation index (i) over all atoms of the molecule j under investigation; the actual value of the physicochemical property k of atom i ($W_{i,k}$); the probe atom with charge +1, radius 1 Å, and hydrophobicity +1 ($W_{prohe,k}$); the attenuation factor (α); and the mutual distance between the probe atom at grid point q and the atom i of the test molecule (r_{iq}). Large values of α will result in a strong attenuation of the distance-dependent consideration of molecular similarity.

The steric, electrostatic, hydrophobic, and hydrogen-bond donor and acceptor properties, which are supposed to contribute mostly to the binding affinity, are used to calculate the fields of similarity indices. For these properties, distance dependence, described by the significantly smoothened Gaussian-type functional form, is equivalently handled. By analogy with the CoMFA approach, the numerical data tables are subjected to a subsequent PLS analysis (Klebe, 1994; Klebe, 1998).

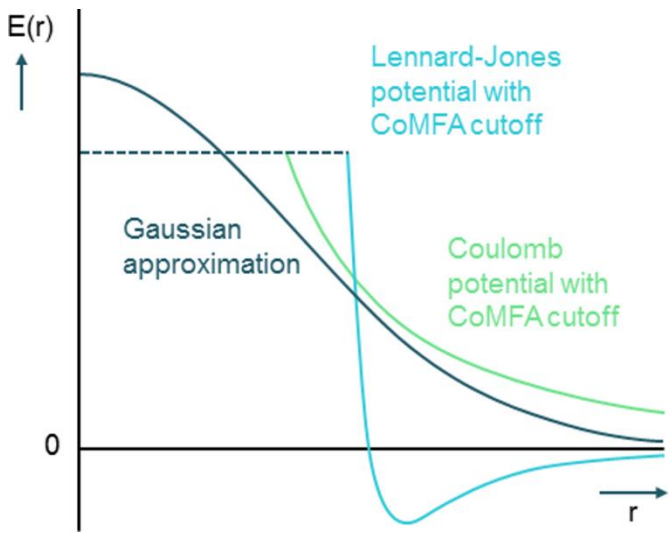

Figure 23. Comparison between the steeper slopes of the Lennard-Jones and Coulomb potentials (CoMFA) and the smoother Gaussian function (CoMSIA), avoiding any singularities and cutoff values. Adapted from Klebe (1998).

2.2.4.2.PLS analysis to build 3D QSAR model – general considerations

PLS analysis is a multivariate statistical technique that is able to extract a weak signal dispersed over many variables even when the number of similarity indices' values exceeds the number of compounds. This is possible because the various similarity indices are intercorrelated and many are unrelated to biological activity (**Figure 24**) (Höltje at al., 2004).

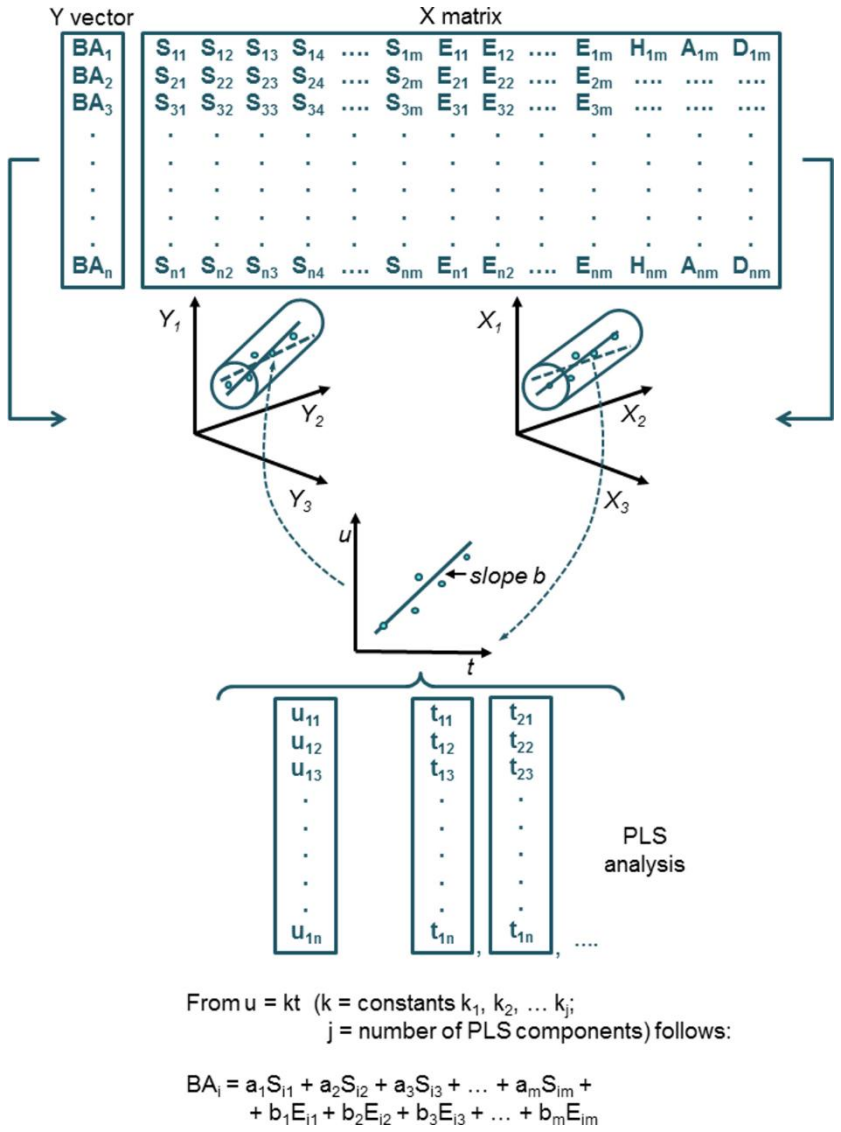

Figure 24. Scheme of the PLS analysis principle: t – latent variables for the X block (S_{ij}, E_{ij}, H_{ij}, A_{ij}, D_{ij} – steric, electrostatic, hydrophobic, HB acceptor and HB donor field variables of molecule *i* in the grid point *j*); u – latent variables for the Y block (BA_i - logarithms of relative affinities or other biological activities). The solid lines in X- and Y-space (the 3D plots) are the principle components, and the dashed lines represent the PLS vectors. These are slightly skewed to account for the correlation between the two data blocks. Adapted from Kubinyi, 1993, 1998.

Because of the multiple variables on which PLS operates, data over-fitting is expected. This implies PLS models' validation, which is performed by a "leave-one-out" (LOO) crossvalidation (**Figure 25**).

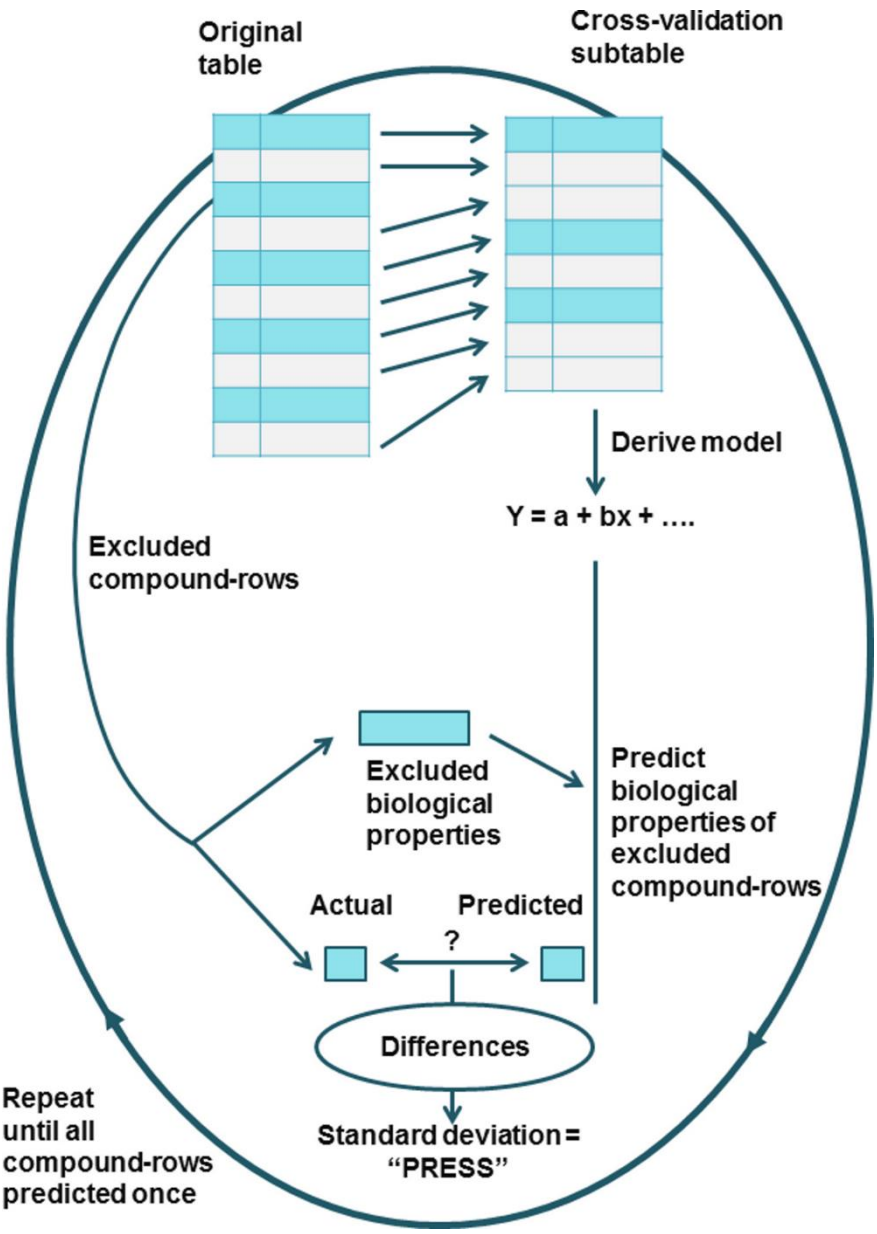

Figure 25. Cross-validation procedure; PRESS = $\Sigma\ (y_{exp\ i} - y_{pred\ i})^2$, where $y_{exp\ i}$ is the experimental (observed) value of the dependent variable, and $y_{pred\ i}$ – the predicted value of the dependent variable. Adapted from Kubinyi, 1993.

The procedure is also used to determine the optimal number of components. The latter suggests that for each model, one of the compounds, in turn, is excluded from the modelling set and its activity is predicted from the model developed without it. When each compound has been predicted once, the observed and predicted potencies are used for the calculation of the q_{cv}^2 value (square of the cross-validated correlation coefficient) and the standard deviation of error prediction value (SDEP, or SEP) according to the following equations:

$$q_{cv}^2 = 1 - \frac{PRESS}{\sum_i (y_{\exp_i} - y_{mean})^2} \qquad \text{Eq. 14}$$

$$SEP = \sqrt{\frac{PRESS}{N - A - 1}} \qquad \text{Eq. 15}$$

where N = number of compounds, A = number of components, (Kubinyi, 1993; Höltje at al., 2004).

The optimal number of components N_{opt} is determined by selecting the smallest SEP and the biggest q^2_{cv} and is subsequently used to derive the final regression 3D QSAR model, characterised by r^2_{pred} (Kubinyi, 1993):

$$r_{pred}^2 = 1 - \frac{\sum (y_{pred}^{test} - y_{\exp}^{test})^2}{\sum (y_{\exp}^{test} - \bar{y}_{\exp}^{train})^2} \qquad \text{Eq. 16}$$

where

$y_{\exp}^{test}$ = experimental (observed) biological activity of the test set

y_{pred}^{test} = predicted biological activity of the test set

$\bar{y}_{\exp}^{train}$ = mean value of the experimental (observed) biological activity in the training set

The sensitivity of the model to chance correlations can be additionally investigated by a Y-randomisation test and by progressive scrambling. In Y-randomisation the best QSAR model is derived on the basis of randomly permuted target activity values, leaving the X-space untouched and preserving the original descriptor selection procedure.

By repeatedly performing this procedure, an array of models is generated with a lower quality standing from the deliberately destroyed structure-activity relationship (Wold and Eriksson, 1995; Baumann et al., 2004). In the progressive scrambling, however, a range of small perturbations is introduced into the Y-space of the model by the scrambling of the responses only within quantiles rather than across the full range (Clark et al., 2001). The statistical parameter used for evaluating the robustness and the predictivity of the PLS model are summarised in **Table 7**:

Table 7. General statistical parameters related to progressive scrambling analysis

Parameter	Description
Q^2	The predictivity of the model after potential effects of redundancy have been removed, i.e. the expected value of q^2 at the specified critical point for $r^2_{yy'}$ (the correlation of the scrambled responses with the unperturbed data)
cSDEP	The estimated cross-validated standard error at the specified critical point
dq/dr	The slope of q^2 – the cross-validated correlation coefficient evaluated at the specified critical point with respect to the correlation of the original dependent variables versus the perturbed dependent variables

2.2.4.3.CoMSIA model development

2.2.4.3.1. Alignment of structures and calculation of fields

The spatial alignment of the structures (170 compounds as described in **Section 2.2.1.2.**) was performed using their docking poses in the PPARγ ligand binding domain that were obtained in a VS procedure developed within this study (**Section 4.3.4.2.**) and the experimental bioactive conformers for the ligands extracted from the PDB complexes. Visual inspection against the template structure and consideration of the docking score (the smallest negative scores preferred) were the criteria driving the final conformer selection for each ligand out of 10 best poses selected after its docking. The template was either the corresponding PDB ligand used as a scaffold in the structure generation or the ligand UNT from 3IA6 PDB complex. The latter was considered appropriate, in view of its high potency (pEC_{50} = 7.886) and relative efficacy (103%), as well as its representativeness with respect to the typical for the full agonists structural features (Casimiro-Garcia et al, 2009; Mahindroo et al., 2005). The alignment of the whole set against the ligand UNT (3IA6 PDB complex) was performed based on substructures that fit to the 4 feature PPARγ pharmacophore model described in **Section 3.3.4.1.** (Tsakovska et al., 2014) and using the "Fit Atoms" procedure in MM software suite SYBYL-X v. 2.1 (Certara USA, Inc.) The aligned structures were subjected to 3D QSAR modelling, using the CoMSIA (Comparative Molecular Similarity Indices Analysis) approach within SYBYL. The electrostatic, steric, hydrogen bond donor, hydrogen bond acceptor, and hydrophobic fields were calculated using the default CoMSIA settings.

2.2.4.3.2. Model development and validation

In order to establish a correlation between the ligands' potency (pEC_{50}) and the similarity indices for the calculated fields, structures were split into a training set used to build multiple CoMSIA models and a test set to externally validate the best one. The PLS was used in the CoMSIA modelling and a Leave-One-Out (LOO) cross-validation analysis was performed for evaluating the models' robustness. The best model was selected based on the following statistical characteristics: cross-validated correlation coefficient, q^2_{cv}; optimal number of PLS components, N_{opt}; and cross-validated standard error of prediction, SEP_{cv}. The non-cross-validated model (characterised by the correlation coefficient, r^2, standard error of estimate, SEE, and the F-value) was obtained for the best cross-validated model with N_{opt}, followed by external validation by prediction of the pEC_{50} values of a predefined test set of full agonists and calculation of the predictive r^2 (r^2_{pr}). Two categories of compounds were excluded from the set of 170 agonists: (i) applicability domain outliers, identified with the "extent of extrapolation" approach (Tropsha et al., 2003; Netzeva et al., 2005) as implemented in Enalos domain leverage node (Melagraki et al., 2009) in the KNIME analytics platform (Berthold et al., 2007) and (ii) response outliers, identified in the analysis of residuals.

2.2.5. Docking procedure

2.2.5.1.Docking – general view

Docking is a structure-based method that allows for a precise calculation of the position and orientation of a potential ligand in a receptor-binding site and for prediction of the free energy of binding. The docking algorithm within MOE (MOE, v. 2014.0901) involves several stages, as shown in **Figure 26.**

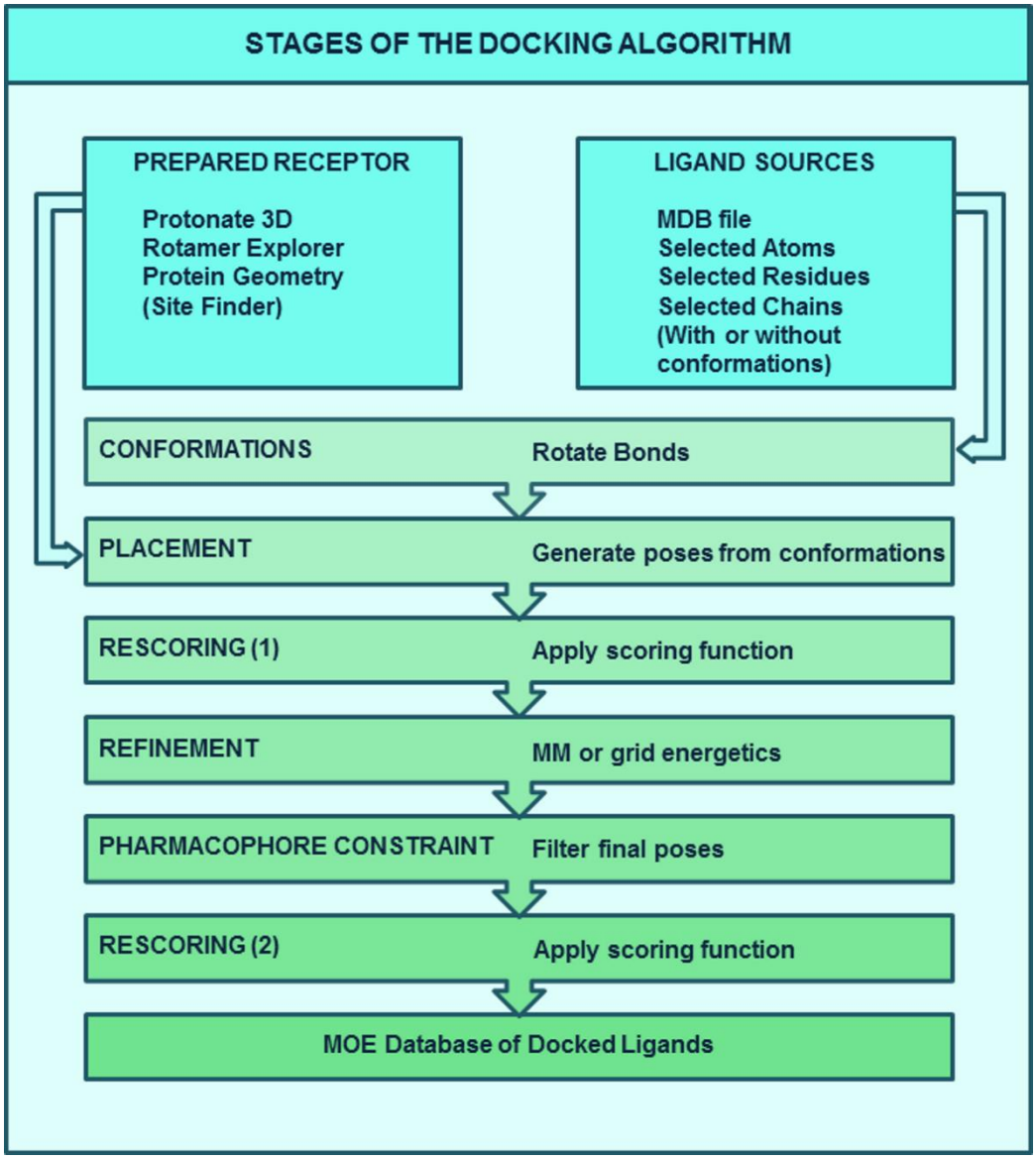

Figure 26. Stages in the docking algorithm (adapted from MOE, v. 2014.0901)

First, an array of conformations is generated by applying a collection of preferred torsion angles to the rotatable bonds. No alternation is induced regarding either the bonds' lengths and angles, or the geometry of the rings. Then, a placement of the generated conformers is performed, which results in a collection of poses with characteristic scores, assigned by the applied placement method. Several methods can be used for pose rescoring with the general understanding that the good poses are supposed to receive low scores. The refinement of the poses follows two possible methods based on either an explicit molecular mechanics force field or a grid-based energetics. A pharmacophore constrain may be applied to the final poses, which requires the selection of the pharmacophore placement method. When the ligand is placed using pharmacophore's features, volume constraints are applied as a final filter but are ignored during the placement stage. The latter is characterised by the following assumptions:

(i) If there are more than two pharmacophore features and they do not lie on or close to a straight line, the pharmacophore search engine is used to orient the ligand.

(ii) If the pharmacophore features lie on or very close to a line, the ligand is anchored by the pharmacophore features and rotated in such a way that a third atom matches an alpha site point.

(iii) If all pharmacophore features lie at a point or very close to one point, the ligand is first anchored at that point. Then, two more atoms on the ligand are matched to two alpha site points to orient the ligand.

(iv) Since the ligand pose changes upon refinement, if there is a refinement stage, the pharmacophore constraints are loosened for placement.

(v) If a pharmacophore search returns too few hits, the pharmacophore constraints are further loosened so that more hits are obtained.

Finally, several alternative scoring schemes are provided to rescore the resulted poses. The assignment of reliable docking scores is crucial for the overall docking algorithm (MOE, v. 2014.0901). The scoring functions are expected to reflect the binding free energies driving the complex formation in order to guarantee the correct prediction of the biological activity. Generally, there are three main groups of scoring functions: empirical scoring functions, force field based functions and knowledge-based potential of mean force.

In VS the scoring functions are used: (i) as a fitness function in the optimisation placement of the ligand during the docking process; (ii) as criteria for ranking the output poses after docking is completed. Different functions could be applied for the two purposes, although one and the same is usually utilised (Höltje at al., 2004). One example is the London dG scoring function, which estimates the free energy of binding of the ligand from a given pose by summing several terms:

$$\Delta G = c + E_{flex} + \sum_{h-bonds} c_{HB} f_{HB} + \sum_{m-lig} c_M f_M + \sum_{atomsi} \Delta D_i \qquad \text{Eq. 17}$$

where c represents the average gain/loss of rotational and translational entropy; E_{flex} is the energy due to the loss of flexibility of the ligand (calculated from ligand topology only); f_{HB} measures geometric imperfections of hydrogen bonds and takes a value in [0,1]; c_{HB} is the energy of an ideal hydrogen bond; f_M measures geometric imperfections of metal ligations and takes a value in [0,1]; c_M is the energy of an ideal metal ligation; and D_i is the desolvation energy of atom i. The difference in desolvation energies is calculated according to the formula:

$$\Delta D_i = c_i R_i^3 \left\{ \iiint_{u \notin A \cup B} |u|^{-6} du - \iiint_{u \notin B} |u|^{-6} du \right\} \qquad \text{Eq. 18}$$

where A and B are the protein and/or ligand volumes with atom i belonging to volume B; R_i is the solvation radius of atom i (taken as the OPLS-AA van der Waals sigma parameter plus 0.5 Å); and c_i is the desolvation coefficient of atom i. The coefficients $\{c, c_{HB}, c_M, c_i\}$ are fitted from ~400 x-ray crystal structures of protein-ligand complexes with available experimental pK_i data. Atoms are categorised into about a dozen atom types for the assignment of the c_i coefficients. The triple integrals are approximated using Generalized Born integral formulas (MOE, v. 2014.0901).

2.2.5.2.Docking in the ligand-binding domain of PPARγ

The ligands (structures prepared according **Section 2.2.1.2.**) were docked into the binding site of the prepared protein structure. The binding pocket of the receptor was specified by using the atoms of the co-crystallised ligand (BRL, or rosiglitazone) of the used PDB complex (PDB ID 1FM6). The virtual screening protocol was applied with a placement method based on a pharmacophore. Then, a rescoring with London dG scoring function was applied to score the poses of the docked ligands (MOE, v. 2014.0901) without subsequent refinement and second rescoring. The highly scored poses of each ligand with a negative value of the scoring function only were kept (**Figure 27**).

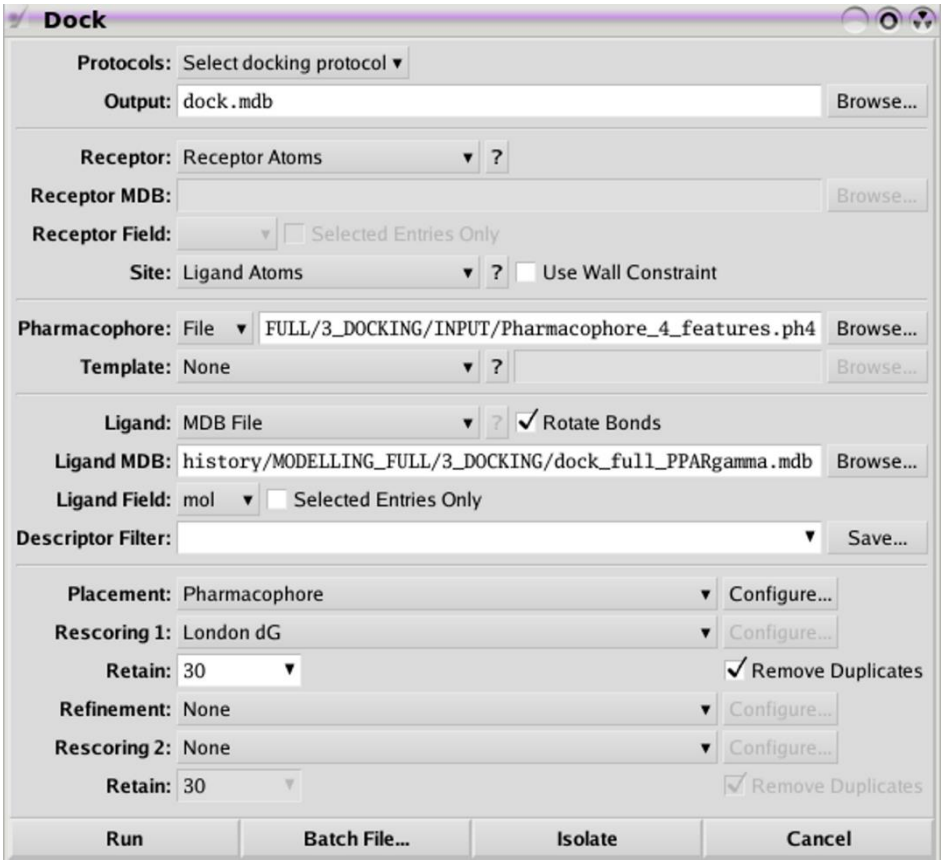

Figure 27. Settings for the docking procedure

CHAPTER 3. RESULTS AND DISCUSSION

3.1. Prosteatotic AOPs

3.1.1. Data harvesting and analysis

Experimental data from studies on hepatocytes and adipocytes were collected and analysed to investigate the possible relationship between PPARγ ligand binding and the development of NAFLD. This involved screening and ranking of more than 300 papers retrieved from NIH PubMed system (http://www.ncbi.nlm.nih.gov/pubmed) according to the following criteria:

(i) completeness in the description of the model system: type of experiment (*in vivo* or *in vitro*), species or cell line used, and genetic properties of the studied subjects which could support a causal link between the MIE and the adverse outcome;

(ii) relevance of the presented experimental evidence to the link KE-AO: availability of qualitative/quantitative data underlining biochemical and histological markers of NAFLD;

(iii) relevance of the presented experimental evidence to the link MIE-KE: availability of qualitative/quantitative data related to the PPARγ-dependent changes in the levels of already identified biochemical and/or histological NAFLD markers;

(iv) availability of appropriate experimental systems approximating the chemical initiation step: experimentally-induced (by diet, pharmacological treatment, or genetic techniques) changes in PPARγ activity and/or expression.

The core set of literature sources was selected based on the availability of information for at least two of the pillars within an AOP, e.g. MIE, intermediate KE and AO, and experimental evidence for their relationship, qualitative or quantitative. This initial pool was further extended by an additional more specific literature search on the causal link between PPARγ dysregulation, the levels of its target proteins, and their corresponding toxicity pathways. The final set of 72 papers, among which 26 are reviews, is organised in several categories (**Table S.2., Appendix A. Supplementary Material**) in relation to the studied subjects (human patients, human cell cultures, animals *in vivo*, and animal cell cultures) and the experimental approaches (PPARγ overexpression, PPARγ overexpression and pharmacological treatment; PPARγ knockout/knockdown; PPARγ knockout/knockdown and pharmacological treatment;

pharmacological treatment; diet manipulation; gene manipulation of PPARγ upstream proteins; gene manipulation of PPARγ upstream proteins and pharmacological treatment). The papers dealing with the AOP methodology, reviews, and research articles containing background information (receptor structure, up- and downstream proteins' functions, etc.) are given in the last two columns of the table. **Figure 28** summarises the data in **Supplementary table S.3.** The analysis of the selected papers served as a basis for building the blocks in the proposed AOPs.

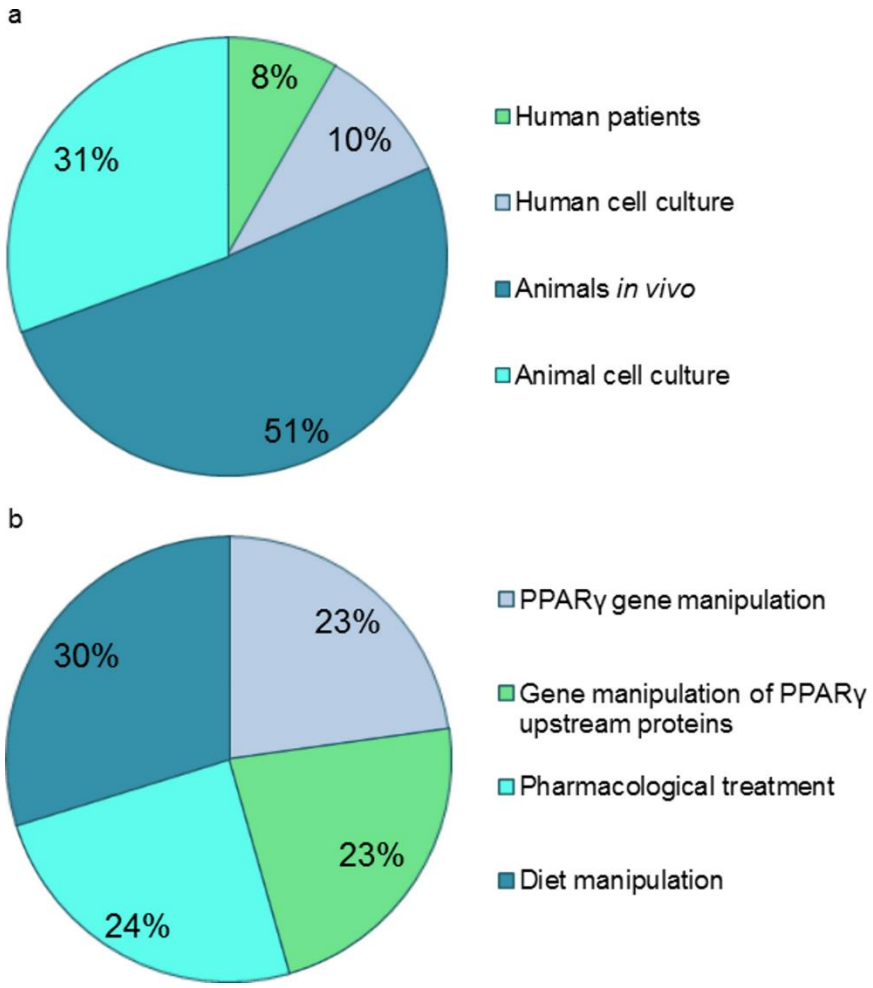

Figure 28. Major categories of (a) subjects and (b) experimental approaches in the selected papers.

3.1.2. Description of the AOPs

Collecting scientific evidence for the relationship between PPARγ signaling and NAFLD was the first step in the development of AOP. The involvement of the receptor in this pathology has been well studied (Lee et al., 2012; He et al., 2011; Videla and Pettinelli, 2012; Nagasaka et al., 2012; Matsusue, 2012; Okumura, 2011). *In vitro* and *in vivo* animal data supporting the role of hepatic PPARγ in the regulation of target lipogenic genes and triglycerides' levels was collected from different experimental settings: receptor overexpression and/or activation, liver-specific knockout/knockdown of the PPARγ gene. While receptor suppression in liver had been shown to correlate with reduced target genes' expression and lowered levels of NAFLD biomarkers, severe liver steatosis and hepatocyte proliferation had been linked to PPARγ upregulation (Lee et al., 2012; Morán-Salvador et al., 2011; Satoh et al., 2013; Yamazaki et al., 2011; Panasyuk et al., 2012). In the present study, data on PPARγ gene nucleotide variations affecting hepatic steatosis, and causing partial lipodystrophy was also considered as strong evidence for the relevance of the receptor to the considered adverse effect (Costa et al., 2010; Semple et al., 2006). AOP development implied analysis of three domains of knowledge by:

(i) identification of the chemical space – known chemical initiators or chemical classes reported as prosteatotic;

(ii) analysis of the MIE: qualitative – by defining the mechanism, the site of action at molecular and higher levels, the key interactions involved; and quantitative – through establishing relationship between the structures of the chemical initiators and the experimental data from *in vitro* model system of the MIE;

(iii) characterisation of the AO, e.g. biomarkers at molecular, cellular, tissue, organ and system levels that are relevant to the MIE and the pathology.

On the basis of the collected evidence, the group of the PPARγ full agonists was outlined as prosteatotic and represents the applicability domain of the *in silico* studies discussed later. Further, two sites of action were considered with different MIEs, respectively – PPARγ inhibition in adipocytes and activation in hepatocytes (Al Sharif et al., 2014). Therefore, the two described AOPs include tissue-specific key events related to pathology-relevant biomarkers (**Figure 29**).

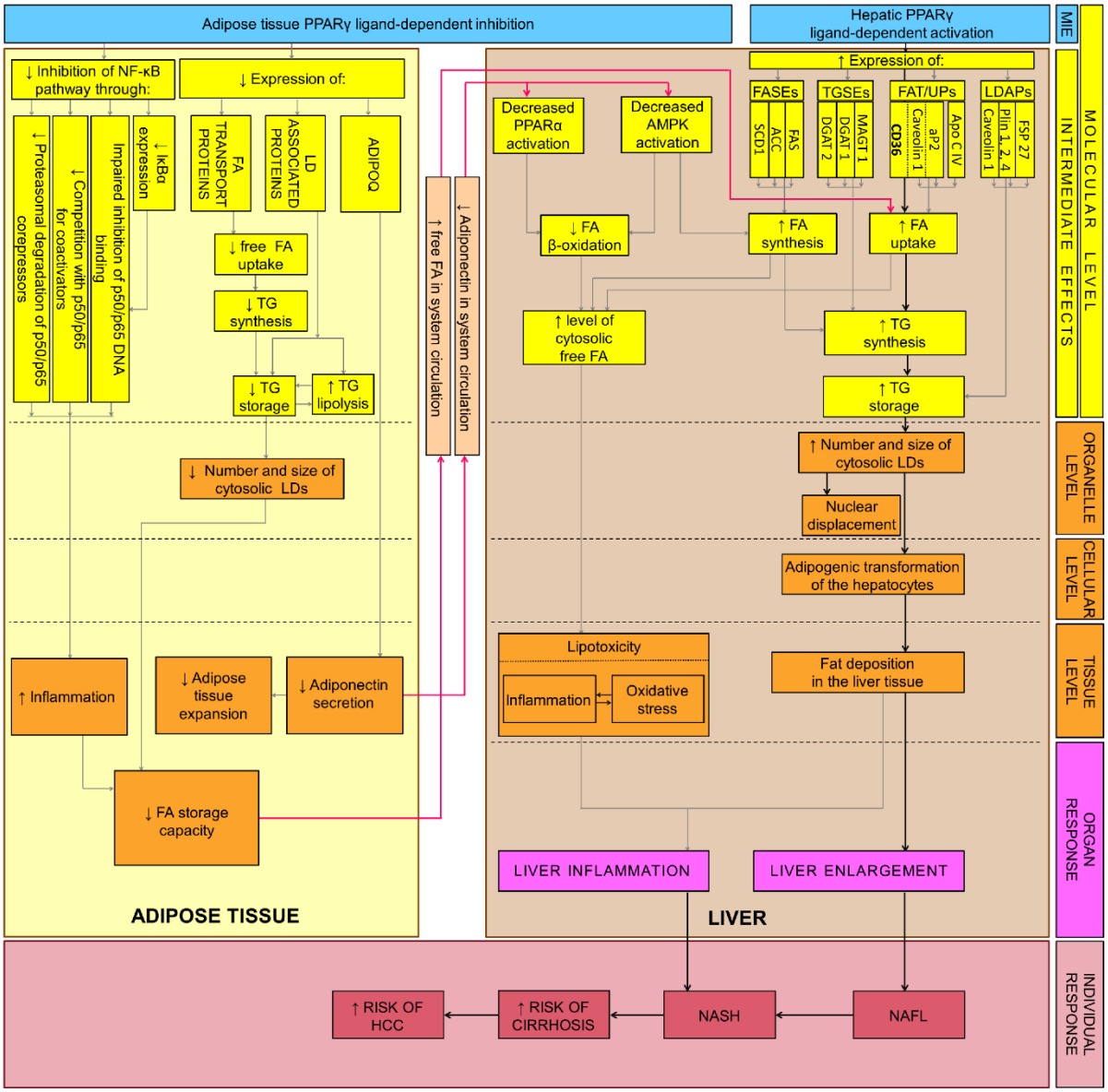

Figure 29. Proposed AOPs from tissue-specific ligand-dependent PPARγ dysregulation to NAFLD: LDAPs – lipid droplet associated proteins; FAT/UPs – fatty acid transport/uptake related proteins; TGSEs – triglyceride synthesising enzymes; FASEs – fatty acid synthesising enzymes; FSP27/CIDE-C – fat-specific protein 27/cell death-inducing DFF45-like effector; Plin 1, 2, 4 – Perilipins 1, 2, and 4; ApoCIV – apolipoprotein C IV; aP2 – adipose fatty acid binding protein; FAT/CD36 (or just CD36) – fatty acid translocase/cluster determinant 36; FAS – fatty acid synthase; ACC – acetyl-CoA carboxylase; SCD1 – stearoyl-CoA desaturase1; MGAT1 – monoacylglycerol O-acyltransferase 1; DGAT1 – diglyceride acyltransferase 1; DGAT2 – diglyceride acyltransferase 2; ADIPOQ – adiponectin; HCC – hepatocellular carcinoma.

3.1.2.1.PPARγ Ligand-Dependent Activation in Hepatocytes

For the proposed AOP initiating with PPARγ activation, the rationale behind the selection of the corresponding MIE lies on the reports of prosteatotic effects of PPARγ agonists (synthetic: rosiglitazone and pioglitazone; endogenous: palmitate, oleate, eicosanoids) and/or liver PPARγ overexpression models (Lee et al., 2012; Morán-Salvador et al., 2011; Videla and Pettinelli, 2012; Okumura, 2011; Maciejewska et al., 2015) as well as the anti-steatotic effects of PPARγ antagonists (BADGE, GW9662), hepatocyte-specific PPARγ knockout/knockdown (Sos et al., 2011; Okumura, 2011), or PPARγ downregulation (He et al., 2015). Although small molecules are the principle initiators of the AOP, studies on PPARγ expression levels were considered as appropriate as the ligand-induced activation of the receptor correlates with qualitative estimations of NAFLD biomarkers. This is justified by the fact that PPARγ is subjected to positive feed-back regulation (Ratushny et al., 2012; Wakabayashi et al., 2009), thus agonist-triggered induction of its own expression is an expected element of the effectuation chain and causes signal amplification.

The toxicity pathways identified within this AOP involve increased synthesis of proteins, responsible for fatty acids':

(i) uptake – lipid transport/binding proteins ApoCIV, aP2, Caveolin 1, FAT/CD36 (Zhu et al., 2011; Lee et al., 2012; Morán-Salvador et al., 2011; Satoh et al., 2013; Yamazaki et al., 2011; Sos et al., 2011; Li et al., 2013; Kumadaki et al., 2011; Gaemers et al., 2011; Larter et al., 2009; Bai et al., 2011; Kim et al., 2008; Larter et al., 2008);

(ii) *de novo* synthesis – the enzymes FAS, ACC, SCD1;

(iii) esterification – the enzymes MGAT1, DGAT1, DGAT2 (Lee et al., 2012; Morán-Salvador et al., 2011; Li et al., 2013; Kumadaki et al., 2011; Larter et al., 2009);

(iv) storage – the lipid droplet associated proteins FSP27/ CIDE-C, Plins (1, 2, 4), Caveolin 1 (Li et al., 2013; He at al., 2011; Matsusue, 2012; Flach et al., 2011; Matsusue, 2010; Bai et al., 2011).

Among the target proteins whose upregulation is relevant to the liver AOP, the most completely characterised were selected for further data summation and analysis. Thus quantitative data was collected for one lipid droplet associated protein (FSP27) and two proteins related to fatty acid uptake and intracellular transport (CD36 and aP2), regarding their expression levels in different

experimental conditions supporting the MIE (**Section 3.1.3.**). Further, the relevance of CD36 to the AOP was placed in the focus of a detailed analysis.

The FA translocase/cluster determinant 36 (FAT/CD36) protein, from the class B scavenger receptor family, is involved in the uptake of oxidised low-density lipoproteins (in macrophages) and fatty acids (in adipocytes, skeletal and heart myocytes). It is well known that the three main membrane structures where CD36 is incorporated are the cell surface caveolae, the intracellular vesicles and the mitochondria. The last is the place of interaction between CD36 and carnitine palmitoyl transferase 1, the key enzyme regulating mitochondrial fatty acids transport and oxidation. Mitochondrial CD36 content has been shown to correlate with mitochondrial fatty acids oxidation in human muscle and to increase upon rosiglitazone treatment (Ring et al., 2006; Ehehalt et al., 2008; Su and Abumrad, 2009). On the other hand, the relocalisation of CD36 from mitochondria to the cellular membrane is among the mechanisms driving the shift from normal to insulin resistant myocytes through excessive fatty acids uptake (Glatz, 2015). It is possible, therefore, for PPARγ full agonists to affect the prosteatotic CD36 localisation in, or redirection toward the cell membrane by elevating its expression levels in hepatocytes.

Furthermore, possible implication of plasma soluble CD36 as a new biomarker of insulin resistance, carotid atherosclerosis, and fatty liver has been suggested (Handberg et al., 2012). A study involving two hundred and twenty-seven NAFLD and eighty-five patients with a histologically normal liver supported the increased serum sCD36 as an independent factor associated with advanced steatosis in NAFLD with a significant correlation between hepatic CD36 and serum sCD36 levels (García-Monzón et al., 2014). The relevance of CD36 is further increased in view of the multiple transcriptional regulators of the translocase, such as cytosolic aryl hydrocarbon receptor (AhR), pregnane X receptor (PXR), liver X receptor (LXR), and PPARγ (He et al., 2011).

Although PPARγ-mediated elevation of CD36 mRNA and protein levels has been clearly related to the adipogenic transformation of liver and exacerbation of steatosis (Zhu et al., 2011; Yamazaki et al., 2011; Larter et al., 2008), consideration of the alternative mechanisms and the extent to which they may distract from the postulated AOP is required for the complete AOP assessment (ENV/JM/MONO(2013)6). Generally, the dysregulation of each of the outlined nuclear receptors can affect the CD36 expression. Moreover, PXR is known as a transcriptional regulator of PPARγ, while PPARγ and LXR regulate their expressions reciprocally (Chawla et al., 2001; Geng et al., 2015).

While AOP networking could reflect such cross-relations, the asymmetric positive feed-back activation that is characteristic for each one of these receptors is neglected by definition. The role of CD36 hepatic overexpression in linking the AOP anchors – PPARγ dysregulation and NAFLD is justified by the growing scientific evidence for these relationships (**Table 8**).

Table 8. Main findings extracted from selected scientific papers supporting the prosteatogenic role of FAT/CD36 in the AOP from PPARγ dysregulation to NAFLD. Legend: Bold, *in vitro* experiments; CD, control diet; HFD, high-fat diet; endpoints: empty cells, endpoint not determined; +, increase; −, decrease; 0, no effect; 1, controls taken for 100%; 0/+ and 0/− are used in cases where a clear-cut decision about the reported effects could not be made

Species	PPARγ related strain characteristics	Diet	Experiment type	Gene manipulation	Pharmacological treatment		Endpoints			Ref
					agent	type	PPARγ	CD36	NAFLD biomarkers	
human	NASH patients							+	+	Zhu et al., 2011
mouse	wild type	HFD					+		+	Le et al., 2012
	liver PPARγ deficient line	HFD					0		0	
	wild type	CD		PPARγ transfected			+	+	+	
	liver PPARγ deficient line	CD		PPARγ transfected			+	+	+	
mouse			**hepatocytes**	**PPARγ transfected**			+	+	+	
					rosiglitazone	**synthetic agonist**	+	++	++	
					palmitate	**endogenous metabolite**	+	++	++	

mouse	functional PPARγ	HFD				+	+	+	
	PPARγ knockout	HFD				0/+	0/+	0/+	
mouse	**functional PPARγ**		**tissue slices**	**oleic acid**	**endogenous agonist**			**+**	Morán-Salvador et al., 2011
	functional PPARγ			**rosiglitazone**	**synthetic agonist**			**+**	
	PPARγ knockout			**oleic acid**	**endogenous agonist**			**0**	
	PPARγ knockout			**rosiglitazone**	**synthetic agonist**			**0**	
	functional PPARγ		**hepatocytes**	**BADGE**	**synthetic antagonist**			**−**	
	functional PPARγ			**oleic acid + BADGE**	**endogenous agonist + synthetic antagonist**			**0/+**	
mouse	Insulin-resistant mice	CD				+	+	+	Satoh et al., 2013
	control mice	CD		pioglitazone	synthetic agonist			0	
	Insulin-resistant mice	CD		pioglitazone	synthetic agonist	0	+	++	
mouse	wild type	HFD - safflower oil				0/+	0	0/+	Yamazaki et al., 2011
	wild type	HFD - butter				+	+	+	
	wild type	HFD - safflower oil	PPARγ2 knockdown			+	0/+	0/+	
	wild type	HFD - butter	PPARγ2 knockdown			+	0/+	0/+	
	wild type	CD	PPARγ transfected			+	+	+	

mouse	JAK2L-thyrosine kinase deficient	CD				+	++	++	Sos et al., 2011
	wild type	CD		GW9662	synthetic antagonist	0	0	0	
	JAK2L-thyrosine kinase deficient	CD		GW9662	synthetic antagonist	+	+	+	
mouse	liver SMS2-overexpressing transgenic line	CD					+	0/+	Li et al., 2013
	lSMS2-deficient knockout line	CD					–	0/–	
	wild type	HFD				1	1	+	
	liver SMS2-overexpressing transgenic line	HFD				+	+	++	
	lSMS2-deficient knockout line	HFD				–	–	–	
	liver SMS2-overexpressing transgenic line	HFD		GW9662	synthetic antagonist			–	
human			**huh7 hepatoma cells**	**ceramide**	**endogenous suppressor**	–	–		

mouse	wild type	CD		Fbw7 knockdown	+	+	++	Kumadaki et al, 2011
	wild type	CD		Fbw7/PPARγ 2 double knockdown	0/–	0/+	+	
	wild type	CD		Fbw7 transfected	–	–	0/–	
mouse	**wild type**		**hepatocytes**	**Fbw7 knockdown**	**+**	**+**	**+**	
mouse	wild type	HFD			+	+	+	Gaemers et al., 2011
	wild type	HFD, liquid, overfeeding			++	++	++	
mouse	wild type	HFD			0/+	0/+	0/+	Larter et al., 2009
	obese, hypercholesterolemic, diabetic foz/foz mice	CD			+	+	0/+	
	obese, hypercholesterolemic, diabetic foz/foz mice	HFD			+	++	+	

The proposed mechanism of the CD36 mediated toxicity pathway is illustrated in **Figure 30** and involves the following steps: gene transcription is suppressed by corepressor binding to the PPARγ-RXRα heterodimer in the absence of PPARγ agonists (1); ligand-induced conformational changes lead to receptor activation, corepressor release and coactivator recruitment necessary for transcription initiation (2); CD36 overexpression and translocation to the plasma membrane markedly increase the hepatic uptake and esterification of free fatty acids (3–6), resulting in excessive and ectopic TG storage in lipid droplets (7).

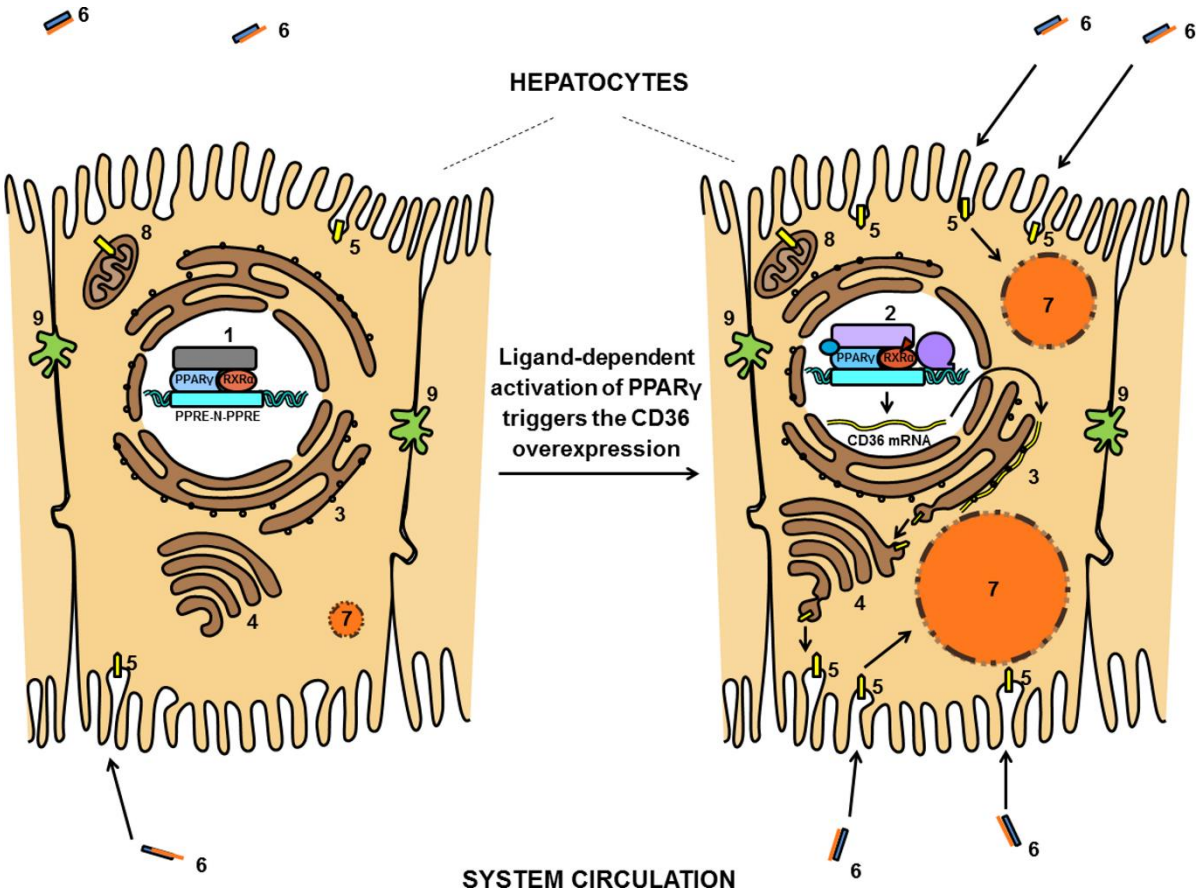

Figure 30. Model of ligand-dependent PPARγ activation as a potential MIE for liver steatosis through CD36 mediated excessive FA uptake and consequent hepatic TG accumulation. (1) PPARγ-RXRα heterodimer interacting with the PPARγ response elements (PPRE-N-PPRE) and transcriptional corepressor complex; (2) ligand-activated PPARγ-RXRα heterodimer with a transcriptional coactivator complex and RNA polymerase II; (3) rough endoplasmic reticulum; (4) Golgi complex; (5) FAT/CD36; (6) plasma fatty acid binding protein (in blue) carrying fatty acid (in orange); (7) growing lipid droplet storing triglycerides and coated with LD associated proteins; (8) mitochondria; (9) bile canaliculus.

Defining uncertainties, inconsistencies and data gaps is another criterion for evaluating the confidence in AOP, in particular for the assessment of key events. In the case with the long-chain FAs transmembrane passage, the earlier hypothesis suggested the cooperative action of two proteins: FABPpm (plasma membrane fatty acid binding protein) – the receptor that facilitates the diffusion of the fatty acid-albumin complex through the unstirred fluid layer, and FAT/CD36 – mediating the fatty acids flip-flop across the bilayer (Chabowski et al., 2007). Later, real-time fluorescence measurements questioned the classification of CD36 as a simple transporter since a mechanism based on rate increase of fatty acids incorporation intoTGs instead of catalysing their translocation across the plasma membrane was proposed. However, the relevance of CD36 for TG accumulation is out of debate, since a study on HEK293 cells overexpressing CD36 has shown the uptake-mediated accumulation of more and larger LDs (Xu et al., 2013).

One of the central elements in the AOP concept is directing the design of alternative risk assessment strategy by suggesting reliable *in vitro* and/or *in silico* predictive models for each key event along the pathway. On the basis of the collected scientific evidence for the CD36-mediated fatty acids uptake, measuring the chemical-induced changes in the levels of CD36 (mRNA and/or protein) in cultured hepatocytes can be used in *in vitro* screening for prosteatotic compounds. However, AOP quantification is necessary in order to estimate the dose-response cutoffs relevant to a real exposure scenario.

Cumulatively, the toxicity pathways involving increased fatty acids' uptake, synthesis, esterification, and storage in lipid droplets lead to an increased number or size of the lipid droplets, e.g. microvesicular or macrovesicular steatosis (Lee et al., 2012; Satoh et al., 2013; Yamazaki et al., 2011; Sos et al., 2011). Among the organ responses of the excessive fat deposition is the significant hepatomegaly (Sos et al., 2011; Li et al., 2013; Kumadaki et al., 2011). The lipid droplets, which are central histological markers of the disease, are metabolically active organelles involved in the cellular homeostasis, rather than only lipid storage depots in the state of hyperlipidemic stress (Manteiga et al., 2013; Guo et al., 2009). A shift toward lipolysis of the content of overloaded lipid droplets induces lipotoxicity which is a prerequisite for the inflammation characteristic for NASH (Sos et al., 2011; Gaemers et al., 2011). Predicting the progression from NAFLD to NASH is another key aspect of understanding the severity of the pathology and its driving molecular mechanisms.

Recently, Yamada et al. (2015) have examined one hundred and three patients diagnosed with NAFLD (simple steatosis: 63, NASH: 40) and reported differential gene expression when comparing the two groups of patients, outlining the progression from simple steatosis to NASH. In particular, increased expression of PPARγ and its target proteins – SCD1 and FAS correlated significantly with the hepatocellular ballooning score. The correlation between the lobular inflammation score and SCD1 levels has also been shown to be significant with a rise in the gene expression during the progress of inflammation in the liver tissue.

Such studies underline the necessity of further monitoring and evaluation of the individual levels of multiple target proteins in pursuit of the biomarkers that are specific to separate stages of the disease development.

3.1.2.2.PPARγ Ligand-Dependent Inhibition in Adipocytes

The developed adipose tissue AOP initiated with PPARγ inhibition is supported by a growing body of evidence that points toward the relevance of this MIE to the considered adverse effect (**Figure 29**). The receptor, whose isoform 2 is predominantly expressed in the adipocytes, is claimed to be a master regulator of adipogenesis (at the stage of terminal differentiation) as it is necessary (Barak et al., 1999; Kubota et al., 1999; Rosen et al., 1999) and sufficient (Tontonoz et al., 1994; Hu et al., 1995; Shao and Lazar, 1997) for establishing the adipocyte phenotype, by regulating the levels of particular metabolic genes and adipokines (Hwang et al., 1997; Rosen and MacDougald, 2006; Lefterova and Lazar, 2009). The role of PPARγ ligands in the regulation of fatty acid uptake into adipocytes and adipocyte differentiation has been shown for thiazolidinediones and other insulin-sensitising agents that are potent receptor's agonists (Grossman and Lessem, 1997). Such lipid sequestration into the adipose tissue lowers the circulating levels of triglycerides and free fatty acids, thus preventing the excessive hepatic lipid uptake and the secondary lipotoxicity in the liver (Rogue et al., 2010; Musso et al., 2009; Park CY and Park SW, 2012). Ligand-induced reduction in adipogenesis and lipid accumulation has been observed in experiments on 3T3-L1 preadipocytes involving cyclic phosphatidic acid, a highly specific endogenous PPARγ antagonist (Tsukahara et al., 2010), and scoparone – a PPARγ inhibitor that has been reported to suppress the rosiglitazone-mediated overexpression of its target genes to a level near the one observed in cells treated with GW9662 (Noh et al., 2013).

The effects observed upon PPARγ loss of function strongly support the relevance of the tissue-specific receptor's suppression for the selected adverse outcome since naturally occurring mutations in human PPARγ-coding sequence have been found to cause lipodystrophy. Cumulating data have been reviewed, supporting the axis PPARγ-deficiency/knockout – impaired adipogenesis as well as its significance for the subsequent elevated levels of plasma free FAs and TGs, and decreased plasma leptin and adiponectin levels, leading to lipodystrophy, insulin resistance and hypotension (Azhar, 2010). The lowered lipid storage capacity due to underdevelopment of adipose tissue has been shown to induce deposition of TG and acyl-CoA in insulin-sensitive tissues, causing not only insulin resistance but often hepatosteatosis (Virtue et al., 2010; Semple et al., 2006). The prosteatotic impairment of the normal function of the adipose tissue has been evidenced by experiments involving adipose tissue loss in JAK2L mice (Sos et al., 2011) and in mouse models of severe lipodystrophy (He at al., 2013; Chen et al.,

2012). On the contrary, the application of antisense oligonucleotide targeting a suppressor of the PPARγ activation (drosophila tribbles homologue 3) has been reported as a PPARγ-dependent mechanism for improving insulin sensitivity through increasing the white adipose tissue mass by 70%. The primary role of PPARγ has been additionally verified by cotreatment with its antagonist (BADGE), reversing the observed effects (Weismann et al., 2011).

The decreased expression of adiponectin is among the key events outlined within this AOP, based on findings that hypoadiponectinemia is strongly associated with a decreased PPARγ expression in adipocytes, development of hepatic steatosis and insulin resistance in obese adolescents. In particular, adiponectin and PPARγ2 expressions have been reported to correlate positively and an inverse relationship has been shown between the adiponectin plasma levels and the hepatic fat content (Kursawe et al., 2010). The massive fat redistribution toward liver due to reduced adiponectin secretion has been confirmed by experiments with foz/foz mice (Larter et al., 2009). As for the strength of the relationship between the MIE and the adiponectin downregulation – the link is supported by studies on the 4-hydroxynonenal-induced activation and upregulation of PPARγ in parallel with the increased adiponectin gene expression both suppressed by T0070907 treatment (PPARγ antagonist) (Wang et al., 2012) as well as the stimulating effects of the eicosapentaenoic acid and its metabolite 15d-PGJ3 on the adiponectin's secretion in 3T3-L1 adipocytes, claimed to be partially mediated by PPARγ (Lefils-Lacourtablaise et al., 2013).

These effects find their mechanistical explanation in the fact that adiponectin is a hormone known to be exclusively expressed in adipocytes and to influence liver lipid metabolism through its hepatic adiponectin receptors 1 and 2 (also PPARγ-regulated proteins). Upon lack of adiponectin, an impaired hepatic β-oxidation of fatty acids is expected by lowered activation of PPARα and AMPK (5'-adenosine monophosphate-activated protein kinase). Normally, adiponectin regulates the AMPK phosphorylation, necessary for the reduction of malonyl-CoA-mediated inhibition of β-oxidation and for lowering the triglyceride synthesis via suppression of SREBP-1 (Sterol regulatory element-binding protein-1) (Anderson and Borlak, 2008).

Decreased PPARγ transactivation activity is also the mechanism involved in the reduced expression of lipid-droplet associated proteins as well as of important transporters in the adipocytes. The remodeling of the lipid droplets (fragmentation, shrinkage, expansion, and/or fusion) is governed by their protein composition. The same holds true for the metabolism of

their lipid contents since lowered levels of some PPARγ targets (FSP27/CIDEC and Plin1) are known to drive the increased lipolysis and release of free fatty acids from the adipocytes to the circulation – a prerequisite for insulin resistance and abnormal hepatic lipid deposition (Manteiga et al., 2013; Lefils-Lacourtablaise et al., 2013).

The role of the fatty acids' uptake/transport is outlined by several studies on compounds (scoparone and extracts from *Zanthoxylum piperitum DC* and *Petalonia binghamiae thalli*) and microorganisms (lactic acid bacteria isolated from Korean pickled fish) suppressing *in vitro* adipocytes differentiation and accumulation of triglycerides by lowering the expression of PPARγ (Gwon et al., 2012; Patk et al., 2013) and its target proteins aP2 and CD36/FAT (Noh et al., 2013; Kang et al., 2010; Patk et al., 2013). Nuclear factor erythroid 2-related factor 2 has been shown to suppress lipid accumulation in white adipose tissue and adipogenesis as well as to induce insulin resistance and hepatic steatosis in Lep (ob/ob) mice. It has been related to the downregulation of PPARγ and aP2 in mouse embryonic fibroblasts (Xu et al., 2012).

Inflammatory and immune responses, in particular NFkB-mediated ones, are among the cellular processes under the transrepressive PPARγ control by: (i) direct interaction with NFkB, preventing its binding to specific responsive elements on target genes; (ii) competing for common coactivators; or (iii) blocking the pro-inflammatory stimulus-induced clearance of corepressor complexes on target genes (Luconi et al., 2010; Rogue et al., 2010; Liao et al., 2012). PPARγ activation by resolvin D1 in lung and by bezafibrate in white adipose tissue has been shown to mediate their anti-inflammatory effects (Liao et al., 2012; Magliano et al., 2013). The transition from steatosis to NASH is claimed to coincide with major changes in adipose tissue. A relationship between its metabolic function and inflammatory state has been shown in overfeeding mouse models of NAFLD. The increased expression of inflammation markers and the lowered PPARγ, adiponectin, CD36 and aP2 expression in white adipose tissue have been reported as strong evidence supporting the understanding that chronic inflammation, increased cytokine production and altered adipokine secretion of white adipose tissue as well as its decreased lipid storage capacity and increased lipid outflow are the driving mechanism behind the metabolic changes and the lipotoxicity in peripheral tissues/organs (Gaemers et al., 2011). Decreased adiponectin secretion and increased free fatty acids' redistribution toward the liver have been outlined as key events bridging the possible toxicity pathways in the adipocytes and the final outcome in the liver. The elevated hepatic lipid uptake, impaired mitochondrial oxidation and increased synthesis of fatty acids cumulatively leads to excessive triglyceride

accumulation and is a prerequisite for hepatocellular injury associated with hepatic lipotoxicity (Anderson and Borlak, 2008; Neuschwander-Tetri, 2010), oxidative stress and inflammation observed in NASH (Serviddio et al., 2013).

3.1.3. Evaluation of the hepatic AOP

A weight-of-evidence was performed for the hepatic AOP, based on two main criteria: (i) the extent of development of the assay supporting a given event and (ii) the relationship between the AOP anchor points MIE-KEs-AO. The following key events within the hepatic AOP were analysed (**Appendix B.AOP evaluation table**):

(i) MIE

(ii) LD associated proteins

(iii) FA transport proteins

(iv) increased FA uptake

(v) increased TG storage

(vi) increased number or size of LD

(vii) NAFLD at tissue and organ level

According to the performed analysis, the most applied assays reflect mRNA and protein levels of PPARγ and its targets, histological markers of NAFLD, hepatic TG content, organ effects and serum levels of markers for liver injury. It is important to note that variations in gene expression are often supported by biochemical or histological confirmation of their relevance to the apical endpoint. Most of the assays (**Figure 31**) are not only robust and reliable methods published in the peer-reviewed literature but also in a form that could allow them to be submitted for prevalidation. However, we did not score the corresponding events as "Strong" but as "Moderate", because the relationships between them and the apical endpoint were not strong and the mechanistic basis was rather probable (**Appendix B. AOP evaluation table**).

The involvement of FSP27 and CD36 in the regulation of fatty acids metabolism and fate has already been discussed (**Sections 3.1.2.1. and 3.1.2.2.**). The other outlined transporter – the fatty acid binding protein 4 (FABP4, aP2) is known to bind specific ligands in the cytosol and to be engaged with their delivery to PPARγ in the nucleus, thus facilitating the ligand-dependent enhancement of the receptor's transcriptional activity (Ayers et al., 2007).

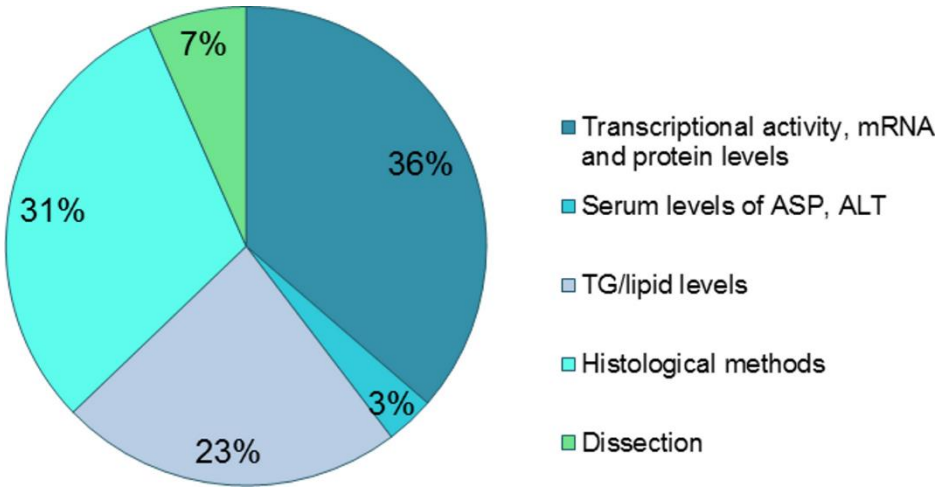

Figure 31. Distribution of the scientific evidence by type of assays.

In **Figure 32,** data for high-fat diet induced changes in the expression are summarised. The colour code corresponds to different literature sources and experimental settings. However, a mixed etiology of the observed effect could be expected since the inductive role of dietary fatty acids could simultaneously act on PPARγ and other nuclear receptors.

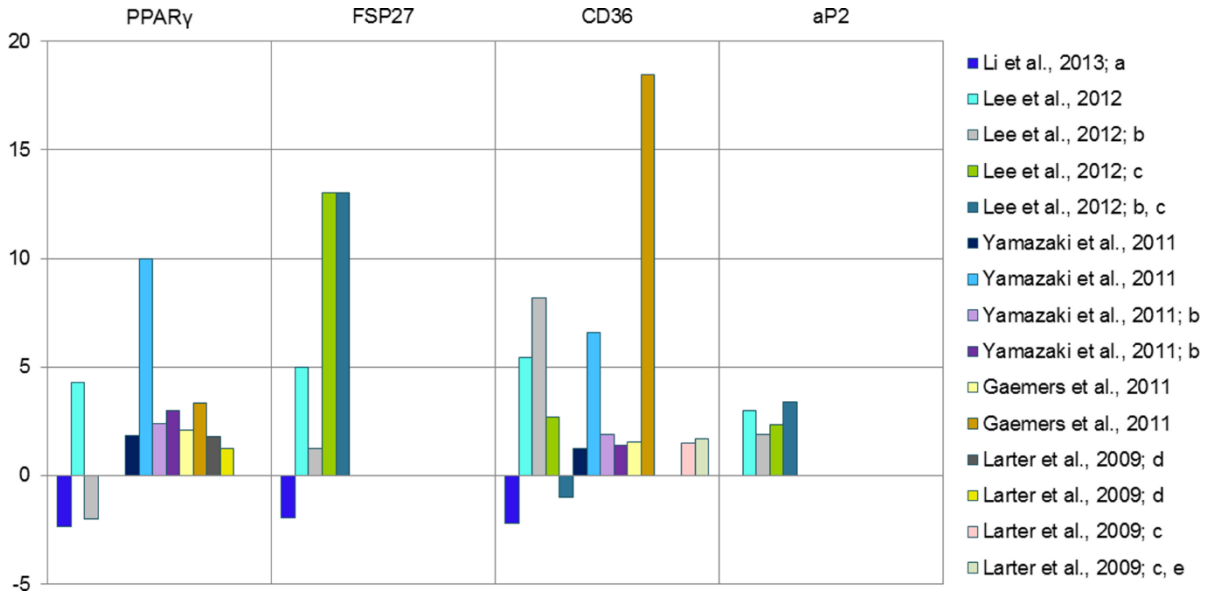

Figure 32. Effect of natural ligands (mainly from diet) on the mRNA levels of PPARγ and some of its targets. General experiment type: wild type + high-fat diet (variants) + quantitative RT-PCR analysis. Exceptions: a – *in vitro* treatment with ceramide (endogenous suppressor); b – PPRAγ deficient line; c – microarray analysis; d – semiquantitative RT-PCR; e – obese, hypercholesterolemic, diabetic line (Supplementary table S.3.).

Additionally, data for genetic manipulations or cell lines with specific genetic background that are related to PPARγ overexpression, knockdown, positive or negative regulation by upstream acting proteins was collected (**Figure 33**).

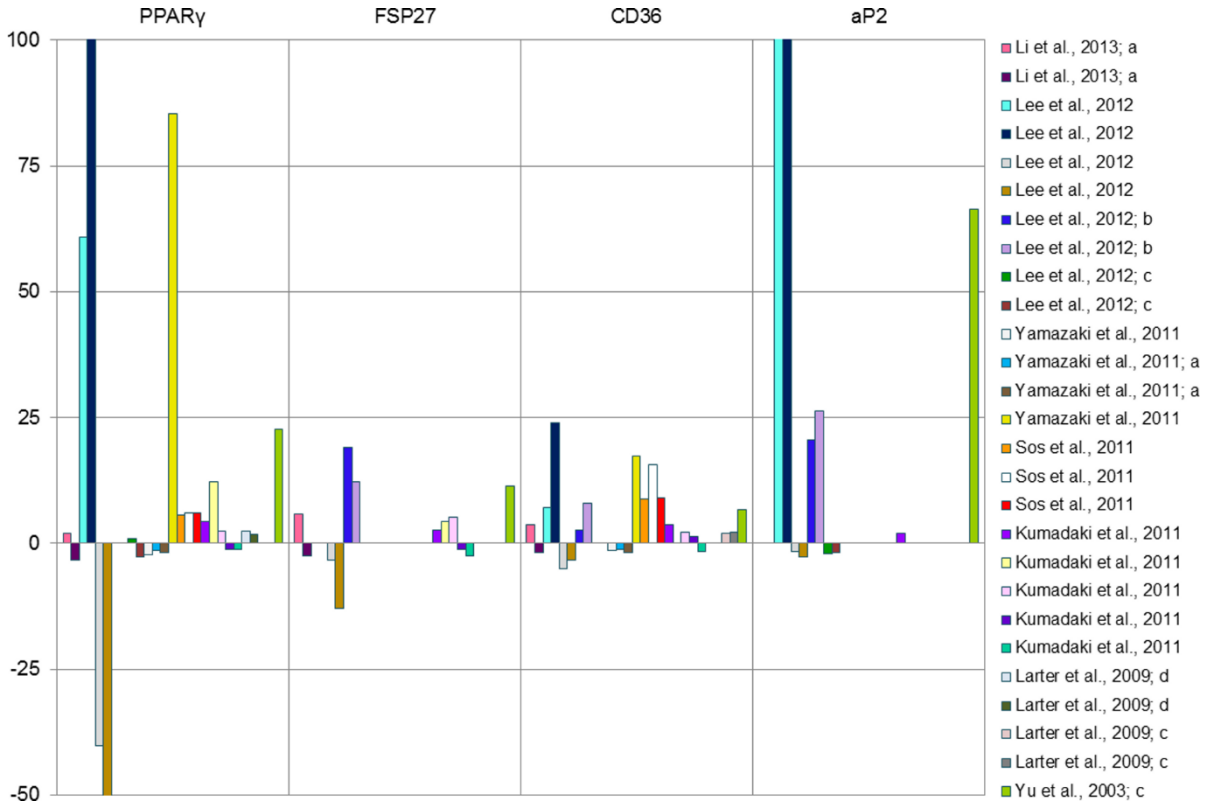

Figure 33. Effect of genetic manipulation and/or genetic background on the mRNA and protein levels of PPARγ and some of its targets. General experiment type: PPARγ up- or downregulation + normal chow diet + quantitative RT-PCR analysis. Exceptions: a – high-fat diet; b – microarray analysis; c – Western blot; d – semiquantitative RT-PCR (Supplementary table S.4.).

At a molecular level we can clearly see the correlation between the availability of PPARγ and its targets. The bars that go outside the plot area stand for knockdown or overexpression data where the normalisation versus zero level produced infinite number. The effects illustrated in **Figure 32** and **Figure 33** support the local interconnections between the MIE and the respective molecular intermediate events, although some of them are associated with the apical endpoint within the source literature by additional histological observations.

3.1.4. The developed AOPs – general analysis and comparison with the AOPs published in the AOP-KB

The complexity of the NAFLD, considered as a spectrum of pathological phenotypes, makes the precise definition of the apical endpoint a challenging task. Studies on the interaction of miRNAs and PPARγ supported the involvement of the receptor in the regulation of triglyceride homeostasis and in the development of hepatic steatosis as a mechanism protecting the extrahepatic tissues from triglyceride accumulation and insulin resistance (Kurtz et al., 2014; Albert et al., 2014). Moreover, there is a general understanding that steatosis can be reversible (Vanni et al., 2010; Tailleux et al., 2012). From that point of view, it can be assumed that steatosis is more likely an adaptive response which by definition is not supposed to be outlined within an AOP neither as a key event nor as an adverse effect. However, fatty liver is both among the prerequisites for disease aggravation and a part of the NASH phenotype, histologically characterised by steatosis, lobular inflammation, hepatocellular ballooning and fibrosis (Takahashi and Fukusato, 2014). If we choose NASH to be the adverse effect in the AOP and consider liver steatosis as one of the histological manifestations of the pathology, then we could represent it as a key event or a non-apical endpoint, preceding the adverse effect. This issue raises the question of the integration of other progressive stages like cirrhosis and hepatocellular carcinoma and their place in a possible AOP network since patients suffering from NASH are particularly predisposed to such outcomes (Wang et al, 2015).

Another inherent limitation of the AOPs is the fact that feedback loops are ignored. This means that the well known positive feedback regulation of PPARγ is not considered. However, as already discussed in the section for protein-ligand interactions, the shifting of the observed ligand's potency toward a lower EC_{50} value as compared to its expected magnitude is rooted in signal amplification. Thus, if ligand-indiced activation of the receptor is involved in its own overexpression, it would result in a different dose-response profile. Another phenomenon that is expected to power the signal amplification is the synergistic action of PPARγ, LXR and PXR, which share common target proteins and/or metabolic pathways involved in the pathogenesis of the selected AO. Moreover, as already discussed, PPARγ and LXR are shown to be targets of PXR as well as to upregulate each other reciprocally (Chawla et al., 2001; Geng et al., 2015).

While AOP networking may solve problems like multi-stage disease representation and cross-relation between parallel signaling pathways, another problem stemming from the complex tissue composition of liver has to be overcome. Since PPARγ-mediated events take place in each of the cell types presented in this organ – hepatocytes, macrophages, hepatic stellate cells (HSCs), defining the individual cell type specific pathways' contributions would bring us a step closer to a more reliable, cumulative predictive model of the organ effect. It is well known that in macrovesicular steatosis the abnormally large LDs, the cellular stress and the morphological changes in the hepatocytes are prerequisites for congestion of the sinusoids, thereby impairing the sinusoidal blood flow. This triggers a pro-inflammatory cascade, which is further enhanced by the complex cross-talk of the sinusoidal epithelial cells, HSCs and activated Kupffer cells, causing congestion, infiltration of lymphocytes and local release of pro-inflammatory cytokines (Sahini and Borlak, 2014). Further, when the lipid storage capacity of the hepatocytes is exceeded, an elevated cytoplasmic lipid oxidation additionally aggravates the inflammatory state of the organ (Alkhouri and McCullough, 2012; Povero and Feldstein, 2016).

On the contrary, PPARγ activation in macrophages is more likely related to the suppression of inflammatory responses while its downregulation in HSCs is considered pro-fibrotic. Whether the anti-inflammatory (in macrophages) and anti-fibrotic (in HSCs) effects of PPARγ activation would be able to compensate the prosteatotic hepatocyte-related events depends on the time of exposure to the chemical initiator, its bioavailability, the feedback/feedforeward regulatory mechanisms, the parallel metabolic pathways regulated by other steatosis-relevant nuclear receptors and the inter-cellular signaling. Therefore, consideration of the individual contributions and cross-talks of the events in different cell types within the same organ could adequately reflect the dynamics and the magnitude of liver toxicity. At the current state of development of the two AOPs, the principles for AOP simplification and the unfilled data-gaps on synergic/interfering mechanism involved in the total individual response suggest quantitative deviations from the real pathway dynamics.

Among the 91 AOPs proposed in the AOP-KB, 12 have a common intercept with key elements of the AOPs reported in the current PhD thesis (**Figure 34**).

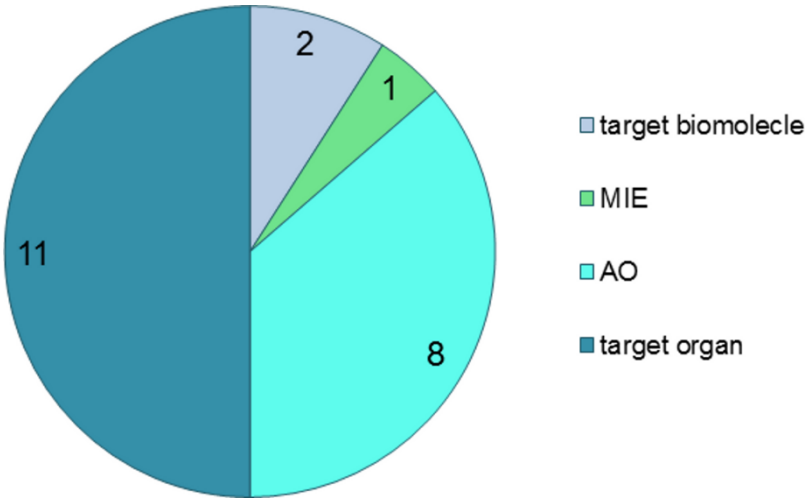

Figure 34. Distribution of the AOPs reported in AOP-KB by key anchors related to the prosteatotic AOPs discussed in the PhD thesis.

None of these except one, namely "LXR Activation to Liver Steatosis", matches both the studied here MIE (PPARγ activation/inhibition) and AO (liver steatosis). However, the mentioned AOP is focused on LXR, while the PPARγ activation was wrongly classified as MIE, since by definition an AOP consists of only one MIE and one adverse outcome (AO) connected by a sequence of key intermediate events. Although the activation of LXR and PPARγ trigger pathways with several common intermediate events and a shared AO, noa direct relation between these MIEs,outlined in the graphical representation of the AOP (https://aopkb.org/aopwiki/index.php/Aop:34). On the other hand, we proposed a complete sequence of events for two PPARγ related AOPs, with weight-of-evidence (WoE) evaluation of key events within the liver-initiated AOP and *in silico* modelling of its MIE. Moreover, the proposed by us AOP triggered by PPARγ activation is one of the few pathways supported by such *in silico* models.

In summary, it has been proposed that the ligand-induced disruption of the PPARγ activity may lead to NAFLD. The toxicity pathways related to this AO are tissue and cell type specific, thus two different AOP have been developed for the PPARγ inhibition in adipocytes and its activation in hepatocytes. Among the evaluated key events, lipid uptake/transport was underlined as the most significant toxicity pathway within the hepatic AOP.

3.2. PPARγ ligands' dataset

A dataset of PPARγ ligands was collected for the modelling purposes. Totally, data for 452 structures was harvested from the Protein Data Bank (PDB) (www.rcsb.org, Berman et al., 2000) and from 32 literature sources, 18 of which deposited a single structure in Protein Data Bank (PDB), 2 – two structures, 1 – three structures, and 11 – no structure. These structures represent 439 different PPARγ ligands. Among them, 5 are standards for PPARγ full agonists, and there is more than one reported experimental measurement (rosiglitazone – 8; pioglitazone – 4; farglitazar – 2; ragaglitazar – 2; tesaglitazar – 2). The structures were generated as described in **Section 2.2.1.2**. The dataset is publicly available at http://biomed.bas.bg/qsarmm/ and includes information about:

1. 2D connection table of the ligand named by its InChi key.
2. SMILES code of the ligands (Open Babel v. 2.3.2 generated "inchified" SMILES).
3. IUPAC names of the ligands.
4. Trivial name of the ligand (where present in the sources).
5. PDB complex and ligand codes (for the complexes deposited in Protein Data Bank by the cited authors).
6. PDB code of the ligand found in Protein Data Bank (even if no complex(es) are deposited in Protein Data Bank by the cited authors).
7. Ligand name / notation in the data source.
8. Data source.
9. Binding affinity data (IC_{50}), error, comments.
10. Transactivation activity data (EC_{50}), error, comments.
11. Relative transactivation efficacy (% max), error, comments.
12. Reference compound used in the relative transactivation efficacy calculation.
13. Species and cell line used in the activity/efficacy determination.
14. Assay names of: (i) *in vitro* binding assays – radioligand binding assay or fluorescence polarisation binding assay for measuring ligands' binding affinity; (ii) cell-based luciferase transcriptional reporter gene assay – used for evaluating the effect of the ligand-dependent PPARγ activation on the expression of a target reporter protein (transactivation activity, potency) and for establishing the percent response in relation to the maximum response of a reference compound (relative transactivation efficacy).

15. Training/test set assignment for the compounds used in 3D QSAR modelling: since the protonation states of the modelled ligands differ from those of the neutral forms presented in this dataset, for some structures two protonation states were shown to coexist and were considered as different ligands in the modelling study (Al Sharif et al., 2016)

The distribution of the collected ligands according to the different human/animal cell lines used for measuring potency and the relative efficacy toward PPARγ is shown in **Figure 35** and summarised in **Table S.5., Appendix A. Supplementary Material.**

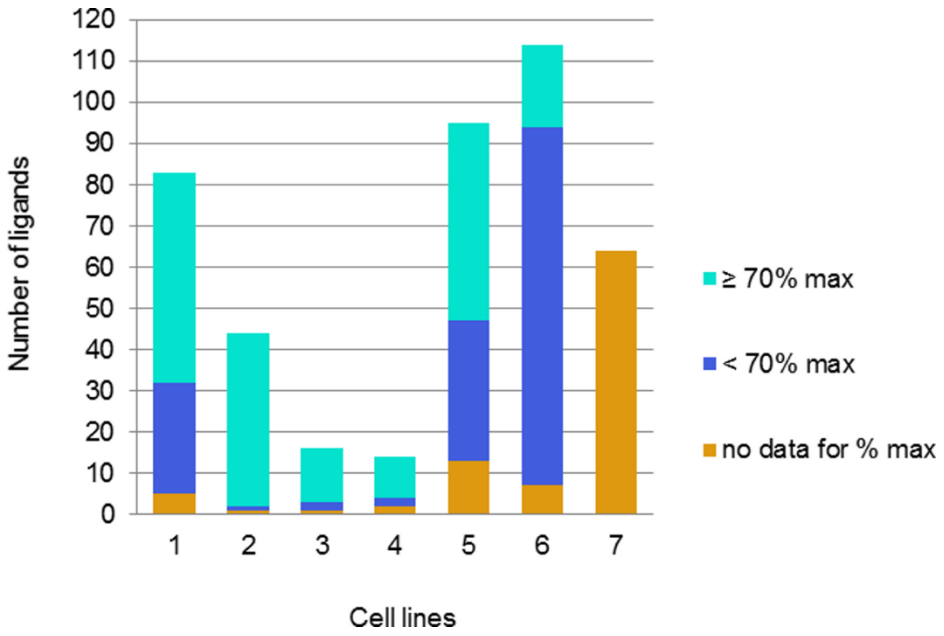

Figure 35. PPARγ agonists' dataset: distribution of the ligands according to the cell line and their relative efficacy toward PPARγ. Numbers 1-7 indicate the different species and cell lines: 1 – hamster/kidney (BHK21 ATCC CCL10), 2-4 – monkey/kidney (COS-1, COS-7, CV-1, respectively), 5 – human/kidney (HEK293), 6 and 7 – human/liver (HepG2, Huh-7, respectively)

In summary, the PPARγ agonists' dataset that has been collected and curated was based on the precise reflection of reported experimental settings. The constructed high quality dataset is suitable for modelling purposes and as a source for building a well organised information pool available on-line.

3.3. Molecular modelling studies

Based on the established causal relationship within the proposed AOPs, the study was logically directed toward molecular modelling of the MIE to develop a mechanistically justified predictive *in silico* approach. Taking into consideration that the prosteatotic genomic activity of PPARγ is specifically triggered by full agonists but not by partial agonists (Chigurupati et al., 2015), and in view of the prevalence of PPARγ-agonist crystallographic complexes over such with antagonists, the modelling strategy was focused on an *in silico* study of the hepatic MIE (PPARγ full activation) as a reliable early signal for hazard identification. This required an analysis of the available data for full agonists (e.g. binding mode, efficacy range) and determined the choice of molecular modelling approaches to be applied for development of a pharmacophore-based virtual screening (VS) procedure and 3D QSAR models (**Figure 36**).

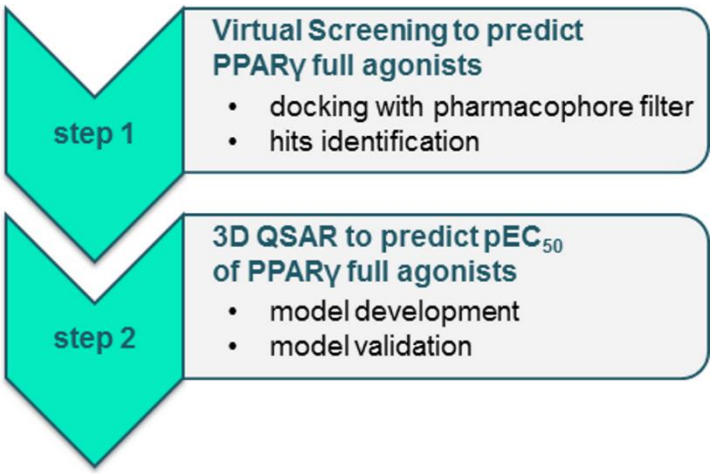

Figure 36. Molecular modelling workflow to study PPARγ full activation: step 1 – VS to predict full agonists and step 2 – 3D QSAR modelling to predict their potency.

3.3.1. Analysis of the deposited PPARγ-ligand complexes

A set of PPARγ-ligand complexes with biological data for the ligands (**Table S.6., Appendix A.Supplementary material**) was constructed, based on data extracted from the PDB and ChEMBL databases (last access: 15 February 2014) (Gaulton et al., 2012). It included 120 complexes of the human PPARγ receptor with binding affinity (K_i, K_d, IC_{50}) and transactivation activity (EC_{50}) data for the corresponding ligands. Complexes differed in terms of the type and/or the number of the bound ligand(s), in case there were any (**Figure 37a**). Some of the complexes had two ligands simultaneously occupying the LBD (Waku et al., 2010; Itoh et al., 2008; Li et al., 2008). Variations also occurred in the type of the non-ligand component, depending on the presence of additional protein subunit(s) or a cofactor as well as the absence of a ligand (apoform) (**Figure 37b**). Only the complexes of PPARγ agonists were selected for subsequent processing and analysis.

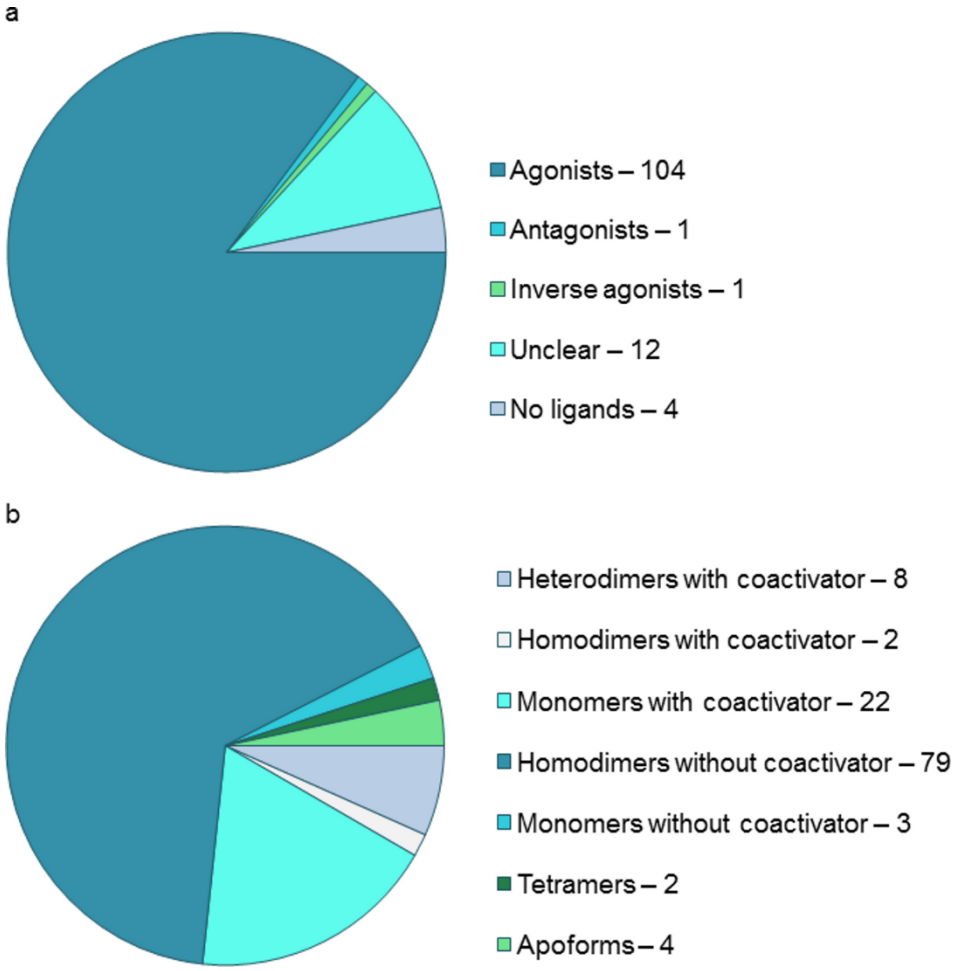

Figure 37. Distribution of the structures according to the type of: (a) the bound ligands; (b) the non-ligand component.

3.3.2. Processing of the PPARγ-ligands'dataset

Selection of a modelling set of 170 ligands out of 439 PPARγ full and partial agonists was performed by:

(i) data gaps removal;

(ii) selection of the full agonists, avoiding duplicates and data uncertainties;

(iii) stereochemical adjustment (S stereoisomers were preferred when potency of racemic mixtures was reported).

A cornerstone in the data processing was the ligands' filtering by type of agonism. Therefore, one of the three proposed thresholds for PPARγ full agonists' relative efficacy had to be selected:

(i) According to Henke et al. (1998), full agonists are those compounds that elicit in average at least 70% activation of PPARγ as compared to rosiglitazone.

(ii) According to Acton et al. (2005), ligands reaching 20–60% of rosiglitazone's maximal activation are deemed partial agonists; therefore %max > 60 could be associated with full agonism.

(iii) According to Bruning et al. (2007), transactivation which is more than 80% as compared to rosiglitazone should be considered full, less than 50% – partial, and between 50% and 80% – intermediate.

Relative efficacy of 70% was considered as a reasonable cutoff for selecting only the full agonists as it is less restrictive toward marginal efficacy and still relevant to the chemical domain of interests.

3.3.3. Analysis of the PPARγ LBD and the ligand-receptor interactions

The PPARγ LBDs were subjected to 3D-protonation at appropriate physiological conditions to assign the correct ionisation state and positions of the missing H-atoms. Then the LBDs were superposed by the C-alpha atoms on a template structure using the "Protein superpose" tool in MOE, and the root-mean-square deviation (RMSD) values were recorded. The X-ray structure of the PPARγ-rosiglitazone complex (PDB ligand ID BRL; complex ID 1FM6; Gampe et al., 2000) was selected for a template since:

(i) the complex represents a physiologically relevant arrangement of agonist-bond LBDs of human RXRα and PPARγ as a heterodimer interacting with coactivator peptides;

(ii) the PPARγ ligand (rosiglitazone) is among the most potent PPARγ full agonists (**Supplementary table S.6.**), thus bearing structural determinants appropriate for the pharmacophore modelling;

(iii) the residue span of the crystallised PPARγ subunit encloses the full length of the LBD (Pro206-Tyr477);

(iv) the complex has the lowest resolution (2.1 Å) compared to the rest of the other PPARγ-rosiglitazone complexes – 4EMA, 3DZY, 2PRG, 3CS8, (Liberato et al., 2012; Chandra at al., 2008; Nolte at al., 1998; Li et al., 2008a), excluding the complex with PDB ID 1ZGY (resolution 1.80 Å; Li et al., 2005) , which lacks the RXRα LBD and, thus, is not a comprehensive representation of the physiological conditions of interest.

Altogether, these considerations make the selected PDB complex a mechanistically justified template for superposition. Since the preliminary superposition on the D-chain produced better RMSDs than the X-chain of the the 1FM6 complex, the latter was used for the final overlay of all bioactive conformations of the PPARγ full agonists. In order to estimate the possible impact of the crystal packing forces on the X-ray ligand conformation, the last was relaxed using the MMFF94s force field and compared with the original structure as extracted from the 1FM6 complex. The superposition on all heavy atoms and on the heteroatoms only (**Figure 38**) revealed just slight deviations with RMSDs of 0.388 Å and 0.377 Å, respectively.

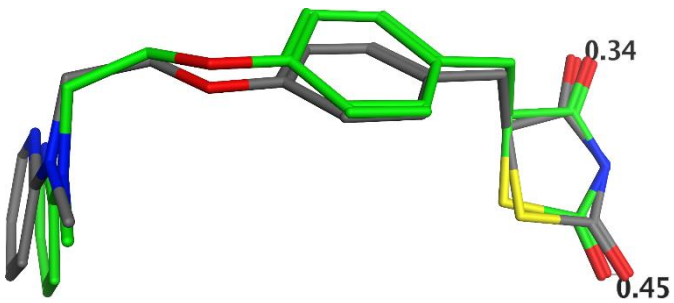

Figure 38. Superposed conformers of rosiglitazone: the X-ray structure as extracted from the complex 1FM6 (in atom type colour) and after optimisation by the MMFF94s force field (carbon atoms are coloured in green). The structures are superposed on the heteroatoms, and the distances between the oxygen atoms in the thiazolidine ring are shown in Å.

As for the heteroatoms relevant to the specific receptor-ligand interactions, albeit the distances between the oxygen atoms (0.34 and 0.45 Å), the nitrogen atoms in the thiazolidine rings were fully overlaid. These results suggested a lack of any significant "tension" in the X-ray conformation, which was further supported by the results of a heavy atoms' superposition, comparing the rosiglitazone's structures extracted from all available complexes (range of the RMSDs: 0.18–0.58 Å; template: rosiglitazone structure from 1FM6 complex, D chain) (**Supplementary table S.6.**). The ligand X-ray structures represent stable bioactive conformations as had been previously underlined upon optimisation of X-ray complexes of another nuclear receptor (human estrogen receptor α) at different levels of protein flexibility (Pencheva et al., 2012). The superposition of 58 full and partial agonists on the PPARγ LBD is shown in **Figure 39a**. **Figure 39b** illustrates the large (~1300 Å3; Nolte et al., 1998), ligand-occupied binding pocket outlined by its surface (within 4.5 Å of the ligand atoms).

The binding pocket has a complex Y-like shape with the so called arms I, II and III, thus allowing for various binding modes and multiple ligands' accommodation. The ligand entry, located between H3 and the β-sheet region, does not coincide with either of the arms but is directed toward their anchor point. Within Arm I, the polar parts of the ligands are directed to H12, which has proved to be crucial for coactivators binding. The analysis of the protein-ligand interactions within the complexes of the nine most active agonists has outlined the amino acid residues forming the receptor-binding pocket (**Figure 40**).

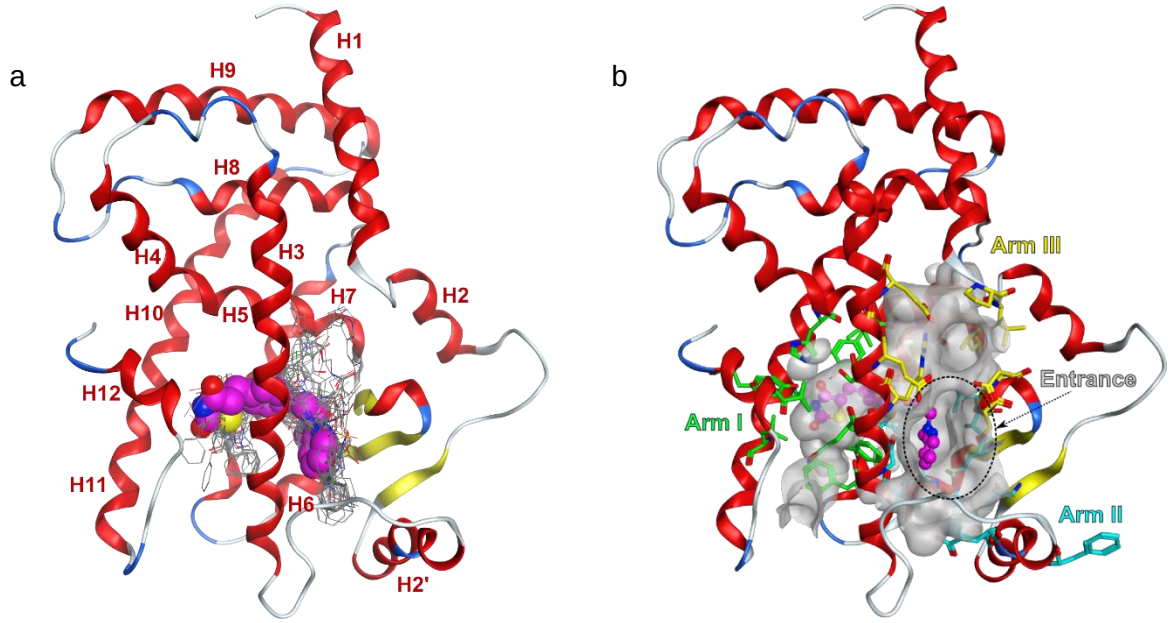

Figure 39. (a) 58 PPARγ agonists superposed in the ligand binding pocket of the receptor on the template complex PDB ID 1FM6 with rosiglitazone (in space-filled rendering and C-atoms coloured in magenta); the other ligands are rendered in lines and coloured according to the atom type; (b) surface map of the binding site (in constant grey colouring) of all agonists and rosiglitazone (in magenta); the different residue colouring designates participation in one of the three "arms" within the binding site: Arm I – green; Arm II – cyan; Arm III – yellow; the entrance to the pocket (outlined with a black dotted line) is located between the arms; the protein backbone is rendered in a ribbon and coloured according to the secondary structure: helix – red; strand – yellow; turn – blue; loop – white; H1–H12 assign the order of the helices in the PPARγ LBD structure.

Indicators for the ligand-driven flexibility of the binding pocket are the sixteen residues detected to participate in protein-ligand interactions in only one or two complexes. Among the 48 residues, 19 are common for the binding sites of all agonists, with Ser289, His323, His449 and Tyr473 (shown in red) involved in hydrogen bond formation. These interactions are illustrated in **Figure 41** of rosiglitazone in the PPARγ complex 1FM6 and GW409544 (PDB ligand ID 544) in complex 1K74 (Xu et al., 2001).

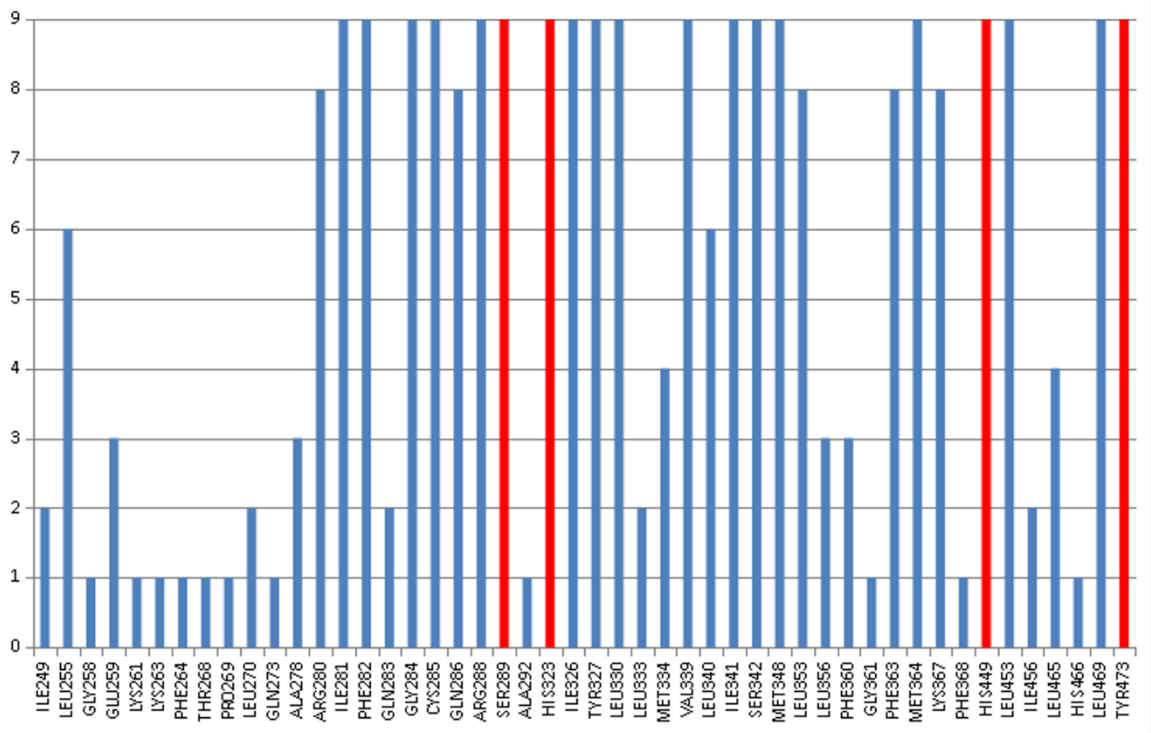

Figure 40. The protein-ligand interaction fingerprints of the nine most active (according to the EC_{50} values in **Supplementary table S.6.**) agonists evinces the number of occurrences of the amino acids involved in the agonists' contacts with the receptor binding pocket; in red – the amino acids that were identified to form hydrogen bonds (HBs) with the most active agonists.

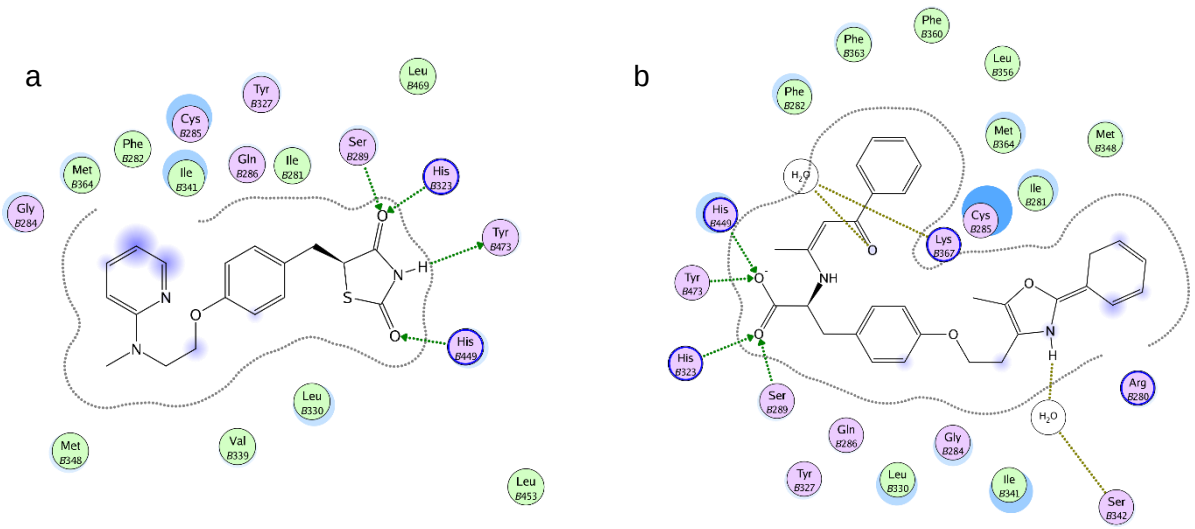

Figure 41. Ligand-interaction diagrams of (a) rosiglitazone and (b) GW409544 within the binding pocket of PPARγ.

Different binding modes were suggested for the full and partial agonists (Bruning et al, 2007) and our inspection of the binding pocket of all complexes has confirmed this observation, emphasising the H12 independent activation of PPARγ by the partial agonists (**Figure 42**).

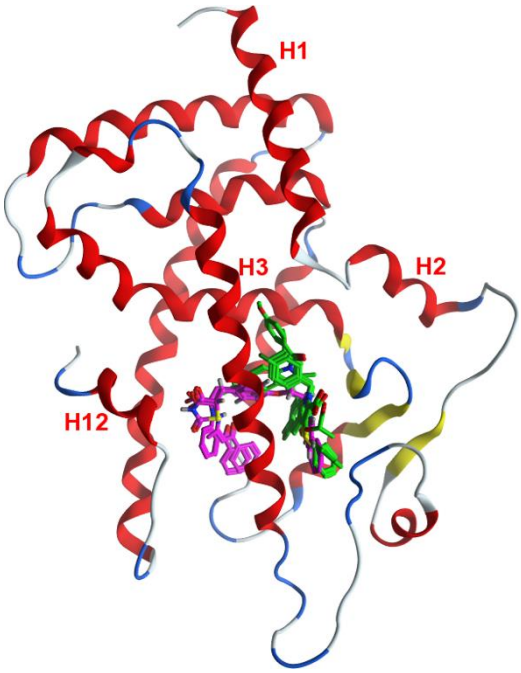

Figure 42. Binding poses of three full agonists (BRL – rosiglitazone; 544 – GW409544 and 570 – farglitazar; in magenta) and three partial agonists (MRL24, SR145, SR147; in green) within the PPARγ binding pocket (template complex 1FM6).

3.3.4. Pharmacophore-based Virtual Screening to predict PPARγ full agonists

3.3.4.1.Pharmacophore model development

The full agonists' complexes selected for pharmacophore modelling were superposed on the template structure 1FM6. Within the range of the calculated RMSD values (0.44 – 1.58 Å; **Supplementary table S.6.**), the complexes were distributed in such a manner that the majority of them shared the interval 0.8–1.2 Å as shown in **Figure 43**.

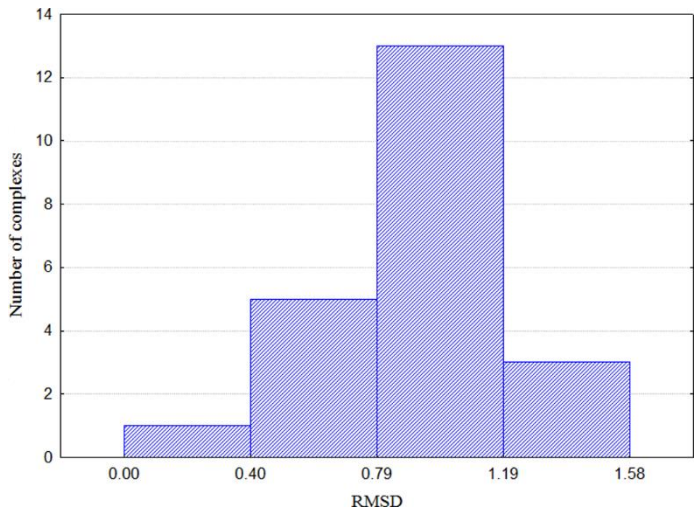

Figure 43. Histogram of the RMSD values (X-axis) of superposed PPARγ-full agonist complexes (Y-axis).

In view of the well aligned helices that enclose the binding site, the observed deviations are to a greatest extent due to the flexibility of the loop between H2' and H3 (**Figure 39a**). This could be rooted in the possible adaptive function of the loop that assists the accommodation of differentially shaped and/or sized ligands, thus maintaining unchanged the positions of the helices in the PPARγ binding site. The stability of the pocket upon ligand binding guaranteed the reliable alignment of the superposed ligands involved in pharmacophore generation. Seven important pharmacophore features were outlined, based on the three most active agonists – rosiglitazone (PDB ID 1FM6), compound 544 (PDB ID 1K74) and compound 570 (PDB ID 1FM9) (**Figure 44**).

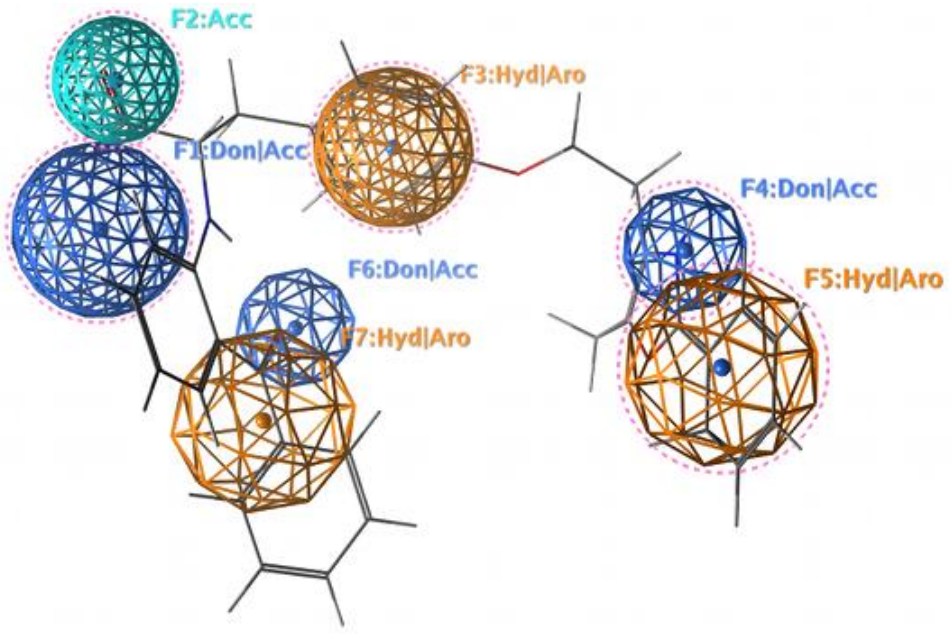

Figure 44. Pharmacophore model of PPARγ full agonists. The features that describe the less restrictive 4/5 point pharmacophore model are surrounded by a dotted line.

They represent two main types of interactions: HB and ionic interactions associated with four polar atoms and functional groups (F1, F2, F4 and F6); and hydrophobic and/or aromatic effects characteristic for three structural elements (F3, F5 and F7). The relative spatial localisation of the latter is crucial for the overall topology of the ligand, which remains anchored within Arms I and II through the terminal features F5 and F7 and is stabilised by the bridging F3. The explicit contribution of the HB and ionic interactions is indirectly mediated by the hydrophobic/aromatic ones which enable the optimal ligand pose into the pocket to ensure protein-ligand interactions that are direct (F1, F2, and F4) or mediated by a water molecule (F6). Details on the mechanistical interpretation of the pharmacophore features are summarised in **Table 9**.

Table 9. Description of the pharmacophore features in the pharmacophore model of the full PPARγ agonists: Don – donor; Acc – acceptor; Hyd – hydrophobic; Aro – aromatic.

Pharmacophore feature	Location	Interactions
F1: Don/Acc	Arm I	Participates in HB interactions (donor and acceptor) with residues His449 (H11) and Tyr473 (H12); responsible for the direct interaction with H12 and stabilises its active position
F2: Acc	Arm I	Participates in HB interactions (acceptor) with Ser289 (H3), His323(H5), Tyr 327 (H5); responsible for the stabilisation of H12 in an active position
F3: Hyd/Aro	Arm I	Fits to the hydrophobic environment; stabilises the positions of F1 and F2 features
F4: Don/Acc	Arm II	Can participate in HB interactions directly or mediated by water molecules with Ser342 (H5), Cys285 (H3) and Arg 288 (H3); stabilises the pose of the ligand into the pocket
F5: Hyd/Aro	Arm II	Fits to the hydrophobic environment; stabilises the pose of the ligand into the pocket
F6: Don/Acc	Arm I	Can participate in HB interactions mediated by water; stabilises the pose of the ligand into the pocket
F7: Hyd/Aro	Arm I	Fits to the hydrophobic environment; stabilises the pose of the ligand into the pocket

For this restrictive pharmacophore model based on the most potent full agonists of PPARγ, further evaluation was performed. A set of 20 full agonists was carefully selected from PDB along with the corresponding potency data (EC_{50} values), based on experimental evidence for full agonistic activity.

A visual inspection of the full agonists as superposed on the 7 pharmacophore features resulted in the generation of substructure-based fingerprints (**Table 10**) and led to the following assumptions:

(i) features F1 or/and F2 and F3 could be outlined as mandatory for full agonism;

(ii) at least one of the features that stabilise the position of the ligand in the pocket (in Arm II – F4 and/or F5 or in Arm I – F6 or/and F7) is necessary for the full agonism.

Since the level of correspondence of the 20 agonists to the 7 feature pharmacophore was related to their activity, the less restrictive 4/5-point pharmacophore model that was built is expected to cover a larger applicability domain (**Figure 44**). Among the previously outlined structural features related to HB and ionic interactions, F1 and F2 were selected as essential within the full agonists' set and F4 – as optional, while the pool of the hydrophobic and aromatic substructures was represented by F3 and F5 only.

A detailed investigation of the 20 full agonists' complexes and the apo-form (1PRG; Nolte et al., 1998) was performed, regarding the HB interactions between H12 and its vicinity, including protein-protein and protein-ligand ones (**Supplementary table S.7.**), leading to the following conclusions:

(i) a number of ligands interact directly with H12 through HBs (e.g. 544, 570, BRL, ZAA), thus fitting with the F1 feature;

(ii) for ligands like M7R, M7S, S44, J53 no interactions are identified with H12; instead, they interact with H3 and/or H5, fitting in this way with the F2 feature;

(iii) unique HBs that take place in complexes only and are not observed in the apo-forms have been found to connect H12 to H3, H4, and H5, thus stabilising its active position (e.g. Ile472 (H12) with Lys319 (H4), Lys474 (after H12) with Lys319 (H4), Tyr477 (after H12) with Glu324 (H5), Hys466 (between H10/11 and H12) with Gln 286 (H3); **Supplementary table S.7.**, highlighted lines);

(iv) for the most active agonists, the H12 stabilising ligand-induced interactions that possibly facilitate coactivator recruitment include: the HB contacts between H12 and H4 as well as those between H12 and H3, which prevail in ligands without F1.

Table 10. Evaluation of the pharmacophore model on a dataset of full agonists: F1–F7, pharmacophore features; +/−, the presence or absence of the particular pharmacophore feature in the particular chemical structure; EC_{50}, transactivation activity; the complexes are ordered according to their EC_{50} values (the lowest value considered when the interval data are reported).

Complex PDB ID	Ligand PDB ID	Pharmacophore features							EC_{50} (nM)
		F1	F2	F3	F4	F5	F6	F7	
1K74	544	+	+	+	+	+	+	+	0.2–2.7
1FM9	570	+	+	+	+	+	+	+	0.339–6
1FM6	BRL	+	+	+	+	+	−	−	2.4–2880
3AN4	M7R	−	+	+	+	+	−	−	3.6
3BC5	ZAA	+	−	+	+	+	+	−	4
3IA6	UNT	+	+	+	+	+	−	−	13
1I7I	AZ2	+	+	+	−	−	−	+	13–3528
3G9E	RO7	+	+	+	+	+	−	−	21
3AN3	M7S	−	+	+	+	+	−	−	22
2ZNO	S44	−	+	+	+	+	−	−	41–70
3GBK	2PQ	+	+	+	+	+	−	−	50
3VJI	J53	−	+	+	−	+	−	−	58
2F4B	EHA	+	−	+	−	+	−	−	70
2Q8S	L92	+	+	+	+	+	−	−	140
1KNU	YPA	+	+	+	+	+	−	+	170
3FEJ	CTM	+	+	+	−	+	−	+	210
2HWR	DRD	+	+	+	−	+	−	−	210
2ATH	3EA	+	+	+	−	+	−	−	230
1NYX	DRF	+	+	+	−	+	−	−	570–600
2GTK	208	+	+	+	+	+	−	+	760
2XKW	P1B	+	+	+	+	+	−	−	1125

3.3.4.2.VS protocol development and validation

Further, a predictive model for PPARγ full agonists was developed as a MOE-based (MOE, v. 2014.0901) VS protocol of three steps: (i) protein preparation (**Section 2.2.1.3.**), (ii) docking of the ligands into the PPARγ binding site (**Section 2.2.5.2.**) and (iii) pharmacophore-based generation and filtering of the full agonists' poses (Tsakovska et al., 2014).

VS protocol validation was performed by the docking of structures from different datasets, using the 5-point pharmacophore model to establish:

(i) Model sensitivity of 85%, where 144 out of 170 PPARγ full agonists selected from the previously collected dataset were correctly predicted as full agonists.

(ii) Model specificity of 44% in relation to the partial agonists, where 38 out of 87 PPARγ partial agonists retrieved from the initial dataset of PPARγ ligands did not pass the filter and were correctly classified as not being full agonists.

(iii) Model specificity of 77% in relation to decoys, where 1949 out of 2527 randomly selected decoys were correctly classified as not being full agonists. Decoys are compounds resembling the receptor binders' physicochemical properties but at the same time topologically dissimilar to minimise the likelihood of actual binding. The random selection of the subset involved extraction of each 10th structure after removal of duplicates from the full set of 25867 PPARγ decoys in DUD-E database (Directory of Useful Decoys – Enhanced, http://dude.docking.org, Mysinger et al., 2012).

While the prediction model for PPARγ full agonists has high sensitivity when discriminating binders from non-binders, discrimination between full and partial agonists is relatively low. The last could be explained by the poorly defined structural differentiation between the two types of agonists sharing the same PPARγ ligand binding pocket. However, for the purposes of the screening, the relatively high number of false positive hits is an acceptable limitation of the approach since its priority is the successful restriction of potentially hepatotoxic PPARγ full agonists.

In summary, the developed pharmacophore model outlines important structural features that are characteristic for PPARγ full agonists. The developed VS protocol is based on a docking algorithm with a pharmacophore filter which involves 5 essential features, thus allowing the identification of the PPARγ full agonists. It is the first step of a combined *in silico* approach for prediction of potential chemical initiators of NAFLD, presented schematically in **Figure 36**. The second step of this alternative approach is discussed in detail in the next section.

3.3.5. 3D QSAR modelling to predict pEC_{50} of PPARγ full agonists

The development of a scientifically sound 3D QSAR model based on the AOP with hepatic MIE implied a careful selection of the dependent variable in order to be:

(i) interpretable in view of the theoretical basis and the inherent limitations of the selected 3D QSAR approach, namely CoMSIA;
(ii) well established, regarding previous modelling attempts;
(iii) biologically relevant to the outlined within the AOP qualitative relationship between PPARγ activation/upregulation and the transcription of its target prosteatotic proteins;
(iv) publicly accepted as a toxicological endpoint.

Although the ligand-induced *in vitro* transactivation (expressed as potency, EC_{50}) covers a series of events, from receptor activation to multiple downstream molecular events triggering gene expression, it starts with receptor binding and thus is expected to be related to the change in the free energy of ligand-receptor complex formation, which is necessary for the CoMSIA modelling. Moreover, the involvement of transactivation activity in computational models has been underlined as both challenging in view of its complex nature and biologically relevant as this endpoint may reflect, in a more complete manner, the molecular determinants of a given pathology (Rücker et al., 2006; Sundriyal et al., 2009). In particular, the toxicity pathways related to the overexpressed PPARγ target proteins are suggested to synergistically drive the NAFLD development and progression as described in the AOP (**Section 3.1.2.1.**). Therefore, *in silico* prediction of PPARγ ligands' transactivation activity is a mechanistically justified rationale for the screening and prioritisation for further testing of potential prosteatotic chemicals. The latter is also supported by the OECD conceptual framework, which includes PPAR transactivation reporter assays among the most promising assays to detect and characterise the chemical effects on the PPAR signaling pathway. These assays are going to be considered for incorporation into new or existing Test Guidelines for the detection of endocrine disrupting chemicals after their refinement and validation (ENV/JM/MONO(2012)23).

A multistep workflow (**Figure 45**) presents the whole 3D QSAR modelling process described below.

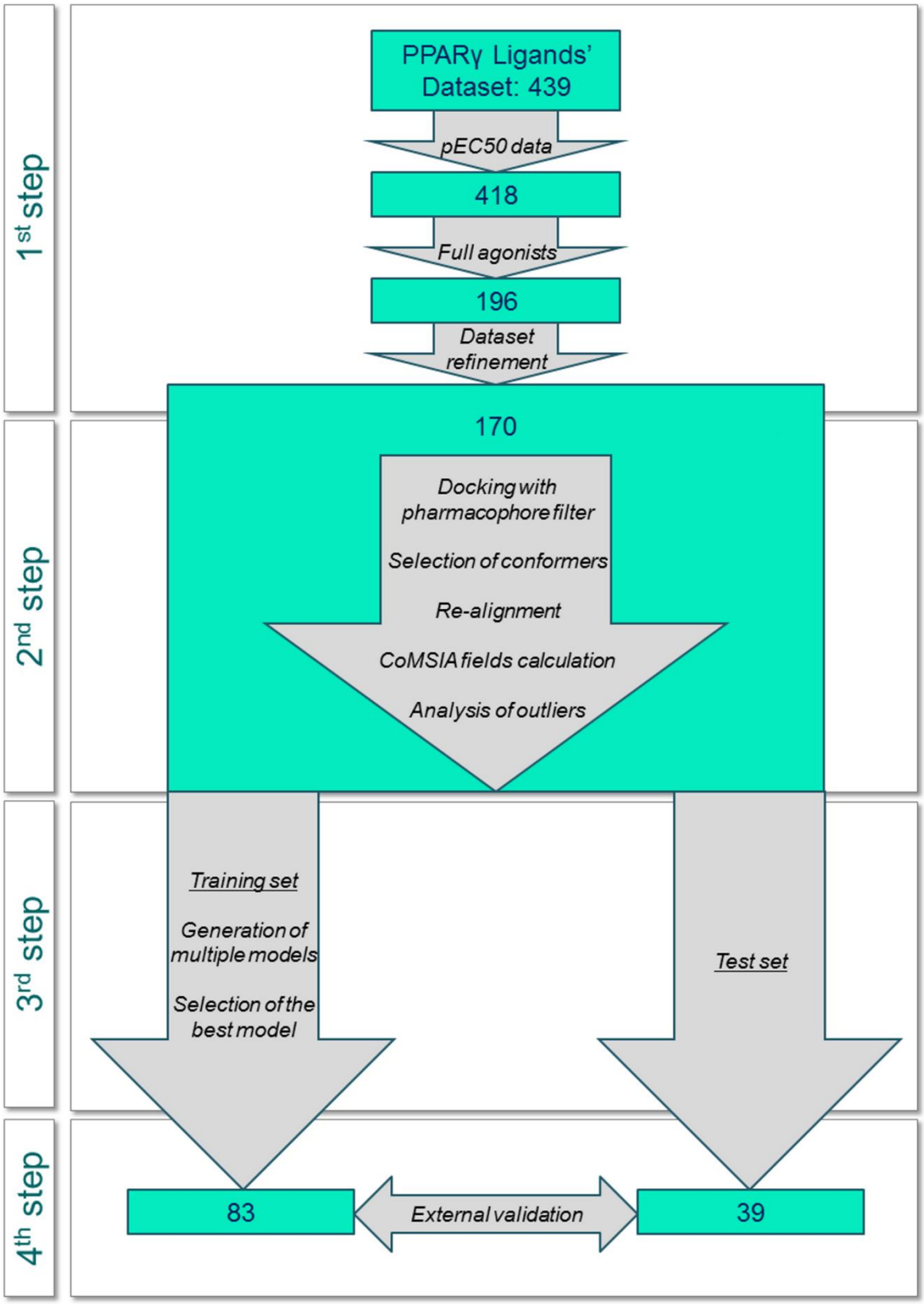

Figure 45. The 3D QSAR modelling workflow to predict the potency of PPARγ full agonists.

3.3.5.1.Dataset processing and structure alignment

The 1st step of the full agonists' selection was performed (Figure 45) according to the criteria in **Section 3.3.2**. The modelling set of 170 ligands from 6 research groups' publications included structures and potency data measured in human (77 ligands) or animal (93 ligands) cell lines. At the 2nd step of the modelling workflow, a structure alignment was performed according to the procedures described in **Section 2.2.4.3.1.** with a 4-feature pharmacophore used as a filter of the generated docking poses. This approach was expected to reproduce the most probable bioactive conformers as well. Based on a preliminary 3D QSAR analysis on the whole dataset and following the criteria defined in **Section 2.2.4.3.2.**, 48 outliers were excluded.

3.3.5.2.Model generation and validation

Since the general performance measures of the preliminary CoMSIA analyses on separated human and animal data were similar, the final analysis covered a combined data set in which nearly 40% of the structures had been tested on human cell lines.

After the outliers' removal, the 3rd step, outlined in **Figure 45,** was splitting the remaining structures into a training set (n=83) assembled to include structures from all selected research groups with a broad structural variety and a wide range of activities (pEC50 = 5.4 – 9.1) and a test set (n=39) with the remaining compounds of similar structural variability and pEC_{50} range (pEC_{50} = 5.5 – 8.1). The robust external validation of the developed model is guaranteed by the relatively high number of the test compounds (about half of the training set). Detailed structural and experimental data regarding the modelled compounds can be found at http://biomed.bas.bg/qsarmm/.

The best CoMSIA model included electrostatic, hydrogen bond acceptor and hydrophobic fields. Its robustness was evaluated through LOO cross-validation procedure based on the cross-validated coefficient q_{cv}^2 = 0.610, the optimal number of principle components N_{opt} = 7, and the cross-validated standard error of prediction, SEP_{CV} = 0.505.

While the statistical parameters are comparable with other pEC_{50}-based models for PPARγ full agonists, the training set considered in this study is the largest of any published. Therefore, a broader applicability domain is achieved by the structural diversity of the modelled compounds, covering as much as possible the available structural data in PDB and the literature.

Ten Y-randomisations were performed to further evaluate the probability of generating a good model by chance. The resulting low average q^2_{cv} = -0.114 and high SEPcv = 0.824 underlined the acceptability of the proposed CoMSIA model. For large redundant datasets the q^2_{cv} obtained from LOO cross-validation may give a false sense of confidence, because a "near-by" molecule with very similar descriptor values to those of each of the omitted molecules is likely to remain in the training data (SYBYL-X, 2013). Therefore, the model's sensitivity to small systemic perturbations of the response variable was assessed by progressive scrambling (maximum: 20 bins, minimum: two bins and critical point: 0.85). The main indications for the robustness of the original unperturbed model are the Q^2 and the dq/dr. Since the introduced noise makes the parameter Q^2 quite conservative, a value of Q^2 above 0.35 is an indication for the robustness of the model. As for the dq/dr – stable models have slopes near unity (SYBYL-X, 2013). Thus, the resulting statistical parameters (Q^2 = 0.437, cSDEP = 0.598, dq/dr = 1.06) further confirmed the stability of the developed CoMSIA model.

At the 4th step, the predictive power of the obtained model was evaluated by external validation and was estimated by the predictive correlation coefficient r_{pred}^2 = 0.552 with training (83) to test set (39) ratio approx. 2:1.

The obtained r_{pred}^2 of the model is comparable to q^2_{cv} and demonstrates a good stability of the predictions in the context of the intra- and inter-laboratory variations in the methodology for measuring the biological data as well as the complex nature of the dependent variable.

Figure 46 presents a plot of the predicted pEC_{50} values obtained by the optimal non-cross-validation 3D QSAR model versus the experimentally observed pEC_{50} values for the training and the test set compounds.

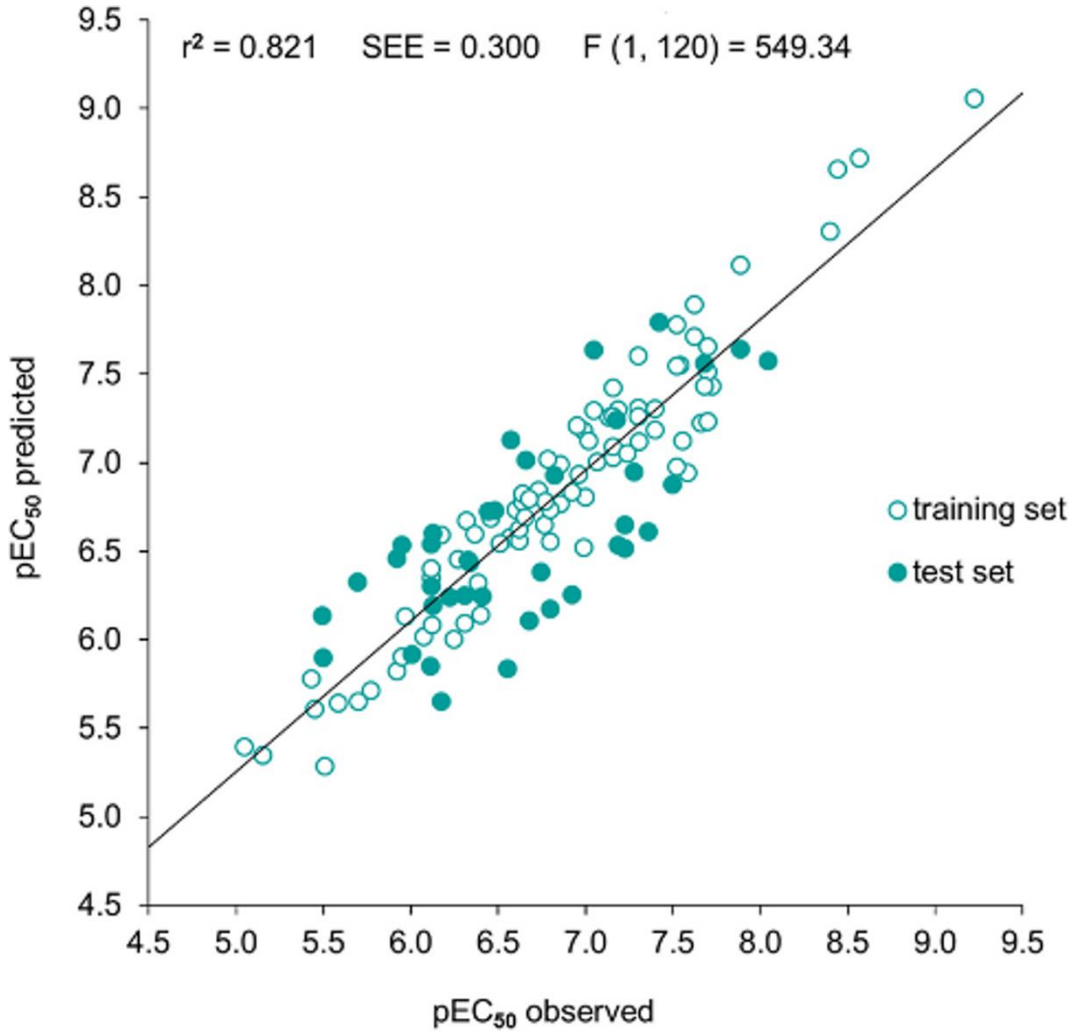

Figure 46. Predicted (pEC_{50} predicted) vs. observed pEC_{50} (pEC_{50} observed) values for training (83) and test (39) set compounds. Regression statistics: r^2 – determination coefficient; SEE – standard error of estimate, F (1, 120) – F-ratio between explained and unexplained variance for the given number of degrees of freedom at 95% level of significance.

The similar fractional contributions of the CoMSIA fields to the differences in the transactivation activity (electrostatic – 0.293, hydrogen bond acceptor – 0.346, hydrophobic – 0.360) indicate that the model is not dominated by any of the three fields. The role of the electrostatic effects has been already emphasised by other authors (Shah et al., 2008; Sundriyal et al., 2009). As for the hydrogen bond acceptor and hydrophobic fields, this is the first pEC_{50}-based 3D QSAR model to explicitly outline their involvement in the pEC_{50} data variations.

The parity between the three types of interactions is not a simple function of their individual contributions but also reflects their synergistic influence on receptor activation. The ligand-receptor interactions are mainly governed by the hydrogen bond acceptor and the electrostatic fields. However, the stabilising role of the hydrophobic effects for the occupancy of the ligand binding domain of PPARγ in terms of optimal orientation and distances of the ligand to key amino acid residues remains significant. These effects have their indirect contribution in driving the electrostatic interactions over the whole interface area and in particular for establishing specific donor-acceptor interactions between the receptor activation helix H12 and the electronegative substructures of the full agonists. Thus, not the simple additivity but the complex interplay between multiple molecular interactions lies in the full agonist-induced stabilisation of the active receptor conformation.

We further analysed the contour maps of our 3D QSAR model and traced out the correspondence between the most contributing CoMSIA molecular fields and the identified pharmacophore features. The contours were estimated by the actual values of the model StDev*Coeff (the standard deviation of the 3D field at each grid point multiplied by the 3D QSAR coefficient) and the contour levels were defined based on the analysis of the field distribution histograms (SYBYL-X, 2013). These maps allow for recognition of regions within the area occupied by the ligands that suggest a particular property field important for the modelled activity.

The analysis of the field contributions allows the characterisation of those spacial features that are mostly responsible for the differences in the observed transactivation activity within the studied series of compounds. This is a good basis for their comparison to the pharmacophore model (**Figure 47**). As seen in the figure, there is a good correspondence between the encapsulated regions of the properties (**Figure 47 a, b and c**) and the pharmacophore features (**Figure 47d**). The relevance of the features F5 and F7 is supported by the corresponding favoured areas (**Figure 47a**; in orange) in the hydrophobic field contour map. The absence of a contour in the area of the pharmacophore feature F3 can be explained by the broad presence of a hydrophobic ring substructure in the compounds within the training set. Further, the appearance of an additional favoured hydrophobic contour in the region between features F1 and F2 outlines the role of a cyclic substructure common for the most active ligands that stabilises the position of the functional groups corresponding to F1 and F2 and thus leads to increased transactivation activity.

The favoured electrostatic field contour (**Figure 47c**; in pink) defines a region where the increased positive charge will result in increased activity, while the disfavoured cyan area suggests that a more negative charge is related to higher activity, instead. These regions perfectly match the donor or/and acceptor features (F1, F2) outlined in the pharmacophore model. In addition, the favoured acceptor contours (**Figure 47b**; in blue) underline the relevance of features F1, F2 and F4.

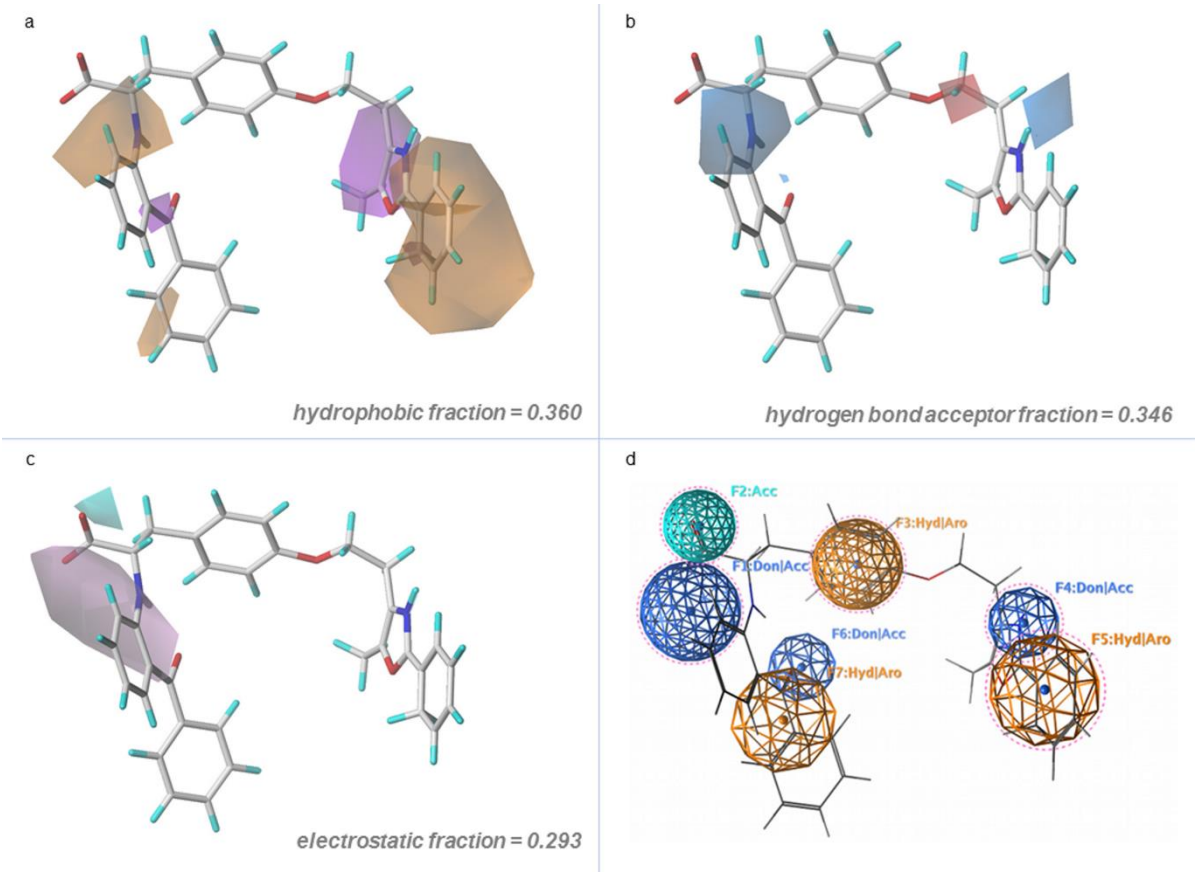

Figure 47. Contour maps (StDev*Coeff) of the favoured/disfavoured CoMSIA fields: (a) hydrophobic (orange/violet at 0.0175/-0.0220 kcal/mol), (b) hydrogen bond acceptor (blue/red at 0.0365/-0.0542 kcal/mol) and (c) electrostatic (pink/cyan at 0.0338/-0.0706 kcal/mol); (d) 7-feature pharmacophore of PPARγ full agonists (shown for comparison). Superimposed onto the maps is the structure of the most active compound (farglitazar, http://biomed.bas.bg/qsarmm/), rendered in sticks and coloured according to the atom type.

3.3.6. Integration of the developed pharmacophore-based VS protocol in battery approaches supporting risk assessment

The developed VS protocol was successfully combined with *in silico* strategies developed in different research groups (Tsakovska et al, 2015; Fioravanzo et al., 2015; Vitcheva et al., 2015) that were focused on:

(i) Consensus molecular modelling of LXRα receptor: Ensemble docking, e-Pharmacophore, fingerprints-based similarity;

(ii) SAR analysis: KNIME workflow (WF) for nuclear receptors (NRs)-mediated liver steatosis alerts (http://knimewebportal.cosmostox.eu/) and ToxPrint Chemotypes Analysis, identifying chemotypes for liver steatosis (Chemotyper, https://chemotyper.org, Yang et al., 2015).

They aimed to identify dual PPARγ/LXR binders and/or to propose an integrated approach to evaluate the prosteatotic potential of predicted PPARγ full agonist. The study showed that molecular modelling and pathology-relevant mining of *in vivo* toxicity data combined with substructure analysis succesfully complement each other within the AOP framework (steps 1 to 4, **Figure 48**).

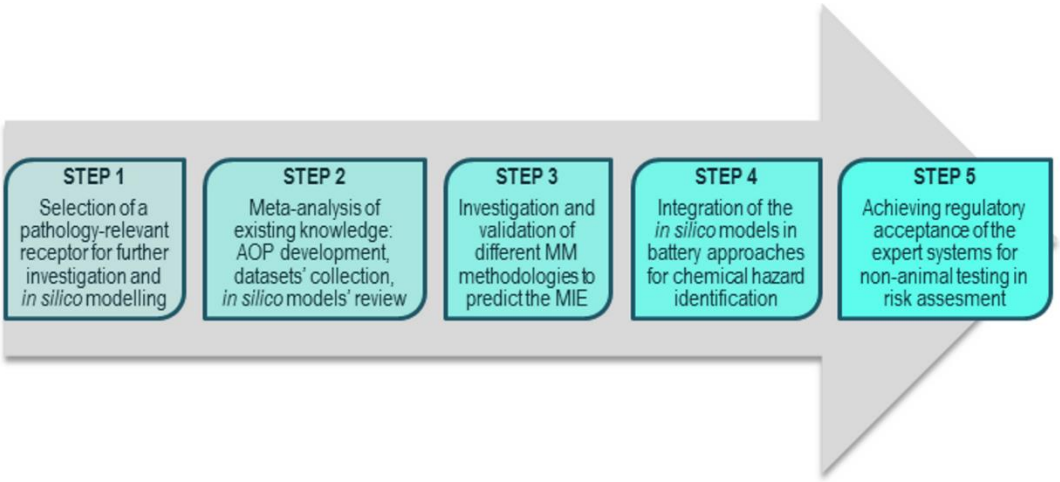

Figure 48. General scheme of the AOP-driven development, validation and integration of *in silico* approaches in expert systems. Modified from Fioravanzo et al. (2015).

Screening of liver toxicity databases was performed to identify potential dual PPARγ/LXRα binders (JRC dataset) or PPARγ full agonists (COSMOS DB). The final aim was to prioritise compounds of potential concern for liver toxicity.

3.3.6.1.Prediction of Dual PPARγ/LXR binders

The JRC case-study dataset included 97 compounds selected for the JRC SEURAT-1 level 2 case study. Among them, 75% were positive (POS) reference chemicals (e.g. experimentally proven to be hepatotoxic). The shaded compounds (**Table 11**) were the hits from the combined application of the rules for structural features and physico-chemical ranges within the KNIME NRs WF with the VS protocol for PPARγ full agonists and the LXR consensus model. Interestingly, sulindac, methotrexate and amodiaquine were classified as dual PPARγ/LXR binders, increasing further their priority for ultimate testing as potential prosteatogenes. Thus, in addition to the already suggested cross-relations between the PPARγ and LXR liver steatosis AOPs (e.g. shared intermediate key events and adverse outcome as well as reciprocal transcriptional regulation), common chemical initiators of the MIEs were identified.

Table 11. JRC case-study dataset chemicals predicted as potential PPARγ full agonists by the VS protocol. The shaded compounds are hits from a battery approach including the VS protocol; the underlined hits are identified as dual PPARγ/LXR binders; NEG – not hepatotoxic compounds; POS – hepatotoxic compounds.

CAS	Name	Hepatotoxicity
111025-46-8	Pioglitazone	NEG
16110-51-3	Cromolyn	NEG
33369-31-2	Zomepirac	NEG
36505-84-7	Buspirone	NEG
38194-50-2	Sulindac	POS
51-03-6	Piperonyl butoxide	POS
59-05-2	Methotrexate	POS
7261-97-4	Dantrolene	POS
86-42-0	Amodiaquine	POS

3.3.6.2.Prediction of piperonyl butoxide

The VS protocol was further combined with the independently performed mechanistic mining of available *in vivo* toxicity data followed by an analysis based on ToxPrint chemotypes (developed by Altamira LLC for FDA CFSAN's CERES). By definition, chemotype is a structural fragment encoded for connectivity and, where required, for physicochemical and electronic properties of atoms, bonds, fragments, and even a whole molecule (Yang et al., 2015). Therefore, the chemotype approach represents a ligand-based screening, driven by empirical prediction of the pathological condition, based on the identification of particular substructures. The procedure was applied to the oRepeatTox DB, part of the COSMOS database (publicly available at: http://cosmosdb.cosmostox.eu) developed within the COSMOS Project. The chemotype analysis matched the substructural fragments present in the chemicals associated with liver steatosis/steatohepatitis/fibrosis with the predefined library of ToxPrint chemotypes. At the same time, the chemicals associated with liver steatosis/steatohepatitis/fibrosis were run through the VS protocol developed. Piperonyl butoxide was identified as a hit through both analyses. Thus it was predicted as a potential prosteatotic PPARγ full agonist (Al Sharif et al., 2016).

This result is a trigger for the development of a next generation *in silico* predictor – the 3D chemotypes for liver steatosis. That involves: (i) coding the essential pharmacophore points as particular substructures extracted from the PPARγ full agonists dataset; (ii) determining the distances between the essential pharmacophoric points; (iii) based on (i) and (ii), coding the disconnected graphs with the spatial distances. At this stage the steps (i) and (ii) have been covered (**Table 12**).

Table 12. Distances (Å) between the essential pharmacophoric points within the PPARγ full agonists

Feature	F1-F2	F1-F3	F1-F5	F2-F3	F2-F5	F3-F5
Average, Å	2.76	6.4	13.1	5.8	13.1	9.3
min÷max, Å	1.9÷3.4	4.9÷9.2	11.2÷15.5	4.4÷7.3	10.8÷15.4	7.1÷11.7

The results above demonstrate that the mechanistically justified integration of multiple approaches (AOPs, molecular modelling, pharmacophore, docking, 3D QSAR and chemotypes) could explain and predict in a more complete manner the complex biological responses characterising the repeated dose toxicity, thus reducing the information gaps and uncertainties that would result from their individual application.

SUMMARY

In summary, the work presented in this thesis has exploited a variety of predictive toxicology methods (pharmacophore modelling, docking, and 3D QSAR analysis) in combination with AOP development in order to investigate the PPARγ-mediated hepatotoxicity and to develop an integrated *in silico* approach supporting hazard identification and characterisation.

On the basis of the collected and systemised experimental evidence, two AOPs focused on the relationship PPARγ dysregulation – NAFLD have been developed, outlining tissue-specific cascades of events initiated by a ligand-induced receptor activation (in liver) or inhibition (in adipose tissue). Moreover, quantitative data have been collected, regarding key events in the liver AOP. The causal relationships within the proposed AOPs underline the relevance of the selected MIEs and emphasise the anchor points for further *in vitro/in silico* exploration. The hepatic AOP, addressing a particular domain of chemical initiators (PPARγ full agonists), became a solid mechanistical basis for the development of predictive models of the MIE as well as their integration in combined approaches.

The structural and biological data for PPARγ full and partial agonists harvested from PDB, ChEMBL and literature sources have resulted in the largest publicly available PPARγ ligands dataset (http://biomed.bas.bg/qsarmm/). It offers high quality data, organised for modelling purposes.

The comprehensive analysis of the key PPARγ-ligand interactions has been performed within the purposefully selected crystallographic complexes, affirming the molecular determinants for the studied MIE and allowing for the development of a pharmacophore model of PPARγ full agonists. Its use within an algorithm for docking into the PPARγ binding pocket produced the core element of a thoroughly validated virtual screening (VS) procedure for identification of full agonists. The successful application of the proposed VS protocol in combination with LXR-based models and chemotype-based read across procedure allowed for the prioritisation of potential prosteatotic chemicals acting as dual PPARγ/LXR binders and for the prediction of the possible mode of action (PPARγ full agonism) of the hepatotoxic piperonyl butoxide.

Using the developed pharmacophore-based docking and the collected full agonists data, a 3D QSAR model has been derived. The CoMSIA approach has been used to correlate the changes in the structures to the variations in their transactivation activities.

The reported goodness-of-fit, robustness and predictivity of the established quantitative structure-activity relationship evidenced the reliability of the model necessary for its regulatory acceptance, while the size and the structural diversity of the training set characterised the superiority of the model's applicability domain compared to previously reported ones.

On the basis of the developed hepatic AOP and predictive molecular models, a mechanistically justified combined *in silico* approach has been proposed to screen for potential prosteatotic chemicals acting through PPARγ full activation (pharmacophore-based VS) and to predict their potency based on characteristic hydrophobic, HB acceptor and electrostatic CoMSIA fields (3D QSAR model).

The developed pathways, dataset and combined *in silico* approach constitute a solid fundamental for further exploration, knowledge transfer and applicability by: (i) AOP refinement and introduction to OECD; (ii) generation of proposals for regulatory assays, which is based on the outlined key events; (iii) development of an enriched PPARγ ligands' database; (iv) further toxicological validation of the developed models against experimentally observed prosteatotic compounds and (v) 3D chemotypes development and validation.

CONTRIBUTIONS

1. **Two tissue-specific AOPs (in liver and in adipose tissue) were developed to link the PPARγ ligand-dependent dysregulation with NAFLD.**
   - Key events within the liver AOP were quantitatively evaluated and the data gaps for further *in vitro* exploration were outlined.
   - The proposed AOPs are a basis for the development of *in silico* models to predict PPARγ ligand-dependent dysregulation and key events in the AOPs.
2. **A dataset with structural and biological data for PPARγ agonists was harvested, curated and released. It is the most complete and largest publicly available dataset of PPARγ agonists (freely available at http://biomed.bas.bg/qsarmm/).**
3. **A pharmacophore model of PPARγ full agonists was build and used for the development of VS protocol.**
   - The developed VS protocol was successfully applied for the prediction of PPARγ full agonistic activity of compounds.
   - The VS protocol was combined with molecular modelling approaches to predict potential dual PPARγ/LXR binders for prioritisation of chemicals of higher concern in view of the expected synergy in their prosteatotic effects.
   - The VS protocol was combined with a chemotype-based read across procedure within an integrated battery approach to predict prosteatotic effects of chemicals and to get an insight into the possible mechanism of the toxic effect (PPARγ full agonism).
4. **A 3D QSAR (CoMSIA) model was developed to predict the transactivation activity of PPARγ full agonists. The model is a good improvement over the previously published ones as it is based on the largest and most structurally diverse dataset, ensuring enlargement of the addressed applicability domain. The statistical parameters resulting from the comprehensive validation performed qualify it as reliable for predictive purposes.**
5. **A two-step *in silico* approach combining the developed VS protocol and 3D QSAR model is proposed for screening and prioritisation of potential prosteatotic ligands.**

DECLARATION FOR ORIGINALITY OF THE RESULTS

I declare that this thesis contains original results obtained within my own research work (with the support and the collaboration of my supervisors). The results that are obtained, reported, and/or published by other scientists, are properly cited in detail in the bibliography.

This thesis has not been submitted for a degree in another higher school, university or research institute.

LITERATURE

37th OECD's Joint Meeting of the Chemicals Committee and the Working Party on Chemicals, Pesticides and Biotechnology, Paris November 17–19, 2004 (http://www.oecd.org/env/ehs/organisationoftheenvironmenthealthandsafetyprogramme.htm)

Ables GP. Update on pparγ and nonalcoholic Fatty liver disease. PPAR Res. 2012;2012:912351. doi: 10.1155/2012/912351. Epub 2012 Aug 16. PubMed PMID: 22966224; PubMed Central PMCID: PMC3431124.

ACD/Labs Percepta suite 2015; Advanced Chemistry development, Inc., http://www.acdlabs.com/products/percepta/

Acton JJ 3rd, Black RM, Jones AB, Moller DE, Colwell L, Doebber TW, Macnaul KL, Berger J, Wood HB. Benzoyl 2-methyl indoles as selective PPARgamma modulators. Bioorg Med Chem Lett. 2005 Jan 17;15(2):357-62. PubMed PMID: 15603954.

Adler S, Basketter D, Creton S, Pelkonen O, van Benthem J, Zuang V, Andersen KE, Angers-Loustau A, Aptula A, Bal-Price A, Benfenati E, Bernauer U, Bessems J, Bois FY, Boobis A, Brandon E, Bremer S, Broschard T, Casati S, Coecke S, Corvi R, Cronin M, Daston G, Dekant W, Felter S, Grignard E, Gundert-Remy U, Heinonen T, Kimber I, Kleinjans J, Komulainen H, Kreiling R, Kreysa J, Leite SB, Loizou G, Maxwell G, Mazzatorta P, Munn S, Pfuhler S, Phrakonkham P, Piersma A, Poth A, Prieto P, Repetto G, Rogiers V, Schoeters G, Schwarz M, Serafimova R, Tähti H, Testai E, van Delft J, van Loveren H, Vinken M, Worth A, Zaldivar JM. Alternative (non-animal) methods for cosmetics testing: current status and future prospects-2010. Arch Toxicol. 2011 May;85(5):367-485. doi: 10.1007/s00204-011-0693-2. Epub 2011 May 1. Review. PubMed PMID: 21533817.

Adverse Outcome Pathway Knowledge Base (AOP-KB), https://aopkb.org/ (last access: 19 August 2015)

Agrawal S, Duseja A. Nonalcoholic Fatty Liver Disease--The Clinician's Perspective. Trop Gastroenterol. 2014 Oct-Dec;35(4):212-21. PubMed PMID: 26349165.

Ahmadian M, Suh JM, Hah N, Liddle C, Atkins AR, Downes M, Evans RM. PPARγ signaling and metabolism: the good, the bad and the future. Nat Med. 2013 May;19(5):557-66. doi: 10.1038/nm.3159. Epub 2013 May 7. Review. PubMed PMID: 23652116; PubMed Central PMCID: PMC3870016.

Al Sharif M, Alov P, Vitcheva V, Pajeva I, Tsakovska I. Modes-of-Action Related to Repeated Dose Toxicity: Tissue-Specific Biological Roles of PPAR γ Ligand-Dependent Dysregulation in Nonalcoholic Fatty Liver Disease. PPAR Res. 2014;2014:432647. doi: 10.1155/2014/432647. Epub 2014 Mar 18. Review. PubMed PMID: 24772164; PubMed Central PMCID: PMC3977565.

Al Sharif M, Tsakovska I, Pajeva I, Alov P, Fioravanzo E, Bassan A, Kovarich S, Yang C, Mostrag-Szlichtyng A, Vitcheva V, Worth AP, Richarz AN, Cronin MTD, The Application of Molecular Modelling in the Safety Assessment of Chemicals: A Case Study on Ligand-Dependent PPARγ Dysregulation, Toxicology, 2016, doi: 10.1016/j.tox.2016.01.009.

Albert JS, Yerges-Armstrong LM, Horenstein RB, Pollin TI, Sreenivasan UT, Chai S, Blaner WS, Snitker S, O'Connell JR, Gong DW, Breyer RJ 3rd, Ryan AS, McLenithan JC, Shuldiner AR, Sztalryd C, Damcott CM. Null mutation in hormone-sensitive lipase gene and risk of type 2 diabetes. N Engl J Med. 2014 Jun 12;370(24):2307-15. doi: 10.1056/NEJMoa1315496. Epub 2014 May 21. PubMed PMID: 24848981; PubMed Central PMCID: PMC4096982.

Alkhouri N, McCullough AJ. Noninvasive Diagnosis of NASH and Liver Fibrosis Within the Spectrum of NAFLD. Gastroenterol Hepatol (N Y). 2012 Oct;8(10):661-8. PubMed PMID: 24683373; PubMed Central PMCID: PMC3969008.

Al-Najjar BO, Wahab HA, Tengku Muhammad TS, Shu-Chien AC, Ahmad Noruddin NA, Taha MO. Discovery of new nanomolar peroxisome proliferator-activated receptor γ activators via elaborate ligand-based modeling. Eur J Med Chem. 2011 Jun;46(6):2513-29. doi: 10.1016/j.ejmech.2011.03.040. Epub 2011 Mar 25. PubMed PMID: 21482446.

Altex Proceedings of the 9th World Congress on Alternatives and Animal Use in the Life Sciences, 24-28 August **2014**, Prague, Czech Republic, Volume 3, No. 1., 2014, ISSN 2194-0479.

Anderson N, Borlak J. Molecular mechanisms and therapeutic targets in steatosis and steatohepatitis. Pharmacol Rev. 2008 Sep;60(3):311-57. doi: 10.1124/pr.108.00001. Review. PubMed PMID: 18922966.

Andrews PR, Drug-receptor interactions in 3D QSAR, In Kubinyi H, (Ed.) 3D QSAR in Drug Design: Vol Drug Design: Volume 1: Theory Methods and Applications, ESCOM, Leiden, 1993, ISBN 90-72199-14-6

Ariens EJ. Affinity and intrinsic activity in the theory of competitive inhibition. I. Problems and theory. Arch Int Pharmacodyn Ther. 1954 Sep 1;99(1):32-49. PubMed PMID: 13229418.

Ayers SD, Nedrow KL, Gillilan RE, Noy N. Continuous nucleocytoplasmic shuttling underlies transcriptional activation of PPARgamma by FABP4. Biochemistry. 2007 Jun 12;46(23):6744-52. Epub 2007 May 22. PubMed PMID: 17516629.

Azhar S. Peroxisome proliferator-activated receptors, metabolic syndrome and cardiovascular disease. Future Cardiol. 2010 Sep;6(5):657-91. doi: 10.2217/fca.10.86. Review. PubMed PMID: 20932114; PubMed Central PMCID: PMC3246744.

Bai L, Jia Y, Viswakarma N, Huang J, Vluggens A, Wolins NE, Jafari N, Rao MS, Borensztajn J, Yang G, Reddy JK. Transcription coactivator mediator subunit MED1 is required for the development of fatty liver in the mouse. Hepatology. 2011 Apr;53(4):1164-74. doi: 10.1002/hep.24155. Erratum in: Hepatology. 2011 Sep 2;54(3):1114. PubMed PMID: 21480322; PubMed Central PMCID: PMC3076129.

Bal-Price A, Crofton KM, Sachana M, Shafer TJ, Behl M, Forsby A, Hargreaves A, Landesmann B, Lein PJ, Louisse J, Monnet-Tschudi F, Paini A, Rolaki A, Schrattenholz A, Suñol C, van Thriel C, Whelan M, Fritsche E. Putative adverse outcome pathways relevant to neurotoxicity. Crit Rev Toxicol. 2015 Jan;45(1):83-91. doi: 10.3109/10408444.2014.981331. Review. PubMed PMID: 25605028.

Barak Y, Nelson MC, Ong ES, Jones YZ, Ruiz-Lozano P, Chien KR, Koder A, Evans RM. PPAR gamma is required for placental, cardiac, and adipose tissue development. Mol Cell. 1999 Oct;4(4):585-95. PubMed PMID: 10549290.

Batista MR, Martínez L. Conformational Diversity of the Helix 12 of the Ligand Binding Domain of PPARγ and Functional Implications. J Phys Chem B. 2015 Dec 17;119(50):15418-29. doi: 10.1021/acs.jpcb.5b09824. Epub 2015 Dec 3. PubMed PMID: 26598113.

Baumann, K.; Stiefl, N. J. Comput. Aided Mol. Des. 2004, 18, 549

Bedogni G, Bellentani S. Fatty liver: how frequent is it and why?. Ann Hepatol. 2004; 3: 63-65; Starley BQ, Calcagno CJ, Harrison SA. Nonalcoholic fatty liver disease and hepatocellular carcinoma: a weighty connection. Hepatology. 2010 May;51(5):1820-32. doi: 10.1002/hep.23594. Review. PubMed PMID: 20432259.

Bénardeau A, Benz J, Binggeli A, Blum D, Boehringer M, Grether U, Hilpert H, Kuhn B, Märki HP, Meyer M, Püntener K, Raab S, Ruf A, Schlatter D, Mohr P. Aleglitazar, a new,

potent, and balanced dual PPARalpha/gamma agonist for the treatment of type II diabetes. Bioorg Med Chem Lett. 2009 May 1;19(9):2468-73. doi: 10.1016/j.bmcl.2009.03.036. Epub 2009 Mar 14. PubMed PMID: 19349176.

Bento AP, Gaulton A, Hersey A, Bellis LJ, Chambers J, Davies M, Krüger FA, Light Y, Mak L, McGlinchey S, Nowotka M, Papadatos G, Santos R, Overington JP. The ChEMBL bioactivity database: an update. Nucleic Acids Res. 2014 Jan;42(Database issue):D1083-90. doi: 10.1093/nar/gkt1031. Epub 2013 Nov 7. PubMed PMID: 24214965; PubMed Central PMCID: PMC3965067

Berger J, Bailey P, Biswas C, Cullinan CA, Doebber TW, Hayes NS, Saperstein R, Smith RG, Leibowitz MD. Thiazolidinediones produce a conformational change in peroxisomal proliferator-activated receptor-gamma: binding and activation correlate with antidiabetic actions in db/db mice. Endocrinology. 1996 Oct;137(10):4189-95. PubMed PMID: 8828476

Berger J, Moller DE. The mechanisms of action of PPARs. Annu Rev Med. 2002;53:409-35. Review. PubMed PMID: 11818483.

Berman HM, Westbrook J, Feng Z, Gilliland G, Bhat TN, Weissig H, Shindyalov IN, Bourne PE. The Protein Data Bank. Nucleic Acids Res. 2000 Jan 1;28(1):235-42. PubMed PMID: 10592235; PubMed Central PMCID: PMC102472.

Berthold, M. R.; Cebron, N.; Dill, F.; Gabriel, T. R.; Kötter, T.; Meinl, T.; Ohl, P.; Sieb, C.; Thiel, K.; Wiswedel, B. KNIME: The Konstanz Information Miner. In Studies in Classification, Data Analysis, and Knowledge Organisation (GfKL 2007); Springer, 2007

Bhatia LS, Curzen NP, Calder PC, Byrne CD. Non-alcoholic fatty liver disease: a new and important cardiovascular risk factor? Eur Heart J. 2012 May;33(10):1190-200. doi: 10.1093/eurheartj/ehr453. Epub 2012 Mar 8. Review. PubMed PMID: 22408036.

Bishop-Bailey D, Wray J. Peroxisome proliferator-activated receptors: a critical review on endogenous pathways for ligand generation. Prostaglandins Other Lipid Mediat. 2003 Apr;71(1-2):1-22. Review. PubMed PMID: 12749590.;

Blaauboer BJ, Barratt MD, Houston JB. The Integrated Use of Alternative Methods in Toxicological Risk Evaluation - ECVAM Integrated Testing Strategies Task Force Report 1. Altern Lab Anim. 1999 Mar-Apr;27(2):229-37. PubMed PMID: 25426587.

Boobis AR, Cohen SM, Dellarco V, McGregor D, Meek ME, Vickers C, Willcocks D, Farland W. IPCS framework for analyzing the relevance of a cancer mode of action for humans. Crit Rev Toxicol. 2006 Nov-Dec;36(10):781-92. PubMed PMID: 17118728.

Boobis AR, Doe JE, Heinrich-Hirsch B, Meek ME, Munn S, Ruchirawat M, Schlatter J, Seed J, Vickers C. IPCS framework for analyzing the relevance of a noncancer mode of action for humans. Crit Rev Toxicol. 2008;38(2):87-96. doi: 10.1080/10408440701749421. Review. PubMed PMID: 18259981.

Brown JD, Plutzky J. Peroxisome proliferator-activated receptors as transcriptional nodal points and therapeutic targets. Circulation. 2007 Jan 30;115(4):518-33. Review. PubMed PMID: 17261671.

Bruning JB, Chalmers MJ, Prasad S, Busby SA, Kamenecka TM, He Y, Nettles KW, Griffin PR. Partial agonists activate PPARgamma using a helix 12 independent mechanism. Structure. 2007 Oct;15(10):1258-71. PubMed PMID: 17937915.

Bugge A, Mandrup S. Molecular Mechanisms and Genome-Wide Aspects of PPAR Subtype Specific Transactivation. PPAR Res. 2010;2010. pii: 169506. doi: 10.1155/2010/169506. Epub 2010 Aug 31. PubMed PMID: 20862367; PubMed Central PMCID: PMC2938449.

Burden N, Mahony C, Müller BP, Terry C, Westmoreland C, Kimber I. Aligning the 3Rs with new paradigms in the safety assessment of chemicals. Toxicology. 2015 Apr 1;330:62-6. Review. PubMed PMID: 25932488.

Burgermeister E, Seger R. MAPK kinases as nucleo-cytoplasmic shuttles for PPARgamma. Cell Cycle. 2007 Jul 1;6(13):1539-48. Epub 2007 May 18. Review. PubMed PMID: 17611413.

Carrieri A, Giudici M, Parente M, De Rosas M, Piemontese L, Fracchiolla G, Laghezza A, Tortorella P, Carbonara G, Lavecchia A, Gilardi F, Crestani M, Loiodice F. Molecular determinants for nuclear receptors selectivity: chemometric analysis, dockings and site-directed mutagenesis of dual peroxisome proliferator-activated receptors α/γ agonists. Eur J Med Chem. 2013 May;63:321-32. doi: 10.1016/j.ejmech.2013.02.015. Epub 2013 Feb 24. PubMed PMID: 23502212.

Casimiro-Garcia A, Bigge CF, Davis JA, Padalino T, Pulaski J, Ohren JF, McConnell P, Kane CD, Royer LJ, Stevens KA, Auerbach B, Collard W, McGregor C, Song K. Synthesis and evaluation of novel alpha-heteroaryl-phenylpropanoic acid derivatives as

PPARalpha/gamma dual agonists. Bioorg Med Chem. 2009 Oct 15;17(20):7113-25. doi: 10.1016/j.bmc.2009.09.001. Epub 2009 Sep 6. PubMed PMID: 19783444.

Casimiro-Garcia A, Bigge CF, Davis JA, Padalino T, Pulaski J, Ohren JF, McConnell P, Kane CD, Royer LJ, Stevens KA, Auerbach BJ, Collard WT, McGregor C, Fakhoury SA, Schaum RP, Zhou H. Effects of modifications of the linker in a series of phenylpropanoic acid derivatives: Synthesis, evaluation as PPARalpha/gamma dual agonists, and X-ray crystallographic studies. Bioorg Med Chem. 2008 May 1;16(9):4883-907. doi: 10.1016/j.bmc.2008.03.043. Epub 2008 Mar 20. PubMed PMID: 18394907.

Chabowski A, Górski J, Luiken JJ, Glatz JF, Bonen A. Evidence for concerted action of FAT/CD36 and FABPpm to increase fatty acid transport across the plasma membrane. Prostaglandins Leukot Essent Fatty Acids. 2007 Nov-Dec;77(5-6):345-53. Review. PubMed PMID: 18240411.

Chandra V, Huang P, Hamuro Y, Raghuram S, Wang Y, Burris TP, Rastinejad F. Structure of the intact PPAR-gamma-RXR- nuclear receptor complex on DNA. Nature. 2008 Nov 20;456(7220):350-6. doi: 10.1038/nature07413. PubMed PMID: 19043829; PubMed Central PMCID: PMC2743566.

Chawla A, Boisvert WA, Lee CH, Laffitte BA, Barak Y, Joseph SB, Liao D, Nagy L, Edwards PA, Curtiss LK, Evans RM, Tontonoz P. A PPAR gamma-LXR-ABCA1 pathway in macrophages is involved in cholesterol efflux and atherogenesis. Mol Cell. 2001 Jan;7(1):161-71. PubMed PMID: 11172721.

Chawla A, Schwarz EJ, Dimaculangan DD, Lazar MA. Peroxisome proliferator-activated receptor (PPAR) gamma: adipose-predominant expression and induction early in adipocyte differentiation. Endocrinology. 1994 Aug;135(2):798-800. PubMed PMID: 8033830.

Chen W, Chang B, Saha P, Hartig SM, Li L, Reddy VT, Yang Y, Yechoor V, Mancini MA, Chan L. Berardinelli-seip congenital lipodystrophy 2/seipin is a cell-autonomous regulator of lipolysis essential for adipocyte differentiation. Mol Cell Biol. 2012 Mar;32(6):1099-111. doi: 10.1128/MCB.06465-11. Epub 2012 Jan 23. PubMed PMID: 22269949; PubMed Central PMCID: PMC3295006.

Cherkasov A, Muratov EN, Fourches D, Varnek A, Baskin II, Cronin M, Dearden J, Gramatica P, Martin YC, Todeschini R, Consonni V, Kuz'min VE, Cramer R, Benigni R, Yang C, Rathman J, Terfloth L, Gasteiger J, Richard A, Tropsha A. QSAR modeling: where have

you been? Where are you going to? J Med Chem. 2014 Jun 26;57(12):4977-5010. doi: 10.1021/jm4004285. Epub 2014 Jan 6. PubMed PMID: 24351051; PubMed Central PMCID: PMC4074254.;

Chigurupati S, Dhanaraj SA, Balakumar P. A step ahead of PPARγ full agonists to PPARγ partial agonists: therapeutic perspectives in the management of diabetic insulin resistance. Eur J Pharmacol. 2015 May 15;755:50-7. doi: 10.1016/j.ejphar.2015.02.043. Epub 2015 Mar 5. Review. PubMed PMID: 25748601.

Choi SS, Kim ES, Koh M, Lee SJ, Lim D, Yang YR, Jang HJ, Seo KA, Min SH, Lee IH, Park SB, Suh PG, Choi JH. A novel non-agonist peroxisome proliferator-activated receptor γ (PPARγ) ligand UHC1 blocks PPARγ phosphorylation by cyclin-dependent kinase 5 (CDK5) and improves insulin sensitivity. J Biol Chem. 2014 Sep 19;289(38):26618-29. doi: 10.1074/jbc.M114.566794. Epub 2014 Aug 6. PubMed PMID: 25100724; PubMed Central PMCID: PMC4176243.

Clark AJ, The Mode of Action of Drugs on Cells, London: Edward Arnold, 1933

Clark, R.D., Sprous, D.G. and Leonard, J.M., In Ho¨ ltje, H.-D. and Sippl, W. (Eds.), Rational Approaches to Drug Design, Prous Science, Barcelona, Spain, 2001, pp. 475– 485.

COM(2013) 135 final, Communication from the Commission to the European Parliament and the Council on the animal testing and marketing ban and on the state of play in relation to alternative methods in the field of cosmetics, Brussels, 11.3.2013

Combes RD. *In silico* methods for toxicity prediction. Adv Exp Med Biol. 2012; 745:96-116. doi: 10.1007/978-1-4614-3055-1_7. Review. PubMed PMID: 22437815.

Costa V, Gallo MA, Letizia F, Aprile M, Casamassimi A, Ciccodicola A. PPARG: Gene Expression Regulation and Next-Generation Sequencing for Unsolved Issues. PPAR Res. 2010;2010. pii: 409168. doi: 10.1155/2010/409168. Epub 2010 Sep 8. PubMed PMID: 20871817; PubMed Central PMCID: PMC2943117.

Cronet P, Petersen JF, Folmer R, Blomberg N, Sjöblom K, Karlsson U, Lindstedt EL, Bamberg K. Structure of the PPARalpha and -gamma ligand binding domain in complex with AZ 242; ligand selectivity and agonist activation in the PPAR family. Structure. 2001 Aug;9(8):699-706. PubMed PMID: 11587644.

Cronin M T D and Livingstone D J, Predicting chemical toxicity and fate, CRC Press, ISBN 0-415-27180-0 2004

Cronin M T D and Richarz A N, Mode of action working group: use of mode of action related to repeated dose systemic toxicity—a framework for capturing Information, in Towards

the Replacement of *In Vivo* Repeated Dose Systemic Toxicity TestIng, T. Gocht andM. Schwarz, Eds., vol. 2,pp. 284–289, 2012.

Cronin M., *In Silico* Toxicology Principles And Applications, 2010, ISBN 13: 9781849730044

Day C. Thiazolidinediones: a new class of antidiabetic drugs. Diabet Med. 1999 Mar;16(3):179-92. Review. PubMed PMID: 10227562.

Dixit A, Saxena AK. QSAR analysis of PPAR-gamma agonists as anti-diabetic agents. Eur J Med Chem. 2008 Jan;43(1):73-80. Epub 2007 Mar 18. PubMed PMID:17482722.

Ebdrup S, Pettersson I, Rasmussen HB, Deussen HJ, Frost Jensen A, Mortensen SB, Fleckner J, Pridal L, Nygaard L, Sauerberg P. Synthesis and biological and structural characterization of the dual-acting peroxisome proliferator-activated receptor alpha/gamma agonist ragaglitazar. J Med Chem. 2003 Apr 10;46(8):1306-17. PubMed PMID: 12672231.

ECETOC (2007). Intelligent testing strategies in ecotoxicology: mode of action approach for specifically acting chemicals. Technical Report 102. Brussels, Belgium.

ECHA (2008), Guidance on information requirements and chemical safety assessment Chapter R.6: QSARs and grouping of chemicals, May, 2008.

ECHA (2013), Guidance on Information Requirements and Chemical Safety Assessment, Chapter R. 7a-Endpoint Specific Guidance, ECHA, Helsinki, Finland, 2013.

Edwards IJ, Berquin IM, Sun H, O'Flaherty JT, Daniel LW, Thomas MJ, Rudel LL, Wykle RL, Chen YQ: Differential effects of delivery of omega-3 fatty acids to human cancer cells by low-density lipoproteins versus albumin. Clin Cancer Res 2004, 10(24):8275–8283.

EFSA (2014), Appendix. A – *In silico* methods for environmental fate and (eco)toxicity In Technical report on a systematic procedure for the identification of emerging chemical risks in the food and feed chain, European Food Safety Authority supporting publication, 2014: EN-547

Ehehalt R, Sparla R, Kulaksiz H, Herrmann T, Füllekrug J, Stremmel W. Uptake of long chain fatty acids is regulated by dynamic interaction of FAT/CD36 with cholesterol/sphingolipid enriched microdomains (lipid rafts). BMC Cell Biol. 2008 Aug 13;9:45. doi: 10.1186/1471-2121-9-45. PubMed PMID: 18700980; PubMed Central PMCID: PMC2533316.

Ehrlich P, Present status of chemotherapy, Ber. Dtsch. Chem. Ges., 1909, 42, 17–47

.

European Food Safety Authority (EFSA),TECHNICAL REPORT: A systematic procedure for the identification of emerging chemical risks in the food and feed chain Appendix. A - *In silico* methods for environmental fate and (eco)toxicity), Parma, Italy, 2014, EFSA supporting publication 2014:EN-547

Fakhrudin N, Ladurner A, Atanasov AG, Heiss EH, Baumgartner L, Markt P, Schuster D, Ellmerer EP, Wolber G, Rollinger JM, Stuppner H, Dirsch VM. Computer-aided discovery, validation, and mechanistic characterisation of novel neolignan activators of peroxisome proliferator-activated receptor gamma. Mol Pharmacol. 2010 Apr;77(4):559-66. doi: 10.1124/mol.109.062141. Epub 2010 Jan 11. PubMed PMID: 20064974; PubMed Central PMCID: PMC3523390.

FAO/WHO (2008) Codex Alimentarius Commission procedural manual, 18th ed. Rome, Food and Agriculture Organization of the United Nations, Codex Alimentarius Commission (ftp://ftp.fao.org/codex/Publications/ProcManuals/Manual_18e.pdf)

Fiévet C, Fruchart JC, Staels B. PPARalpha and PPARgamma dual agonists for the treatment of type 2 diabetes and the metabolic syndrome. Curr Opin Pharmacol. 2006 Dec;6(6):606-14. Epub 2006 Sep 14. Review. PubMed PMID: 16973418.

Fioravanzo E, Kovarich C, Bassan A, Ciacci A, Al Sharif M, Pajeva I, Alov P, Richarz AN, Worth AP, Palczewska A, Steinmetz FP, Yang C, Tsakovska I (2015) Use of molecular modelling approaches for the evaluation of potential binding to nuclear receptors involved in liver steatosis, SEURAT-1 Final Symposium, 4 December 2015, Brussels, Belgium

Flach RJ, Qin H, Zhang L, Bennett AM. Loss of mitogen-activated protein kinase phosphatase-1 protects from hepatic steatosis by repression of cell death-inducing DNA fragmentation factor A (DFFA)-like effector C (CIDEC)/fat-specific protein 27. J Biol Chem. 2011 Jun 24;286(25):22195-202. doi: 10.1074/jbc.M110.210237. Epub 2011 Apr 26. PubMed PMID: 21521693; PubMed Central PMCID: PMC3121364.

Fothergill JM. On Digitalis: Its Mode of Action and its Use. Br Med J. 1871 Jul 1;2(548):5-7. PubMed PMID: 20746286; PubMed Central PMCID: PMC2261609.

Fournier T, Tsatsaris V, Handschuh K, Evain-Brion D. PPARs and the placenta. Placenta. 2007 Feb-Mar;28(2-3):65-76. Epub 2006 Jul 10. Review. PubMed PMID: 16834993.

Fowler BA. Biomarkers in toxicology and risk assessment. EXS. 2012;101:459-70. doi: 10.1007/978-3-7643-8340-4_16. Review. PubMed PMID: 22945579.

Gaemers IC, Stallen JM, Kunne C, Wallner C, van Werven J, Nederveen A, Lamers WH. Lipotoxicity and steatohepatitis in an overfed mouse model for non-alcoholic fatty liver disease. Biochim Biophys Acta. 2011 Apr;1812(4):447-58. doi: 10.1016/j.bbadis.2011.01.003. Epub 2011 Jan 7. PubMed PMID: 21216282.

Gampe RT Jr, Montana VG, Lambert MH, Miller AB, Bledsoe RK, Milburn MV, Kliewer SA, Willson TM, Xu HE. Asymmetry in the PPARgamma/RXRalpha crystal structure reveals the molecular basis of heterodimerization among nuclear receptors. Mol Cell. 2000 Mar;5(3):545-55. PubMed PMID: 10882139.

García-Monzón C, Lo Iacono O, Crespo J, Romero-Gómez M, García-Samaniego J, Fernández-Bermejo M, Domínguez-Díez A, Rodríguez de Cía J, Sáez A, Porrero JL, Vargas-Castrillón J, Chávez-Jiménez E, Soto-Fernández S, Díaz A, Gallego-Durán R, Madejón A, Miquilena-Colina ME. Increased soluble CD36 is linked to advanced steatosis in nonalcoholic fatty liver disease. Eur J Clin Invest. 2014 Jan;44(1):65-73. doi: 10.1111/eci.12192. Epub 2013 Nov 23. PubMed PMID: 24134687.

Garg A. Acquired and inherited lipodystrophies. N Engl J Med. 2004 Mar 18;350(12):1220-34. Review. PubMed PMID: 15028826.

Gaulton A, Bellis LJ, Bento AP, Chambers J, Davies M, Hersey A, Light Y, McGlinchey S, Michalovich D, Al-Lazikani B, Overington JP. ChEMBL: a large-scale bioactivity database for drug discovery. Nucleic Acids Res. 2012 Jan;40(Database issue):D1100-7. doi: 10.1093/nar/gkr777. Epub 2011 Sep 23. PubMed PMID: 21948594; PubMed Central PMCID: PMC3245175.

Gee VM, Wong FS, Ramachandran L, Sethi G, Kumar AP, Yap CW. Identification of novel peroxisome proliferator-activated receptor-gamma (PPARγ) agonists using molecular modeling method. J Comput Aided Mol Des. 2014 Nov;28(11):1143-51. doi: 10.1007/s10822-014-9791-6. Epub 2014 Aug 29. PubMed PMID: 25168706.

Geenen S, Taylor PN, Snoep JL, Wilson ID, Kenna JG, Westerhoff HV. Systems biology tools for toxicology. Arch Toxicol. 2012 Aug;86(8):1251-71. doi: 10.1007/s00204-012-0857-8. Epub 2012 May 9. Review. PubMed PMID: 22569772.; Hartung T, Hoffmann S. Food for thought ... on *in silico* methods in toxicology. ALTEX. 2009;26(3):155-66. PubMed PMID: 19907903.;

Geng T, Xia L, Russo S, Kamara D, Cowart LA. Prosteatotic genes are associated with unsaturated fat suppression of saturated fat-induced hepatic steatosis in C57BL/6 mice.

Nutr Res. 2015 Sep;35(9):812-22. doi: 10.1016/j.nutres.2015.06.012. Epub 2015 Jul 2. PubMed PMID: 26277244.

Glatz JF. Lipids and lipid binding proteins: a perfect match. Prostaglandins Leukot Essent Fatty Acids. 2015 Feb;93:45-9. doi: 10.1016/j.plefa.2014.07.011. Epub 2014 Jul 19. Review. PubMed PMID: 25154384.

Gleeson MP, Modi S, Bender A, Robinson RL, Kirchmair J, Promkatkaew M, Hannongbua S, Glen RC. The challenges involved in modeling toxicity data *in silico*: a review. Curr Pharm Des. 2012;18(9):1266-91. Review. PubMed PMID: 22316153.

Gocht T, Berggren E, Ahr HJ, Cotgreave I, Cronin MT, Daston G, Hardy B, Heinzle E, Hescheler J, Knight DJ, Mahony C, Peschanski M, Schwarz M, Thomas RS, Verfaillie C, White A, Whelan M. The SEURAT-1 approach towards animal free human safety assessment. ALTEX. 2015;32(1):9-24. doi: http://dx.doi.org/10.14573/altex.1408041. Epub 2014 Nov 5. PubMed PMID: 25372315.

Goebel M, Wolber G, Markt P, Staels B, Unger T, Kintscher U, Gust R. Characterisation of new PPARgamma agonists: benzimidazole derivatives-importance of positions 5 and 6, and computational studies on the binding mode. Bioorg Med Chem. 2010 Aug 15;18(16):5885-95. doi: 10.1016/j.bmc.2010.06.102. Epub 2010 Jul 3. PubMed PMID: 20656494.

Gonzalez IC, Lamar J, Iradier F, Xu Y, Winneroski LL, York J, Yumibe N, Zink R, Montrose-Rafizadeh C, Etgen GJ, Broderick CL, Oldham BA, Mantlo N. Design and synthesis of a novel class of dual PPARgamma/delta agonists. Bioorg Med Chem Lett. 2007 Feb 15;17(4):1052-5. Epub 2006 Nov 15. PubMed PMID: 17129725.

Graham DJ, Ouellet-Hellstrom R, MaCurdy TE, Ali F, Sholley C, Worrall C, Kelman JA. Risk of acute myocardial infarction, stroke, heart failure, and death in elderly Medicare patients treated with rosiglitazone or pioglitazone. JAMA. 2010 Jul 28;304(4):411-8. doi: 10.1001/jama.2010.920. Epub 2010 Jun 28. PubMed PMID: 20584880.

Greenberg AS, Coleman RA, Kraemer FB, McManaman JL, Obin MS, Puri V, Yan QW, Miyoshi H, Mashek DG. The role of lipid droplets in metabolic disease in rodents and humans. J Clin Invest. 2011 Jun;121(6):2102-10. doi: 10.1172/JCI46069. Epub 2011 Jun 1. Review. PubMed PMID: 21633178; PubMed Central PMCID: PMC3104768.

Grether U, Bénardeau A, Benz J, Binggeli A, Blum D, Hilpert H, Kuhn B, Märki HP, Meyer M, Mohr P, Püntener K, Raab S, Ruf A, Schlatter D. Design and biological evaluation

of novel, balanced dual PPARalpha/gamma agonists. ChemMedChem. 2009 Jun;4(6):951-6. doi: 10.1002/cmdc.200800425. PubMed PMID: 19326383.

Grossman SL, Lessem J. Mechanisms and clinical effects of thiazolidinediones. Expert Opin Investig Drugs. 1997 Aug;6(8):1025-40. PubMed PMID: 15989661.

Grygiel-Górniak B. Peroxisome proliferator-activated receptors and their ligands: nutritional and clinical implications--a review. Nutr J. 2014 Feb 14;13:17. doi: 10.1186/1475-2891-13-17. Review. PubMed PMID: 24524207; PubMed Central PMCID: PMC3943808.

Guasch L, Sala E, Castell-Auví A, Cedó L, Liedl KR, Wolber G, Muehlbacher M, Mulero M, Pinent M, Ardévol A, Valls C, Pujadas G, Garcia-Vallvé S. Identification of PPARgamma partial agonists of natural origin (I): development of a virtual screening procedure and *in vitro* validation. PLoS One. 2012;7(11):e50816. doi: 10.1371/journal.pone.0050816. Epub 2012b Nov 30. PubMed PMID: 23226391; PubMed Central PMCID: PMC3511273.

Guasch L, Sala E, Mulero M, Valls C, Salvadó MJ, Pujadas G, Garcia-Vallvé S. Identification of PPARgamma partial agonists of natural origin (II): *in silico* prediction in natural extracts with known antidiabetic activity. PLoS One. 2013;8(2):e55889. doi: 10.1371/journal.pone.0055889. Epub 2013 Feb 6. PubMed PMID: 23405231; PubMed Central PMCID: PMC3566095.

Guasch L, Sala E, Valls C, Blay M, Mulero M, Arola L, Pujadas G, Garcia-Vallvé S. Structural insights for the design of new PPARgamma partial agonists with high binding affinity and low transactivation activity. J Comput Aided Mol Des. 2011 Aug;25(8):717-28. doi: 10.1007/s10822-011-9446-9. Epub 2011 Jun 21. PubMed PMID: 21691811.

Guasch L, Sala E, Valls C, Mulero M, Pujadas G, Garcia-Vallvé S. Development of docking-based 3D-QSAR models for PPARgamma full agonists. J Mol Graph Model. 2012a Jun;36:1-9. doi: 10.1016/j.jmgm.2012.03.001. Epub 2012 Mar 14. PubMed PMID: 22503857.

Guo Y, Cordes KR, Farese RV Jr, Walther TC. Lipid droplets at a glance. J Cell Sci. 2009 Mar 15;122(Pt 6):749-52. doi: 10.1242/jcs.037630. PubMed PMID: 19261844; PubMed Central PMCID: PMC2714424.

Gwon SY, Ahn JY, Kim TW, Ha TY. Zanthoxylum piperitum DC ethanol extract suppresses fat accumulation in adipocytes and high fat diet-induced obese mice by regulating adipogenesis. J Nutr Sci Vitaminol (Tokyo). 2012;58(6):393-401. PubMed PMID: 23419397.

Handberg A, Højlund K, Gastaldelli A, Flyvbjerg A, Dekker JM, Petrie J, Piatti P, Beck-Nielsen H; RISC Investigators. Plasma sCD36 is associated with markers of atherosclerosis, insulin resistance and fatty liver in a nondiabetic healthy population. J Intern Med. 2012 Mar;271(3):294-304. doi: 10.1111/j.1365-2796.2011.02442.x. Epub 2011 Sep 14. PubMed PMID: 21883535.

Hartung T, Hoffmann S. Food for thought ... on *in silico* methods in toxicology. ALTEX. 2009;26(3):155-66. PubMed PMID: 19907903.

He J, Lee JH, Febbraio M, Xie W. The emerging roles of fatty acid translocase/CD36 and the aryl hydrocarbon receptor in fatty liver disease. Exp Biol Med (Maywood). 2011 Oct;236(10):1116-21. doi: 10.1258/ebm.2011.011128. Epub 2011 Sep 1. Review. PubMed PMID: 21885479.

He Q, Li JK, Li F, Li RG, Zhan GQ, Li G, Du WX, Tan HB. Mechanism of action of gypenosides on type 2 diabetes and non-alcoholic fatty liver disease in rats. World J Gastroenterol. 2015 Feb 21;21(7):2058-66. doi: 10.3748/wjg.v21.i7.2058. PubMed PMID: 25717238; PubMed Central PMCID: PMC4326140.

He Z, Zhu HH, Bauler TJ, Wang J, Ciaraldi T, Alderson N, Li S, Raquil MA, Ji K, Wang S, Shao J, Henry RR, King PD, Feng GS. Nonreceptor tyrosine phosphatase Shp2 promotes adipogenesis through inhibition of p38 MAP kinase. Proc Natl Acad Sci U S A. 2013 Jan 2;110(1):E79-88. doi: 10.1073/pnas.1213000110. Epub 2012 Dec 10. PubMed PMID: 23236157; PubMed Central PMCID: PMC3538237.

Heim M, Johnson J, Boess F, Bendik I, Weber P, Hunziker W, Fluhmann B: Phytanic acid, a natural peroxisome proliferator-activated receptor (PPAR) agonist, regulates glucose metabolism in rat primary hepatocytes. FASEB J 2002, 16(7):718–720.

Hemmeryckx B, Gaekens M, Gallacher DJ, Lu HR, Lijnen HR. Effect of rosiglitazone on liver structure and function in genetically diabetic Akita mice. Basic Clin Pharmacol Toxicol. 2013 Nov;113(5):353-60. doi: 10.1111/bcpt.12104. Epub 2013 Jul 11. PubMed PMID: 23789962.

Hengstler JG, Marchan R, Leist M. Highlight report: towards the replacement of *in vivo* repeated dose systemic toxicity testing. Arch Toxicol. 2012 Jan;86(1):13-5. doi: 10.1007/s00204-011-0798-7. PubMed PMID: 22187068.

Henke BR, Blanchard SG, Brackeen MF, Brown KK, Cobb JE, Collins JL, Harrington WW Jr, Hashim MA, Hull-Ryde EA, Kaldor I, Kliewer SA, Lake DH, Leesnitzer LM, Lehmann JM, Lenhard JM, Orband-Miller LA, Miller JF, Mook RA Jr, Noble SA, Oliver W Jr,

Parks DJ, Plunket KD, Szewczyk JR, Willson TM. N-(2-Benzoylphenyl)-L-tyrosine PPARgamma agonists. 1. Discovery of a novel series of potent antihyperglycemic and antihyperlipidemic agents. J Med Chem. 1998 Dec 3;41(25):5020-36. PubMed PMID: 9836620.

Höltje HD, Sippl W, Rognan D, Folkers D, Molecular Modeling: Basic Principles and Applications, 3rd Revised edition, WILEY-VCH Verlag GmbH & Co. KGaA, 2004, ISBN: 978-0-471-47878-2

http://biomed.bas.bg/qsarmm/

http://cactus.nci.nih.gov

http://cosmosdb.cosmostox.eu

http://knimewebportal.cosmostox.eu/

https://www.ebi.ac.uk/chembl/

Hu E, Tontonoz P, Spiegelman BM. Transdifferentiation of myoblasts by the adipogenic transcription factors PPAR gamma and C/EBP alpha. Proc Natl Acad Sci U S A. 1995 Oct 10;92(21):9856-60. PubMed PMID: 7568232; PubMed Central PMCID:PMC40901.

Huh D, Hamilton GA, Ingber DE. From 3D cell culture to organs-on-chips. Trends Cell Biol. 2011 Dec;21(12):745-54. doi: 10.1016/j.tcb.2011.09.005. Epub 2011 Oct 25. Review. PubMed PMID: 22033488; PubMed Central PMCID: PMC4386065.

Hwang CS, Loftus TM, Mandrup S, Lane MD. Adipocyte differentiation and leptin expression. Annu Rev Cell Dev Biol. 1997;13:231-59. Review. PubMed PMID: 9442874.

IPCS (2004) Risk assessment terminology. Geneva, World Health Organisation, International Programme on Chemical Safety.

Itoh T, Fairall L, Amin K, Inaba Y, Szanto A, Balint BL, Nagy L, Yamamoto K, Schwabe JW. Structural basis for the activation of PPARgamma by oxidized fatty acids. Nat Struct Mol Biol. 2008 Sep;15(9):924-31. PubMed PMID: 19172745; PubMed Central PMCID: PMC2939985.

Houck KA, Richard AM, Judson RS, Martin MT, Reif DM, and Shah I, ToxCast: predicting toxicity potential through high-throughput bioactivity profiling In High-Throughput ScreenIng Methods in Toxicity TestIng, P. Steinberg, Ed., pp. 1–31, JohnWiley & Sons, Hoboken, NJ, USA, 2013.

Kamenecka TM, Busby SA, Kumar N, Choi JH, Banks AS, Vidovic D, Cameron MD, Schurer SC, Mercer BA, Hodder P, Spiegelman BM, Griffin PR. Potent Anti-Diabetic Actions

of a Novel Non-Agonist PPARγ Ligand that Blocks Cdk5-Mediated Phosphorylation. 2011 Jul 5 [updated 2013 Mar 7]. Probe Reports from the NIH Molecular Libraries Program [Internet]. Bethesda (MD): National Center for Biotechnology Information (US); 2010-. Available from http://www.ncbi.nlm.nih.gov/books/NBK143191/PubMed PMID: 23762958.

Kang SI, Kim MH, Shin HS, Kim HM, Hong YS, Park JG, Ko HC, Lee NH, Chung WS, Kim SJ. A water-soluble extract of Petalonia binghamiae inhibits the expression of adipogenic regulators in 3T3-L1 preadipocytes and reduces adiposity and weight gain in rats fed a high-fat diet. J Nutr Biochem. 2010 Dec;21(12):1251-7. doi: 10.1016/j.jnutbio.2009.11.008. Epub 2010 Mar 23. PubMed PMID: 20332066.

Kawano Y, Cohen DE. Mechanisms of hepatic triglyceride accumulation in non-alcoholic fatty liver disease. J Gastroenterol. 2013 Apr;48(4):434-41. doi: 10.1007/s00535-013-0758-5. Epub 2013 Feb 9. Review. PubMed PMID: 23397118; PubMed Central PMCID: PMC3633701.

Keller DA, Juberg DR, Catlin N, Farland WH, Hess FG, Wolf DC, Doerrer NG. Identification and characterisation of adverse effects in 21st century toxicology. Toxicol Sci. 2012 Apr;126(2):291-7. doi: 10.1093/toxsci/kfr350. Epub 2012 Jan 19. PubMed PMID: 22262567; PubMed Central PMCID: PMC3307604.

Kim E, Li K, Lieu C, Tong S, Kawai S, Fukutomi T, Zhou Y, Wands J, Li J. Expression of apolipoprotein C-IV is regulated by Ku antigen/peroxisome proliferator-activated receptor gamma complex and correlates with liver steatosis. J Hepatol. 2008 Nov;49(5):787-98. doi: 10.1016/j.jhep.2008.06.029. Epub 2008 Sep 7. PubMed PMID: 18809223; PubMed Central PMCID: PMC2644636.

Klebe G, Abraham U, Mietzner T. Molecular similarity indices in a comparative analysis (CoMSIA) of drug molecules to correlate and predict their biological activity. J Med Chem. 1994 Nov 25;37(24):4130-46. PubMed PMID: 7990113.

Klebe G, Comparative molecular similarity indices analysis: CoMSIA, In Kubinyi H, Folkers G and Martin YC (Eds.) 3D QSAR in Drug Design: Vol 3, Kluwer Academic Publishers, Dordrecht, Boston, London, 1998, p. 87-104

Kouskoumvekaki, I.; Petersen, R.K.; Fratev, F.; Taboureau, O.; Nielsen, T.E.; Oprea, T.I.; Sonne, S.B.; Flindt, E.N.; Jónsdóttir, S.Ó.; Kristiansen, K. Discovery of a Novel Selective PPARγ Ligand with Partial Agonist Binding Properties by Integrated *in Silico*/*in Vitro* Work Flow. J. Chem. Inf. Model. 2013, 53, 923–937.

Krewski D., Acosta D. Jr., Andersen M., Anderson H., Bailar J.C. 3rd, Boekelheide K., Brent R., Charnley G., Cheung V.G., Green S. Jr, Kelsey K.T., Kerkvliet N.I., Li A.A., McCray L., Meyer O., Patterson R.D., Pennie W., Scala R.A., Solomon G.M., Stephens M., Yager J., Zeise L., 2010. Toxicity testing in the 21st century: a vision and a strategy. J. Toxicol. Environ. Health. B. Crit. Rev. 13, 51-138. doi: 10.1080/10937404.2010.483176

Kubinyi H, Comparative molecular field analysis (CoMFA). In: SchleyerP.V.R., Allinger NL, Clark T, Gasteiger J, Kollman P., Schaefer HF, Schreiner PR III, editors. The Encyclopedia of Computational Chemistry. Chichester, UK: John Wiley & Sons; p. 448–460, 1998

Kubinyi H, QSAR: Hansch Analysis and Related Approaches, In Mannhold R, Krogsgaard-Larsen P, Timmerman H (Eds.) Methods and principles in medicinal chemistry ; Vol. I), Weinheim- ; New York ; Basil ; Cambridge ; Tokyo : VCH, 1993

Kubota N, Terauchi Y, Miki H, Tamemoto H, Yamauchi T, Komeda K, Satoh S, Nakano R, Ishii C, Sugiyama T, Eto K, Tsubamoto Y, Okuno A, Murakami K, Sekihara H, Hasegawa G, Naito M, Toyoshima Y, Tanaka S, Shiota K, Kitamura T, Fujita T, Ezaki O, Aizawa S, Kadowaki T, et al. PPAR gamma mediates high-fat diet-induced adipocyte hypertrophy and insulin resistance. Mol Cell. 1999 Oct;4(4):597-609. Larter CZ, Yeh MM, Williams J, Bell-Anderson KS, Farrell GC. MCD-induced steatohepatitis is associated with hepatic adiponectin resistance and adipogenic transformation of hepatocytes. J Hepatol. 2008 Sep;49(3):407-16. doi: 10.1016/j.jhep.2008.03.026. Epub 2008 Apr 30. PubMed PMID: 18534710. PubMed PMID: 10549291.

Kuhn B, Hilpert H, Benz J, Binggeli A, Grether U, Humm R, Märki HP, Meyer M, Mohr P. Structure-based design of indole propionic acids as novel PPARalpha/gamma co-agonists. Bioorg Med Chem Lett. 2006 Aug 1;16(15):4016-20. Epub 2006 Jun 5. PubMed PMID: 16737814.

Kumadaki S, Karasawa T, Matsuzaka T, Ema M, Nakagawa Y, Nakakuki M, Saito R, Yahagi N, Iwasaki H, Sone H, Takekoshi K, Yatoh S, Kobayashi K, Takahashi A, Suzuki H, Takahashi S, Yamada N, Shimano H. Inhibition of ubiquitin ligase F-box and WD repeat domain-containing 7α (Fbw7α) causes hepatosteatosis through Krüppel-like factor 5 (KLF5)/peroxisome proliferator-activated receptor γ2 (PPARγ2) pathway but not SREBP-1c protein in mice. J Biol Chem. 2011 Nov 25;286(47):40835-46. doi:

10.1074/jbc.M111.235283. Epub 2011 Sep 12. PubMed PMID: 21911492; PubMed Central PMCID: PMC3220464.

Kursawe R, Narayan D, Cali AM, Shaw M, Pierpont B, Shulman GI, Caprio S. Downregulation of ADIPOQ and PPARγ2 gene expression in subcutaneous adipose tissue of obese adolescents with hepatic steatosis. Obesity (Silver Spring). 2010 Oct;18(10):1911-7. doi: 10.1038/oby.2010.23. Epub 2010 Feb 18. PubMed PMID: 20168312; PubMed Central PMCID: PMC3898705.

Kurtz M, Capobianco E, Careaga V, Martinez N, Mazzucco MB, Maier M, Jawerbaum A. Peroxisome proliferator-activated receptor ligands regulate lipid content, metabolism, and composition in fetal lungs of diabetic rats. J Endocrinol. 2014 Feb 10;220(3):345-59. doi: 10.1530/JOE-13-0362. Print 2014 Mar. PubMed PMID: 24389592.

Kus V, Flachs P, Kuda O, Bardova K, Janovska P, Svobodova M, Jilkova ZM, Rossmeisl M, Wang-Sattler R, Yu Z, Illig T, Kopecky J. Unmasking differential effects of rosiglitazone and pioglitazone in the combination treatment with n-3 fatty acids in mice fed a high-fat diet. PLoS One. 2011;6(11):e27126. doi: 10.1371/journal.pone.0027126. Epub 2011 Nov 3. PubMed PMID: 22073272; PubMed Central PMCID: PMC3207833.

Kuwabara N, Oyama T, Tomioka D, Ohashi M, Yanagisawa J, Shimizu T, Miyachi H. Peroxisome proliferator-activated receptors (PPARs) have multiple binding points that accommodate ligands in various conformations: phenylpropanoic acid-type PPAR ligands bind to PPAR in different conformations, depending on the subtype. J Med Chem. 2012 Jan 26;55(2):893-902. doi: 10.1021/jm2014293. Epub 2012 Jan 10. PubMed PMID: 22185225.

Lamers C, Schubert-Zsilavecz M, Merk D. Therapeutic modulators of peroxisome proliferator-activated receptors (PPAR): a patent review (2008-present). Expert Opin Ther Pat. 2012 Jul;22(7):803-41. doi: 10.1517/13543776.2012.699042. Epub 2012 Jun 15. Review. PubMed PMID: 22697317.

Landesmann B., Goumenou M., Munn S., and Whelan M., Description of prototype modes-of-action related to repeated dose toxicity, Reference Report By the Joint Research Centre of the European Commission, Institute for Health and Consumer Protection, 2012.

Larter CZ, Yeh MM, Van Rooyen DM, Teoh NC, Brooling J, Hou JY, Williams J, Clyne M, Nolan CJ, Farrell GC. Roles of adipose restriction and metabolic factors in progression of steatosis to steatohepatitis in obese, diabetic mice. J Gastroenterol Hepatol. 2009

Oct;24(10):1658-68. doi: 10.1111/j.1440-1746.2009.05996.x. PubMed PMID: 19788606.

Le TA, Loomba R. Management of Non-alcoholic Fatty Liver Disease and Steatohepatitis. J Clin Exp Hepatol. 2012 Jun;2(2):156-73. doi: 10.1016/S0973-6883(12)60104-2. Epub 2012 Jul 21. PubMed PMID: 25755424; PubMed Central PMCID: PMC3940181.;

Lee YJ, Ko EH, Kim JE, Kim E, Lee H, Choi H, Yu JH, Kim HJ, Seong JK, Kim KS, Kim JW. Nuclear receptor PPARγ-regulated monoacylglycerol O-acyltransferase 1 (MGAT1) expression is responsible for the lipid accumulation in diet-induced hepatic steatosis. Proc Natl Acad Sci U S A. 2012 Aug 21;109(34):13656-61. doi: 10.1073/pnas.1203218109. Epub 2012 Aug 6. PubMed PMID: 22869740; PubMed Central PMCID: PMC3427113.

Lefils-Lacourtablaise J, Socorro M, Géloën A, Daira P, Debard C, Loizon E, Guichardant M, Dominguez Z, Vidal H, Lagarde M, Bernoud-Hubac N. The eicosapentaenoic acid metabolite 15-deoxy-δ(12,14)-prostaglandin J3 increases adiponectin secretion by adipocytes partly via a PPARγ-dependent mechanism. PloS One. 2013 May 29;8(5):e63997. doi: 10.1371/journal.pone.0063997. Print 2013. PubMed PMID: 23734181; PubMed Central PMCID: PMC3666990.

Lefterova MI, Lazar MA. New developments in adipogenesis. Trends Endocrinol Metab. 2009 Apr;20(3):107-14. doi: 10.1016/j.tem.2008.11.005. Epub 2009 Mar 9. Review. PubMed PMID: 19269847.

Lewis SN, Garcia Z, Hontecillas R, Bassaganya-Riera J, Bevan DR. Pharmacophore modeling improves virtual screening for novel peroxisome proliferator-activated receptor-gamma ligands. J Comput Aided Mol Des. 2015 May;29(5):421-39. doi: 10.1007/s10822-015-9831-x. Epub 2015 Jan 24. PubMed PMID: 25616366; PubMed Central PMCID: PMC4395532.

Li Y, Choi M, Suino K, Kovach A, Daugherty J, Kliewer SA, Xu HE. Structural and biochemical basis for selective repression of the orphan nuclear receptor liver receptor homolog 1 by small heterodimer partner. Proc Natl Acad Sci U S A. 2005 Jul 5;102(27):9505-10. Epub 2005 Jun 23. PubMed PMID: 15976031; PubMed Central PMCID: PMC1157103.

Li Y, Dong J, Ding T, Kuo MS, Cao G, Jiang XC, Li Z. Sphingomyelin synthase 2 activity and liver steatosis: an effect of ceramide-mediated peroxisome proliferator-activated receptor γ2 suppression. Arterioscler Thromb Vasc Biol. 2013 Jul;33(7):1513-20. doi:

10.1161/ATVBAHA.113.301498. Epub 2013 May 2. PubMed PMID: 23640498; PubMed Central PMCID: PMC3784343.

Li Y, Kovach A, Suino-Powell K, Martynowski D, Xu HE. Structural and biochemical basis for the binding selectivity of peroxisome proliferator-activated receptor gamma to PGC-1alpha. J Biol Chem. 2008a Jul 4;283(27):19132-9. doi: 10.1074/jbc.M802040200. Epub 2008 May 9. PubMed PMID: 18469005; PubMed Central PMCID: PMC2441548.

Li Y, Zhang J, Schopfer FJ, Martynowski D, Garcia-Barrio MT, Kovach A, Suino-Powell K, Baker PR, Freeman BA, Chen YE, Xu HE. Molecular recognition of nitrated fatty acids by PPAR gamma. Nat Struct Mol Biol. 2008b Aug;15(8):865-7. doi: 10.1038/nsmb.1447. Epub 2008 Jul 6. PubMed PMID: 18604218; PubMed Central PMCID: PMC2538624.

Liao C, Xie A, Zhou J, Shi L, Li Z, Lu XP. 3D QSAR studies on peroxisome proliferator-activated receptor gamma agonists using CoMFA and CoMSIA. J Mol Model. 2004 Jun;10(3):165-77. Epub 2004 Mar 12. PubMed PMID: 15022104.

Liao Z, Dong J, Wu W, Yang T, Wang T, Guo L, Chen L, Xu D, Wen F. Resolvin D1 attenuates inflammation in lipopolysaccharide-induced acute lung injury through a process involving the PPARγ/NF-κB pathway. Respir Res. 2012 Dec 2;13:110. doi: 10.1186/1465-9921-13-110. PubMed PMID: 23199346; PubMed Central PMCID: PMC3545883.

Liberato MV, Nascimento AS, Ayers SD, Lin JZ, Cvoro A, Silveira RL, Martínez L, Souza PC, Saidemberg D, Deng T, Amato AA, Togashi M, Hsueh WA, Phillips K, Palma MS, Neves FA, Skaf MS, Webb P, Polikarpov I. Medium chain fatty acids are selective peroxisome proliferator activated receptor (PPAR) γ activators and pan-PPAR partial agonists. PLoS One. 2012;7(5):e36297. doi: 10.1371/journal.pone.0036297. Epub 2012 May 23. PubMed PMID: 22649490; PubMed Central PMCID: PMC3359336.

Lin CH, Peng YH, Coumar MS, Chittimalla SK, Liao CC, Lyn PC, Huang CC, Lien TW, Lin WH, Hsu JT, Cheng JH, Chen X, Wu JS, Chao YS, Lee HJ, Juo CG, Wu SY, Hsieh HP. Design and structural analysis of novel pharmacophores for potent and selective peroxisome proliferator-activated receptor gamma agonists. J Med Chem. 2009 Apr 23;52(8):2618-22. doi: 10.1021/jm801594x. PubMed PMID: 19301897.

Lu Y, Guo Z, Guo Y, Feng J, Chu F. Design, synthesis, and evaluation of 2-alkoxydihydrocinnamates as PPAR agonists. Bioorg Med Chem Lett. 2006 Feb 15;16(4):915-9. Epub 2005 Nov 21. PubMed PMID: 16300944.

Luconi M, Cantini G, Serio M. Peroxisome proliferator-activated receptor gamma (PPARgamma): Is the genomic activity the only answer? Steroids. 2010 Aug-Sep;75(8-9):585-94. doi: 10.1016/j.steroids.2009.10.012. Epub 2009 Nov 10. Review. PubMed PMID: 19900469.

Machado M, Marques-Vidal P, Cortez-Pinto H. Hepatic histology in obese patients undergoing bariatric surgery. J Hepatol. 2006 Oct;45(4):600-6. Epub 2006 Jul 25. PubMed PMID: 16899321.

Maciejewska D, Ossowski P, Drozd A, Ryterska K, Jamioł-Milc D, Banaszczak M, Kaczorowska M, Sabinicz A, Raszeja-Wyszomirska J, Stachowska E. Metabolites of arachidonic acid and linoleic acid in early stages of non-alcoholic fatty liver disease-A pilot study. Prostaglandins Other Lipid Mediat. 2015 Sep;121(Pt B):184-9. doi: 10.1016/j.prostaglandins.2015.09.003. Epub 2015 Sep 25. PubMed PMID: 26408952.

Magliano DC, Bargut TC, de Carvalho SN, Aguila MB, Mandarim-de-Lacerda CA, Souza-Mello V. Peroxisome proliferator-activated receptors-alpha and gamma are targets to treat offspring from maternal diet-induced obesity in mice. PLoS One. 2013 May 20;8(5):e64258. doi: 10.1371/journal.pone.0064258. Print 2013. PubMed PMID: 23700465; PubMed Central PMCID: PMC3658968.

Mahindroo N, Huang CF, Peng YH, Wang CC, Liao CC, Lien TW, Chittimalla SK, Huang WJ, Chai CH, Prakash E, Chen CP, Hsu TA, Peng CH, Lu IL, Lee LH, Chang YW, Chen WC, Chou YC, Chen CT, Goparaju CM, Chen YS, Lan SJ, Yu MC, Chen X, Chao YS, Wu SY, Hsieh HP. Novel indole-based peroxisome proliferator-activated receptor agonists: design, SAR, structural biology, and biological activities. J Med Chem. 2005 Dec 29;48(26):8194-208. PubMed PMID: 16366601.

Mahindroo N, Peng YH, Lin CH, Tan UK, Prakash E, Lien TW, Lu IL, Lee HJ, Hsu JT, Chen X, Liao CC, Lyu PC, Chao YS, Wu SY, Hsieh HP. Structural basis for the structure-activity relationships of peroxisome proliferator-activated receptor agonists. J Med Chem. 2006b Oct 19;49(21):6421-4. PubMed PMID: 17034149.

Mahindroo N, Wang CC, Liao CC, Huang CF, Lu IL, Lien TW, Peng YH, Huang WJ, Lin YT, Hsu MC, Lin CH, Tsai CH, Hsu JT, Chen X, Lyu PC, Chao YS, Wu SY, Hsieh HP. Indol-1-yl acetic acids as peroxisome proliferator-activated receptor agonists: design, synthesis, structural biology, and molecular docking studies. J Med Chem. 2006a Feb 9;49(3):1212-6. PubMed PMID: 16451087.

Manteiga S, Choi K, Jayaraman A, Lee K. Systems biology of adipose tissue metabolism: regulation of growth, signaling and inflammation. Wiley Interdiscip Rev Syst Biol Med. 2013 Jul-Aug;5(4):425-47. doi: 10.1002/wsbm.1213. Epub 2013 Feb 13. Review. PubMed PMID: 23408581.

Marciano DP, Kuruvilla DS, Boregowda SV, Asteian A, Hughes TS, Garcia-Ordonez R, Corzo CA, Khan TM, Novick SJ, Park H, Kojetin DJ, Phinney DG, Bruning JB, Kamenecka TM, Griffin PR. Pharmacological repression of PPARγ promotes osteogenesis. Nat Commun. 2015 Jun 12;6:7443. doi: 10.1038/ncomms8443. PubMed PMID: 26068133; PubMed Central PMCID: PMC4471882.

Markt P, Petersen RK, Flindt EN, Kristiansen K, Kirchmair J, Spitzer G, Distinto S, Schuster D, Wolber G, Laggner C, Langer T. Discovery of novel PPAR ligands by a virtual screening approach based on pharmacophore modeling, 3D shape, and electrostatic similarity screening. J Med Chem. 2008 Oct 23;51(20):6303-17. doi: 10.1021/jm800128k. Epub 2008 Sep 27. PubMed PMID: 18821746.

Markt P, Schuster D, Kirchmair J, Laggner C, Langer T. Pharmacophore modeling and parallel screening for PPAR ligands. J Comput Aided Mol Des. 2007 Oct-Nov;21(10-11):575-90. Epub 2007 Oct 25. PubMed PMID: 17960326.

Matsusue K. [Novel mechanism for hepatic lipid accumulation: a physiological role for hepatic PPARγ-fsp27 signal]. Yakugaku Zasshi. 2012;132(7):823-9. Review. Japanese. PubMed PMID: 22790028.

Matsusue K. A physiological role for fat specific protein 27/cell death-inducing DFF45-like effector C in adipose and liver. Biol Pharm Bull. 2010;33(3):346-50. Review. PubMed PMID: 20190390.

Meek ME, Bucher JR, Cohen SM, Dellarco V, Hill RN, Lehman-McKeeman LD, Longfellow DG, Pastoor T, Seed J, Patton DE. A framework for human relevance analysis of information on carcinogenic modes of action. Crit Rev Toxicol. 2003;33(6):591-653. Review. PubMed PMID: 14727733.

Melagraki, G., Afantitis, A., Sarimveis, H., Koutentis, P.A., Kollias, G., Igglessi-Markopoulou, O., 2009. Predictive QSAR workflow for the *in silico* identification and screening of novel HDAC inhibitors. Mol. Diversity 13, 301–311. doi:10.1007/s11030-009-9115-2

Mellor CL, Steinmetz FP, Cronin MT. The identification of nuclear receptors associated with hepatic steatosis to develop and extend adverse outcome pathways. Crit Rev Toxicol. 2015 Oct 9:1-15. [Epub ahead of print] PubMed PMID: 26451809.

Merk D, Schubert-Zsilavecz M. Nuclear receptors as pharmaceutical targets: rise of FXR and rebirth of PPAR? Future Med Chem. 2012 Apr;4(5):587-8. doi: 10.4155/fmc.12.8. PubMed PMID: 22458677.

MOE (Molecular Operating Environment), version 2014.0901; Chemical Computing Group Inc., 2015, http://www.chemcomp.com.

Morán-Salvador E, López-Parra M, García-Alonso V, Titos E, Martínez-Clemente M, González-Périz A, López-Vicario C, Barak Y, Arroyo V, Clària J. Role for PPARγ in obesity-induced hepatic steatosis as determined by hepatocyte- and macrophage-specific conditional knockouts. FASEB J. 2011 Aug;25(8):2538-50. doi: 10.1096/fj.10-173716. Epub 2011 Apr 19. PubMed PMID: 21507897.

Mostrag-Szlichtyng, A.S et al. (2014) Poster presented at SOT 53rd Annual Meeting, 24–27 March 2014, Phoenix, Arizona, USA

Moya, M.; Gómez-Lechón, M.J.; Castell, J.V.; Jover, R. Enhanced steatosis by nuclear receptor ligands: A study in cultured human hepatocytes and hepatoma cells with a characterised nuclear receptor expression profile. Chem. Biol. Interact. 2010, 184, 376–387.

Mueller, J.J., Schupp, M., Unger, T., Kintscher, U., Heinemann, U. Binding Diversity of Pioglitazone by Peroxisome Proliferator-Activated Receptor-Gamma. doi:10.2210/pdb2xkw/pdb

Musso G, Gambino R, Cassader M. Recent insights into hepatic lipid metabolism in non-alcoholic fatty liver disease (NAFLD). Prog Lipid Res. 2009 Jan;48(1):1-26. doi: 10.1016/j.plipres.2008.08.001. Epub 2008 Sep 9. Review. PubMed PMID: 18824034.

Mysinger MM, Carchia M, Irwin JJ, Shoichet BK. Directory of useful decoys, enhanced (DUD-E): better ligands and decoys for better benchmarking. J Med Chem. 2012 Jul 26;55(14):6582-94. doi: 10.1021/jm300687e. Epub 2012 Jul 5. PubMed PMID: 22716043; PubMed Central PMCID: PMC3405771.

Nagasaka H, Miida T, Inui A, Inoue I, Tsukahara H, Komatsu H, Hiejima E, Fujisawa T, Yorifuji T, Hiranao K, Okajima H, Inomata Y. Fatty liver and anti-oxidant enzyme activities along with peroxisome proliferator-activated receptors γ and α expressions in the liver of Wilson's disease. Mol Genet Metab. 2012 Nov;107(3):542-7. doi: 10.1016/j.ymgme.2012.08.004. Epub 2012 Aug 11. PubMed PMID: 22940187.

NC3Rs (https://www.nc3rs.org.uk/the-3rs)

Netzeva, T.I., Worth, A., Aldenberg, T., Benigni, R., Cronin, M.T., Gramatica, P., Jaworska, J.S., Kahn, S., Klopman, G., Marchant, C.A., Myatt, G., Nikolova-Jeliazkova, N.,

Patlewicz, G.Y., Perkins, R., Roberts, D., Schultz, T., Stanton, D.W., van de Sandt, J.J., Tong, W., Veith, G., Yang, C., 2005. Current status of methods for defining the applicability domain of (quantitative) structure-activity relationships. The report and recommendations of ECVAM Workshop 52. Altern Lab Anim. 33, 155-173

Neuschwander-Tetri BA. Hepatic lipotoxicity and the pathogenesis of nonalcoholic steatohepatitis: the central role of nontriglyceride fatty acid metabolites. Hepatology. 2010 Aug;52(2):774-88. doi: 10.1002/hep.23719. Review. PubMed PMID: 20683968.

Nissen SE et al. Rosiglitazone revisited. An updated meta analysis of risk for myocardial infarction and cardiovascular mortality. Arch Intern Med doi:10.1001/archinternmed.2010.207.

Noh JR, Kim YH, Hwang JH, Gang GT, Yeo SH, Kim KS, Oh WK, Ly SY, Lee IK, Lee CH. Scoparone inhibits adipocyte differentiation through down-regulation of peroxisome proliferators-activated receptor γ in 3T3-L1 preadipocytes. Food Chem. 2013 Nov 15;141(2):723-30. doi: 10.1016/j.foodchem.2013.04.036. Epub 2013 Apr 19. PubMed PMID: 23790840.

Nolte, R.T.; Wisely, G.B.; Westin, S.; Cobb, J.E.; Lambert, M.H.; Kurokawa, R.; Rosenfeld, M.G.; Willson, T.M.; Glass, C.K.; Milburn, M.V. Ligand binding and co-activator assembly of the peroxisome proliferator-activated receptor-gamma. Nature 1998, 395, 137–143.

North American Free Trade Agreement (NAFTA), Technical Working Group on Pesticides (TWG). (2011). (Quantitative) Structure Activity Relationship ((Q)SAR) Guidance Document.

Nosjean O, Boutin JA. Natural ligands of PPARgamma: are prostaglandin J(2) derivatives really playing the part? Cell Signal. 2002 Jul;14(7):573-83. Review. PubMed PMID: 11955950.

Nuclear Receptors Nomenclature Committee. A unified nomenclature system for the nuclear receptor superfamily. Cell. 1999 Apr 16;97(2):161-3. PubMed PMID: 10219237.

OECD (2007), Guidance document on the validation of (quantitative)structure-activity relationships [(Q)SAR] models, OECD Environment Health and Safety Publications Series on Testing and Assessment No. 69, OECD, Paris, France, ENV/JM/MONO(2007)2.

OECD (2008). Report of the Second Survey on Available Omics Tools. OECD Environment, Health and Safety Publications Series on Testing and Assessment No. 100. ENV/JM/MONO(2008)35.

OECD (2011). Report of the Workshop on Using Mechanistic Information in Forming Chemical Categories. OECD Environment, Health and Safety Publications Series on Testing and Assessment No. 138. ENV/JM/MONO(2011)8.

OECD (2012) Detailed review paper on the state of the science on novel *in vitro* and *in vivo* screening and testing methods and endpoints for evaluating endocrine disruptors Series on Testing & Assessment No. 178, ENV/JM/MONO(2012)23;

OECD (2013), Guidance Document on Developing and Assessing Adverse Outcome Pathways, Series on Testing and Assessment No. 184, OECD, Paris, France, ENV/JM/MONO(2013)6.

OECD (www.oecd.org/chemicalsafety/testing/adverse-outcome- pathways-molecular-screening-and-toxicogenomics.htm)

OECD, List of projects on the Adverse Outcome Pathways development programme workplan (http://www.oecd.org/chemicalsafety/testing/projects-adverse-outcome-pathways.htm; last access: 19 August 2015)

Ohashi M, Oyama T, Nakagome I, Satoh M, Nishio Y, Nobusada H, Hirono S, Morikawa K, Hashimoto Y, Miyachi H. Design, synthesis, and structural analysis of phenylpropanoic acid-type PPARγ-selective agonists: discovery of reversed stereochemistry-activity relationship. J Med Chem. 2011 Jan 13;54(1):331-41. doi: 10.1021/jm101233f. Epub 2010 Dec 3. PubMed PMID: 21128600.

Ohashi M, Oyama T, Putranto EW, Waku T, Nobusada H, Kataoka K, Matsuno K, Yashiro M, Morikawa K, Huh NH, Miyachi H. Design and synthesis of a series of α-benzyl phenylpropanoic acid-type peroxisome proliferator-activated receptor (PPAR) gamma partial agonists with improved aqueous solubility. Bioorg Med Chem. 2013 Apr 15;21(8):2319-32. doi: 10.1016/j.bmc.2013.02.003. Epub 2013 Feb 14. PubMed PMID: 23490155.

Okumura T. Role of lipid droplet proteins in liver steatosis. J Physiol Biochem. 2011 Dec;67(4):629-36. doi: 10.1007/s13105-011-0110-6. Epub 2011 Aug 17. Review. PubMed PMID: 21847662.

Pan, H.J.; Lin, Y.; Chen, Y.E.; Vance, D.E.; Leiter, E.H. Adverse hepatic and cardiac responses to rosiglitazone in a new mouse model of type 2 diabetes: Relation to dysregulated phosphatidylcholine metabolism. Vascul. Pharmacol. 2006, 45, 65–71.

Panasyuk G, Espeillac C, Chauvin C, Pradelli LA, Horie Y, Suzuki A, Annicotte JS, Fajas L, Foretz M, Verdeguer F, Pontoglio M, Ferré P, Scoazec JY, Birnbaum MJ, Ricci JE, Pende M. PPARγ contributes to PKM2 and HK2 expression in fatty liver. Nat Commun. 2012 Feb 14;3:672. doi: 10.1038/ncomms1667. PubMed PMID: 22334075; PubMed Central PMCID: PMC3293420.

Park CY, Park SW. Role of peroxisome proliferator-activated receptor gamma agonist in improving hepatic steatosis: Possible molecular mechanism. J Diabetes Investig. 2012 Mar 28;3(2):93-5. doi: 10.1111/j.2040-1124.2012.00204.x. PubMed PMID: 24843551; PubMed Central PMCID: PMC4020725.

Park JE, Oh SH, Cha YS. Lactobacillus plantarum LG42 isolated from gajami ik-hae inhibits adipogenesis in 3T3-L1 adipocyte. Biomed Res Int. 2013;2013:460927. doi: 10.1155/2013/460927. Epub 2013 Feb 28. PubMed PMID: 23555088; PubMed Central PMCID: PMC3600254.

Patlewicz G, Ball N, Booth ED, Hulzebos E, Zvinavashe E, Hennes C. Use of category approaches, read-across and (Q)SAR: general considerations. Regul Toxicol Pharmacol. 2013 Oct;67(1):1-12. doi: 10.1016/j.yrtph.2013.06.002. Epub 2013 Jun 11. PubMed PMID: 23764304.; Gleeson MP, Modi S, Bender A, Robinson RL, Kirchmair J, Promkatkaew M, Hannongbua S, Glen RC. The challenges involved in modeling toxicity data *in silico*: a review. Curr Pharm Des. 2012;18(9):1266-91. Review. PubMed PMID: 22316153.;

Pencheva T, Jereva D, Miteva MA, Pajeva I. Post-docking optimization and analysis of protein-ligand interactions of estrogen receptor alpha using AMMOS software. Curr Comput Aided Drug Des. 2013 Mar;9(1):83-94. PubMed PMID: 23106778.

Pingali H, Jain M, Shah S, Makadia P, Zaware P, Goel A, Patel M, Giri S, Patel H, Patel P. Design and synthesis of novel oxazole containing 1,3-dioxane-2-carboxylic acid derivatives as PPAR alpha/gamma dual agonists. Bioorg Med Chem. 2008 Aug 1;16(15):7117-27. doi: 10.1016/j.bmc.2008.06.050. Epub 2008 Jun 28. PubMed PMID: 18625559.

Polvani S, Tarocchi M, Galli A. PPARγ and Oxidative Stress: Con(β) Catenating NRF2 and FOXO. PPAR Res. 2012;2012:641087. doi: 10.1155/2012/641087. Epub 2012 Mar 5. PubMed PMID: 22481913; PubMed Central PMCID: PMC3317010.

Povero D, Feldstein AE. Novel Molecular Mechanisms in the Development of Non-Alcoholic Steatohepatitis. Diabetes Metab J. 2016 Feb;40(1):1-11. doi: 10.4093/dmj.2016.40.1.1. Review. PubMed PMID: 26912150; PubMed Central PMCID: PMC4768045.

Prieto P., Testai E., Cronin M., and Mahony C., Current state of the art in repeated dose systemic toxicity testing, in Towards the Replacement of *In Vivo* Repeated Dose Systemic Toxicity TestIng, T. Gocht and M. Schwarz, Eds., vol. 1, pp. 38–46, 2011.

Rabinowitz JR, Goldsmith MR, Little SB, Pasquinelli MA. Computational molecular modeling for evaluating the toxicity of environmental chemicals: prioritising bioassay requirements. Environ Health Perspect. 2008 May;116(5):573-7. doi: 10.1289/ehp.11077. PubMed PMID: 18470285; PubMed Central PMCID: PMC2367647

Rachek LI, Yuzefovych LV, Ledoux SP, Julie NL, Wilson GL. Troglitazone, but not rosiglitazone, damages mitochondrial DNA and induces mitochondrial dysfunction and cell death in human hepatocytes. Toxicol Appl Pharmacol. 2009 Nov 1;240(3):348-54. doi: 10.1016/j.taap.2009.07.021. Epub 2009 Jul 24. PubMed PMID: 19632256; PubMed Central PMCID: PMC2767118.

Raffa RB, Chapter 3: Experimental Approaches to Determine the Thermodynamics of Protein-Ligand Interactions, In Böhm HJ and Schneider G (Eds.) Protein-Ligand Interactions: From Molecular Recognition to Drug Design, Wiley-VCH, Weinheim, 2003, p. 51-72

Ratushny AV, Saleem RA, Sitko K, Ramsey SA, Aitchison JD. Asymmetric positive feedback loops reliably control biological responses. Mol Syst Biol. 2012 Apr 24;8:577. doi: 10.1038/msb.2012.10. PubMed PMID: 22531117; PubMed Central PMCID: PMC3361002.

Regulation 1223/2009/EC of the European Parliament and of the Council of 30 November 2009 on cosmetic products, OJ L 342, 22.12.2009, p. 59.

Richarz A.-N., Berthold M. N., Fioravanzo E.,. Neagu D,. Péry A. R. R, Worth A. P., Yang C. and Cronin M. T. D., II-7-504 Computational approaches for the safety assessment of cosmetics-related chemicals: results from the COSMOS Project, Abstracts of the 9th World Congress, Prague, 2014, Volume 3, No. 1, ISSN 2194-0479.

Ring A, Le Lay S, Pohl J, Verkade P, Stremmel W. Caveolin-1 is required for fatty acid translocase (FAT/CD36) localization and function at the plasma membrane of mouse embryonic fibroblasts. Biochim Biophys Acta. 2006 Apr;1761(4):416-23. Epub 2006 Apr 19. PubMed PMID: 16702023.

Rogue A, Anthérieu S, Vluggens A, Umbdenstock T, Claude N, de la Moureyre-Spire C, Weaver RJ, Guillouzo A. PPAR agonists reduce steatosis in oleic acid-overloaded HepaRG cells. Toxicol Appl Pharmacol. 2014 Apr 1;276(1):73-81. doi: 10.1016/j.taap.2014.02.001. Epub 2014 Feb 15. PubMed PMID: 24534255.

Rogue A, Spire C, Brun M, Claude N, Guillouzo A. Gene Expression Changes Induced by PPAR Gamma Agonists in Animal and Human Liver. PPAR Res. 2010;2010:325183. doi: 10.1155/2010/325183. Epub 2010 Oct 19. PubMed PMID: 20981297; PubMed Central PMCID: PMC2963138.

Rosen ED, MacDougald OA. Adipocyte differentiation from the inside out. Nat Rev Mol Cell Biol. 2006 Dec;7(12):885-96. Review. PubMed PMID: 17139329.

Rosen ED, Sarraf P, Troy AE, Bradwin G, Moore K, Milstone DS, Spiegelman BM, Mortensen RM. PPAR gamma is required for the differentiation of adipose tissue *in vivo* and *in vitro*. Mol Cell. 1999 Oct;4(4):611-7. PubMed PMID: 10549292.

Ross E, Chapter 2. Pharmacodynamics: Mechanisms of Drug Action and the Relationship Between Drug Concentration and Effect in Goodman & Gilman's The pharmacological basis of therapeutics, 9-th edition, McGraw-Hill Co., New York, 1996.

Rücker C, Scarsi M, Meringer M. 2D QSAR of PPARgamma agonist binding and transactivation. Bioorg Med Chem. 2006 Aug 1;14(15):5178-95. Epub 2006 May 2. PubMed PMID: 16650995.

Rull A, Geeraert B, Aragonès G, Beltrán-Debón R, Rodríguez-Gallego E, García-Heredia A, Pedro-Botet J, Joven J, Holvoet P, Camps J. Rosiglitazone and fenofibrate exacerbate liver steatosis in a mouse model of obesity and hyperlipidemia. A transcriptomic and metabolomic study. J Proteome Res. 2014 Mar 7;13(3):1731-43. doi: 10.1021/pr401230s. Epub 2014 Jan 30. PubMed PMID: 24479691.;

Russell WMS, Burch RL (1959) The Principles of Humane Experimental Technique, London:Methuen, London, 1959. (http://altweb.jhsph.edu/pubs/books/humane_exp/chap1a)

Rusu E, Enache G, Jinga M, Dragut R, Nan R, Popescu H, Parpala C, Homentcovschi C, Nitescu M, Stoian M, Costache A, Posea M, Rusu F, Jinga V, Mischianu D, Radulian G. Medical nutrition therapy in non-alcoholic fatty liver disease - a review of literature.

J Med Life. 2015 Jul-Sep;8(3):258-62. Review. PubMed PMID: 26351523; PubMed Central PMCID: PMC4556902.

Sahini N, Borlak J. Recent insights into the molecular pathophysiology of lipid droplet formation in hepatocytes. Prog Lipid Res. 2014 Apr;54:86-112. doi: 10.1016/j.plipres.2014.02.002. Epub 2014 Mar 6. Review. PubMed PMID: 24607340.

Sass DA, Chang P, Chopra KB. Nonalcoholic fatty liver disease: a clinical review. Dig Dis Sci. 2005 Jan;50(1):171-80. Review. PubMed PMID: 15712657.

Satoh H, Ide N, Kagawa Y, Maeda T. Hepatic steatosis with relation to increased expression of peroxisome proliferator-activated receptor-γ in insulin resistant mice. Biol Pharm Bull. 2013;36(4):616-23. Epub 2013 Feb 2. PubMed PMID: 23386130.

Sauerberg P, Bury PS, Mogensen JP, Deussen HJ, Pettersson I, Fleckner J, Nehlin J, Frederiksen KS, Albrektsen T, Din N, Svensson LA, Ynddal L, Wulff EM, Jeppesen L. Large dimeric ligands with favorable pharmacokinetic properties and peroxisome proliferator-activated receptor agonist activity in vitro and in vivo. J Med Chem. 2003 Nov 6;46(23):4883-94. PubMed PMID: 14584939.

Sauerberg P, Mogensen JP, Jeppesen L, Svensson LA, Fleckner J, Nehlin J, Wulff EM, Pettersson I. Structure-activity relationships of dimeric PPAR agonists. Bioorg Med Chem Lett. 2005 Mar 1;15(5):1497-500. PubMed PMID: 15713415.

Sauerberg P, Pettersson I, Jeppesen L, Bury PS, Mogensen JP, Wassermann K, Brand CL, Sturis J, Wöldike HF, Fleckner J, Andersen AS, Mortensen SB, Svensson LA, Rasmussen HB, Lehmann SV, Polivka Z, Sindelar K, Panajotova V, Ynddal L, Wulff EM. Novel tricyclic-alpha-alkyloxyphenylpropionic acids: dual PPARalpha/gamma agonists with hypolipidemic and antidiabetic activity. J Med Chem. 2002 Feb 14;45(4):789-804. PubMed PMID: 11831892.

Scheen AJ. Hepatotoxicity with thiazolidinediones: is it a class effect? Drug Saf. 2001;24(12):873-88. Review. PubMed PMID: 11735645.

Schneider G, Baringhaus KH, Kubinyi H (Foreword by), Molecular Design: Concepts and Applications, Wiley-VCH Verlag GmbH & Co. KGaA, 2008, ISBN: 978-3-527-31432-4

Schultz, T.W. (2010). Adverse outcome pathways: A way of linking chemical structure to *in vivo* toxicological hazards. In: Cronin, M.T.D. and Madden, J.C. eds., In Silico Toxicology: Principles and Applications, The Royal Society of Chemistry, Cambridge, UK, pp. 346-371.

Schultz, p. c., cited in OECD (2013) ENV/JM/MONO(2013)6 as Schultz, personal communication

Schupp M, Lazar MA. Endogenous ligands for nuclear receptors: digging deeper. J Biol Chem. 2010 Dec 24;285(52):40409-15. doi: 10.1074/jbc.R110.182451. Epub 2010 Oct 18. Review. PubMed PMID: 20956526; PubMed Central PMCID: PMC3003339.

Seed J, Carney EW, Corley RA, Crofton KM, DeSesso JM, Foster PM, Kavlock R, Kimmel G, Klaunig J, Meek ME, Preston RJ, Slikker W Jr, Tabacova S, Williams GM, Wiltse J, Zoeller RT, Fenner-Crisp P, Patton DE. Overview: Using mode of action and life stage information to evaluate the human relevance of animal toxicity data. Crit Rev Toxicol. 2005 Oct-Nov;35(8-9):664-72. Review. PubMed PMID: 16417033.

Semple RK, Chatterjee VK, O'Rahilly S. PPAR gamma and human metabolic disease. J Clin Invest. 2006 Mar;116(3):581-9. Review. PubMed PMID: 16511590; PubMed Central PMCID: PMC1386124.

Serviddio G, Bellanti F, Vendemiale G. Free radical biology for medicine: learning from nonalcoholic fatty liver disease. Free Radic Biol Med. 2013 Dec;65:952-68. doi: 10.1016/j.freeradbiomed.2013.08.174. Epub 2013 Aug 29. Review. PubMed PMID: 23994574.

SEURAT-1 (http://www.seurat-1.eu)

Shah P, Mittal A, Bharatam PV. CoMFA analysis of dual/multiple PPAR activators. Eur J Med Chem. 2008 Dec;43(12):2784-91. doi: 10.1016/j.ejmech.2008.01.017. Epub 2008 Jan 30. PubMed PMID: 18321611.

Shao D, Lazar MA. Peroxisome proliferator activated receptor gamma, CCAAT/enhancer-binding protein alpha, and cell cycle status regulate the commitment to adipocyte differentiation. J Biol Chem. 1997 Aug 22;272(34):21473-8. PubMed PMID: 9261165.

Sharma MC. Prospective QSAR-based prediction models with pharmacophore studies of oxadiazole-substituted α-isopropoxy phenylpropanoic acids on with dual activators of PPARα and PPARγ. Interdiscip Sci. 2014 Sep 2. [Epub ahead of print] PubMed PMID: 25183350.

Shen C, Meng Q, Zhang G. Species-specific toxicity of troglitazone on rats and human by gel entrapped hepatocytes. Toxicol Appl Pharmacol. 2012 Jan 1;258(1):19-25. doi: 10.1016/j.taap.2011.10.020. Epub 2011 Nov 6. PubMed PMID: 22085495.

Sohn YS, Lee Y, Park C, Hwang S, Kim S, Baek A, Son M, Suh JK, Kim HH, and Lee KW. Peroxisome Proliferator-Activated Receptor Agonist Design Bull. Korean Chem. Soc. 2011, Vol. 32, No. 1 201 DOI 10.5012/bkcs.2011.32.1.201

Sohn YS, Park C, Lee Y, Kim S, Thangapandian S, Kim Y, Kim HH, Suh JK, Lee KW. Multi-conformation dynamic pharmacophore modeling of the peroxisome proliferator-activated receptor γ for the discovery of novel agonists. J Mol Graph Model. 2013 Nov;46:1-9. doi: 10.1016/j.jmgm.2013.08.012. Epub 2013 Aug 22. PubMed PMID: 24104184.

Sonich-Mullin C, Fielder R, Wiltse J, Baetcke K, Dempsey J, Fenner-Crisp P, Grant D, Hartley M, Knaap A, Kroese D, Mangelsdorf I, Meek E, Rice JM, Younes M; International Programme on Chemical Safety. IPCS conceptual framework for evaluating a mode of action for chemical carcinogenesis. Regul Toxicol Pharmacol. 2001 Oct;34(2):146-52. PubMed PMID: 11603957.

Sos BC, Harris C, Nordstrom SM, Tran JL, Balázs M, Caplazi P, Febbraio M, Applegate MA, Wagner KU, Weiss EJ. Abrogation of growth hormone secretion rescues fatty liver in mice with hepatocyte-specific deletion of JAK2. J Clin Invest. 2011 Apr;121(4):1412-23. doi: 10.1172/JCI42894. Erratum in: J Clin Invest. 2011 Aug 1;121(8):3360. Dosage error in article text. PubMed PMID: 21364286; PubMed Central PMCID: PMC3069761.

Souza-Mello V. Peroxisome proliferator-activated receptors as targets to treat non-alcoholic fatty liver disease. World J Hepatol. 2015 May 18;7(8):1012-9. doi: 10.4254/wjh.v7.i8.1012. PubMed PMID: 26052390; PubMed Central PMCID: PMC4450178

Stephenson RP. A modification of receptor theory. Br J Pharmacol Chemother. 1956 Dec;11(4):379-93. PubMed PMID: 13383117; PubMed Central PMCID: PMC1510558.

Su X, Abumrad NA. Cellular fatty acid uptake: a pathway under construction. Trends Endocrinol Metab. 2009 Mar;20(2):72-7. doi: 10.1016/j.tem.2008.11.001. Epub 2009 Jan 29. Review. PubMed PMID: 19185504; PubMed Central PMCID: PMC2845711.

Sun H, Berquin IM, Edwards IJ: Omega-3 polyunsaturated fatty acids regulate syndecan-1 expression in human breast cancer cells. Cancer Res 2005, 65(10):4442–4447.

Sun H, Berquin IM, Owens RT, O'Flaherty JT, Edwards IJ: Peroxisome proliferator-activated receptor γ-mediated up-regulation of syndecan-1 by n-3 fatty acids promotes apoptosis of human breast cancer cells. Cancer Res 2008, 68(8):2912–2919.

Sundriyal S, Bharatam PV. 'Sum of activities' as dependent parameter: a new CoMFA-based approach for the design of pan PPAR agonists. Eur J Med Chem. 2009 Jan;44(1):42-53. doi: 10.1016/j.ejmech.2008.03.014. Epub 2008 Mar 28. PubMed PMID: 18448203.

SYBYL-X, version 2.1, Tripos International, 2013, https://www.certara.com/

Tailleux A, Wouters K, Staels B. Roles of PPARs in NAFLD: potential therapeutic targets. Biochim Biophys Acta. 2012 May;1821(5):809-18. doi: 10.1016/j.bbalip.2011.10.016. Epub 2011 Oct 25. Review. PubMed PMID: 22056763.

Takahashi Y, Fukusato T. Histopathology of nonalcoholic fatty liver disease/nonalcoholic steatohepatitis. World J Gastroenterol. 2014 Nov 14;20(42):15539-48. doi: 10.3748/wjg.v20.i42.15539. Review. PubMed PMID: 25400438; PubMed Central PMCID: PMC4229519.

Teboul L, Gaillard D, Staccini L, Inadera H, Amri EZ, Grimaldi PA. Thiazolidinediones and fatty acids convert myogenic cells into adipose-like cells. J Biol Chem. 1995 Nov 24;270(47):28183-7. PubMed PMID: 7499310.

Tontonoz P, Hu E, Spiegelman BM. Stimulation of adipogenesis in fibroblasts by PPAR gamma 2, a lipid-activated transcription factor. Cell. 1994 Dec 30;79(7):1147-56. Erratum in: Cell 1995 Mar 24;80(6):following 957. PubMed PMID: 8001151.

Törnqvist E, Annas A, Granath B, Jalkesten E, Cotgreave I, Öberg M. Strategic focus on 3R principles reveals major reductions in the use of animals in pharmaceutical toxicity testing. PLoS One. 2014 Jul 23;9(7):e101638. doi: 10.1371/journal.pone.0101638. eCollection 2014. PubMed PMID: 25054864; PubMed Central PMCID: PMC4108312.

TOX21 (http://www.epa.gov/ncct/Tox21/)

Trombetta A, Maggiora M, Martinasso G, Cotogni P, Canuto RA, Muzio G: Arachidonic and docosahexaenoic acids reduce the growth of A549 human lung-tumor cells increasing lipid peroxidation and PPARs. Chem Biol Interact 2007, 165(3):239–250.

Tropsha, A., Gramatica, P., Gombar, V., 2003. The importance of being earnest: validation is the absolute essential for successful application and interpretation of QSPR models. QSAR Comb. Sci. 2, 69–77. doi: 10.1002/qsar.200390007

Tsakovska I, Al Sharif M, Alov P, Diukendjieva A, Fioravanzo E, Cronin MT, Pajeva I. Molecular modelling study of the PPARγ receptor in relation to the mode of action/adverse outcome pathway framework for liver steatosis. Int J Mol Sci. 2014 May 5;15(5):7651-66. doi: 10.3390/ijms15057651. PubMed PMID: 24857909; PubMed Central PMCID: PMC4057697.

Tsakovska I, Al Sharif M, Fioravanzo E, Bassan A, Kovarich S, Vitcheva V, Mostrag-Szlichtyng A, Yang C, Steinmetz F, Cronin M (2015) *In silico* approaches to support liver toxicity screening of chemicals: Case study on molecular modelling of ligands - nuclear receptors interactions to predict potential steatogenic effects. 51st Congress of the European Societies of Toxicology (EUROTOX), 13-16 September 2015, Porto, Portugal

Tsukahara T, Tsukahara R, Fujiwara Y, Yue J, Cheng Y, Guo H, Bolen A, Zhang C, Balazs L, Re F, Du G, Frohman MA, Baker DL, Parrill AL, Uchiyama A, Kobayashi T, Murakami-Murofushi K, Tigyi G. Phospholipase D2-dependent inhibition of the nuclear hormone receptor PPARgamma by cyclic phosphatidic acid. Mol Cell. 2010 Aug 13;39(3):421-32. doi: 10.1016/j.molcel.2010.07.022. PubMed PMID: 20705243; PubMed Central PMCID: PMC3446787.

U.S. EPA (U.S. Environmental Protection Agency). (1999) Guidelines for carcinogen risk assessment (review draft). Risk Assessment Forum, Washington, DC. NCEA-F-0644. Available from: http://www.epa.gov/ncea/raf/cancer.htm

Valerio LG Jr. *In silico* toxicology for the pharmaceutical sciences. Toxicol Appl Pharmacol. 2009 Dec 15;241(3):356-70. doi: 10.1016/j.taap.2009.08.022. Epub 2009 Aug 28. Review. PubMed PMID: 19716836.

Vanni E, Bugianesi E, Kotronen A, De Minicis S, Yki-Järvinen H, Svegliati-Baroni G. From the metabolic syndrome to NAFLD or vice versa? Dig Liver Dis. 2010 May;42(5):320-30. doi: 10.1016/j.dld.2010.01.016. Epub 2010 Mar 6. Review. PubMed PMID: 20207596.

Vedani A, Descloux AV, Spreafico M, Ernst B. Predicting the toxic potential of drugs and chemicals *in silico*: a model for the peroxisome proliferator-activated receptor gamma (PPAR gamma). Toxicol Lett. 2007 Aug 30;173(1):17-23. Epub 2007 Jun 20. PubMed PMID: 17643875.

Viccica G, Francucci CM, Marcocci C. The role of PPARγ for the osteoblastic differentiation. J Endocrinol Invest. 2010;33(7 Suppl):9-12. Review. PubMed PMID: 20938219.

Videla LA, Pettinelli P. Misregulation of PPAR Functioning and Its Pathogenic Consequences Associated with Nonalcoholic Fatty Liver Disease in Human Obesity. PPAR Res. 2012;2012:107434. doi: 10.1155/2012/107434. Epub 2012 Dec 9. PubMed PMID: 23304111; PubMed Central PMCID: PMC3526338.

Vidović D, Busby SA, Griffin PR, Schürer SC. A combined ligand- and structure-based virtual screening protocol identifies submicromolar PPARγ partial agonists. ChemMedChem.

2011 Jan 3;6(1):94-103. doi: 10.1002/cmdc.201000428. PubMed PMID: 21162086; PubMed Central PMCID: PMC3517154.

Villeneuve DL, Garcia-Reyero N. Vision & strategy: Predictive ecotoxicology in the 21st century. Environ Toxicol Chem. 2011 Jan;30(1):1-8. doi: 10.1002/etc.396. PubMed PMID: 21182100.

Vinken M, Pauwels M, Ates G, Vivier M, Vanhaecke T, Rogiers V. Screening of repeated dose toxicity data present in SCC(NF)P/SCCS safety evaluations of cosmetic ingredients. Arch Toxicol. 2012 Mar;86(3):405-12. doi: 10.1007/s00204-011-0769-z. Epub 2011 Oct 29. PubMed PMID: 22038139.

Virtue S, Vidal-Puig A. Adipose tissue expandability, lipotoxicity and the Metabolic Syndrome--an allostatic perspective. Biochim Biophys Acta. 2010 Mar;1801(3):338-49. doi: 10.1016/j.bbalip.2009.12.006. Epub 2010 Jan 6. Review. PubMed PMID: 20056169.

Vitcheva V, Mostrag-Szlichtyng A, Sacher O, Bienfait B, Shwab C, Tzakovska I, Al Sharif M, Pazeva I, Yang C(2015) *In vivo* data mining and *in silico* metabolic profiling to predict diverse hepatotoxic phenotypes: Case study of piperonyl butoxide. 51st Congress of the European Societies of Toxicology (EUROTOX), 13-16 September 2015, Porto, Portugal

Wakabayashi K, Okamura M, Tsutsumi S, Nishikawa NS, Tanaka T, Sakakibara I, Kitakami J, Ihara S, Hashimoto Y, Hamakubo T, Kodama T, Aburatani H, Sakai J. The peroxisome proliferator-activated receptor gamma/retinoid X receptor alpha heterodimer targets the histone modification enzyme PR-Set7/Setd8 gene and regulates adipogenesis through a positive feedback loop. Mol Cell Biol. 2009 Jul;29(13):3544-55. doi: 10.1128/MCB.01856-08. Epub 2009 May 4. PubMed PMID: 19414603; PubMed Central PMCID: PMC2698772.

Waku T, Shiraki T, Oyama T, Maebara K, Nakamori R, Morikawa K. The nuclear receptor PPARγ individually responds to serotonin- and fatty acid-metabolites. EMBO J. 2010 Oct 6;29(19):3395-407. doi: 10.1038/emboj.2010.197. Epub 2010 Aug 17. PubMed PMID: 20717101; PubMed Central PMCID: PMC2957204.

Wang XJ, Zhang J, Wang SQ, Xu WR, Cheng XC, Wang RL. Identification of novel multitargeted PPARα/γ/δ pan agonists by core hopping of rosiglitazone. Drug Des Devel Ther. 2014 Nov 7;8:2255-62. doi: 10.2147/DDDT.S70383. eCollection 2014. PubMed PMID: 25422585; PubMed Central PMCID: PMC4232041.;

Wang Y, Liu Z, Zou W, Hong H, Fang H, Tong W. Molecular regulation of miRNAs and potential biomarkers in the progression of hepatic steatosis to NASH. Biomark Med.

2015 Nov;9(11):1189-200. doi: 10.2217/bmm.15.70. Epub 2015 Oct 28. PubMed PMID: 26506944.

Wang Z, Dou X, Gu D, Shen C, Yao T, Nguyen V, Braunschweig C, Song Z. 4-Hydroxynonenal differentially regulates adiponectin gene expression and secretion via activating PPARγ and accelerating ubiquitin-proteasome degradation. Mol Cell Endocrinol. 2012 Feb 26;349(2):222-31. doi: 10.1016/j.mce.2011.10.027. Epub 2011 Nov 10. PubMed PMID: 22085560; PubMed Central PMCID: PMC3594100.

Watanabe KH, Andersen ME, Basu N, Carvan MJ 3rd, Crofton KM, King KA, Suñol C, Tiffany-Castiglioni E, Schultz IR. Defining and modeling known adverse outcome pathways: Domoic acid and neuronal signaling as a case study. Environ Toxicol Chem. 2011 Jan;30(1):9-21. doi: 10.1002/etc.373. PubMed PMID: 20963854.

Weaver S, Gleeson MP. The importance of the domain of applicability in QSAR modeling. J Mol Graph Model. 2008 Jun;26(8):1315-26. doi: 10.1016/j.jmgm.2008.01.002. Epub 2008 Jan 18. PubMed PMID: 18328754.

Weismann D, Erion DM, Ignatova-Todorava I, Nagai Y, Stark R, Hsiao JJ, Flannery C, Birkenfeld AL, May T, Kahn M, Zhang D, Yu XX, Murray SF, Bhanot S, Monia BP, Cline GW, Shulman GI, Samuel VT. Knockdown of the gene encoding Drosophila tribbles homologue 3 (Trib3) improves insulin sensitivity through peroxisome proliferator-activated receptor-γ (PPAR-γ) activation in a rat model of insulin resistance. Diabetologia. 2011 Apr;54(4):935-44. doi: 10.1007/s00125-010-1984-5. Epub 2010 Dec 29. PubMed PMID: 21190014; PubMed Central PMCID: PMC4061906.

Wermuth, CG , Ganellin, CR , Lindberg, P , Mitscher, LA, Glossary of Terms Used in Medicinal Chemistry (IUPAC Recommendations 1998); Pure & Appl. Chem. 70:5 (1998) 1129–1143.

Wold, S; Eriksson, L. In Chemometric Methods in Molecular Design; van de Waterbeemd, H., Ed.; VCH: Weinheim, 1995; pp 309–318. 59.

World Gastroenterology Organisation Global Guidelines. Nonalcoholic Fatty Liver Disease and Nonalcoholic Steatohepatitis, 2012.

WHO, World Health Organisation (2009a), Chapter 2 Risk Assessment and its Role in Risk Analysis In Environmental Health Criteria 240: Principles and Methods for the Risk Assessment of Chemicals in Food. WHO, Geneva, http://www.who.int/foodsafety/publications/chemical-food/en/

WHO, World Health Organisation (2009b), Annex 1: Glossary of Terms, page A-24 In Environmental Health Criteria 240: Principles and Methods for the Risk Assessment of

Chemicals in Food. WHO, Geneva, http://www.who.int/foodsafety/publications/chemical-food/en/

Xiao B, Su M, Kim EL, Hong J, Chung HY, Kim HS, Yin J, Jung JH. Synthesis of PPAR-γ activators inspired by the marine natural product, paecilocin A. Mar Drugs. 2014 Feb 13;12(2):926-39. doi: 10.3390/md12020926. PubMed PMID: 24531188; PubMed Central PMCID: PMC3944523.

Xu HE, Lambert MH, Montana VG, Plunket KD, Moore LB, Collins JL, Oplinger JA, Kliewer SA, Gampe RT Jr, McKee DD, Moore JT, Willson TM. Structural determinants of ligand binding selectivity between the peroxisome proliferator-activated receptors. Proc Natl Acad Sci U S A. 2001 Nov 20;98(24):13919-24. Epub 2001 Nov 6. PubMed PMID: 11698662; PubMed Central PMCID: PMC61142.

Xu J, Kulkarni SR, Donepudi AC, More VR, Slitt AL. Enhanced Nrf2 activity worsens insulin resistance, impairs lipid accumulation in adipose tissue, and increases hepatic steatosis in leptin-deficient mice. Diabetes. 2012 Dec;61(12):3208-18. doi: 10.2337/db11-1716. Epub 2012 Aug 30. PubMed PMID: 22936178; PubMed Central PMCID: PMC3501889.

Xu S, Jay A, Brunaldi K, Huang N, Hamilton JA. CD36 enhances fatty acid uptake by increasing the rate of intracellular esterification but not transport across the plasma membrane. Biochemistry. 2013 Oct 15;52(41):7254-61. doi: 10.1021/bi400914c. Epub 2013 Oct 3. PubMed PMID: 24090054.

Yamada K, Mizukoshi E, Sunagozaka H, Arai K, Yamashita T, Takeshita Y, Misu H, Takamura T, Kitamura S, Zen Y, Nakanuma Y, Honda M, Kaneko S. Characteristics of hepatic fatty acid compositions in patients with nonalcoholic steatohepatitis. Liver Int. 2015 Feb;35(2):582-90. doi: 10.1111/liv.12685. Epub 2014 Oct 10. PubMed PMID: 25219574.

Yamazaki T, Shiraishi S, Kishimoto K, Miura S, Ezaki O. An increase in liver PPARγ2 is an initial event to induce fatty liver in response to a diet high in butter: PPARγ2 knockdown improves fatty liver induced by high-saturated fat. J Nutr Biochem. 2011 Jun;22(6):543-53. doi: 10.1016/j.jnutbio.2010.04.009. Epub 2010 Aug 30. PubMed PMID: 20801631.

Yang C, Tarkhov A, Marusczyk J, Bienfait B, Gasteiger J, Kleinoeder T, Magdziarz T, Sacher O, Schwab CH, Schwoebel J, Terfloth L, Arvidson K, Richard A, Worth A, Rathman J. New publicly available chemical query language, CSRML, to support chemotype representations for application to data mining and modeling. J Chem Inf Model. 2015 Mar 23;55(3):510-28. doi: 10.1021/ci500667v. Epub 2015 Feb 19. PubMed PMID: 25647539.; https://chemotyper.org

Yang ZH, Miyahara H, Iwasaki Y, Takeo J, Katayama M: Dietary supplementation with long-chain monounsaturated fatty acids attenuates obesity-related metabolic dysfunction and increases expression of PPAR gamma in adipose tissue in type 2 diabetic KK-Ay mice. Nutr Metab (Lond) 2013, 10(1):16.

Yu S, Matsusue K, Kashireddy P, Cao WQ, Yeldandi V, Yeldandi AV, Rao MS, Gonzalez FJ, Reddy JK. Adipocyte-specific gene expression and adipogenic steatosis in the mouse liver due to peroxisome proliferator-activated receptor gamma1 (PPARgamma1) overexpression. J Biol Chem. 2003 Jan 3;278(1):498-505. Epub 2002 Oct 24. PubMed PMID: 12401792.

Zhang H, Ryono DE, Devasthale P, Wang W, O'Malley K, Farrelly D, Gu L, Harrity T, Cap M, Chu C, Locke K, Zhang L, Lippy J, Kunselman L, Morgan N, Flynn N, Moore L, Hosagrahara V, Zhang L, Kadiyala P, Xu C, Doweyko AM, Bell A, Chang C, Muckelbauer J, Zahler R, Hariharan N, Cheng PT. Design, synthesis and structure-activity relationships of azole acids as novel, potent dual PPAR alpha/gamma agonists. Bioorg Med Chem Lett. 2009 Mar 1;19(5):1451-6. doi: 10.1016/j.bmcl.2009.01.030. Epub 2009 Jan 15. PubMed PMID: 19201606.

Zhu L, Baker SS, Liu W, Tao MH, Patel R, Nowak NJ, Baker RD. Lipid in the livers of adolescents with nonalcoholic steatohepatitis: combined effects of pathways on steatosis. Metabolism. 2011 Jul;60(7):1001-11. doi: 10.1016/j.metabol.2010.10.003. Epub 2010 Nov 13. PubMed PMID: 21075404.

PUBLICATIONS AND ACTIVITIES RELATED TO THE PhD THESIS

PUBLICATIONS

SCIENTIFIC PAPERS IN JOURNALS WITH IMPACT FACTOR

1. **Al Sharif M**, Tsakovska I, Pajeva I, Alov P, Fioravanzo E, Bassan A, Kovarich S, Yang C, Mostrag-Szlichtyng A, Vitcheva V, Worth AP, Richarz AN, Cronin MTD, The Application of Molecular Modelling in the Safety Assessment of Chemicals: A Case Study on Ligand-Dependent PPARγ Dysregulation, Toxicology, **2016**, doi: 10.1016/j.tox.2016.01.009.

   IF = 3.621 (2014)

2. **Al Sharif M**, Alov P, Vitcheva V, Pajeva I, Tsakovska I. Modes-of-action related to repeated dose toxicity: tissue-specific biological roles of PPARγ ligand-dependent dysregulation in nonalcoholic fatty liver disease, PPAR Research (a special issue PPARs and Metabolic Syndrome), **2014**, Article ID 432647.

   IF = 2.509 (2014)

   3 citations in:

   - *Mellor CL, Steinmetz FP, Cronin MT. The identification of nuclear receptors associated with hepatic steatosis to develop and extend adverse outcome pathways, Crit Rev Toxicol. 2016 Feb;46(2):138-52. doi: 10.3109/10408444.2015.1089471*
   - *Barbosa AM, Francisco PC, Motta K, Chagas TR, dos Santos C, Rafacho A, Nunes E. Fish Oil Supplementation Attenuates the Changes in the Plasma Lipids Caused by Dexamethasone Treatment in Rats, Appl Physiol Nutr Metab, 2015, doi: 10.1139/apnm-2015-0487*
   - *V. Zuang,B. Desprez, J. Barroso, S. Belz, E. Berggren,, C. Bernasconi, J.Bessems, S.e Bopp, S. Casati, S. Coecke, R. Corvi, C. Dumont, V. Gouliarmou, C. Griesinger, M. Halder, A. Janusch-Roi, A. Kienzler, B. Landesmann, F. Madia, A. Milcamps, S. Munn, A. Price, P. Prieto, M. Schäffer, J. Triebe, C. Wittwehr, A. Worth, M. Whelan.. EURL ECVAM status report on the development, validation and regulatory acceptance of alternative methods and approaches, European Union, 2015, pp. 1-114*

3 Tsakovska I., **Al Sharif M**, Alov P, Diukendjieva A, Fioravanzo E, Cronin M.T.D, Pajeva I. Molecular modelling study of PPARγ receptor in relation to the mode of action / adverse outcome pathway framework for liver steatosis. Int. J. Mol. Sci. **2014**, 15, 7651-7666. (ISSN 1422-0067).

IF = 2.862 (2014)

2 citations in:

- *Defining Molecular Initiating Events in the Adverse Outcome Pathway Framework for Risk Assessment By: Allen, Timothy E. H.; Goodman, Jonathan M.; Gutsell, Steve; et al. CHEMICAL RESEARCH IN TOXICOLOGY Volume: 27 Issue: 12 Pages: 2100-2112 Published: DEC 2014*
- *Zuang V, Desprez B, Barroso J, Belz S, Berggren E, Bernasconi C, Bessems J, Bopp S, Casati S, Coecke S, Corvi R, Dumont C, Gouliarmou V, Griesinger C, Halder M, Janusch-Roi A, Kienzler A, Landesmann B, Madia F, Milcamps A, Munn S, Price A, Prieto P, Schäffer M, Triebe J, Wittwehr C, Worth A, Whelan M. EURL ECVAM status report on the development, validation and regulatory acceptance of alternative methods and approaches, European Union, 2015, pp. 1-114.*

REPORTS IN PROCEEDINGS

1. **Al Sharif M**, Alov P, Tsakovska I, Pajeva I. (**2015**) *In silico* modelling of full PPARγ agonists: a step towards liver steatosis risk assessment, International Conference Of Young Scientists, 11 – 12 June **2015**, Plovdiv, Bulgaria, Scientific Researches of the Union of Scientists in Bulgaria – Plovdiv, Series G. Medicine, Pharmacy and Dental medicine, Vol. XVII, p. 182-186, ISSN1311-9427

ABSTRACTS IN JOURNAL PROCEEDINGS

1. Tsakovska I, **Al Sharif M**, Fioravanzo E, Bassan A, Kovarich S, Vitcheva V, Mostrag-Szlichtyng A, Yang C, Steinmetz F, Cronin M (**2015**) *In silico* approaches to support liver toxicity screening of chemicals: Case study on molecular modelling of ligands–nuclear receptors interactions to predict potential steatogenic effects. Toxicology Letters 238 Supplement: S173 **IF = 3.262 (2014)**
2. Vitcheva V, **Al Sharif M**, Tsakovska I, Alov P, Mostrag-Szlichtyng A, Cronin MTD, Yang C, Pajeva I (**2014**) Description of the MoA/AOP linked with PPARgamma receptor dysregulation leading to liver fibrosis. Toxicology Letters 229 Supplement: S49

IF = 3.262 (2014)

3. Diukendjieva A, **Al Sharif M**, Alov P, Tsakovska I, Pajeva I (**2014**) PPARγ agonists and liver steatosis: mode-of-action characterisation and *in silico* study, Journal of Biomedical and Clinical Research, vol.7, n.1, suppl.1, p.39
4. **Al Sharif M**, Tsakovska I, Alov P, Vitcheva V, Pajeva I (**2014**) PPARγ-related hepatotoxic mode-of-action: quantitative characterization and *in silico* study of the molecular initiating event involving receptor activation. Altex Proceedings 3, 1/14: 56-57

   IF = 5.467 (2014)
5. **Al Sharif M**, Alov P, Cronin M, Fioravanzo E, Tsakovska I, Vitcheva V, Worth A, Yang C, Pajeva I (**2013**) Toward better understanding of liver steatosis MoA: Molecular modelling study of PPAR gamma receptor. Toxicology Letters 221 Supplement: S85

   IF = 3.262 (2014)

   1 citation in:

   - *Sullivan KM, Manuppello JR, Willett CE. Building on a solid foundation: SAR and QSAR as a fundamental strategy to reduce animal testing. SAR QSAR Environ Res. 2014, 25: 357-365.*

CONTRIBUTIONS TO INTERNATIONAL SCIENTIFIC EVENTS

POSTERS

1. Fioravanzo E, Kovarich C, Bassan A, Ciacci A, **Al Sharif M**, Pajeva I, Alov P, Richarz AN, Worth AP, Palczewska A, Steinmetz FP, Yang C, Tsakovska I **(2015)** Use of molecular modelling approaches for the evaluation of potential binding to nuclear receptors involved in liver steatosis, SEURAT-1 Final Symposium, 4 December **2015**, Brussels, Belgium
2. Tsakovska I, **Al Sharif M**, Fioravanzo E, Bassan A, Kovarich S, Vitcheva V, Mostrag-Szlichtyng A, Yang C, Steinmetz F, Cronin M (**2015**) *In silico* approaches to support liver toxicity screening of chemicals: Case study on molecular modelling of ligands - nuclear receptors interactions to predict potential steatogenic effects. 51st Congress of the European Societies of Toxicology (EUROTOX), 13-16 September **2015**, Porto, Portugal
3. Vitcheva V, Mostrag-Szlichtyng A, Sacher O, Bienfait B, Shwab C, Tzakovska I, **Al Sharif M**, Pazeva I, Yang C(**2015**) *In vivo* data mining and *in silico* metabolic profiling to predict diverse hepatotoxic phenotypes: Case study of piperonyl butoxide. 51st Congress of the European Societies of Toxicology (EUROTOX), 13-16 September **2015**, Porto, Portugal
4. Tsakovska I, Kovarich S, Bassan A, Ciacci A, **Al Sharif M**, Pajeva I, Alov P, Cronin MTD, Worth A, Palczewska A, Steinmetz FP, Yang C, Fioravanzo E (**2015**) Modelling studies to

support the prediction of molecular initiating events for liver steatosis: LXR and PPARγ binding, SEURAT-1 Fifth Annual Meeting, 21-22 January **2015**, Barcelona, Spain

5. Jereva D, **Al Sharif M**, Diukendjieva A, Alov P, Pencheva T, Tsakovska I., Pajeva I (**2014**) Nuclear ERα and PPARγ: receptor- and ligand-based analysis. 16th Congress of the European Neuroendocrine Association, 10-13 September **2014**, Sofia, Bulgaria, Book of Abstracts - Basic Metabolism, Abstract-ID: 564, p. 88 **(Poster award)**
6. Vitcheva V, **Al Sharif M**, Tsakovska I, Alov P, Mostrag-Szlichtyng A, Cronin MTD, Yang C, Pajeva I (**2014**) Description of the MoA/AOP linked with PPARgamma receptor dysregulation leading to liver fibrosis. 50th Congress of the European Societies of Toxicology (EUROTOX), 7-10 September **2014**, Edinburgh, Scotland, UK
7. Tsakovska I, **Al Sharif M**, Alov P, Vitcheva V, Fioravanzo E, Mostrag-Szlichtyng A, Yang C, Cronin MTD, Pajeva I (2014) *In silico* ligand screening based on a pharmacophore model of PPARγ full agonists. 16Th International Workshop on Quantitative Structure-Activity Relationships in Environmental and Health Sciences, 16-20 June **2014**, Milan, Italy
8. Kovarich S, **Al Sharif M**, Alov P, Bassan A, Cronin MTD, Fioravanzo E, Mostrag-Szlichtyng A, Pajeva I, Tsakovska I, Vitcheva V, Worth AP, Yang C (2014) Molecular Modelling Studies of LXR and PPAR gamma Receptors in Relation to the MoA/AOP Framework for Liver Steatosis. SEURAT-1 4th Annual Meeting, 5-6 February **2014**, Barcelona, Spain
9. Tsakovska I, Jereva D, **Al Sharif M**, Alov P, Diukendjieva A, Pencheva T, Fioravanzo E, Cronin M, Worth A, Yang C, Pajeva I (2013) Structure- and ligand-based analysis of ligand-nuclear receptor ERα and PPARγ complexes. CMTPI-2013 - 7th International Symposium on Computational Methods in Toxicology and Pharmacology Integrating Internet Resources, 8–11 October **2013**, Seoul, Korea
10. Tsakovska I, **Al Sharif M**, Diukendjieva A, Alov P, Vitcheva V, Fioravanzo E, Cronin M, Worth A, Yang C, Pajeva I (2013) From PPARγ activation to liver steatosis: adverse outcome pathways description and molecular modelling study. CMTPI-2013 - 7th International Symposium on Computational Methods in Toxicology and Pharmacology Integrating Internet Resources, 8–11 October **2013**, Seoul, Korea
11. **Al Sharif M**, Alov P, Cronin M, Fioravanzo E, Tsakovska I, Vitcheva V, Worth A, Yang C, Pajeva I (2013) Toward better understanding of liver steatosis MoA: Molecular modelling study of PPAR gamma receptor. 49th Congress of the European Societies of Toxicology (EUROTOX), 2 September **2013**, Interlaken, Switzerland

ORAL PRESENTATIONS

1. **Al Sharif M**, Alov P, Tsakovska I, Pajeva I. (**2015**) Study of the ligand-dependent dysregulation of PPARγ – adverse outcome pathways and molecular modelling. Humboldt Kolleg, Bulgarian-German Scientific Cooperation: Past, Present and Future, 26 – 28 November **2015**, Sofia, Bulgaria, Book of abstracts, p. 36

2. **Al Sharif M**, Alov P, Tsakovska I, Pajeva I. (**2015**) *In silico* screening approach to predict liver toxicity of potential PPARγ agonists. 2nd International Conference on Natural Products Utilization: from Plant to Pharmacy Shelf (ICNPU), 14 – 17 October **2015**, Plovdiv, Bulgaria, Book of abstracts, SL-9, p. 46 **(Oral presentation award)**
3. **Al Sharif M**, Tsakovska I, Alov P, Pajeva P, Fioravanzo E, Bassan A, Kovarich S, Mostrag-Szlichtyng A, Vitcheva V, Yang C (**2015**) From PPARγ ligand dependent dysregulation to liver steatosis: MoA description and molecular modelling study. CMTPI-2015 - 8th International Symposium on Computational Methods in Toxicology and Pharmacology Integrating Internet Resources, 21-25 June **2015**, Chios, Greece
4. **Al Sharif M**, Alov P, Tsakovska I, Pajeva I. (**2015**) *In silico* modelling of full PPARγ agonists: a step towards liver steatosis risk assessment, International Conference Of Young Scientists, 11 – 12 June **2015**, Plovdiv, Bulgaria
5. **Al Sharif M**, Tsakovska I, Alov P, Vitcheva V, Pajeva I (2014) PPARγ-related hepatotoxic mode-of-action: quantitative characterisation and *in silico* study of the molecular initiating event involving receptor activation. 9th World Congress on Alternatives and Animal Use in the Life Sciences, 24-28 August **2014**, Prague, Czech Republic, Abstract in ALTEX proceedings, Volume 3, No. 1., Theme II Predictive toxicology, Session II Pathways approaches in toxicology: 1c-212, p. 56-57, ISSN 2194-0479.
6. **Al Sharif M**, Tsakovska I, Alov P, Vitcheva V, Pajeva I. COSMOS General Assembly Meeting, Erlangen'**2014**
7. **Al Sharif M**, Tsakovska I, Alov P, Vitcheva V, Pajeva I. COSMOS General Assembly Meeting, Milan'**2014**
8. **Al Sharif M**, Tsakovska I, Alov P, Vitcheva V, Pajeva I. COSMOS General Assembly Meeting, Barcelona'**2014**
9. **Al Sharif M**, Tsakovska I, Alov P, Vitcheva V, Pajeva I. COSMOS General Assembly Meetings, Ljubljana'**2013**

CONTRIBUTIONS TO NATIONAL SCIENTIFIC EVENTS

POSTERS

1. Diukendjieva A, **Al Sharif M**, Alov P, Tsakovska I, Pajeva I, PPARγ agonists and liver steatosis: mode-of-action characterisation and *in silico* study, VII-th National Congress of Pharmacology, 17 – 19 October **2014**, Medical University Pleven, Bulgaria

PRESENTATIONS

1. **Al Sharif M**, Tsakovska I, Alov P, Vitcheva V, Pajeva I (**2014**) From ligand-dependent dysregulation of PPARγ to nonalcoholic fatty liver disease. Scientific session for students and young scientists "Biomedicine and Quality of Life", 2 October **2014**, IBPhBME-BAS, Sofia, Bulgaria, Book of abstracts, p. 24

2. **Al Sharif M**, Tsakovska I, Alov P, Vitcheva V, Pajeva I (**2013**) Modes-of-action related to repeated dose toxicity: from PPARγ ligand-dependent dysregulation to non-alcoholic fatty liver disease, 8th Workshop "Biological activity of metals, synthetic compounds and natural products", 27-29 November **2013**, Sofia, Bulgaria, Proceedings ofthe eighthworkshop on biological activity of metals, synthetic compounds and natural products, Edited by: Dimitar Kadiysky and Radostina Alexandrova, D01., p.108-109, ISSN 2367 – 5683

PARTICIPATION IN SCIENTIFIC PROJECTS/GRANTS

1. EU Project n° 266835 (“Integrated *in silico* models for the prediction of human repeated dose toxicity of cosmetics to optimise safety (COSMOS)”) - Research project funded by the European Community’s 7th Framework Program (FP7/2007-2013) and from Cosmetics Europe

2. Project BG051PO001-3.3.06-0040 "Establishment of interdisciplinary teams of young scientists in the field of fundamental and applied research relevant to medical practice", implemented with financial support of the operative program Human Resources Development" financed by the European Social Fund of the European Union

APPENDIX A. SUPPLEMENTARY MATERIAL

Table S.1. PPARγ ligands retrieved from PDB (nd % max – no data for relative efficacy)

Complex PDB ID	Ligand PDB ID	In the dataset	Scaffold	Comment	Ref.
3BC5	ZAA	no	yes	nd % max	Zhang et al., 2009
3G9E	RO7	no	yes	67 % max	Bénardeau et al., 2009
3KDU	NKS	no	yes	PPARα ligand	Li et al., 2010
3VSO	EK1	no	yes	nd %max	Ohashi et al., 2013
1FM9	570	yes	yes		Gampe et al., 2000
1KNU	YPA	yes	yes		Sauerberg et al., 2002
2GTK	208	yes	yes		Kuhn et al., 2006
2Q8S	L92	yes	yes		Casimiro-Garcia et al., 2008
3FEJ	CTM	yes	yes		Grether et al., 2009
3IA6	UNT	yes	yes		Casimiro-Garcia et al., 2009
1FM6	BRL	yes	no		Gampe et al., 2000
1NYX	DRF	yes	no		Ebdrup et al., 2003.
2XKW	P1B	yes	yes		Mueller et al., DOI:10.2210/pdb2xkw/pdb
1I7I	AZ2	yes	no	nd %max	Cronet et al., 2001
1K74	544	yes	no	nd %max	Xu et al., 2001
2ATH	3EA	yes	no	nd %max	Mahindroo et al., 2005
2F4B	EHA	yes	no	nd %max	Mahindroo et al., 2006a
2HWR	DRD	yes	no	nd %max	Mahindroo et al., 2006b
3AN3	M7S	yes	no	nd %max	Ohashi et al., 2011
3AN4	M7R	yes	no	nd %max	Ohashi et al., 2011
3GBK	2PQ	yes	no	nd %max	Lin et al., 2009
3VJI	J53	yes	no	nd %max	Kuwabara et al., 2012

Table S.2. Classification of the selected papers according to the experimental subjects and approaches: HP – human patients; HC – human cell culture; A*iv* – animal *in vivo*; AC – animal cell culture; PPARγ↑ – PPARγ overexpression; PPARγ↑ + PT – PPARγ overexpression and pharmacological treatment; PPARγ↓ – PPARγ knockout / knockdown; PPARγ↓ + PT – PPARγ knockout / knockdown and pharmacological treatment; PT – pharmacological treatment; DM – diet manipulation; GM*up* – gene manipulation of PPARγ upstream proteins; GM*up* + PT – gene manipulation of PPARγ upstream proteins and pharmacological treatment; AOPP – AOP-related papers; BP – Background-related papers

Experimental subject				**Experimental approach**										
HP	**HC**	**A*iv***	**AC**	**PPARγ↑**	**PPARγ↑ + PT**	**PPARγ↓**	**PPARγ↓ + PT**	**PT**	**DM**	**GM*up***	**GM*up* + PT**	**AOPP**	**BP**	**Ref**
												✓		Krewski et al., 2010
												✓		ECHA, 2013
												✓		Prieto et al., 2011
												✓		Cronin and Richarz, 2012
												✓		ENV/JM/MONO(2013)6
													✓	Sass et al., 2005
												✓		Landesmann et al., 2012
													✓	Virtue and Vidal-Puig, 2010
													✓	Azhar, 2010
													✓	Fournier et al., 2007
													✓	Costa et al., 2010
													✓	Luconi et al., 2010
													✓	Ahmadian et al., 2013
													✓	Chandra et al., 2008
✓														Zhu et al., 2011
		✓	✓	✓	✓				✓					Lee et al., 2012
		✓	✓			✓	✓		✓					Morán-Salvador et al., 2011
		✓						✓						Satoh et al., 2013
		✓		✓		✓			✓					Yamazaki et al., 2011
		✓						✓						Sos et al., 2011
	✓	✓						✓	✓					Li et al., 2013
		✓	✓			✓				✓				Kumadaki et al., 2011

Experimental subject					Experimental approach									
HP	**HC**	**A*iv***	**AC**	**PPARγ↑**	**PPARγ↑ + PT**	**PPARγ↓**	**PPARγ↓ + PT**	**PT**	**DM**	**GM*up***	**GM*up* + PT**	**AOPP**	**BP**	**Ref**
		✓							✓					Gaemers et al., 2011
		✓							✓					Larter et al., 2009
													✓	He et al., 2011
													✓	Kawano and Cohen, 2013
													✓	Videla and Pettinelli, 2012
✓														Nagasaka et al., 2012
		✓	✓			✓	✓							Matsusue, 2012
													✓	Okumura, 2011
		✓		✓						✓	✓			Panasyuk et al., 2012
													✓	Semple et al., 2012
	✓	✓							✓	✓	✓			Flach et al., 2011
													✓	Matsusue, 2010
		✓		✓		✓			✓	✓				Bai et al., 2011
	✓									✓				Kim et al., 2008
		✓							✓					Larter et al., 2008
													✓	Handberg et al., 2012
													✓	Ring et al., 2006
													✓	Ehehalt et al., 2008
													✓	Su and Abumrad, 2009
													✓	Chabowski et al., 2007
													✓	Xu et al., 2013
													✓	Manteiga et al., 2013
													✓	Guo et al., 2009
													✓	Rogue et al., 2010
													✓	Musso et al., 2009
			✓					✓						Park and Park, 2012
		✓	✓						✓	✓				He et al., 2013

Experimental subject						Experimental approach								
HP	**HC**	**A*iv***	**AC**	**PPARγ↑**	**PPARγ↑ + PT**	**PPARγ↓**	**PPARγ↓ + PT**	**PT**	**DM**	**GM*up***	**GM*up* + PT**	**AOPP**	**BP**	**Ref**
		✓	✓							✓	✓			Chen et al., 2012
		✓							✓	✓	✓			Weismann et al., 2011
	✓	✓	✓					✓						Tsukahara et al., 2010
			✓					✓						Noh et al., 2013
													✓	Anderson and Borlak, 2008
	✓													Chen et al., 2013
✓														Kursawe et al., 2010
		✓	✓					✓	✓					Wang et al., 2012
		✓	✓					✓	✓					Lefils-Lacourtablaise et al., 2013
													✓	Greenberg et al., 2011
		✓	✓					✓	✓					Gwon et al., 2012
		✓	✓					✓	✓					Kang et al., 2010
			✓					✓						Park et al., 2013
		✓	✓					✓	✓	✓				Xu et al., 2012
		✓						✓						Liao et al., 2012
		✓						✓	✓					Magliano et al., 2013
													✓	Neuschwander-Tetri, 2010
													✓	Serviddio et al., 2013
													✓	Polvani et al., 2012
													✓	Bugge and Mandrup, 2010
													✓	Schupp and Lazar, 2010
													✓	Burgermeister and Seger, 2007
												✓		Houck et al., 2013
3	**5**	**25**	**15**	**4**	**1**	**5**	**2**	**14**	**17**	**9**	**4**	**7**	**32**	**Total**

Table S.3. Effect of natural ligands (mainly from diet) on the mRNA levels of PPARγ and some of its targets: WT – wild type; HFD – high-fat diet; CD – normal chow diet; qRT-PCR – quantitative reverse transcription polymerase chain reaction; sRT-PCR – semiquantitative RT-PCR; wks – weeks; * – endogenous suppressor.

PPARγ-related genetic background	Diet / Pharmacological treatment*	Assay	Fold change				Normalisation	Ref
			PPARγ	FSP27	CD36	aP2		
huh7 hepatoma cells	ceramide*	qRT-PCR	-2.32	-1.93	-2.21		vs vehicle	Li et al., 2013
WT	HFD	qRT-PCR	4.30	5.00	5.42	3.00	normalised expression - represent the mean ± SD diet effect	Lee et al., 2012
liver PPARγ-deficient line	HFD	qRT-PCR	-2.00	1.24	8.19	1.92	normalised expression - represent the mean ± SD diet effect	Lee et al., 2012
WT	HFD	Microarray		13.00	2.71	2.36	HFD vs CD	Lee et al., 2012
liver PPARγ-deficient line	HFD	Microarray		13.00	-1.02	3.38	HFD vs CD	Lee et al., 2012
WT	HFD (safflower oil); 10 wks	qRT-PCR	1.84		1.22		HFD vs CD; 10 wks	Yamazaki et al., 2011
WT	HFD (butter); 10 wks	qRT-PCR	10.00		6.57		HFD vs CD; 10 wks	Yamazaki et al., 2011
WT	HFD (safflower oil)	qRT-PCR	2.39		1.91		HFD butter vs CD; knockdown 5 days	Yamazaki et al., 2011

PPARγ-related genetic background	Diet / Pharmacological treatment*	Assay	Fold change				Normalisation	Ref
			PPARγ	FSP27	CD36	aP2		
WT	HFD (butter)	qRT-PCR	2.98		1.38		HFD butter vs CD); knockdown 5 days	Yamazaki et al., 2011
WT	HFD, 3 wks	qRT-PCR	2.09		1.52		vs CD WT; PPARγ/18S – normalisation	Gaemers et al., 2011
WT	HFD (liquid, overfed); 3 wks	qRT-PCR	3.34		18.44		vs CD WT; PPARγ/18S – normalisation	Gaemers et al., 2011
WT	HFD	sRT-PCR	1.81				vs WT CD	Larter et al., 2009
obese, hypercholesterolemic, diabetic foz/foz mice	HFD	sRT-PCR	1.25				vs foz CD	Larter et al., 2009
WT	HFD	Microarray			1.48		vs WT CD	Larter et al., 2009
obese, hypercholesterolemic, diabetic foz/foz mice	HFD	Microarray			1.70		vs foz CD	Larter et al., 2009

Table S.4. Effect of genetic manipulation and/or genetic background on the mRNA and protein levels of PPARγ and some of its targets: Ad-PPARγ2 – adenovirus-mediated transfection of PPARγ2; GFP – adenovirus-mediated transfection of green fluorescent protein.

PPARγ-related genetic background	PPARγ-related genetic manipulation	Diet	Assay	Fold change				Normalisation	Ref
				PPARγ	FSP27	CD36	aP2		
liver SMS2-overexpressing transgenic line	PPARγ upregulation	HFD	qRT-PCR	2.09	5.82	3.70		vs HFD WT	Li et al., 2013
lSMS2-deficient knockout line	PPARγ downregulation	HFD	qRT-PCR	-3.23	-2.56	-1.92		vs HFD WT	Li et al., 2013
liver PPARγ-deficient line		CD	qRT-PCR	-1000.00		7.00			Lee et al., 2012
wild type	PPARγ-transfected	CD	qRT-PCR	60.83		7.14	1000.00		Lee et al., 2012
liver PPARγ-deficient line	PPARγ-transfected	CD	qRT-PCR	1000.00		24.00	1000.00		Lee et al., 2012
liver PPARγ-deficient line		CD	qRT-PCR	-40.19	-3.21	-5.02	-1.67	normalised expression - represent the mean ± SD gene effect	Lee et al., 2012
liver PPARγ-deficient line		HFD	qRT-PCR	-346.00	-12.97	-3.33	-2.62	normalised expression - represent the mean ± SD gene effect	Lee et al., 2012
wild type	PPARγ-transfected	CD	Microarray		19.15	2.57	20.48	Ad-PPARγ2 vs Ad-GFP	Lee et al., 2012
liver PPARγ-deficient line	PPARγ-transfected	CD	Microarray		12.16	7.97	26.37	Ad-PPARγ2 vs Ad-GFP	Lee et al., 2012

PPARγ-related genetic background	PPARγ-related genetic manipulation	Diet	Assay	Fold change				Normalisation	Ref
				PPARγ	FSP27	CD36	aP2		
liver PPARγ-deficient line		CD	Western blot	1.00			-2.00		Lee et al., 2012
liver PPARγ-deficient line	PPARγ-transfected	CD	Western blot	-2.73			-1.86		Lee et al., 2012
wild type	PPARγ2 knockdown; 5 days	CD	qRT-PCR	-2.17		-1.45		CD (knockdown/functional); 5 days	Yamazaki et al., 2011
wild type	PPARγ2 knockdown; 5 days	HFD (safflower oil)	qRT-PCR	-1.46		-1.13		HFD saf (knockdown/functional); 5 days	Yamazaki et al., 2011
wild type	PPARγ2 knockdown; 5 days	HFD (butter)	qRT-PCR	-1.89		-1.77		HFD butt (knockdown/functional); 5 days	Yamazaki et al., 2011
wild type	PPARγ2-transfected	CD	qRT-PCR	85.30		17.30		CD (WT/PPARγ2-transfected)	Yamazaki et al., 2011
Lit-con		CD	qRT-PCR	5.54		8.81			Sos et al., 2011
Con-JAK2L		CD	qRT-PCR	6.06		15.73			Sos et al., 2011
Lit-JAK2L		CD	qRT-PCR	6.17		9.00			Sos et al., 2011
wild type	Fbw7 knockdown	CD	qRT-PCR	4.32	2.58	3.72	2.05	vs CD WT	Kumadaki et al., 2011
wild type	Fbw7 knockdown in litteramates	CD	qRT-PCR	12.30	4.43			vs CD WT	Kumadaki et al., 2011

PPARγ-related genetic background	PPARγ-related genetic manipulation	Diet	Assay	Fold change				Normalisation	Ref
				PPARγ	FSP27	CD36	aP2		
wild type	Fbw7 knockdown	CD	qRT-PCR	2.36	5.24	2.15		vs CD WT	Kumadaki et al., 2011
wild type	Fbw7/PPARγ2 - double knockdown	CD	qRT-PCR	-1.24	-1.11	1.34		vs CD WT	Kumadaki et al., 2011
wild type	Fbw7 transfected	CD	qRT-PCR	-1.14	-2.56	-1.51		vs CD WT	Kumadaki et al., 2011
obese, hypercholesterolemic, diabetic foz/foz mice		CD	sRT-PCR	2.51				vs WT CD	Larter et al., 2009
obese, hypercholesterolemic, diabetic foz/foz mice		HFD	sRT-PCR	1.73				vs WT HFD	Larter et al., 2009
obese, hypercholesterolemic, diabetic foz/foz mice		CD	Microarray			1.99		vs WT CD	Larter et al., 2009
obese, hypercholesterolemic, diabetic foz/foz mice		HFD	Microarray			2.27		vs WT HFD	Larter et al., 2009
PPARα -/-	PPARγ1-transfected	CD	Microarray	22.70	11.50	6.80	66.50		Yu et al., 2003

Table S.5. PPARγ ligands dataset: distribution of the ligands according to the experimental subject and the relative efficacy toward PPARγ (nd – no data).

Range of the %max	Hamster / kidney	Monkey / kidney			Human / kidney	Human / liver		№ of ligands	pEC_{50} data
	BHK21 ATCC CCL10	COS-1	COS-7	CV-1	HEK293	HepG2	Huh-7		
≥ 70% max	51	42	13	10	48	20	0	184	184
< 70% max	27	1	2	2	34	87	0	153	153
nd	5	1	1	2	13	7	64	95	93
total by cell line	83	44	16	14	95	114	64	432	430
total by species	83	74			273				
total human and animal data	157				273				

Table S.6. Information about PPARγ-full agonist complexes extracted from PDB: complex ID, ligand (agonist) ID, activity data of the PPARγ agonists extracted from PDB and CheMBL databases; RMSD values are recorded after the superposition of all extracted agonist-PPARγ complexes on the template structure from the 1FM6 complex.

Complex PDB ID	**Ligand PDB ID**	**Biological activity**				**RMSD**
		EC_{50} (nM)	**K_i (nM)**	**K_d (nM)**	**IC_{50} (nM)**	
1K74	544	0.2–2.7	1			1.07
1FM9	570	0.339–6	1–1.1	25–217		0.44
1FM6	BRL	2.4–2880	8–440	7–4980	30–2000	0 (template)
3AN4	M7R	3.6				1.20
3BC5	ZAA	4		5		1.51
3IA6	UNT	13			3	0.85
1I7I	AZ2	13–3528	18–200	200–350		1.01
3G9E	RO7	21		19		0.63
3AN3	M7S	22				1.06
2ZNO	S44	41–70				1.15
3GBK	2PQ	50				1.03
3VJI	J53	58				1.04
2F4B	EHA	70			50	1.01
2Q8S	L92	140	140			0.85
1KNU	YPA	170			170	1.58
3FEJ	CTM	210	740	740		0.62
2HWR	DRD	210				0.79
2ATH	3EA	230		152–152.05		0.90
2XKW	P1B	1125				1.03
1NYX	DRF	570–600	90	92		1.15
2GTK	208	760		250		0.67

Table S.7. Analysis of the HB contacts between amino acids in H12 and in other helices and between full agonists and the receptor in the LBD of the 21 PPARγ complexes extracted from PDB; 1PRG, apo-form.

Complex PDB ID	Ligand PDB ID	HBs between amino acids in the vicinity of H12				HBs between ligand and receptor		
		AA1		AA2		PHF	AA	SE
		AA	SE	AA	SE			
1K74	544	Glu460	H10/11_H12	Arg357	H6_H7	F1	Tyr473	H12
		Ile472	H12	Lys319	H4	F1	His449	H10/11
		Lys474	H12_	Lys319	H4	F2	His323	H5
		Tyr477	H12_	Glu324	H5	F2	Ser289	H3
1FM9	570	Glu460	H10/11_H12	Arg357	H6_H7	F1	Tyr473	H12
		Ile472	H12	Lys319	H4	F1	His449	H10/11
		Lys474	H12_	Lys319	H4	F2	His323	H5
		Tyr477	H12_	Glu324	H5	F2	Ser289	H3
		His449	H10/11	Lys367	H7			
		Lys367	H7	Phe363	loop in H7			
1FM6	BRL	Glu460	H10/11_H12	Arg357	H6_H7	F1	His449	H10/11
		Arg357	H6_H7	Glu276	H2'_H3	F2	His323	H5
		Ile472	H12	Lys319	H4	F2	Ser289	H3
		Lys474	H12_	Lys319	H4			
		Tyr477	H12_	Glu324	H5			
3AN4	M7R	Glu460	H10/11_H12	Arg357	H6_H7	F2	His323	H5
		Arg357	H6_H7	Glu276	H2'_H3	F2	Tyr327	H5
		Ser464	H10/11_H12	Gln286	H3	F4	Cys285	H3
		Leu465	H10/11_H12	Gln286	H3			
		His466	H10/11_H12	Gln286	H3			
		Ile472	H12	Lys319	H4			
		Lys474	H12_	Lys319	H4			
		His449	H10/11	Lys367	H7			
		Lys367	H7	Phe363	loop in H7			
3BC5	ZAA	Ser464	H10/11_H12	Gln283	H3	F1	Tyr473	H12
		His466	H10/11_H12	Gln286	H3	F1	His449	H10/11
		Asp475	H12	Lys319	H4			

Complex PDB ID	Ligand PDB ID	HBs between amino acids in the vicinity of H12				HBs between ligand and receptor		
		AA1		AA2		PHF	AA	SE
		AA	SE	AA	SE			
		His449	H10/11	Lys367	H7			
		Lys367	H7	Phe363	turn in H7			
3IA6	UNT	Glu460	H10/11_H12	Arg357	H6_H7	F1	Tyr473	H12_
		Arg357	H6_H7	Glu276	H2'_H3	F1	His449	H10/11
		His466	H10/11_H12	Gln286	H3	F2	His323	H5
		Ile472	H12	Lys319	H4	F2	Ser289	H3
		His449	H10/11	Lys367	H7			
		Lys367	H7	Phe363	loop in H7			
1I7I	AZ2	His466	H10/11_H12	Gln286	H3	F1	Tyr473	H12
		Gln470	H12	Lys474	H12_	F1	His449	H10/11
		Ile472	H12	Lys319	H4	F2	His323	H5
		Lys474	H12_	Lys319	H4	F2	Ser289	H3
		His449	H10/11	Lys367	H7			
		Lys367	H7	Phe363	loop in H7			
3G9E	RO7	Glu460	H10/11_H12	Arg357	H6_H7	F1	Tyr473	H12
		Arg357	H6_H7	Lys358	H6_H7	F1	His449	H10/11
		Arg357	H6_H7	Glu276	H2'_H3	F2	His323	H5
		Met463	H10/11_H12	Lys275	H2'_H3	F2	Ser289	H3
		His466	H10/11_H12	Gln286	H3			
		Ile472	H12	Lys319	H4			
		Lys474	H12_	Lys319	H4			
		His449	H10/11	Lys367	H7			
		Lys367	H7	Phe363	H7			
		Arg397	H8_H9	Glu324	H5			
		Asp396	H8_H9	Arg443	H10/11			
3AN3	M7S	Glu460	H10/11_H12	Arg357	H6_H7	F2	Tyr327	H5
		Ser464	H10/11_H12	Gln286	H3	F4	Cys285	H3
		Leu465	H10/11_H12	Gln286	H3	F4	Ser342	H5_H6
		His466	H10/11_H12	Gln286	H3			
		Ile472	H12	Lys319	H4			
		Lys474	H12_	Lys319	H4			

Complex PDB ID	Ligand PDB ID	HBs between amino acids in the vicinity of H12				HBs between ligand and receptor		
		AA1		AA2		PHF	AA	SE
		AA	SE	AA	SE			
		Leu476	H12_	Tyr320	H4			
		His449	H10/11	Lys367	H7			
		Lys367	H7	Phe363	loop in H7			
2ZNO	S44	Glu460	H10/11_H12	Thr459	H10/11	F4	Cys285	H3
		Arg357	H6_H7	Glu276	H2'_H3			
		Ile472	H12	Lys319	H4			
		Glu471	H12	Lys319	H4			
		Lys474	H12_	Lys319	H4			
		His449	H10/11	Lys367	H7			
		Lys367	H7	Phe363	turn in H7			
3GBK	2PQ	Glu460	H10/11_H12	Arg357	H6_H7	F1	Tyr473	H12
		Arg357	H6_H7	Glu276	H2'_H3	F1	His449	H10/11
		His466	H10/11_H12	Gln286	H3	F2	His323	H5
		Ile472	H12	Lys319	H4	F2	Ser289	H3
		Tyr477	H12_	Glu324	H5			
		Arg397	H8_H9	Glu324	H5			
		Asp396	H8_H9	Arg443	H10/11			
		His449	H10/11	Lys367	H7			
		Lys367	H7	Phe363	H7			
3VJI	J53	Glu460	H10/11_H12	Arg357	H6_H7	F2	Tyr327	H5
		Ser464	H10/11_H12	Gln286	H3	F4	Cys285	H3
		Leu465	H10/11_H12	Gln286	H3			
		Ile472	H12	Lys319	H4			
		Lys474	H12_	Lys319	H4			
		His449	H10/11	Lys367	H7			
		Lys367	H7	Phe363	loop in H7			
		Arg397	H8_H9	Glu324	H5			
		Arg443	H10/11	Glu324	H5			
2F4B	EHA	Glu460	H10/11_H12	Arg357	H6_H7	F1	Tyr473	H12
		Glu460	H10/11_H12	Thr459	H10/11	F1	His449	H10/11
		Arg357	H6_H7	Glu276	H2'_H3			

Complex PDB ID	Ligand PDB ID	HBs between amino acids in the vicinity of H12				HBs between ligand and receptor		
		AA1		AA2		PHF	AA	SE
		AA	SE	AA	SE			
		Ile472	H12	Lys319	H4			
		Lys474	H12_	Lys319	H4			
		Tyr477	H12_	Glu324	H5			
		Arg397	H8_H9	Glu324	H5			
		Asp396	H8_H9	Arg443	H10/11			
		His449	H10/11	Lys367	H7			
		Lys367	H7	Phe363	turn in H7			
2Q8S	L92	Glu460	H10/11_H12	Arg357	H6_H7	F1	Tyr473	H12
		Ser464	H10/11_H12	Gln283	H3	F2	His323	H5
		Ile472	H12	Lys319	H4	F4	Tyr327	H5
		Glu471	H12	Lys319	H4			
		His449	H10/11	Lys367	H7			
		Lys367	H7	Phe363	turn in H7			
		Arg397	H8_H9	Glu324	H5			
1KNU	YPA	Glu460	H10/11_H12	Arg357	H6_H7	F1	Tyr473	H12
		Arg357	H6_H7	Glu276	H2'_H3	F1	His449	H10/11
		Met463	H10/11_H12	Gln283	H3	F2	His323	H5
		Leu465	H10/11_H12	Gln286	H3	F2	Ser289	H3
		His466	H10/11_H12	Gln286	H3			
		Asp475	H12_	Lys319	H4			
		Ile472	H12	Lys319	H4			
		His449	H10/11	Lys367	H7			
		Lys367	H7	Phe363	loop in H7			
		Arg397	H8_H9	Glu324	H5			
3FEJ	CTM	Glu460	H10/11_H12	Arg357	H6_H7	F1	Tyr473	H12
		Asp462	H10/11_H12	Lys275	H2'_H3	F1	His449	H10/11
		Arg357	H6_H7	Glu276	H2'_H3	F2	His323	H5
		His466	H10/11_H12	Gln286	H3	F2	Ser289	H3
		Ile472	H12	Lys319	H4	F4	Arg288	H3
		Lys474	H12_	Lys319	H4			

Complex PDB ID	Ligand PDB ID	HBs between amino acids in the vicinity of H12				HBs between ligand and receptor		
		AA1		AA2		PHF	AA	SE
		AA	SE	AA	SE			
		His449	H10/11	Lys367	H7			
		Lys367	H7	Phe363	loop in H7			
		Arg397	H8_H9	Glu324	H5			
		Asp396	H8_H9	Arg443	H10/11			
2HWR	DRD	Glu460	H10/11_H12	Arg357	H6_H7	F2	His323	H5
		Arg357	H6_H7	Glu276	H2'_H3	F2	Ser289	H3
		His466	H10/11_H12	Gln286	H3			
		Ile472	H12	Lys319	H4			
		Lys474	H12_	Lys319	H4			
		Arg397	H8_H9	Glu324	H5			
		Asp396	H8_H9	Arg443	H10/11			
2ATH	3EA	Thr459	H10/11_H12	Val455	H10/11	F1	Tyr473	H12_
		Glu460	H10/11_H12	Arg357	H6_H7			
		Arg357	H6_H7	Glu276	H2'_H3			
		Asp462	H10/11_H12	Gln286	H3			
		His466	H10/11_H12	Phe287	H3			
		Lys474	H12_	Tyr320	H4			
		His449	H10/11	Lys367	H7			
		Arg397	H8_H9	Glu324	H5			
		Asp396	H8_H9	Arg443	H10/11			
2XKW	P1B	Glu460	H10/11_H12	Arg357	H6_H7			
		Arg357	H6_H7	Glu276	H2'_H3			
		Ser464	H10/11_H12	Gln286	H3			
		His466	H10/11_H12	Gln286	H3			
		Ile472	H12	Lys319	H4			
		Lys474	H12_	Lys319	H4			
		Leu476	H12_	Tyr320	H4			
		His449	H10/11	Lys367	H7			
		Lys367	H7	Phe363	loop in H7			
		Arg397	H8_H9	Glu324	H5			
		Asp396	H8_H9	Arg443	H10/11			

Complex PDB ID	Ligand PDB ID	HBs between amino acids in the vicinity of H12				HBs between ligand and receptor		
		AA1		AA2		PHF	AA	SE
		AA	SE	AA	SE			
		Arg443	H10/11	Glu324	H5			
1NYX	DRF	Glu460	H10/11_H12	Arg357	H6_H7	F1	Tyr473	H12_
		Ser464	H10/11_H12	Gln286	H3	F2	His323	H5
		Asp475	H12_	Tyr320	turn in H4			
		His449	H10/11	Lys367	H7			
		Met364	H6_H7	Lys367	H7			
		Arg 397	H8_H9	Glu324	H5			
2GTK	208	Glu460	H10/11_H12	Arg357	H6_H7	F1	Tyr473	H12
		Arg357	H6_H7	Glu276	H2'_H3	F1	His449	H10/11
		His466	H10/11_H12	Gln286	H3	F2	His323	H5
		Ile472	H12	Lys319	H4	F2	Ser289	H3
		Lys474	H12_	Lys319	H4			
		His449	H10/11	Lys367	H7			
		Lys367	H7	Phe363	loop in H7			
		Arg397	H8_H9	Glu324	H5			
		Asp396	H8_H9	Arg443	H10/11			
1PRG chain A		Glu460	H10/11_H12	Arg357	H6_H7			
		Arg357	H6_H7	Glu276	H2'_H3			
		Leu468	H12	His466	H10/11_H12			
		Asp475	H12_	Gln454	H10/11			
		Arg397	H8_H9	Glu324	H5			
		Asp396	H8_H9	Lys438	turn in H10/11			
		Met364	loop in H7	Lys367	H7			
		Lys367	H7	Phe363	loop in H7			
		Ser289	H3	Cys285	H3			
1PRG chain B		Glu471	H12	Lys474	H12_			
		His449	H10/11	Lys367	H7			
		Arg397	H8_H9	Glu324	H5			
		Asp396	H8_H9	Lys438	H10/11			

APPENDIX B. AOP EVALUATION TABLE

The table, containing the data for the AOP evaluation, is available in electronic format onto the CD attached to the inside cover (Appendix_B_AOP_evaluation_table.xls).

BULGARIAN
ACADEMY
of SCIENCES
1869